HETEROGENIZED N-HETEROCYCLIC CARBENE METAL COMPLEXES FOR SELECTIVE CATALYSIS

Alberto Martínez Lombardía

ALBERTO MARTÍNEZ LOMBARDÍA

HETEROGENIZED *N*-HETEROCYCLIC CARBENE METAL COMPLEXES FOR SELECTIVE CATALYSIS

DOCTORAL THESIS

Supervised by

Prof. Dr. Carmen Claver and Dr. Cyril Godard

Departament de Química Física I Inorgànica

UNIVERSITAT ROVIRA i VIRGILI

Tarragona, June 2016

UNIVERSITAT ROVIRA I VIRGILI
HETEROGENIZED N-HETEROCYCLIC CARBENE METAL COMPLEXES FOR SELECTIVE CATALYSIS
Alberto Martínez Lombardía

UNIVERSITAT ROVIRA i VIRGILI

Departament de Química Física i Inorgànica,
Facultat de Química
C/ Marcel·lí Domingo s/n,
43007, Tarragona

Prof. Dr. Carmen Claver Cabrero, and Dr. Cyril Godard from the Department of Physical and Inorganic Chemistry at Universitat Rovira I Virgili,

STATE that the present study, entitled "**Heterogenized N-Heterocyclic Carbenes Transition Metal Complexes for Selective Catalysis**", presented by Alberto Martínez Lombardía for the award of the degree of Doctor, has been carried out under our supervision at the Department of Physical and Inorganic Chemistry at Universitat Rovira I Virgili and that it fulfils all the requirements to be eligible for the International Doctorate Award.

Tarragona, 10 May, 2016

Doctoral Thesis Supervisor/s

Prof. Dr. Carmen Claver Cabrero Dr. Cyril Godard

UNIVERSITAT ROVIRA I VIRGILI
HETEROGENIZED N-HETEROCYCLIC CARBENE METAL COMPLEXES FOR SELECTIVE CATALYSIS
Alberto Martínez Lombardía

The present Doctoral Thesis has been carried out thanks to the "Programa d'ajuts per a la contractació de personal investigador novell (FI-DGR) (Reference: 2011F1_B2 00216) financed by the Generalitat de Catalunya.

The work developed in this doctoral thesis has been possible thanks to the finantial support from the following research projects:

- 246461 SYNFLOW European 7th Framework Programme
- CTQ2010-14938
- 2009 SGR 116
- CTQ2013-43438-R
- 2014 SGR 670

Generalitat de Catalunya

UNIVERSITAT ROVIRA I VIRGILI
HETEROGENIZED N-HETEROCYCLIC CARBENE METAL COMPLEXES FOR SELECTIVE CATALYSIS
Alberto Martínez Lombardía

ACKNOWLEDGEMENTS

En primer lugar, quiero agradecerles a Carmen y a Cyril la oportunidad que me han brindado de poder llevar a cabo una tesis doctoral en su grupo. A Cyril, te agradezco lo mucho que he aprendido durante estos años, tu accesibilidad y tu ayuda la hora de resolver problemas de química. A Carmen, te agradezco mucho tu apoyo, tu confianza, tu cercanía a pesar de tu apretada agenda y el exquisito trato recibido. Y por supuesto, las incontables oportunidades que se me han puesto al alcance durante estos años, congresos, conferencias, estancias... Gracias por fomentar siempre el buen ambiente y motivarnos con cenas de navidad llenas de villancicos, cenas de verano en el jardín, excursiones al valle...

Gracias a Eduardo Peris por darme la oportunidad de conocer el mundo de la investigación, y por posibilitar mi estancia Erasmus en Toulouse, y por ayudarme a recalar en Tarragona para así poder hacer la tesis.

Aunque dudo que lo lea nunca, muchas gracias a Jamin, por empezar la química a la que he dedicado buena parte de estos 4 años, y por enseñarme a trabajar en el laboratorio con un rigor que yo no tenía.

Le quiero agradecer a Sergio Castillón su disponibilidad, su trato auténtico, y sus fantásticas explicaciones, provistas de fundamento y utilidad práctica, cosas ambas no siempre compatibles en un laboratorio.

Quiero agradecer a todos los compañeros que he tenido durante estos 4 años y medio, ya que todos me han aportado algo de una forma u otra. Gente del mundo boro, Amadeu y su pedazo cena de tesis en el restaurante Gaudir, Henrik y sus horarios tarde-noche y su amabilidad, Cristina Pubill poniendo reacciones con su camisa de cuadros y riéndose por todo, Jess Cid y su sentido del humor siempre a punto, Cristy Solé, la energía incontenible, Xavi Sanz "com li fots" XD, Yérard y su asombrosa habilidad con los idiomas y las imitaciones, Enrico, sangre siciliana, Ana B, 10 como química, 11 como persona..., los baby borons Nuria y sus anillos, Marc petit y sus complicados compuestos, y Jordi Royes el del Madriz XD, Alba que estuvo poquito tiempo, Adam, que

vino de estancia, y Eric Bowes, cómo te lo montas, gran reencuentro en Ottawa :D

Azucarillos (oscarcitos), Javi Mazuela, pásate algún paper, Mercé y su amor por los animales, Sabina, Magre, alcalde de Valls, Jèeessica M, lo milloret del Perelló, Charly, todo clase y espectaculares raquetukis en Sapeira, Maria, la mejor calçotada de mi vida, Zahra, la alegría en persona, Albert, un crak del nàstic, Efrem y Carles, todo por delante.

Gente CO_2, Siham, Marlene, encantadora como siempre 4 años después, Laia, danza del vientre de Els Pallaresos, Anna M Masdeu, siempre buen rollo.

Carmencitos, Angy y Vero, Bernabé, "no tocar" "Bernabé", Jessi, Eli, mítica, gatitos, cristales por doquier, criadora de pollos como yo por ejemplo, Franciscooooooo el hípster madrugador de Reus capital, Nanette, se te echa en falta, Antón, ya te quedan menos columnas XD ;) J Creus, gracias por traerme ligandos en vialitos desde Barcelona, Laura y Aarón, se os quiere, Myriam, welcome to the jungleeeee nanananananana,

Carmencitos de la acera de enfrente (CTQ), Quique, Doctor Colavida, VAMOS!!!!! Jorge, soluciona problemas, y baila, Bianca y Mónica, Repsol se os queda muy pequeño, Dolores, Stefano, no le puedes caer mal a nadie, Xavi Castilla, se echan en falta las quedadas toulousans, a ver si nos vemos pronto, Olga, Míriam de los apellidos muy largos, Isabel y Aitor, parejita feliz, Olivia, Itzi, gracias por buscarme amigos en Bilbo por Navidad y por tener tanto flow ;)

Vamos con el staff, Raquel por ser una crack y la number one de los técnicos de la uni, Josep, siempre un placer poder contar contigo. Sílvia, siempre me has echado una manita con lo que sea, Yolanda, también, gracias por preocuparte por mi beca, Elisenda, gracias por todo, siempre me has solucionado la papeleta. Ramón, paciencia, bondad y eficiencia a partes iguales. Toni de la Torre, gracias por buscarme un hueco siempre para hacer ICPs... Débora, gracias por ser tan atenta y tan simpática.

I'd like to say thank you to Giancarlo Franciò for being my advisor and helping me during my time in Aachen, and also to Walter Leitner for the great opportunity to spend three months at the ITMC. En el terreno

personal conocí a gente de la que no me voy a olvidar. Maren, I felt like home during my time in Aachen (actually better than at home). Really one the best periods in my life, just thanks for everything, hope to keep in contact and get the chance to share some more fabulous times :D . Laura, congrats, I guess u'r a doctor now, I was fortunate to meet you, thanks for helping me socializing in Aachen and I wish u the best, u r a fantastic person. Daniel, er del shiringuito de Cái, gracias por todo, te lo curraste un montón, aunque tu jefe piense que no trabajes XD, José, me contaste muchas cosas interesantes, un placer siempre compartir ratos contigo, y gracias por la ayudita con la cuenta corriente ;), Raquel, me parto contigo, molas mazo, ánimo que ya lo tienes eso. Olga, a ver si nos vemos por Tarragona. De los demás Pedro, gracias por ayudarme un montón, César, Bernhard, Kylie, Fabian, Martin, Pascal, Katerina, Katerina, Giuliana, Dominik, Benjamin, Stefan, Sandra... I've forgotten some names, so sorry for that, and thanks to everyone, my time in Aachen was awesome.

A la gente que conocí en Toulouse y que me metió el gusanillo de la investigación. Noel, Fany, Xavi, Richi, Jordi... Además de eso me quedo con las impagables anécdotas durante las cenas en l'Aubrac, los cafés en el pasillo exterior, los motes bien buscados, las excursiones y las bodas en Pravia (y las prebodas) XD.

A mis amigos, los del tenis, los de la bici, el Comando Cork, los carbonatos por las farras máximas, y las que quedan, y a mis mejores amigos, Lucas, Roberto y Rober, que últimamente no nos vemos un carajo, pero siempre puedo contar con vosotros pa to.

Muchas gracias Judi, por aguantarme estos últimos meses y por echarme un cable.

Por último, gracias papá y mamá por apoyarme siempre en todo, en las buenas y en las malas y por estar SIEMPRE ahí.

UNIVERSITAT ROVIRA I VIRGILI
HETEROGENIZED N-HETEROCYCLIC CARBENE METAL COMPLEXES FOR SELECTIVE CATALYSIS
Alberto Martínez Lombardía

"It always seems imposible until it's done"

Nelson Mandela

UNIVERSITAT ROVIRA I VIRGILI
HETEROGENIZED N-HETEROCYCLIC CARBENE METAL COMPLEXES FOR SELECTIVE CATALYSIS
Alberto Martínez Lombardía

Table of contents

UNIVERSITAT ROVIRA I VIRGILI
HETEROGENIZED N-HETEROCYCLIC CARBENE METAL COMPLEXES FOR SELECTIVE CATALYSIS
Alberto Martínez Lombardía

Glossary of acronyms and abbreviations

υ(CO) CO stretching frequency

$[Rh(\mu\text{-}Cl)(COD)]_2$ Chloro(1,5-cyclooctadiene)rhodium(I) dimer

A

acac acetylacetonate

Ad Adamantyl

AIBN Azobisisobutyronitrile

API Active Pharmaceutical Ingredient

B

BIAN Bis(imino) acenaphtene

BINAM 1,1'-binaphtyl-2,2'-diamine

BINAP 2,2'-bis(diphenylphosphanyl)-1,1'-binaphthyl

C

CNTs Carbon Nanotubes

COD 1,5-cyclooctadiene

CP-MAS Cross Polarization-Magic Angle Spinning

CuAAC Cu-catalyzed Alkyne Azyde Cycloaddition

Cy Cyclohexyl

D

d doublet

DCE 1,2-dichloroethane

DDQ 2,3-dichloro-dichloro-5,6-dicyano-1,4-benzoquinone

DME 1,2-dimethoxyethane

DMF Dimethyl formamide

DMSO Dimethyl sulfoxide

DMPA 2,2-dimethoxy-2-phenylacetophenone

E

EDX Energy-dispersive X-Ray Photoelectron Spectroscopy

ee enantiomeric excess

Et Ethyl

ESI-TOF Electrospray Ionization-Time-of-Flight

F

FG Functional group

FWHM Full Width at Half Maximum

G

GC-FID Gas Chromatography-Flame Ionization Detector

GC-MS Gas Chromatography-Mass Spectrometry

H

HBCat Catecholborane

HBPin Pinacolborane

HPLC High Pressure Liquid Chromatography

HR-MS High Resolution-Mass spectrometry

I

ICP-AES Inductively Coupled Plasma-Atomic Emission Spectroscopy

ID Internal diameter

IL Ionic Liquid

IMes 1,3-dimesityl-2-imidazolylidene

iPr isopropyl

IPr 1,3-bis(2,6-diisopropylphenyl)-2-imidazolylidene

J

J Coupling constant

M

m multiplet

MCM Mobile Composition of Matter

MCF Mesostructured Cellular Foam

Me Methyl

Mes Mesityl

MOF Metal Organic Framework

MS Mass Spectrometry

MSU Michigan State University

MWCNTs Multi-Walled Carbon Nanotubes

N

NHC *N*-Heterocyclic Carbene

NMR Nuclear Magnetic Resonance

NPs Nanoparticles

O

OTs Tosylate

P

P123 Pluronic P-123

$Pb(OAc)_2$ Lead (II) acetate

$Pd_2(dba)_3$ Tris(dibenzylideneacetone) dipalladium(o)

$Pd(acac)_2$ Palladium (II) acetylacetonate

$Pd(OAc)_2$ Palladium (II) acetate

Ph Phenyl

PHIP *para*-Hydrogen Induced Polarization

PMO Periodic Mesoporous Organosilica

ppm parts per milion

Pr Propyl

PR_3 Trialkyl phosphine

P*t*Bu_3 Tris(*tert*-butyl) phosphine

PTFE Poly trifluoroethylene

PUFA Polyunsaturated fatty acid

S

s singlet

SBA Santa Barbara Acids

sept septuplet

SIMes Saturated backbone IMes

SIPr Saturated backbone IPr

SM Suzuki-Miyaura

S_N^2 Bimolecular nucleophilic substitution

SWCNT's Single-Walled Carbon Nanotubes

T

t triplet

T temperature

tBu *tert*-butyl

TEM Transmission Electron Microscopy

TEOS Tetraethyl orthosilicate

THF Tetrahydrofuran

TLC Thin Layer Chromatography

TMS Trimethylsilane

TMSCl Chloro trimethylsilane

TOF Turnover Frequency

TON Turnover Number

TSH Transfer Semi-Hydrogenation

U

UV-Vis Ultraviolet-Visible Spectroscopy

UHV Ultra-High Vaccuum

X

XRD X-Ray Diffraction

XPS X-Ray Photoelectron Spectrocopy

UNIVERSITAT ROVIRA I VIRGILI
HETEROGENIZED N-HETEROCYCLIC CARBENE METAL COMPLEXES FOR SELECTIVE CATALYSIS
Alberto Martínez Lombardía

Summary

SUMMARY

Catalysis is a crucial tool in the development of sustainable chemical processes. The manufacture of bulk chemicals mostly relies on heterogeneous catalysts, with reactions usually taking place between a solid catalyst and a gaseous feedstock at high temperatures. For the production of molecules of high complexity, the reactions usually take place in an organic solvent containing a dissolved catalyst, which in most cases is a transition-metal based complex. In spite of the huge potential of this class of catalysts for the manufacture of specialty chemicals, pharmaceuticals, agrochemicals, flavors and fragrances or advanced materials, their implementation in large scale industrial processes has been limited because of the difficulties in separating the catalysts from the products. Therefore, the development of strategies that allow the recovery and reuse of this type of catalyst is an issue of economic and environmental concern.

Among the various approaches described to tackle this problem, the immobilization of homogeneous metal complexes onto solid supports combines the advantages of heterogeneous catalysis such as the easy handling of the catalyst and product separation with the ability of homogeneous catalysts to promote very selective transformations under mild reaction conditions.

The general objective of this PhD work is the development of N-heterocyclic carbene transition metal catalysts immobilized onto solid supports and the evaluation of their performance in various reactions, with special attention on the issue of catalyst recovery and reuse. The testing of the catalysts performance under continuous flow operation is also addressed.

After an introduction to establish the “state of the art” in **Chapter 1** and the definition of the objectives in **Chapter 2**, in **Chapter 3,** the synthesis of well-defined Pd complexes bearing functionalized monodentate NHC ligands was described. An important part of the work consisted in the design of a suitable synthetic route for the introduction of functional groups in the ligand structure for the subsequent immobilization of the corresponding Pd complexes onto inorganic oxide solid supports. The nature of the immobilized molecular species was studied in order to

confirm the integrity of the [Pd(NHC)] complexes upon immobilization, and the final materials were appropriately characterized.

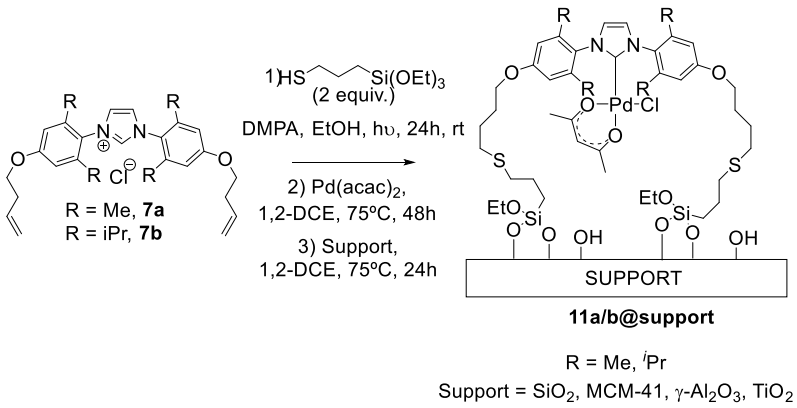

Scheme 1. Procedure followed for the immobilization of well-defined [Pd(NHC)] complexes onto inorganic supports.

In **Chapter 4**, the supported complexes described above were evaluated in various C-C cross coupling reactions, namely Suzuki-Miyaura, Heck and Sonogashira (Scheme 2). Exploration of the most suitable reaction conditions for the Suzuki-Miyaura reaction led to the use of a biphasic aqueous/organic solvent mixture. However, rapid catalyst degradation was observed under these conditions, and attempts to recycle and reuse the catalyst resulted in a rapid decay of the activity after the first catalytic cycle. Operating under non-aqueous reaction conditions was beneficial for the stability of the catalyst, and under these conditions the deactivation pathway was slowed down.

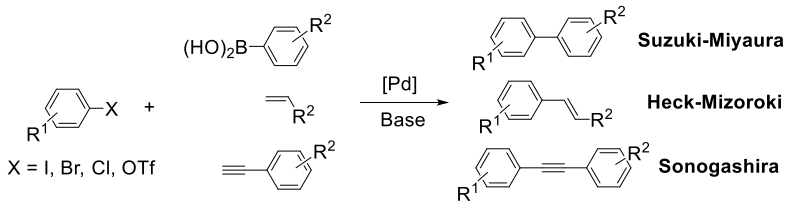

Scheme 2. General reaction scheme of the Suzuki, Heck and Sonogashira couplings, catalyzed by Pd.

These non-aqueous reaction conditions were used to determine the influence of the different supports on the performance of the catalysts.

Summary

Increased robustness was displayed by materials based on γ-Al_2O_3 and TiO_2 when the catalyst was reused in successive cycles. The robustness of the silica-, γ-Al_2O_3, and TiO_2-supported catalysts was further evaluated in continuous flow Suzuki-Miyaura experiments. When the reaction was run over a two hours period, silica-based materials showed some deactivation, whereas this tendency was not observed in the case of γ-Al_2O_3, and TiO_2-supported catalysts.

Application of the supported catalysts in the Heck coupling of aryl bromides with electron poor alkenes led to the desired coupling product in excellent yields. However, recycling of the catalyst resulted in greatly diminished product yields after the first reaction run. The causes for this deactivation remain unclear.

The Sonogashira couplings between *p*-bromoacetophenone and various alkynes catalyzed by the supported catalysts were also described. As in the case of the Suzuki-Miyaura reaction, materials based on γ-Al_2O_3, and TiO_2 displayed superior stability compared to their silica analogues. The former supported catalysts were evaluated in the Sonogashira coupling between *p*-bromoacetophenone and phenylacetylene under continuous flow conditions, and no drop in activity was observed after two hours on stream.

In **Chapter 5**, the γ-Al_2O_3-, and TiO_2-supported catalysts were tested in the (*Z*)-selective semi-reduction of alkynes to alkenes (Scheme 3)

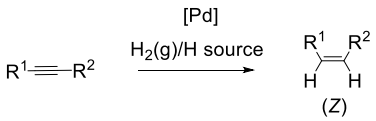

Scheme 3. Pd-catalyzed (*Z*)-selective semi-reduction of alkynes.

Two methodologies were used to realize this transformation: using H_2 (g) as the reductant and using an equimolar mixture of HCO_2H/Et_3N as the hydrogen donor.

The semi-hydrogenation using H_2 (g) as the reductant provided good activity under mild reaction conditions in the reduction of internal alkynes. However, under these conditions, important amounts of overhydrogenated alkane products were obtained at high alkyne

conversions. The same selectivity issue was encountered when this process was run in a continuous flow microreactor.

This transformation could also be performed in the presence of the supported Pd catalysts and an equimolar mixture of HCO_2H/Et_3N as the hydrogen donor, and through the addition of a catalytic amount of PPh_3, overreduction was prevented. Internal alkynes and alkynols were transformed to the corresponding (*Z*)-alkenes in high yields. This system could also be applied to several terminal alkynes.

Besides the reduction of alkynes under transfer hydrogenation conditions, the supported catalysts promoted the isomerization of (*Z*)-stilbene to (*E)*-stilbene. Under appropriate reaction conditions, diphenylacetylene was converted to (*E*)-stilbene in 90% yield, *via* indirect (*E*)-selective transfer semi-hydrogenation.

Recycling of the supported catalysts in the (*Z*)-selective transfer semi-hydrogenation of diphenylacetylene was studied. Complete deactivation of the catalysts occurred after the first reaction run. Pd leaching was detected by ICP-OES analysis of the reaction mixtures, however, these values were insufficient to explain the complete loss of activity in the second reaction run. It was hypothesized that the active catalyst species may *in situ* aggregate into clusters, nanoparticles and/or bulk Pd. This issue was investigated by XRD and TEM analysis, but neither the presence of characteristic diffraction patterns of Pd(0) nor the formation of NP's could be evidenced.

In **Chapter 6** Rh complexes bearing chiral bis(NHC) ligands functionalized with pyrene moieties were synthesized, and were subsequently immobilized onto the surface of MWCNT's *via* π-π stacking interactions. Two strategies were described for the introduction of a pyrene moiety in the structure of atropoisomeric 1,1'-binaphtyl-2,2'-bis(4-phenyl-1,2,3-triazol).

- A pyrene tag bearing a 4C-linker chain was introduced through alkylation of the N3 position of the triazol compound using 4-(pyren-1-yl)butyl triflate as reagent. In this manner, a ditriflate salt bearing two pyrene tags was obtained. By careful methylation of one of the two N3 positions a BINAM-based monomethylated triazolium triflate compound

Summary

could be obtained, and subsequent reaction with 4-(pyren-1-yl)butyl triflate afforded a bistriazolium preligand only one pyrene tag.

- The second strategy involved a key Cu-catalyzed alkyne azide cycloaddition step using propargyl pyrenebutyl ether as the alkyne reagent. This strategy provided a BINAM-based bistriazole compound bearing two pyrene tags in 34% yield.

Metalation of the ditriflate salt precursors was achieved in the presence of $[Rh(\mu\text{-}Cl)(COD)]_2$ and KO^tBu. The corresponding [Rh(I)bis(NHC)] chelate complexes were isolated in yields above 70% after purification by precipitating the crude mixtures in THF/Et_2O.

The complexes depicted in Scheme 4, containing one and two pyrene tags, respectively, were immobilized onto the surface of MWCNTs.

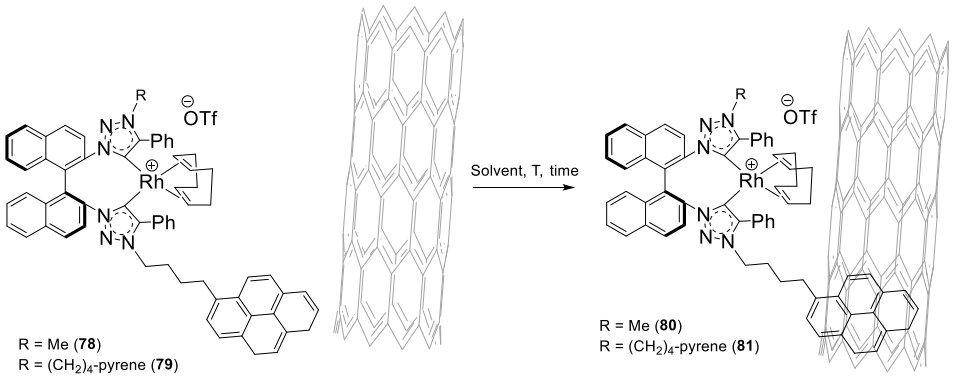

Scheme 4. Non-covalent immobilization of Rh complexes bearing chiral bis(NHC) ligands functionalized with pyrene moieties.

The presence of a second pyrene moiety in the ligand resulted in a higher metal loading in the corresponding hybrid material. Moreover, the solvent used to carry out the immobilization procedure also influenced the catalyst loading in the hybrid materials.

Finally, the non-pyrene-tagged Rh complex was used in order to explore the potential of these novel catalysts in asymmetric reduction processes. Hydrosilylation of isobutyrophenone resulted in only 8% ee at 25% conversion. A slight increase in the reaction temperature resulted in increased conversion but only 2% ee was obtained in this case. The use of

bulkier silane partners to enhance the enantioselectivity of the process resulted in no conversion. The same Rh complex was also tested in the asymmetric hydroboration of styrene with pinacolborane. The catalyst was active and 100% conversion was observed at room temperature. The branched and linear regioisomers were obtained in 1:1 ratio, and GC analysis revealed that the branched regioisomer was obtained as a racemic mixture. This complex was also active in the hydrogenation of dimethylitaconate. However, the alkane product was obtained as a racemic mixture. Further work is currently ongoing to design a selective process mediated by these complexes, and to study their recycling in successive reaction runs.

Chapter 1

"Introduction"

UNIVERSITAT ROVIRA I VIRGILI
HETEROGENIZED N-HETEROCYCLIC CARBENE METAL COMPLEXES FOR SELECTIVE CATALYSIS
Alberto Martínez Lombardía

1.1. Homogeneous and heterogeneous catalysis

In principle, a catalyst participates in a chemical reaction resulting in an increase of the reaction rate, without consumption of the catalyst partner, so that fresh reagents may be fed in the system upon completion of the reaction, yielding again the expected reaction products. In a catalyzed reaction the total free energy from reactants to products does not change compared to its non-catalyzed counterpart but the catalyst provides an alternative reaction pathway involving different and lower-energy transition states. Therefore the presence of a catalyst affects the kinetic aspects of a reaction by lowering the activation energy without affecting its thermodynamics, *i.e.* the product distribution at equilibrium (Figure 1.1).[1]

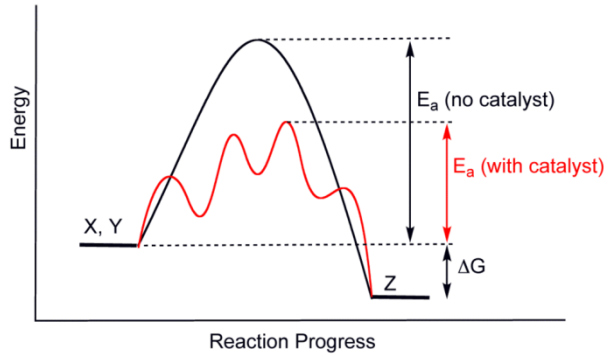

Figure 1.1. Energy profile for a catalyzed multi-step reaction (in red) and an uncatalyzed reaction (in black).

In industry, catalysis plays a key role, enabling a wide range of chemical transformations and reducing cost, time, and in many cases preventing the use of stoichiometric reagents, thus minimizing waste and contributing to the development of more environmentally friendly processes.[2] Leaving enzymes apart, catalysts may be generally divided into homogeneous and heterogeneous catalysts, depending on whether the catalysts are in the same or a distinct phase than the reagents.

Typical heterogeneous catalysts are oxides, or supported metal particles. Important factors influencing the activity of these catalysts include the rate of diffusion of reactants towards the catalytic body, adsorption of reactants, desorption of the products, the presence of catalytically active sites which is related to the surface area of the solid, etc... In general

heterogeneous catalysts require harsh reaction conditions, such as high temperatures or pressures in order to overcome these series of rate-determining processes, however their solid nature has greatly helped their implementation in industrial processes due to the ease of separation from the products which lie in a different phase, and due to the easy handling of these catalysts, which are generally very robust and can be used under rather extreme reaction conditions without decomposition.[3] Some examples of the application of this kind of catalysts in industry are the production of sulphuric acid which uses a vanadium catalyst,[4] the Haber-Bosch process[5] for the production of ammonia which uses a heterogeneous iron catalyst or the zeolites used in the cracking of hydrocarbons mixtures. Heterogeneous catalysis is usually associated to the bulk chemical industry.

In contrast, homogeneous catalysis is more related to the field of fine chemistry, although some industrially relevant processes for the production of bulk chemicals also rely on homogeneous catalysis (Scheme 1.1 and 1.2). In contrast with heterogeneous catalysts, homogeneous species have a well-defined structure, and every single catalytic entity can act as a single active site, which makes them intrinsically more active and selective. Several classes of chemical compounds can function as homogeneous catalysts, namely Brønsted and Lewis acids, bases, organic molecules such as proline or quinine... but nowadays, the term homogeneous catalyst usually refers to organometallic or coordination complexes. With this type of catalysts, the choice of the metal and the design of the ligands have an important influence on the reactivity and selectivity of the reaction. Moreover, the reaction mechanisms are considerably easier to study since powerful spectroscopic methods such as NMR can be used to assign structures and follow reaction kinetics. Moreover, diffusion and dissipation of heat rarely is a problem.[6,7]

Over the last decades, scientific research has led to enormous progress in this field. Nowadays, myriads and myriads of transition metal complexes have been developed showing excellent activity and selectivity in almost any organic transformation known and have helped to discover and develop new chemical processes. Furthermore, they are

usually very versatile and able to transform various types of substrates under mild reaction conditions.

Industrial processes based on homogeneous catalysis for the production of bulk chemicals

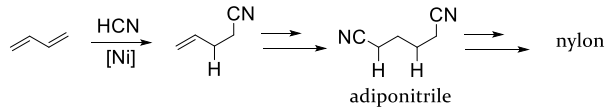

Hydrocyanation of butadiene using a Ni catalyst, DuPont

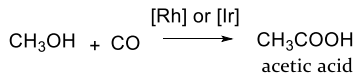

Carbonylation of methanol using a Rh catalyst, Monsanto Process, or an Ir catalyst, CATIVA Process by BP Ltd.

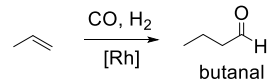

Hydroformylation of propene using a Rh catalyst, RuhrChemie/Rhone-Poulenc Process

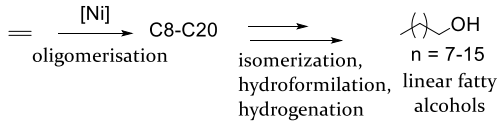

Production of linear alcohols from ethylene using a Ni catalyst, Shell Higher Olefin Process (SHOP)

Scheme 1.1. Examples of homogeneous catalysis-based industrial processes for the production of bulk chemicals.

However, to date, heterogeneous catalysts have been more widely used by industry. The main drawbacks associated with soluble transition metal catalysts are their intrinsic thermal instability and the difficulties in separating them from the products, which result in toxic metal contamination of the products and hamper the recovery and reuse of the often very expensive catalysts (Table 1.1).

Table 1.1. Properties associated to homogeneous and heterogeneous catalysts.

PROPERTY	HOMOGENEOUS	HETEROGENEOUS
Catalyst recovery	Difficult and expensive	Easy and cheap
Thermal stability	Poor	Good
Selectivity	Excellent/good-single active site	Good/poor-multiple active sites
Activity	Mild reaction conditions	Require harsh reaction conditions

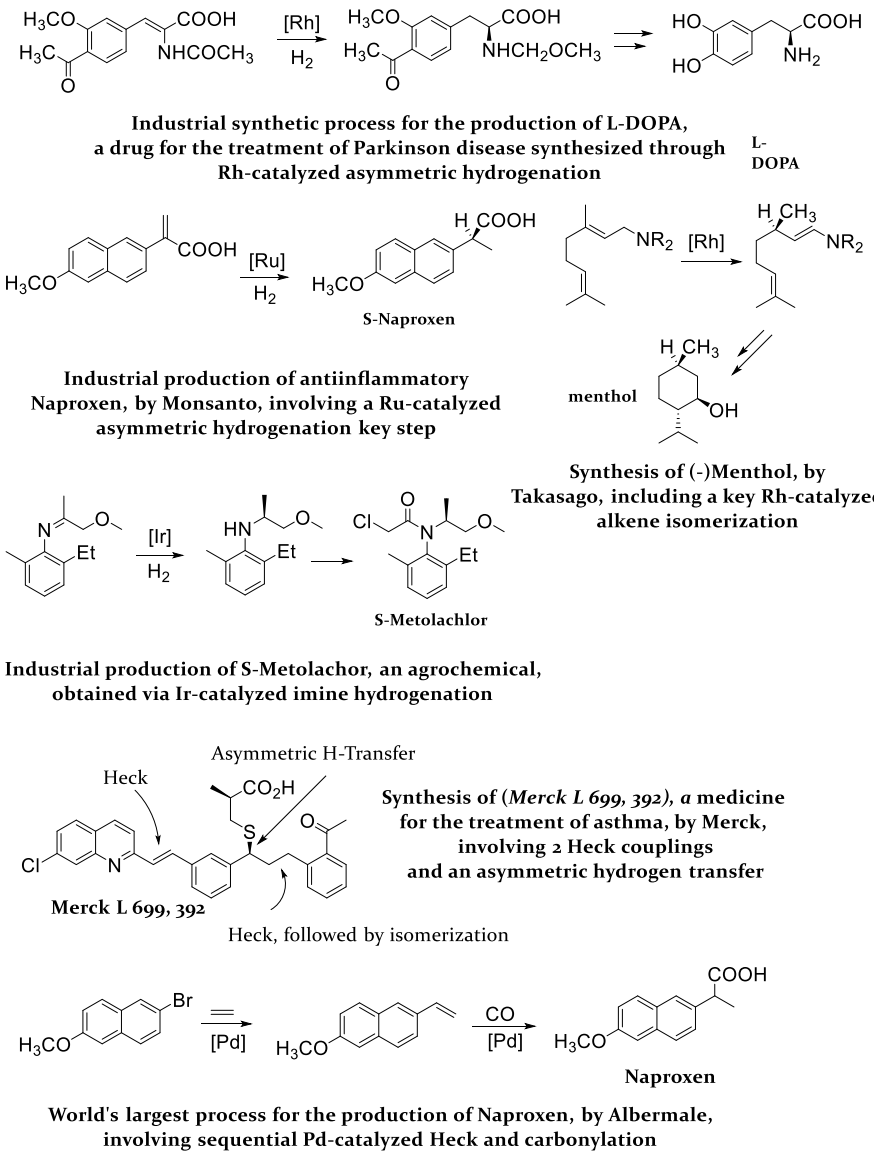

Scheme 1.2. Examples of industrially relevant fine chemicals produced through homogeneous catalysis.

The recognition of this inherent limitation of homogeneous catalysts has led to a flourishing activity attempting to device heterogenized versions with the aim of combining the advantages of homogeneous catalysts with the facility of heterogeneous systems to recover and reuse the catalyst.[8] Many very ingenious approaches are being studied in this regard which will be described in the next section.

1.2. Supported homogeneous catalysis and flow chemistry

During the last decade, continuous flow technology has attracted much interest in the production of fine chemicals because it provides a series of advantages compared with traditional batch-based protocols.[9] The literal definition of Flow Chemistry is operating a chemical process in a continuous manner. [10] However, this term is primarily associated with sectors where the traditional mode of operation is batch, such as specialty and fine chemicals or pharmaceutical manufacturing. Some of the most appealing features of flow methodologies are the improvement of mass and heat transfer, safety of operation (smaller volumes are involved, since the reaction takes place in confined microchannels), precise control over residence (reaction) time, isolation of sensitive reactions from air and moisture, ease of scale-up by applying scaling-up, numbering-up or scaling-out principles, and possibility to establish integrated processes, which are largely automated and involve less operation units. [11,12,13,14,15,16]

The continuous flow systems reported so far in the literature can be generally divided into four types, as suggested by Kobayashi and co-workers (Figure 1.2).[17] In type I, substrates (A and B) are passed through a column or hollow loop, inside which reactions occur. Unreacted A or B or any by-products are not separated. In type II, one of the substrates (B) is supported in a column. If an excess amount of B is used, one substrate (A) is consumed. However, once the supported B is consumed, the column must be changed. In type III, A reacts with B in the presence of a homogeneous catalyst. Although catalysis proceeds smoothly, the catalyst cannot be separated. In type IV, A reacts with B in the presence of a heterogeneous catalyst. If catalysis proceeds smoothly, no separation is required. The recent regulations of 'green sustainable chemistry' mean that synthesis with catalysts is preferable to synthesis without catalysts because of energy savings and waste reduction. Consequently, types III and IV are recommended in continuous-flow systems.

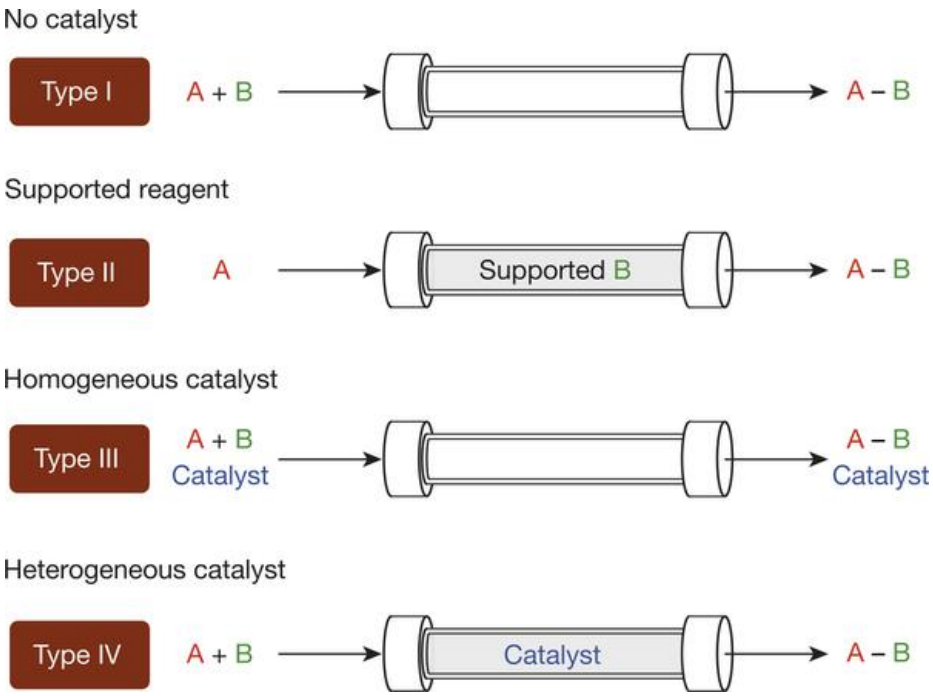

Figure 1.2. Types of continuous flow systems as suggested by Kobayashi.[15]

In type III, a homogeneous catalyst is employed; the catalyst flows through the reactor together with the reactants. Therefore, at the end, a separation step of the product from the catalyst (and possible by-products) is required. In type IV, the catalyst resides into the reactor, while the reagents passed by; in this case, an immobilization step of the catalyst onto a solid support is required, but, in principle, no separation of the product from the catalyst is needed; Therefore, type IV is regarded as the best method for continuous-flow synthesis.[18,14,19,20]

In direct relation with this growing interest in flow chemistry, the design of efficient catalysts which can be implemented in continuous microreactors has become a scientific challenge of economic and environmental relevance.[21,22]

1.3. Catalyst separation, recovery and recycling

1.3.1. Overview of the different approaches

Numerous approaches have been developed with the aim of recovering and reusing homogeneous catalysts and to warrant appropriate separation of the catalyst from the products.[23,24] Different criteria may be considered in order to classify the various approaches towards catalyst recovery and reuse. In scheme 1.3) recyclable catalysts are divided in two groups depending on whether catalyst and substrates are involved in a monophasic or a multiphasic reaction. Monophasic recyclable systems where the reaction takes place in a homogeneous phase may have benefits in terms of mass transfer and diffusion of reactants to the active catalyst sites.

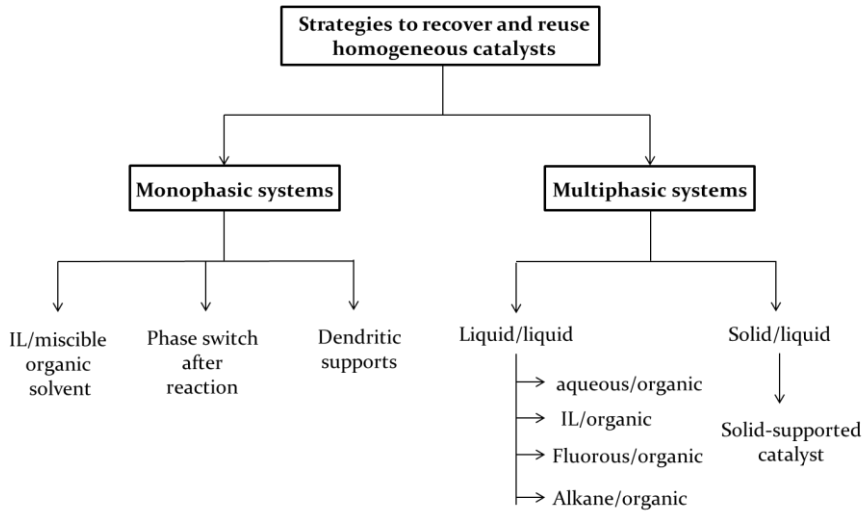

Scheme 1.3. Most important approaches reported for the recovery and reuse of homogeneous catalysts.

Various systems of this class can be identified. One case is the use of ionic liquids (IL) in combination with a miscible organic solvent, for example CH_2Cl_2. The reaction takes place in one phase containing the catalyst, the substrates and the products. Upon completion, the organic solvent is evaporated, and the products are extracted with a second solvent which does not dissolve the ionic liquid phase containing the catalyst, which may be reused in successive cycles.[25] In a similar manner,

the reaction can be performed in a single phase containing pure IL, and then extracting the products after the reaction with an immiscible organic solvent.[26] This approach is frequent for Ru catalysts for olefin metathesis.[27] A second case comprises the use of catalysts supported on materials which may switch from the reaction phase to a separate phase upon a stimulus such as heat, light, bubbling CO_2 or by changing the conditions (T, pH, solvent...).[28,29,30,31] Some of these types of catalysts involve phase-switchable polymeric supports, which form a second phase upon cooling of the reaction mixture, however they stand out as gels and recovery is sometimes troublesome.[32]

The use of supercritical fluids represents a promising strategy for catalyst recycling, although its elevated price limits its wider applicability.[33] Another type of recyclable systems operating under homogeneous reaction conditions are dendrimer-supported catalysts. They are based on the concept of size enlargement of a molecular catalyst without differentiation of its molecular and single-site properties with respect to the original smaller-size analogue. Compared with catalysts immobilized on hyperbranched solid polymers their main advantage is their homogeneity, in contrast to somewhat more unpredictable surface morphology of solid supported catalysts.[34] To date, the main limitation of this type of catalysts is the elevated cost of well-defined dendritic materials, and lack of "affordable" molecular filtration protocols, since the necessary set-ups are still expensive.

The other group of recyclable catalysts includes all the systems which are in a different phase to that containing the reactants and the products (Multiphasic systems in Scheme 1.3). This group has received comparatively more attention. Since the substrates are always in solution, when the catalyst is dissolved in an immiscible solvent these systems are called biphasic liquid/liquid and rely on solubility-tailored catalysts. Introduction of suitable functionality dictates the preferential solubility of the catalyst between two liquid phases, whereas reactants and products reside in the other phase, and catalysis takes place at the interphase (Scheme 1.4). Systems of this type are usually referred to as "biphasic catalysis". At the end of the reaction, the phase containing the products is removed and fresh reactants and reagents can be fed into the phase containing the catalyst.

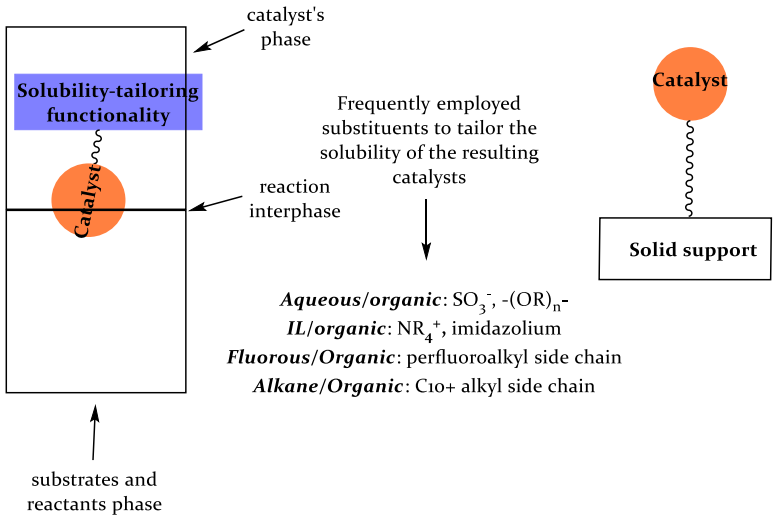

Scheme 1.4. Biphasic and solid-supported recyclable systems. Most common solubility-tailoring functionality.

Water soluble catalysts are usually prepared by introduction of a sulfonate group, or a polyether chain like in ethyleneglycol.[35,36] When immobilization of the catalyst in an IL is desired, ammonium or imidazolium-based tags are the most frequently used.[37,38] Perfluoroalkyl chains are useful to confer solubility in a fluorous solvent.[39] Long hydrophobic alkylic groups are chosen to solubilize the catalyst in an apolar phase, such as heptane.[40]

1.3.2. Methodologies for the immobilization of homogeneous catalysts onto solid supports

The attachment of homogeneous catalysts to the surface or to the inner structure of a solid support material is undoubtedly the dominant approach towards the design of so called "heterogenized catalysts".[6] A variety of strategies have been described to successfully immobilize molecular metal catalysts onto solid supports. The classification of the different strategies is usually based on the type of interaction between the catalyst and the support (Figure 1.3). Among them, the most common ones are convalent binding, electrostatic interaction, encapsulation and adsorption.

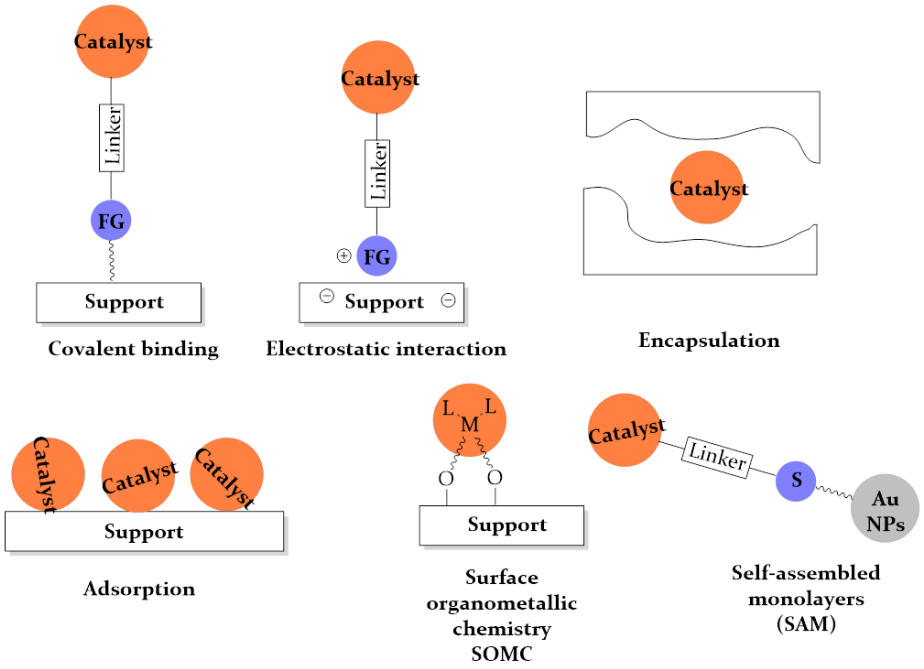

Figure 1.3. Main strategies for the immobilization of homogeneous catalysts onto solid supports.

Less common methods exist, as is the case of Surface Organometallic Chemistry (SOMC),[41] or interaction with gold NPs through a thiol group, forming self-assembled monolayers (SAM).[42] According to the strength of the linkage between the catalyst and the support, the covalent binding and electrostatic interactions represent the strongest types of interactions. When weaker interactions are used, the most relevant types are encapsulation and adsorption. Examples from the latter include catalysts attached to the surface of the support through either Van der Waals forces, hydrogen bonding and hydrophobic interactions. A very interesting type of recyclable systems arising from weak interactions with the support are Supported Liquid Phase Catalysts (SILP),[43,44] where a thin film of a liquid phase is physisorbed at the surface of the support (usually a thin film of water, or ionic liquid), and the catalyst is dissolved in this thin film. The actual aspect of the supported catalyst is solid, since very low amounts of the liquid film are usually introduced.

1.3.2.1. *Immobilization of homogeneous catalysts onto solid supports through covalent interactions*

The covalent binding of a metal complex onto a solid support implies the need of a chemical reaction to establish a covalent bond between one of the ligands in the complex and the support. Therefore, the ligand must be appropriately functionalized. Additional synthetic efforts are thus required to introduce such functionality, and care needs to be taken to avoid undesired interactions between the *pro*-immobilizable functional groups and the metal center. However, the enhanced stability provided by this binding usually makes the resulting heterogenized complexes more robust, and less prone to metal leaching compared to *softer* immobilization strategies.[8] This approach can be applied to almost any type of support material, since functional groups on the support can serve as anchoring points (Scheme 1.5).

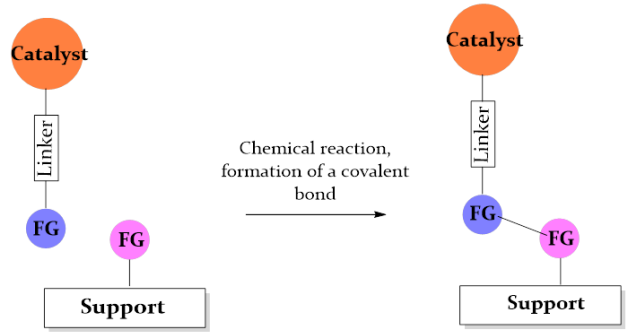

FG	FG	FG—FG	Type of support
$RSi(OR)_3$	OH	SiR–O–Support	Unfunctionalized inorganic oxide support
BnR–Br	RSH	RBn—SR—Support	Inorganic oxide support functionalized with thiol groups
ROH	CH_2Cl	$HO–CH_2–$Support	Merrifield resin
RCOOH	NH_2	R–C(=O)–N(H)—Support	PS-PEG polymers
ROH	C(=O)–Cl	HO–C(=O)–Support	Oxidized carbon nanotubes
$RSi(OR)_3$	OH	SiR–O–Support	silica-coated magnetic NPs (composite material)

Scheme 1.5. Illustration of various linkages created through covalent binding between differently functionalized catalysts and different types of supports.

Inorganic oxide supports (either amorphous such as silica gel or mesoporous crystalline such as MCM-41) can be directly functionalized with a catalyst through their available surface hydroxyl groups.[45] Alternatively, functional groups can be introduced onto the solid surface prior to catalyst immobilization. Amino-[46] and thiosilicas[47] bearing an alkyl linker between the functional group and the support are common examples of this type. Carbonaceous materials, such as carbon nanotubes, usually undergo oxidative treatment to generate hydroxyl or carboxylic groups which are subsequently used to generate ester, amide or ether linkages.[48] Other types of materials that offer the possibility of covalent functionalization are composite materials (such as silica coated maghemite NP's)[49], or membranes.[50]

The covalent binding has been extensively applied, and especially in the case of inorganic oxides and polymeric supports various synthetic alternatives have been described.[8] For the former type of supports, *grafting* methods, *sol-gel synthesis* or *solid-phase synthesis* have been described, resulting in different properties of the final materials. In the case of polymers, *grafted polymers, copolymers* or *self-supported catalysts* are among the alternatives to obtain heterogenized materials.

1.3.2.2. Immobilization of homogeneous catalysts onto solid supports through electrostatic interactions

In order to immobilize a catalyst onto a solid support through electrostatic interactions, the support and the catalyst must be electrically charged, but in contrast with covalent binding, no chemical reaction is required between the catalyst and the support. There are two possible ways to immobilize a catalyst onto a support via electrostatic interactions, depending on whether the neat charge is situated in one of the ligands or at the metal center.

To situate the charge on one of the ligands, appropriate (charged) functional groups need to be introduced. Most frequently, ammonium (NR_4^+) or sulphonate (RSO_3^-) groups are used. [51] Polymers and inorganic solids can be functionalized in such a way.[52] Morover, this option has been applied for the immobilization of catalysts onto layered solids, such as clays or Layered Double Hydroxides (LDH).[53] The former

supports have exchangeable cations and a negatively charged matrix, whereas the latter have a positively charged matrix and exchangeable hydroxide anions (Scheme 1.6).

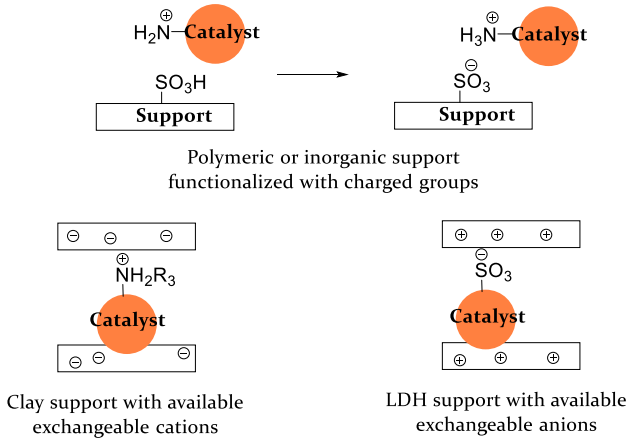

Scheme 1.6. Catalyst immobilization through electrostatic interactions between charges within the ligand and charges in the support.

Alternatively, the electrostatic interaction can be established between the support and the charged metal center in ionic complexes. [54] This strategy does not require the functionalization of one of the ligands with charged groups. Usually, inorganic supports containing exchangeable cations are used. A cation exchange takes place between the charged metal ion in the complex and a cation present in the support, usually Na, or H^+ (Scheme 1.7).

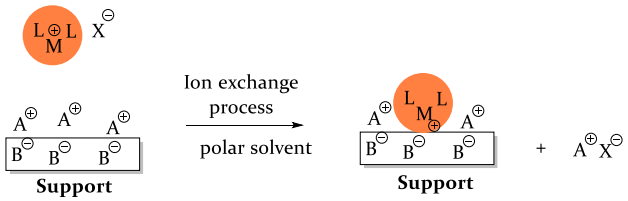

Scheme 1.7. Heterogenization of a metal complex through electrostatic interaction between the metal center and the support.

Typical catalysts that can be immobilized by this approach include Rh(I)(diphosphine), Mn(III)(salen) or Cu complexes with various types of ligands. This approach has provided good results in some cases,[55] however the biggest limitation of this method is that any change in the

oxidation state of the metal center during the course of the catalytic reaction may affect the electrostatic interaction resulting in leaching of the catalyst.[56]

In conclusion, the immobilization of catalysts through electrostatic interactions provides robust systems, although appropriate solvents must be selected to reinforce the interactions between the catalyst and the support and special attention must be paid to operate under reaction conditions where ion exchange cannot occur.

1.3.2.3. Immobilization of homogeneous catalysts onto solid supports through encapsulation

When a catalyst is immobilized onto a solid support through encapsulation, the catalyst molecules get occluded within the pores of the resulting solid and cannot diffuse out whereas reactants and reagents do not have any diffusion restriction in principle. The immobilization thus responds to a physical confinement and further interactions between the catalyst and the support are not required. Therefore, rigid supports with constant pore sizes are preferred over more flexible matrices in order to minimize metal leaching, if the pore and catalyst sizes are adequate. Two main strategies have been described to encapsulate homogeneous catalysts (Scheme 1.8). They consist on either building the catalyst inside the pores of the support, or alternatively building the support around a preformed catalyst. In principle, both strategies may lead to identical immobilized catalysts.

Building the support around the preformed metal complex is usually selected when the catalyst is too large in relation to the pore size of the support. For instance, metalloporphyrins or larger metallophthalocyanines which have been encapsulated within the supercages of zeolite Y.[57]

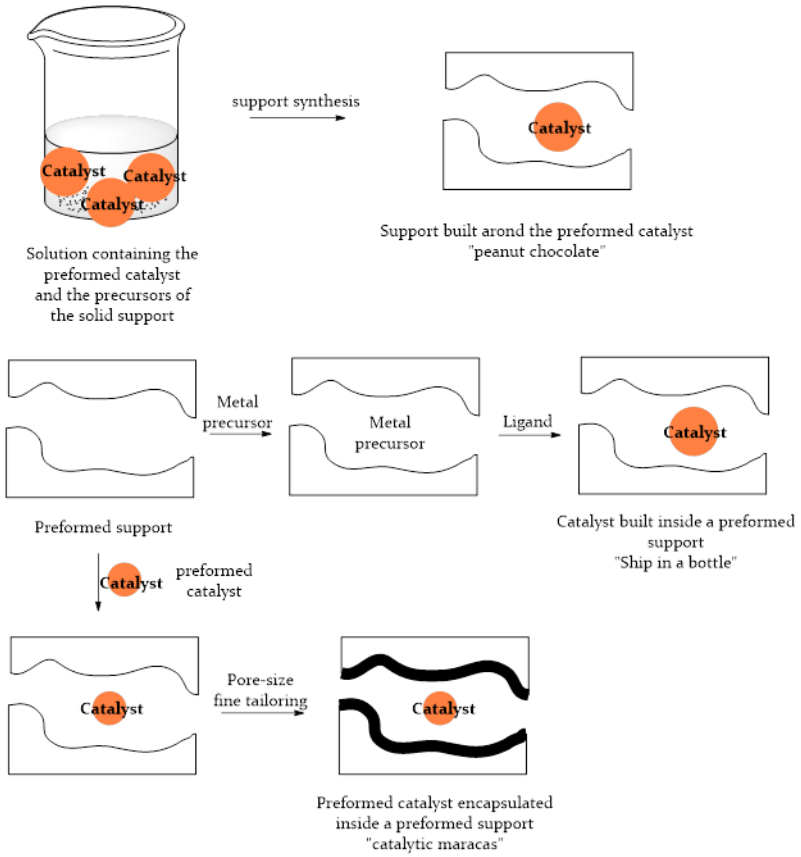

Scheme 1.8. Possible strategies for encapsulating homogeneous catalysts in the pore structure of a solid support.

Zeolites have also been used to encapsulate catalysts *via* the method called *"ship in a bottle"*. Usually, a metal cation is introduced first by ion exchange, and then the ligand is introduced, yielding the complex.[58,59]. Support materials with larger pore sizes can help to overcome diffusion limitations that are sometimes encountered with microporous materials. This is the case of Ordered Mesoporous Silicas (OMS) with supercage-like structures (mimicking the crystalline structure of zeolites). To prevent catalyst diffusion out of the nanocages of the material, the size of the entrance to these spaces is reduced by treating the material with a silylating agent.[60] Following this approach, the catalyst can be either built inside the support, or introduced as a preformed complex if the pore sizes are large enough compared to the size of the molecular catalyst. In the latter case, the presence of

uncomplexed metal that may act as competing catalytic species is avoided.

1.3.2.4. Immobilization of homogeneous catalysts onto solid supports through adsorption

Immobilizing homogeneous catalysts onto a solid by mere physisorption may be considered as the most straightforward strategy available, since in principle, neither catalyst nor support have to be modified. The main drawback associated to this strategy, however is the weak van der Waals forces associated to the physisorption phenomenon, so leaching of the catalyst into the solution is usually observed.[61] To overcome this problem, efficient catalyst adsorption must rely on stronger interactions, such as hydrogen bonding,[62] hydrophobic effect[63] or π-π stacking interactions.[64] Hydrogen bonding interactions can be established between a polar (or charged) functional group in one of the ligands and surface hydroxyl groups present on the support, such as sulfonate groups for instance.[65] In the case of cationic metal complexes, the counteranion can establish hydrogen bonds with the support.[66]

Hydrophobic interactions can also be used to attach the catalyst to a support. The most typical example of this strategy involves the use of hydrophobic silicas, obtained after trialkylsilylation of the surface hydroxyl groups.[67]

Other interactions that can be included among these type of relatively weak surface interactions are those occurring between polyaromatic systems and carbonaceous surfaces, namely π-π stacking interactions. For these interactions a direct relationship between aromatic ring size and strength of the interaction was demonstrated.[64] Using this method, very robust catalytic systems bearing pyrene moieties have been reported, with negligible metal leaching.[68] Their most important drawback is that during catalysis, factors such as the polarity of the solvent, or the reaction temperature must be well controlled to avoid metal leaching.[61]

1.3.2.5. Immobilization of homogeneous catalysts onto solid supports through the SLPC concept

An elegant application of adsorption interactions consists on the surface immobilization of a thin liquid film containing the dissolved metal complex onto the surface of a solid support. This concept is known as Supported Liquid Phase Catalysts (SLPC).[69] The most appealing features of this approach are that the catalyst remains in solution, thus acting as a genuine homogeneous species. The most frequently used support is silica, due to its availability, low price and large surface area. Polar liquid phases are used, taking advantage of the hydrophilic nature of silica. Supported Aqueous Phase Catalysts (SAPC) can be prepared by aqueous phase impregnation of the silica support.[69] Importantly for the success of this approach, the metal complex used must present a high solubility for the supported liquid phase. In the case of using an aqueous phase, complexes bearing sulfonated ligands have been reported.[42] The use of water has the intrinsic limitation of its relatively high volatility, causing the depletion of the liquid film during the course of the reaction.[70]

In order to overcome these limitations, ionic liquid films have been introduced. The corresponding materials are known as Supported Ionic Liquid Phase Catalysts (SILPC) (Figure 1.4). Furthermore, these solvents display advantageous properties, such as low volatility, low toxicity, and very good solubility of organic and inorganic compounds. As in the case of SAPC, high solubility of the catalyst within the IL phase is required, so usually solubility-tailoring tags, such as sulfonated,[41] or imidazolium-containing groups are used.[71] This approach has provided robust systems, which have been successfully applied under continuous flow conditions showing long-term stability.[67] The most important drawback of this approach is that even a low ionic liquid solubility in the liquid substrate/product mixture can be sufficient to remove the catalyst from the carrier over time. Another issue of concern is the possibility of physical removal of the thin immobilized catalyst layer by mechanical forces, for example by a convective liquid flow.

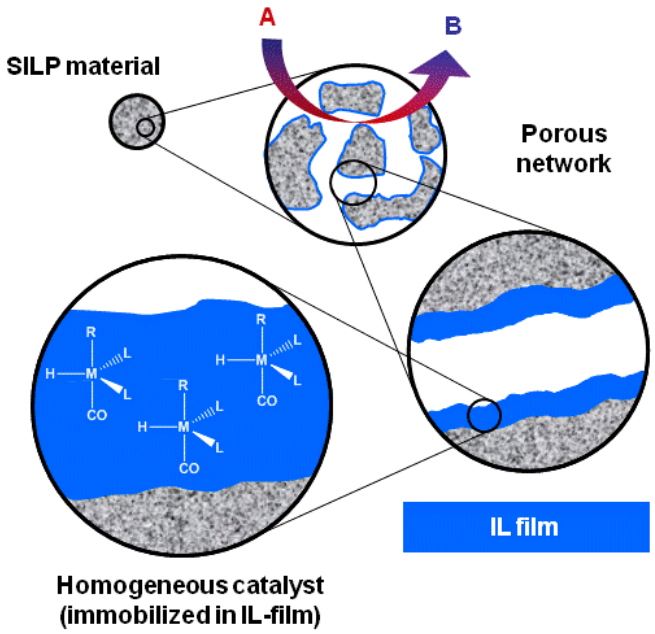

Figure 1.4. Schematic view of a supported ionic liquid phase catalyst [Ref. 44]

1.4. *N*-Heterocyclic Carbenes, versatile ligands in Transition Metal Catalysis

Carbenes are formally defined as neutral compounds containing a divalent carbon atom with a six electron valence shell (Figure 1.5)

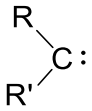

Figure 1.5. Schematic representation of a carbene

Their incomplete electron octet and coordinative unsaturation, however, render free carbenes inherently unstable and they have been traditionally considered only as highly reactive transient intermediates in organic transformations such as cyclopropanation. Despite attempted syntheses from as early as 1835,[72] the isolation and unambiguous characterization of free, uncoordinated carbenes remained elusive until pioneering studies in the late 1980s and early 1990s.[73]

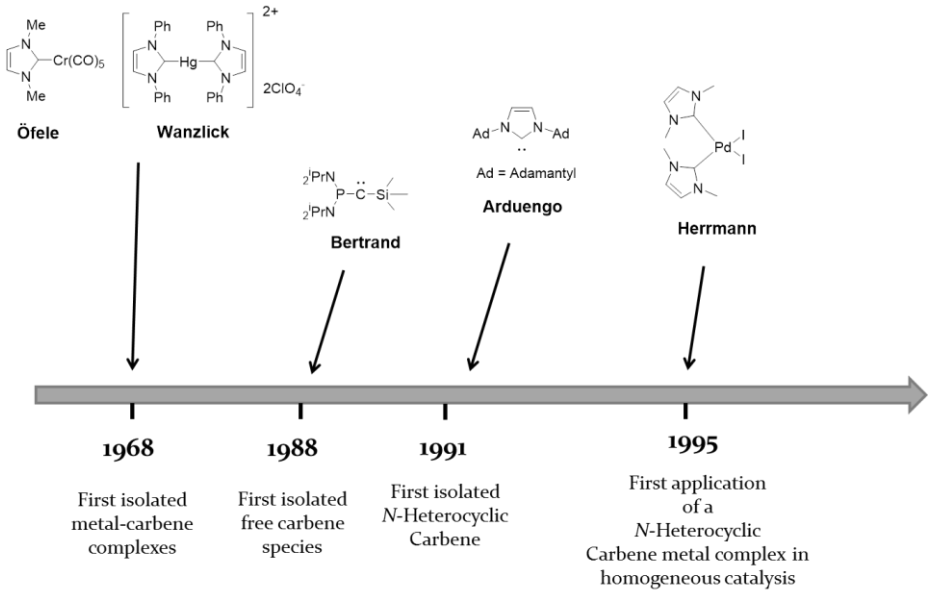

Scheme 1.9. Most important breakthroughs achieved in the development of carbene chemistry.

In a seminal publication in 1988, Bertrand and co-workers reported the preparation of the first isolable carbene stabilized by interactions with adjacent phosphorus and silicon substituents.[74] Three years later, Arduengo *et al.* isolated the first *N*-Heterocyclic Carbene.[75] With structural features inspired by earlier insightful studies by Wanzlick[76] and Öfele[77] on metal-carbene complexes, the remarkable stability and relatively simple synthesis of the first *N*-Heterocyclic Carbene (NHC) l,3-di(adamantyl)imidazol-2-ylidene (IAd, Scheme 1.9) led to an explosion of experimental and theoretical studies on novel NHCs.

1.4.1. Carbenes: electronic and steric considerations

When considering a prototype carbene, the divalent carbon atom can present either a bent or linear geometry, each geometry responding to a certain degree of hybridization of the carbonic carbon. The linear geometry implies an *sp*- hybridized carbene center with two nonbonding degenerate orbitals (p_x and p_y). Bending the molecule breaks this degeneracy, and the carbon atom adopts an sp^2-type hybridization: the p_y orbital remains almost unchanged (it is

usually called p_π) whilst the orbital that starts as pure p_x orbital is stabilized since it acquires some *s* character (it is therefore called σ). The linear geometry is an extreme case, and most carbenes are bent, and the frontier orbitals are systematically designed as σ and p_π (Scheme 1.10). Considering this scenario, four different electronic configurations can be envisioned regarding the lone pair of electrons on the carbene atom (Scheme 1.11). The two nonbonding electrons can be in two different orbitals with parallel spins (triplet state); hence, the molecule is correctly described by the configuration $\sigma^1 p_\pi^1$ ($^3B_1$ state).

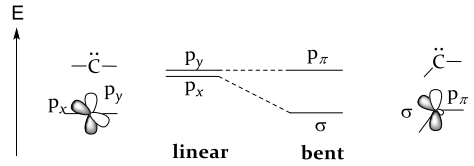

Scheme 1.10. Relationship between the carbene bond angle and the nature of the frontier orbitals.

In contrast, for singlet carbenes, the two nonbonding electrons can be paired in the same σ or p_π orbital. Therefore, there are two different $^1A_1$ states, the σ^2 being generally more stable than the p_π^2. Last, an excited singlet state with a $\sigma^1 p_\pi^1$ configuration can also be envisaged ($^1B_1$ state).

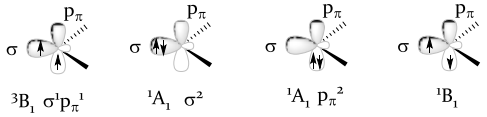

Scheme 1.11. Electronic configurations of carbenes.

The ground state spin multiplicity is a fundamental feature of carbenes that dictates their reactivity.[78] This multiplicity is determined by the relative energy of the σ and p_π orbitals, which will be greatly influenced by the steric and electronic profile of the carbene substituents.

1.4.1.1. Steric effects of the carbene substituents

Sterically demanding substituents stabilize kinetically all types of carbenes by preventing dimerization.[79] Moreover, when the influence of electronic effects is negligible, steric parameters may dictate the ground state spin multiplicity. Since the electronic

stabilization of the triplet relative to the singlet state is at a maximum when the carbene frontier orbitals are degenerate (Scheme 1.7) a linear geometry will favor the triplet state. Hence, increasing the steric bulk of the carbene substituents broadens the carbene angle and favors a triplet ground state configuration. Steric factors definitely play an important role in stabilizing carbene species, but electronic effects from the substituents of the carbene center usually have a larger impact on the reactivity and stability of the carbene.

1.4.1.2. Electronic effects of the carbene substituents

The role of the substituents of the carbene center is very important in the design of stable carbenes. The effects derived from the interaction between the orbitals of the carbene center and those in the substituents can be separated into *inductive* and *mesomeric* effects which refer to the interaction between σ-σ and π-π orbitals respectively. The presence of electropositive substituents such as lithium favors a triplet carbene, whereas electronegative substituents such as fluorine favor the singlet. On the basis of perturbation molecular orbitals, σ-electron withdrawing substituents inductively stabilize the σ-non bonding orbital of the carbene by increasing its s character, and leave the p_π unchanged (Scheme 1.12 a).

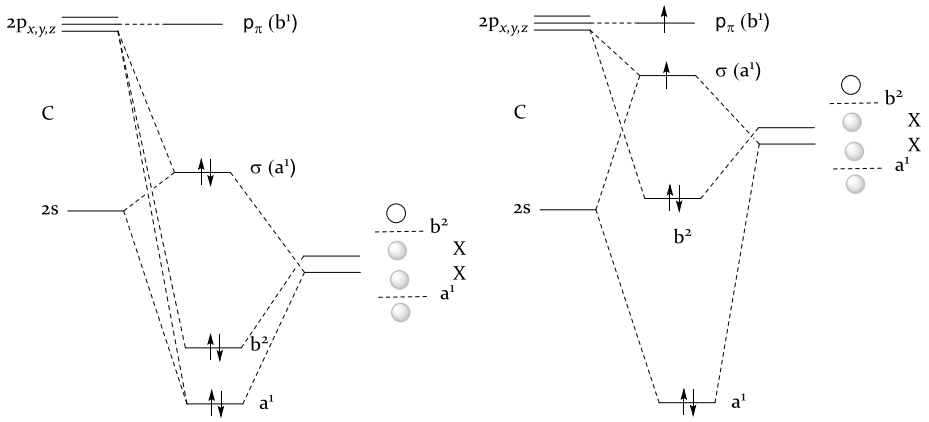

a) σ-electron withdrawing substituents

b) σ-electron donating substituents

Scheme 1.12. Inductive effect of the substituents on the relative energy of the frontier orbitals σ and pπ.

The σ-p_π gap thus increases, favoring the singlet state. In contrast, σ-donating substituents destabilize the σ-non bonding orbital, which increases in energy, and gets closer to the p_π orbital, so favoring the excitation to a triplet state (Scheme 1.9 b). Besides inductively modifying the energy of the carbene orbitals, substituents also display mesomeric effects. These type of electronic effects consist on the interaction of the carbene *s* and *p* orbitals with appropriate *p* or π orbitals of the two carbene substituents. In this regard, the substituents of the carbene can be classified into π-electron withdrawing, and π-electron donating, denoted as X and Z respectively. X-type substituents include –F, -Cl, -Br, -I, -NR_2, -PR_2, -OR, -SR, -SR_3..., whereas –COR, -CN, -CF_3, -BR_2, -SiR_3^+, PR_3^+ belong to the Z-type. A combination of X,X substitution results in a destabilization of the LUMO p_π orbital, which increases its energy, whereas the σ orbital remains unchanged (Scheme 1.13 a).

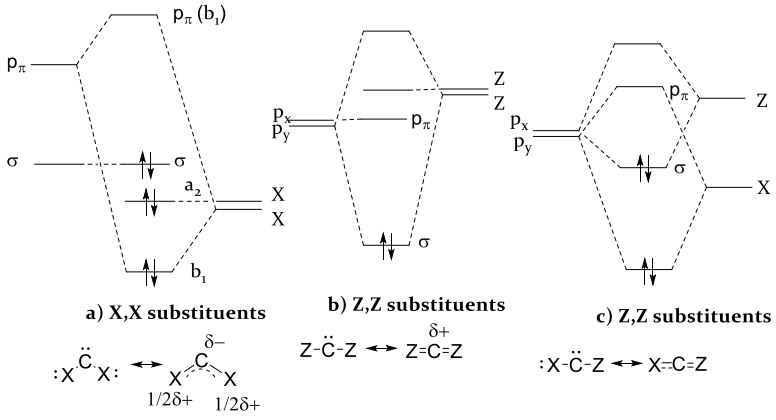

Scheme 1.13. Stabilization of a carbene center through mesomeric effects from the substituents.

Carbenes of this type are predicted to have a bent geometry, since the HOMO σ orbital containing a lone pair of electrons is not involved in any interaction and thus an sp^2-like hybridization is the most energetically favored. The carbene possesses a partial negative charge. In Z,Z carbenes, the p_x orbital gets stabilized as it releases some electron density through combination with an empty orbital on the substituent, and therefore it reduces its energy, whereas the energy of the unoccupied p_y is not modified. These types of carbenes are linear, in

accordance to an *sp*-like hybridization of the carbon orbitals. The carbene center has a partial positive charge (Scheme 1.13 b). Lastly, in carbenes combining X,Z substitution, both of the previous effects apply, that is, the vacant p_y orbital interacts with the X substituent, and increases its energy; the filled p_x orbital releases some electron density into an empty orbital of the Z substituent, and therefore decreases its energy. A linear geometry is also characteristic of these type of carbenes, in consequence of a *sp* hybridization of the carbene (Scheme 1.13 c).

In all of the three cases depicted a singlet ground state configuration is favored. Compared to triplet carbenes, singlet carbenes are more easily stabilized by electronic effects through the design of a suitable substitution pattern. The three most important types of stable singlet carbenes are diaminocarbenes, diborylcarbenes and phosphinosilyl and phosphinophosphoniocarbenes, which correspond to (X,X), (Z,Z) and (X,Z) substitution on the carbene center as explained in Scheme 1.13.

1.4.2. *N*-Heterocyclic Carbenes

1.4.2.1. Stabilizing factors and modularity

Among the group of aminocarbenes, *N*-Heterocyclic Carbenes (NHC's) undoubtedly stand out as the most illustrious members.[80,79] NHC's are defined as heterocyclic species containing a carbene carbon and at least one nitrogen atom within the ring structure.[81] Their persistent carbene character due to efficient stabilization combined with their strong nucleophilic character has enabled a wide range of applications, including homogeneous transition metal catalysis,[82] organometallic materials,[83] metallopharmaceuticals,[84] coordination to surfaces,[85] and organocatalysis[86] to cite some of the most remarkable. An explanation to their success may count on their high σ-donor character, stability, the facility to tune steric and electronic properties, and their accessibility through many well established synthetic routes.[87] Usually, NHC's generally feature bulky substituents adjacent to the carbene carbon, which help to kinetically stabilize the species by sterically disfavoring dimerization to the corresponding olefin (Wanzlick equilibrium).[88] The electronic stabilization, however, provided by the nitrogen atoms is a much more important factor. NHC's exhibit a singlet ground state electronic

configuration, with the HOMO and LUMO frontier orbitals best described as a formally sp^2 hybridized lone pair and an unoccupied p orbital on the C^2 carbon.

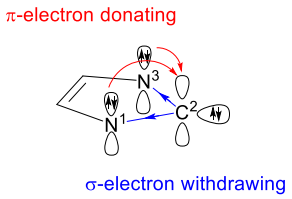

Scheme 1.14. Representation of the *push,push* mesomeric-*pull,pull* inductive effect by the N substituents at NHC's.

The cyclic structure also favors this type of hybridization by forcing a rather small carbene angle compared to acyclic variants. The adjacent N atoms electronically stabilize the structure by means of a combined *push, push* mesomeric-*pull,pull* inductive effect (Scheme 1.14). The inductive effect of the more electronegative N atoms, withdraw electron density from the HOMO σ, lowering its energy, and mesomeric donation to the empty p orbital results in a very efficient stabilization of the carbene lone pair of electrons. The great π-donor ability of adjacent amino groups plays a very important role through mesomeric stabilization. This fact was illustrated when comparing the stability of bis(dimethylamino) carbene with that of dimethoxycarbene. The first can be observed by NMR at room temperature,[89] whereas the latter has only been characterized in matrices at low temperature, and has an estimated lifetime in solution at room temperature of 2 ms.[90] Experimental data collected from studies on a series of NHC's as well as acyclic diaminocarbenes[91] revealed that the N-C-N angles typically range from 100-110°, in accordance with the values expected for singlet carbenes. The C-N bond distances varied from 1,32-1,37 Å, slightly less than in the cationic iminium precursors, thus pointing out a partial multiple bond character. This was further confirmed by rather large energies of rotation (13-21 Kcal/mol) around the C-N bond observed for acyclic diaminocarbenes. Moreover, NHC's derived from heteroaromatic compounds benefit from a greater degree of stabilization by virtue of their partial aromaticity. This effect, which has been calculated to be around 25 Kcal·mol^{-1} for model imidazole-2-ylidenes,[92] allows for a lesser demand of proximal steric bulk.

An appealing feature of NHC ligands is the possibility to tune their steric and electronic properties by changing different parts of the ligand structure (Figure 1.6).

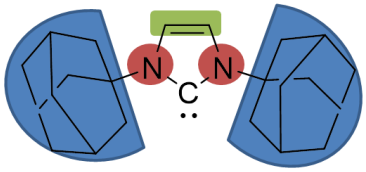

Fine tuning of the NHC properties:

- Electronic effects: type of heterocycle (ring size, number of heteroatoms (1, 2, 3, 4), type of heteroatoms (O, S...); introduction of substituents at the NHC backbone; N substituents.
- Steric effects: ring size, N substituents

Figure 1.6. Versatility in the variation of the steric and electronic parameters of the NHC ligands.

The electronic parameters can be modified by introducing changes within the cyclic core structure,[93] such as varying the number and identity of heteroatoms present, or the location of the carbene center within the ring. Introduction of electron withdrawing substituents at the C4-C5 positions has been shown to greatly influence the properties of the NHC ligands by reducing their electron density.[94]

The steric demand of the NHC ligand can be modulated by changing the substituents on the N wingtips, and also by varying the ring size.

1.4.2.2. [M(NHC)]: steric and electronic considerations

The carbene metal complexes are divided into two types, according to the nature of the formal metal-carbon bond, namely Fischer and Schrock metal carbene complexes (Scheme 1.15).[95,96] Fischer type carbenes involve a singlet carbene interacting with a low valent late transition metal. The most extreme case for this situation is when the metal complex contains π-acceptor ligands, such as CO, and the carbene has π-donor substituents, such as NR_2 and OR. Fischer carbenes are predominantly L-type σ donors *via* the lone pair, but the empty *p* orbital on carbon is also a weak acceptor for π back donation from the M(d_π) orbitals.

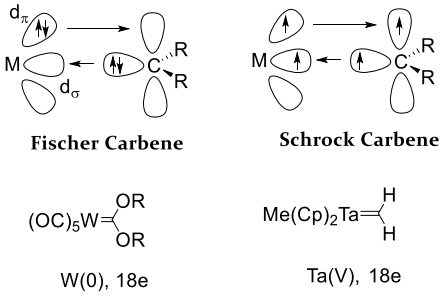

Scheme 1.15. Representation of Fischer and Schrock type metal carbene complexes.

This said, late transition metals are more electronegative than early transition metals, this means that they have more stable M(d_π) orbitals. Moreover, the presence of π-acceptor ligands further stabilizes the M(d_π) levels. This situation leads to an electrophilic (δ+) carbene carbon because direct C→M donation is only partially compensated by M→C back donation.

On the contrary, Schrock type carbenes involve the interaction between a triplet carbene and an early transition metal in high oxidation state, where the metal complex does not contain any π-acceptor ligands and the carbene substituents are not π-donor. Two covalent bonds are formed between the triplet carbene and the metal fragment having two unpaired electrons.

For the case of electropositive early transition metals, without π-acceptor ligands, the M(d_π) orbitals are less stable, and electron loss is easier, thus resulting in the polarization of the M-C bonds since C is more electronegative. Therefore, Schrock carbenes act as X_2 ligands, and the carbene carbon is nucleophilic (δ-) as for bis-alkyl carbenes. Each type represents a different formulation of the bonding of the CR_2 group to the metal, and real cases probably fall somewhere between the two.

The suitability of NHCs as ligands for transition metals can be rationalized by their inherent σ-donor ability with a formal sp^2 hybridized lone pair available for donation into a σ accepting orbital of the transition metal. Due to their singlet ground state configuration and the presence of two π-donor substituents at the carbene center, *N*-Heterocyclic Carbene complexes may be classified at a first glance as

Fischer-type compounds. However, NHC's bind to transition metals predominantly through σ donation, whereas in the most cases π back bonding from the metal is almost negligible.[97] These characteristic binding properties are easily understandable since the energy of the vacant p_π orbital at the carbene center is considerably increased by the strong π donation from the adjacent N atoms (Scheme 1.13, a). This argument is supported by the experimentally observed potential for rotation around the metal-C^2 bond. Therefore, metal-C^2 coordination is drawn as a single rather than as a double bond with π contributions restricted to delocalization within the NHC ring (Figure 1.7).

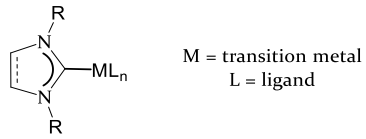

Figure 1.7. Representation of the coordination of a NHC ligand to a transition metal.

The strong σ donor and comparatively weak π acceptor properties of NHC's bear similarities to the coordination characteristics of phosphines and they were initially considered as mimics for the latter in transition metal coordination chemistry.[98] There are however, a number of differences between the two classes of ligands. NHC's such as those based on imidazole-2-ylidene and imidazolin-2-ylidene tend to be more donor than even the most Lewis basic phosphines according to their lower measured Tolman Electronic Parameters (TEP) and CO stretching frequencies (Table 1.2). The most widely used method to evaluate the donor properties of NHC's has been to measure the CO stretching frequencies of carbonyl metal complexes by IR spectroscopy. The more electron-donating the ligand of interest the more electron-rich the metal centre becomes, increasing the degree of π-backbonding into the carbonyl ligands and thus reducing their bond order and infrared stretching frequency. This provides a direct probe for the donor properties of the ligand, since a linear correlation between the average CO stretching frequency, υ_{av}(CO), and TEP has been established by Crabtree and coworkers.[99] The stronger electron donating properties of NHC relative to phosphines leads to thermodynamically stronger metal-ligand bonds which is reflected in greater bond dissociation energies

and shorter metal-ligand bond lengths in comparison with their phosphines counterparts. In consequence, this stronger metal-ligand interaction renders NHC-metal coordination less labile than metal-phosphine binding and the complexes are more thermally stable.[100]

Table 1.2. Comparison of CO stretching frequencies between NHC and PR_3 ligands in $[L_2RhClCO]$ complexes.

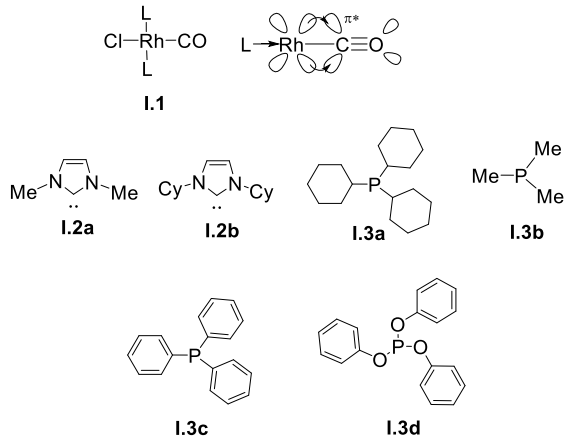

Ligand	I.2a	I.2b	I.3a	I.3b	I.3c	I.3d
υ_{CO} (cm^{-1})	1924	1929	1939	1957	1983	2018

A comparison of the steric properties of NHC's and phosphines also reveals significant differences. Whereas the sp^3-hybridization of phosphines results in a cone-shaped spatial arrangement of the steric bulk, most classes of NHCs, including the most commonly employed imidazole-derived types can best be described as fan- or umbrella-shaped with the nitrogen-substituents adjacent to the carbene carbon oriented more towards the metal. The steric properties of NHCs can be conveniently quantified using the 'buried volume' parameter *(% V_{bur})* developed by Nolan, Cavallo and co-workers (Figure 1.8).[101]

The *%Vbur* value of an NHC refers to the percentage of a sphere occupied or 'buried' by the ligand upon coordination to a metal at the centre of the sphere. Fixed parameters of 2 Å for the metal-carbene bond distance *d* and 3 A or 3.5 A for the sphere radius rare typically used with a larger *% V_{bur}* value signifying a greater steric influence of the ligand on the metal centre. The buried volume can be determined from

crystallographic data or from theoretical calculations with the free NHC, various NHC-metal complexes or the azolium salt precursor being suitable data sources. The derived % V_{bur} values, however, may vary greatly depending on the system used and care must be taken to compare only values determined using the same approach.

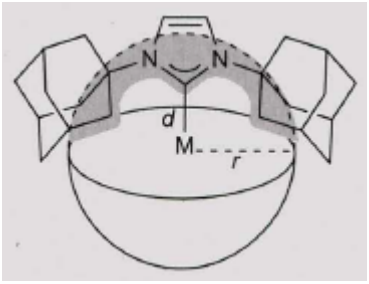

Figure 1.8. Quantification of the steric demand of metal ligated NHC through the measurement of the % buried volume. [Ref. 79]

1.4.2.3. Strategies for the metalation of N-Heterocyclic Carbenes

At least eight different strategies have been reported for the synthesis of [M(NHC)] complexes (Scheme 1.16), all of them starting from an azolium salt, with the exception of *viii)*.

i) The first method shown in Scheme 1.16 involves inserting the metal into an electron-rich olefin (enetetramine). Enetetramines are obtained by treatment of the azolium salt with a base under conditions analogous to those leading to a free NHC. Lower steric hinderance favors the formation of the enetetramine through dimerization of the free NHC.[102] Lappert is responsible for most of these studies, hence this process is usually referred to as the "Lappert method".[103]

ii) The proton abstraction method involves deprotonating the C2 carbon with a base. Herrmann was the first to report this type of protocol, by using liquid ammonia in combination with a stoichiometric amount of NaH at -40°C.[104] Other bases, such as $KN(Si(CH_3)_3)_2$ have also been reported to promote proton abstraction.[96]

iii) In 1998 Wang and Lin reported a new method for making M-NHC complexes that involved making a silver NHC complex and then transmetallating it to gold and palladium.[105]

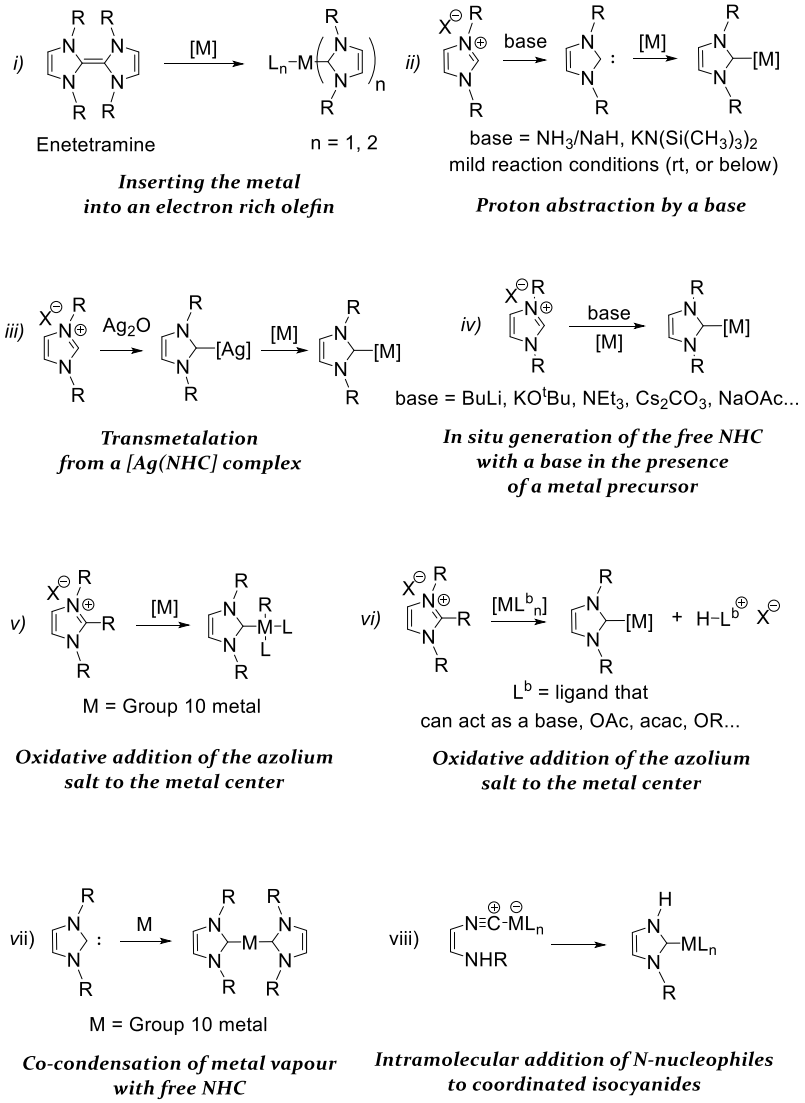

Scheme 1.16. Synthetic strategies for the synthesis of [M(NHC)] complexes.

This method takes advantage of the the straightforward formation of [Ag(NHC)] complexes which are usually very labile in solution, and efficiently transmetalate the NHC fragment to other metal center. This method was later applied to a wide variety of transition metals.[106]

iv) Arguably the most popular way to synthesize [M(NHC)] complexes involves generating the NHC in situ with bases such as NaH, *n*BuLi, or *t*BuOK followed by addition (or in the presence) of the metal precursor in a one-pot synthesis. Elimination of synthesis and isolation of the NHC is a clear advantage because the NHC is often air/moisture-sensitive. This process can also be achieved in the presence of milder bases, such as NaOAc,[107] Cs_2CO_3,[108] or Et_3N[94] among others. Some authors point out that the free carbene may not always be generated through this methodology, but a base assisted C-H activation may occur generating a carbene species that ultimately will coordinate to the metal precursor.[109]

v) The oxidative addition method was first reported in 1974,[110] yet was only rediscovered by Cavell in 2001.[111] The metal effectively activates a C2-R bond on the azolium salt precursor (R = H, halogen, alkyl). This method predominantly occurs with group 10 metals.

vi) The in situ generation of the free NHC-complexation can be achieved in the absence of an external base by using a metal precursor having a lingand that can actually act as the base, such as acetate[112], acetylacetonate[113] or alkoxy groups.[114]

vii) A more unusual method consists on the co-condensation of group 10 metal vapor with imidazol-2-ylidenes. Two-coordinate homoleptic metal carbene complexes have been obtained in this manner,[115] however this route is limited by the experimental conditions.

viii) Finally, an alternative route has been reported that involves the intramolecular addition of a N-nucleophile to coordinated isocyanides.[116]

In this context, taking into account the interest in the immobilization of homogeneous catalysts as well as the possibilities offered by *N*-Heterocyclic Carbene ligands in transition metal catalysis, the research developed in this Thesis focuses on the objectives described in the following Chapter 2.

1.5. References

[1] P.W.N.M. Van Leeuwen, *Homogeneous Catalysis: Understanding the art*, Kluwer, Dordrecht, **2004**.
[2] A. Behr, A.J. Vorholt, T. Seidensticker, *Chem. BioEng. Rev.* **2015**, *2*, 6.
[3] A. Corma, *Cat. Rev.* **2004**, *46*, 369.
[4] J. Clark, *The Contact Process*, **2002**.
[5] M. Appl, "Ammonia", , *Ullmann's Encyclopedia of Industrial Chemistry,* **2005** *Weinheim: Wiley-VCH*
[6] L.A. Oro, E. Sola, *Fundamentos y aplicaciones de la Catálisis Homogénea,* Prensas Universitarias de Zaragoza, Zaragoza, **2000**.
[7] B. Cornils and W.A. Herrmann, *Applied homogeneous catalysis with organometallic compounds*, Wiley-VCH, Wienheim, **1996**.
[8] *Heterogenized homogeneous catalysts for fine chemical production*, Catalysis by Metal Complexes. **2010**, Eds. P. Barbaro, F. Liguori, Springer.
[9] R. Porta, M. Benaglia, A. Puglissi, *Org. Process Res. Dev.*, **2016**, *20*, 2.
[10] D.M. Roberge, *Chimica Oggi*, **2015**, *33*, 4.
[11] P. T. Anastasas, M. M. Kirchhoff, *Acc. Chem. Res.*, **2002**, *35*, 686.
[12] C. Wiles, P. Watts, *Green Chem.*, **2012**, *14*, 38.
[13] T. Noel, S. L. Buchwald, *Chem. Soc. Rev.*, **2011**, 40, 5010.
[14] C. G. Frost, L. Mutton, *Green Chemistry*, **2010**, *12*, 1687.
[15] D. Webb, T. F. Jamison, *Chem. Sci.*, **2010**, *1*, 675.
[16] A. Cukalovic, J.-C. M. R. M. Monbaliu, C. V. Stevens, *Top. Heterocycl. Chem.*, **2010**, *23*, 161.
[17] T. Tsugobo, H. Oyamada, S. Kobayashi, *Nature*, **2015**, *520*, 329.
[18] A. Kirschning, W. Solodenko, K. Mennecke, *Chemistry*, **2006**, *12*, 5972.
[19] T. Tsugobo, T. Ishiwata, S. Kobayashi, *Angew. Chem. Int. Ed.* **2013**, 6590.
[20] C. Battilocchio, J.M. Hawkins, S.W.A. Ley, *Org. Lett.* **2013**, *15*, 2278.
[21] G. S. Newman and K. Jensen, F., *Green Chemistry*, **2013**, *15*, 1456.
[22] L. Vaccaro, D. Lanari, A. Marrocchi and G. Strappaveccia, *Green Chemistry*, **2014**, *16*, 3680.
[23] *Catalyst separation, recovery and recycling; chemistry and process design,* **2006**, Eds. D.J. Cole-Hamilton, R.P. Tooze, Springer, Dordrecht.
[24] Ed. M. Benaglia, *Recoverable and reciclable catalysts*, **2009**, Wiley-Blackwell, Chichester.
[25] H. Clavier, N. Audic, J.-C. Guillemin, M. Mauduit, *J. Organomet. Chem.,* **2005**, *690*, 3585.
[26] S. Lee, J. Y. Shin, S.-G. Lee, *Chem. Asian. J.*, **2013**, *8(9)*, 1990.
[27] C.P. Ferraz, B. Autenrieth, W. Frey, M.R. Buchmeiser, *ChemCatChem*, **2014**, *6*, 191.
[28] X.L. Zheng, J.Y. Jiang, X.Z. Liu, Z.L. Jin, *Catal. Today*, **1998**, *44*, 175.
[29] A. Andreetta, G. Barberis, G. Gregorio, *Chim. Ind.*, **1978**, *60*, 887.
[30] A. Andreetta, G. Gregorio, *Can. Patent*, **1978**, 1023729.
[31] S.L. Desset, D.J. Cole-Hamilton, *Angew. Chem. Int. Ed.*, **2009**, *48*, 1472.
[32] C. Hobbs, Y.-C. Yang, J. Ling, S. Nicola, H.-L. Su, H.S. Bazzi, D.E. Bergbreiter, *Org. Lett.*, **2011**, *13*, 3904.

[33] U. Hintermair, G. Franciò, W. Leitner, *Chem. Commun*., **2011**, *47*, 3691.
[34] Z.J. Zheng, J. Chen, Y.-S. Li, *J. Organomet. Chem.*, **2004**, *689*, 3040.
[35] H. Díaz Velazquez, F. Verpoort, *Chem. Soc. Rev.* **2012**, *41*, 7032.
[36] F. Godoy, C. Segarra, M. Poyatos, E. Peris, *Organometallics* **2011**, *30*, 684.
[37] S.-W. Chen, J.H. Kim, K.Y. Ryu, W.-W. Lee, J. Hong, S.-G. Lee, *Tetrahedron*, **2009**, *65*, 3397.
[38] K. Skowerski, C,. Bierzvicka, G. Szczepaniak, L. Gulaiski, M. Bieniek, K. Grela, *Green Chem.*, **2012**, *14*, 3264.
[39] L. Wan, H. Yu, C. Cai, *J. Fluor. Chem.* **2012**, *140*, 107.
[40] Y. F. Yang, N. Priyadarshani, T. Khamatnurova, J. Suriboot, D. E. Bergbreiter, *J. Am. Chem. Soc.* **2012**, *134*, 14714.
[41] J.R. Severn, J.C. Chadwick, R. Duchateau, N. Friedrichs, *Chem. Rev.*, **2005**, *105*, 4073.
[42] K. Marubayashi, S. Takizawa, T. Kawakusu, T. Arai, H. Sasai, *Org. Lett*. **2003**, 5, 4409.
[43] J.P. Arhancet, M.E. Davis, J.S. Merola, B.E. Hanson, *Nature*, **1989**, *339*, 454.
[44] A. Riisager, R. Fehrmann, S. Flicker, R. van Hal, M. Haumann, P. Wasserscheid, *Angew. Chem. Int. Ed.* **2005**, *44*, 815.
[45] A. Corma, H. García, *Adv. Synth. Catal*., **2006**, *348*, 1391.
[46] H. Hagiwara, K. Hyeok Ko, T. Hoshi, T, Suzuki, *Synlett*, **2008**, *4*, 0611.
[47] M. Al-Hashimi, A. Qazi, A.C. Sullivan, J.R.H. Wilson, *J. Mol. Catal. A Chem.*, **2007**, *278*, 160.
[48] D. Tasis, N. Tagmatarchis, A. Bianco, M. Prato, *Chem. Rev*. **2006,** *106*, 1105.
[49] P.D. Stevens, G. Li, J. Fan, M. Yen, Y. Gao, *Chem. Commun*., **2005**, 4435.
[50] I.F.J. Vankelecom, *Chem. Rev.*, **2002**, *102*, 3779.
[51] Y. Arakawa, N. Haraguchi, S. Itsuno, *Tetrahedron Lett*. **2006**, *47*, 3229.
[52] F. Rajabi, D. Schaffner, S. Follmann, C. Wilhelm, S. Ernst, W.R. Thiel, *ChemCatChem*, **2015**, *7*, 3513.
[53] L. Barloy, P. Battioni, D. Mansuy, *J. Chem. Soc. Chem. Commun.*, **1990**, 1365.
[54] J.M. Fraile, J.I. García, J.A. Mayoral, *Chem.Rev.*, **2009**, *109*, 360.
[55] W.P. Hems, P. McMorn, S. Riddel, S. Watson, F.E. Hancock, G.J. Hutchings, *Org. Biomol. Chem.*, **2005**, *3*, 1547.
[56] C. Simons, U. Hanefeld, I.W.C.E. Arends, R.A. Sheldon, T MaschMeyer, *Chem. A. Eur. J.* **2004**, *10*, 5829.
[57] B.Z. Zhan, X.Y. Li, *Chem.Commun.* **1998**, 349.
[58] W. Kahlen, A. Janssen, W.F. Holderich, *Stud. Surf. Sci.Cata.*, *108*, 469.
[59] A. Zsigmond, K. Bogar, F. Notheisz, *Catal. Lett.*, **2006**, *83*, 55.
[60] Q.H. Yang, D.F. Han, H.Q. Yang, C. Li, *Chem. Asian. J.*, **2008**, 3, 1214.
[61] M. Inoue, K. Ohta, N. Ishizuka, S. Enomoto, *Chem. Pharm. Bull.*, **1983**, *31*, 3371.
[62] P. Gamez, F. Fache, M. Lemaire, *Bull. Soc.. Chim. Fr.*, **1994**, 131, 600.
[63] N. Ishizuka, M. Togashi, M. Inoue, S. Enomoto, *Chem. Pharm.Bull.*, **1987**, *35*, 1686.
[64] S. Latil, M. Heggie, J. Charlier, F. Tournus, *Phys. Rev.* **2005**, *72*, 075431.
[65] P. Barbaro, C. Bianchini, V. Dal Santo, A. Meli, S. Moneti, R. Psaro, A. Scaffidi, L. Sordelli, F. Vizza, *J. Am. Chem. Soc.*, **2006**, *128*, 7065.
[66] F.M. de Rege, D.K. Morita, K.C. Ott, W. Tumas, R.D. Broene, *Chem. Commun.*, **2000**, 1797.

[67] P. Handa, K. Holmberg, M. Sauthier, Y. Castanet, A. Mortreux, *Micropor. Mesopor. Mater.*, **2008**, *116*, 424.
[68] S. Sabater, J.A. Mata, E. Peris, *ACS Catal.*, **2014**, *4*, 2038.
[69] S. Minakata, M. Komatsu, *Chem. Rev.*, **2009**, *109*, 711.
[70] F.Y. Zhao, S.I. Fujita, M. Arai, *Curr. Org. Chem.*, **2006**, *10*, 1681.
[71] S. Doherty, P. Goodrich, C. Hardacre, V. Parvulescu, C. Paun, *Adv. Synth. Catal.*, **2008**, *350*, 295.
[72] J.B. Dumas, E. Peligot, *Ann. Chim. Phys.***1835**, *58*, 5.
[73] J.A.III. Arduengo, R. Krafczyk, *Chem. Unserer Zeit*, **1998**, *32*, 6.
[74] A. Igau, H. Grutzmacher, A. Baceiredo, G. Bertrand, *J. Am. Chem. Soc.* **1988,** *110*, 6463.
[75] A.J.III. Arduengo, R.L. Harlow, M.A. Kline, *J. Am.Chem. Soc.* **1991**, *113*, 361.
[76] H.-W. Wanzlick, H.-J. Schönherr, Angew. *Chem. Int. Ed. Engl.*, **1968**, *7*, 141.
[77] K. Öfele, *J. Organomet. Chem.*, **1968**, *12*, 42.
[78] G.B. Schuster, *Adv. Phys. Org. Chem.* **1986**, *22*, 311.
[79] M.N. Hopkinson, C. Richter, M. Schedler, F. Glorius, *Nature*, **2010**, *510*, 485.
[80] D.J. Nelson, S.P. Nolan, *N-Heterocyclic Carbenes* in N-Heterocyclic Carbenes, **2014**. Ed. S.P. Nolan, 1.
[81] P. de Frémont, N. Marion, S.P. Nolan, *Coord. Chem. Rev.*, **2009**, *253*, 862.
[82] S. Díez-González, N. Marion, S.P. Nolan, *Chem. Rev.*, **2009**, *109*, 3612.
[83] L. Mercs, M. Albrecht, *Chem. Soc. Rev.*, **2010**, *39*, 1903.
[84] K.M. Hindi, M.J. Panzner, C.A. Tessier, C.L. Cannon, *Chem. Rev.*, **2009**, *109*, 3859.
[85] P. Lara, O. Rivada-Wheelaghan, S. Conejero, R. Poteau, K. Philippot, B. Chaudret, *Angew. Chem. Int. Ed.* **2011,** *50*, 12080.
[86] D. Enders, O. Niemeier, A. Henseler, *Chem. Rev.* **2007**, *107*, 5606.
[87] L. Benhamou, E. Chardon, G. Lavigne, S. Bellemin-Laponnaz, V. César, *Chem. Rev.* **2011**, *111*, 2705.
[88] H.W. Wanzlick, E. Shikora, *Angew. Chem., Int. Ed.* **1960**, *72*, 494.
[89] R.W. Alder, M.E. Blake, *J. Chem. Soc., Chem. Commun.* **1997**,1513.
[90] R.A. Moss, M. Wlotowski, S. Shen, K. Krogh-Jespersen, A. Matro, *J. Am. Chem. Soc.* **1988**, *110*, 4443.
[91] D. Bourissou, O. Guerret, F.P.Gabbaï, G. Bertrand, *Chem. Rev.* **2000,** *100,* 39.
[92] C. Heinmann, T. Müller, Y. Apeloig, H. Schwarz, *J. Am. Chem.. Soc.* **1996**, *118*, 2023.
[93] T. Dröge, F. Glorius, *Angew. Chem. Int. Ed*. **2010**, *49*, 6940.
[94] M. Viciano, E. Mas-Marzá, M. Sanaú, E. Peris, *Organometallics*, **2006**, *25*, 3063.
[95] *Principles and Applications of Organotransition Metal Chemistry,* **1987**.; eds. J.P. Collman, L.S. Hegedus, J.R. Norton, R.G. Finke, University Science Books: Mill Valley,
[96] *The Organometallic Chemistry of the Transition Metals*, 5th ed., R.H. Crabtree, Wiley, **2009**.
[97] J.C. Green, R.G. Scurr, P.L. Arnold, F.G.N. Cloke, J. *Chem.Soc., Chem. Commun.* **1997**, 1963.
[98] R.H. Crabtree, *J. Organomet. Chem.*, **2005**, *690*, 5451.

[99] A. R. Chianese, X. Li, M. C. Janzen, J. W. Faller and R. H. Crabtree, *Organometallics*, **2003**, *22*, 1663.
[100] C.M. Crudden, D.P. Allen, *Coord. Chem. Rev.*, **2004**, *248*, 2247.
[101] A.C. Hillier, J.W. Sommer, S.B. Yong, J.L. Petersen, L. Cavallo, S.P. Nolan, *Organometallics*, **2003**, *22*, 4322.
[102] *New chiral di-N-Heterocyclic Carbene Ligands and their application in Enantioselective Hydrogenation, Hydroformilation, and 1,4-conjugate addition reactions. A study towards rational development of di-N-Heterocyclic Carbene Complexes in Enantioselective Catalysis*, M.S. Jeletic, PhD Thesis manuscript, University of Florida, **2010**.
[103] M.F. Lappert, *J. Organomet. Chem.* **1988**, *358*, 185.
[104] W.A. Herrmann, M. Elison, J. Fischer, C. Kocher, G.R.J. Artus, *Chem-Eur J* **1996**, *2*, 772.
[105] H.M.J. Wang, I.J.B. Lin, *Organometallics* **1998**, *17*, 972.
[106] I.J.B. Lin, C.S. Vasam, *Coord. Chem. Rev.* **2007**, *251*, 642.
[107] W.-L. Duan, M. Shi, G.-B. Rong, *Chem. Commun.*, **2003**, 2916.
[108] A. Pontes da Costa, M. Viciano, M. Sanaú, S. Merino, J. Tejeda, E. Peris, B. Royo, *Organometallics*, **2008**, *27*, 1305.
[109] K.F. Donnely, A. Petronilho, M. Albrecht, *Chem. Commun.*, **2013**, *49*, 1145.
[110] P.J. Fraser, W.R. Roper, F.G.A. Stone, *J. Chem. Soc., Dalton Trans.* **1974**, 760.
[111] D.S. McGuinness, K.J. Cavell, B.F. Yates, *Chem. Commun.* **2001**, 355.
[112] I. Peñafiel, I.M. Pastor, M. Yus, M.A. Esteruelas, M. Oliván, E. Oñate, *Eur. J. Org. Chem.*, **2011**, *35*, 7174.
[113] N. Marion, P. de Frémont, I.M. Puijk, E.C. Ecarnot, D. Amoroso, A, Bell, S.P. Nolan, *Adv. Synth. Catal*. **2007**, *349*, 2380.
[114] I. Peñafiel, I.M. Pastor, M. Yus, M.A. Esteruelas, M. Oliván, *Organometallics*, **2012**, *31*, 6154.
[115] P.L. Arnold, F.G.N. Cloke, T. Geldbach, P.B. Hitchcock, *Organometallics* **1999**, *18*, 3228.
[116] C.Y. Liu, D.Y. Chen, G.H. Lee, S.M. Peng, S.T. Liu, *Organometallics*, **1996**, *15*, 1055., and references therein.

UNIVERSITAT ROVIRA I VIRGILI
HETEROGENIZED N-HETEROCYCLIC CARBENE METAL COMPLEXES FOR SELECTIVE CATALYSIS
Alberto Martínez Lombardía

Chapter 2

"General objectives"

UNIVERSITAT ROVIRA I VIRGILI
HETEROGENIZED N-HETEROCYCLIC CARBENE METAL COMPLEXES FOR SELECTIVE CATALYSIS
Alberto Martínez Lombardía

General objectives

The general objective of this PhD work deals with the design, synthesis and catalytic application of NHC-based organometallic complexes heterogenized onto solid supports. The recycling and application of these materials under flow conditions are also included in this general objective.

The specific objectives of thes thesis are classified by chapters and can be summarized as follows:

- **CHAPTER 3**:
  - The synthesis and characterization of well-defined [Pd(NHC)]-based complexes incorporating functional groups for their subsequent immobilization onto inorganic solids.
  - The synthesis and characterization of inorganic oxide solid-supported catalysts.
- **CHAPTER 4**:
  - The evaluation of the catalytic performance of the immobilized catalysts described in Chapter 3 in C-C cross-coupling reactions, namely Suzuki-Miyaura, Heck and Sonogashira reactions.
  - The study of the recycling and reuse of these catalytic materials under batch conditions.
  - The evaluation of the most efficient catalysts under flow conditions.
- **CHAPTER 5**:
  - The evaluation of the catalytic performance of the immobilized catalysts described in Chapter 3 in hydrogenation and transfer hydrogenation of alkynes and alkynols.
  - The study of the recycling and reuse of these catalyst materials under batch conditions.
  - The evaluation of the most efficient catalysts under flow conditions.

- **CHAPTER 6**:
  - The synthesis and characterization of chiral Rh complexes bearing bis(triazolylidene) ligands functionalized with pyrene moieties.
  - The immobilization of these species onto CNT's and the characterization of the resulting materials.
  - The evaluation of these complexes as catalysts in reduction processes.

UNIVERSITAT ROVIRA I VIRGILI
HETEROGENIZED N-HETEROCYCLIC CARBENE METAL COMPLEXES FOR SELECTIVE CATALYSIS
Alberto Martínez Lombardía

UNIVERSITAT ROVIRA I VIRGILI
HETEROGENIZED N-HETEROCYCLIC CARBENE METAL COMPLEXES FOR SELECTIVE CATALYSIS
Alberto Martínez Lombardía

Chapter 3

"Covalent immobilization of [Pd(NHC)] complexes onto inorganic solid supports. Synthesis and characterization."

UNIVERSITAT ROVIRA I VIRGILI
HETEROGENIZED N-HETEROCYCLIC CARBENE METAL COMPLEXES FOR SELECTIVE CATALYSIS
Alberto Martínez Lombardía

> Covalent immobilization of [Pd(NHC)] complexes onto inorganic solid supports. Synthesis and characterization

3.1. Introduction

As previously commented in Chapter 1, the covalent attachment of a homogeneous catalyst onto a support requires the introduction of a functional group able to establish a covalent bond with the surface of the support, thus adding complexity to the synthesis of the ligand. Furthermore, the introduction of such functional groups in the structure of the ligand may have some effect on the original steric and electronic properties of the ligand and/or on the stability of the resulting catalyst. Nevertheless, covalent anchoring has been the most widely used method to date, since the robustness of this binding should make the supported catalyst able to withstand rather harsh reaction conditions, and minimize metal leaching.

3.1.1. Heterogenization of organometallic catalysts onto inorganic supports

A variety of inorganic supports have been used for the immobilization of homogeneous catalysts.[1] These solid supports must have a large particle size and must be mechanically stable to be recovered and reused by means of filtration or centrifugation. Moreover, they must have a large surface area and sufficiently large mean pore size in order to grant good accessibility of the reagents and products to active sites and leave the solid with ease. It is also important to have a regular distribution of anchoring points.

3.1.1.1. Silica and other inorganic oxide supports

When it comes to inorganic supports, many materials can be envisioned for the attachment of organometallic catalysts.[2] The most common are metal oxide supports such as silicates,[3] including the huge families of zeolites[4] and clays,[5] and carbonaceous supports,[6] namely activated carbon, carbon nanotubes,[7] graphenes[8] or fullerenes.[9] Alternative supports have also been reported such as metal nanoparticles. In particular, magnetic metal NPs are attractive since catalyst separation can be easily performed by applying an external magnetic field.[10] Finally, among the group of composite materials that are supports combining two different materials attached to each other, silica coated magnetic nanoparticles or heteropolyanions supported on

silica constitute remarkable examples of this class.[11] To date, without any doubt, silica materials have been the most widely used inorganic supports.[12,13,14,15] A wide array of materials with different structures, particle sizes, morphologies and textural properties have been described and characterized under the generic SiO_2 formula. Among the different types of silicas, amorphous silica gel offers some advantageous properties such as chemical, thermal and mechanical stability, good accessibility, defined narrow distribution of pore size and developed surface area. In this case, the presence of silanol groups provides immobilization sites and organic groups can be robustly anchored to the surface (Scheme 3.1).[16,17,18,19] These Si-OH groups confer hydrophilicity and a slight acidity to this surface. However, this hydrophilic character can be modulated by capping the surface with silanes bearing hydrophobic chains, the most commonly used being trimethylsilane (Scheme 3.1). Besides the extensive use of amorphous silica gel, other alternatives among silica materials offer interesting features. This is the case of mesostructured crystalline silicas or periodic mesoporous organosilicas (PMO). In contrast to amorphous silica they show long-range order in the mesoporous systems but not short-range order. Therefore, a more regular distribution of immobilization sites is expected. Moreover, their pore size can be tailored according to the preparation conditions.

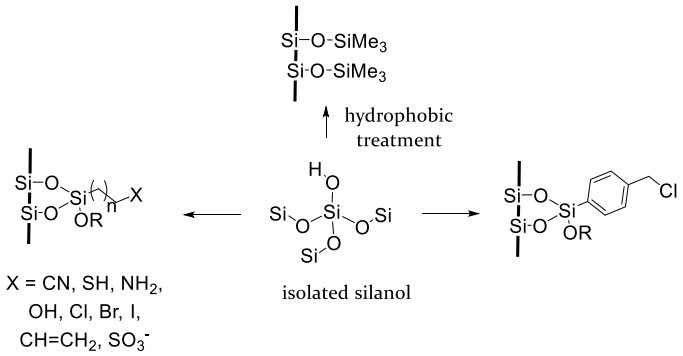

Scheme 3.1. Functionalization of surface silanol groups in silica materials.

Among the various types (MCM, SBA, MCF or MSU), MCM-41[20] and SBA-15[21] have been widely used. In the case of MCM-41, it has a *honeycomb*-like pore structure consisting in an hexagonal arrangement of 1D pores (Figure 3.1). This type of inorganic material usually presents

a higher surface area compared to amorphous silica gel, around 1000 m^2/g, and a uniform distribution of pore size, which can be tailored in the 1,5 to 20 nm range. The group of PMO is a class of hybrid organic-inorganic materials, obtained by hydrolysis-condensation of an organic molecule (usually the ligand) and an inorganic monomer such as tetraethylorthosilicate (TEOS) in the presence of a template. This type of materials present a more regular distribution of the organic molecules over the solid structure (Figure 3.1). In complementary fashion to the silica materials, other metal oxide supports can provide distinct properties to the supported catalysts.[22]

MCM-41

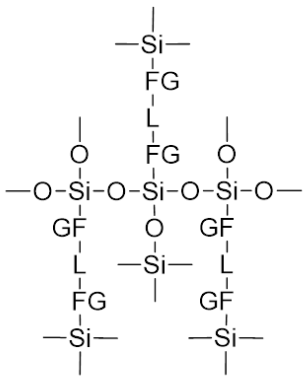

Periodic mesoporous organosilica (PMO)
L = ligand
FG = Functional group

Figure 3.1. Structure of MCM-41 and PMO ordered silica materials.

Alumina materials represent another class of well-studied supports which have been applied for anchoring organometallic catalysts.[23] They comprise all the forms of aluminum oxide (Al_2O_3). Like silica materials, aluminas can be amorphous such as alumina gel or activated alumina or can present a crystalline structure as in gibbsite, boehmite and corundum.[5] Finally, other metal oxides have also been used as supports for metal complexes, NPs or other inorganic species. This is the case of MgO, ZnO, ZrO_2, B_2O_3, or TiO_2. Titania is a crystalline solid, for which three different structures are known: ilmenite, rutile and anatase. Compared with the above described supports, titanium oxide is a

microporous solid, having a much smaller surface area and pore size. However, it has been successfully applied as support for heterogeneous catalysts,[24] and also for organometallic complexes.[25]

In all these inorganic oxide supports the presence of isolated hydroxyl groups on the surface serves as anchoring points for the immobilization of catalysts *via* covalent bonding.

3.1.1.2. Strategies to establish a support-ligand covalent interaction

To anchor an organometallic catalyst onto a solid support through a covalent bond with one of the ligands in the coordination sphere of the complex, several possibilities can be foreseen (Scheme 3.2). The catalyst can be attached to the preformed solid support, which is known as *grafting*. This is quite a simple protocol to carry out; the catalyst must provide an appropriate functional group able to establish a covalent bond with the support.[2] Usually, immobilization is achieved by suspending the solid support in an organic solvent, adding the catalyst and heating this mixture for a few hours.[26] Alternatively, immobilization of the catalyst onto the support can be done by *sol-gel synthesis*. In this way the catalyst and a suitable support precursor such as TEOS are hydrolyzed and condensed, in the presence or not of a structure directing agent known as template, which is removed at a later stage of the synthesis by calcination. Compared to grafting methods, materials prepared using this method present a more uniform distribution of the catalytic entities throughout the solid structure. On the other side the preparation of supported catalysts by sol-gel synthesis is more complex.[13] Moreover, the length of spacer, the density of catalytic units, the physical properties of the final hybrid materials or the synthetic process itself can have an influence on the catalytic results and therefore need to be controlled and optimized. Finally, two additional approaches can be followed: a preformed organometallic catalyst can be immobilized onto the support, or the support can be functionalized first with a ligand and subsequently can be treated with a metal precursor under suitable reaction conditions to coordinate the metal center to the immobilized ligand. This metalation step must be carefully controlled by either choosing the right metal precursor or protecting the free silanol groups in order to avoid the

coordination of the metal to the support, creating non-selective catalytic sites.[27]

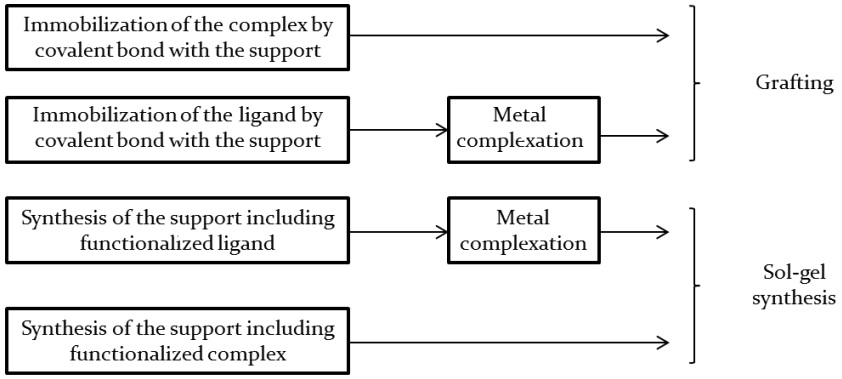

Scheme 3.2. Strategies for the covalent immobilization of organometallics catalysts onto inorganic solid supports.

Grafting a preformed complex reduces the possibility of formation of non-selective catalytic sites due to uncomplexed metal ions or metal oxide clusters. Moreover, this immobilization route allows full characterization of the complex prior to grafting, allowing a better control.

3.1.2. Synthetic strategies reported for the covalent attachment of NHC-based catalysts onto inorganic oxide supports

The success of *N*-heterocyclic carbenes (NHCs) such as the imidazol-2-ylidenes IMes[28,29,30,31] and IPr[32,33,34,35] (and their ring-saturated counterparts) and other sterically demanding architectures[36,37,38,39] as ligands in a wide variety of metal-catalyzed processes has spurred the exploration and development of new solid-supported NHC-bound metal complexes.[40,41] Irrespective of the approach followed for the incorporation of the NHC-based catalysts on the inorganic oxide support, the functionalization of the NHC salt precursor with trialkoxysilyl groups constitutes the most straightforward and efficient manner to establish a covalent bond by condensation with suitable functional groups present on the support (Scheme 3.3).[42] The number of [M(NHC)] catalysts immobilized onto inorganic solid supports through

covalent binding will be classified in two subgroups. A first group will include those catalysts where the NHC presents at least one N-alkyl wingtip substituent. The second group, will involve those NHC-based catalysts bearing the more bulky N,N'-diaryl substitution profile.

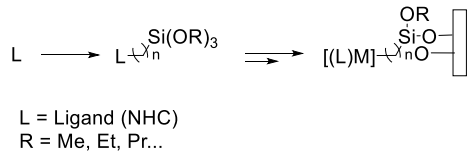

Scheme 3.3. Functionalization of the ligand with trialkoxysilyl groups for their subsequent immobilization on metal oxide supports.

3.1.2.1. Solid-supported [Pd(N- alkylimidazolylidenes)]

The majority of work on solid-supported NHC-based catalysts has focused on *N*-alkylimidazolylidene NHCs due to their straightforward synthesis, involving an S_N^2 substitution reaction between an *N*-aryl or alkyl-substituted imidazole and a straight-chain haloalkyl-containing tether moiety such as an alkoxysilane (Scheme 3.4).[38,43,44,45,46,47,27,48,49]

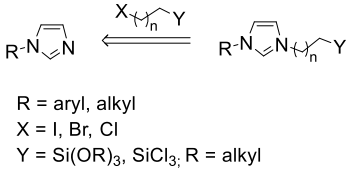

Scheme 3.4. Introduction of a trialkoxysilyl containing alkyl chain into one of the NHC N-wingtips.

Pleixats et al. reported on the preparation of two different [Pd(NHC)]-containing PMO catalytic materials by sol-gel synthesis (Scheme 3.5).[48] In the first step N-mesitylimidazole was converted into 1-mesityl-3-(3-triethoxysilyl)propyl imidazolium chloride. This compound was then metalated by using two different Pd precursors. Finally, a hydrolysis-condensation process using TEOS and NH_4F afforded the solid supported [Pd(NHC)] materials. This synthesis exemplifies the solid-support immobilization of a preformed [Pd(NHC)] complex by sol-gel synthesis.

Covalent immobilization of [Pd(NHC)] complexes onto inorganic solid supports. Synthesis and characterization

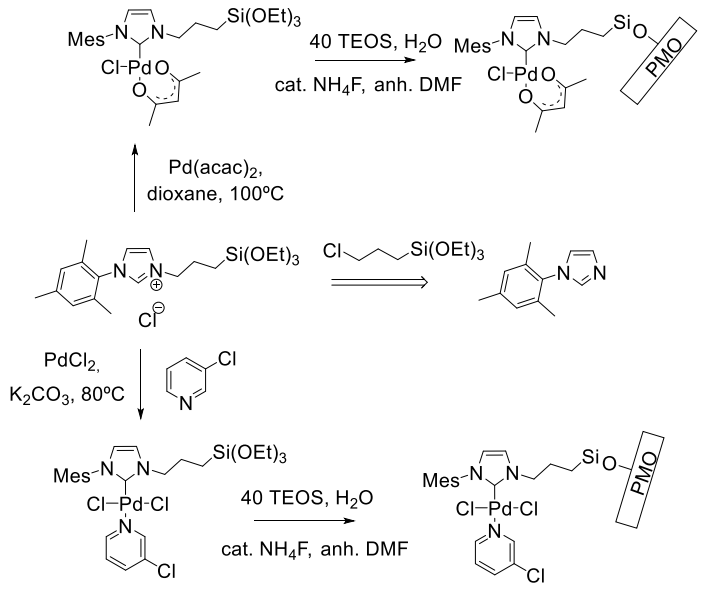

Scheme 3.5. Preparation of [Pd(NHC)]-containing PMO by sol-gel synthesis.

Alternatively, [Pd(NHC)] complexes can be attached onto the surface of the support by grafting methods. Again, the success of this approach relies on the functionalization of the NHC salt precursor with a linker containing a trialkoxysilyl group.

Scheme 3.6 a) and Scheme 3.6 b) provide two examples of the covalent attachment of the ligand onto the surface of the support by a condensation reaction with the surface silanol groups. [50,51] Then, this functional material is washed to remove any unreacted salt, and dried, and the content of the grafted imidazolium salts in the solid can be calculated by means of elemental analysis or even by determining the weight gain.Then this solid is usually suspended in an organic solvent and treated with a suitable metal precursor, such as $Pd(OAc)_2$; In all the examples displayed in Scheme 3.6, a substoichiometric amount of Pd was added in order to favor the formation of [Pd(bis(NHC))] species. A drawback of the immobilization-metalation sequence, is the difficulty in confirming the coordination around the metal center. In this regard, Tyrrell et al. have compared the catalytic profile of materials prepared via these two different methodologies (Scheme 3.6 c)).[47]

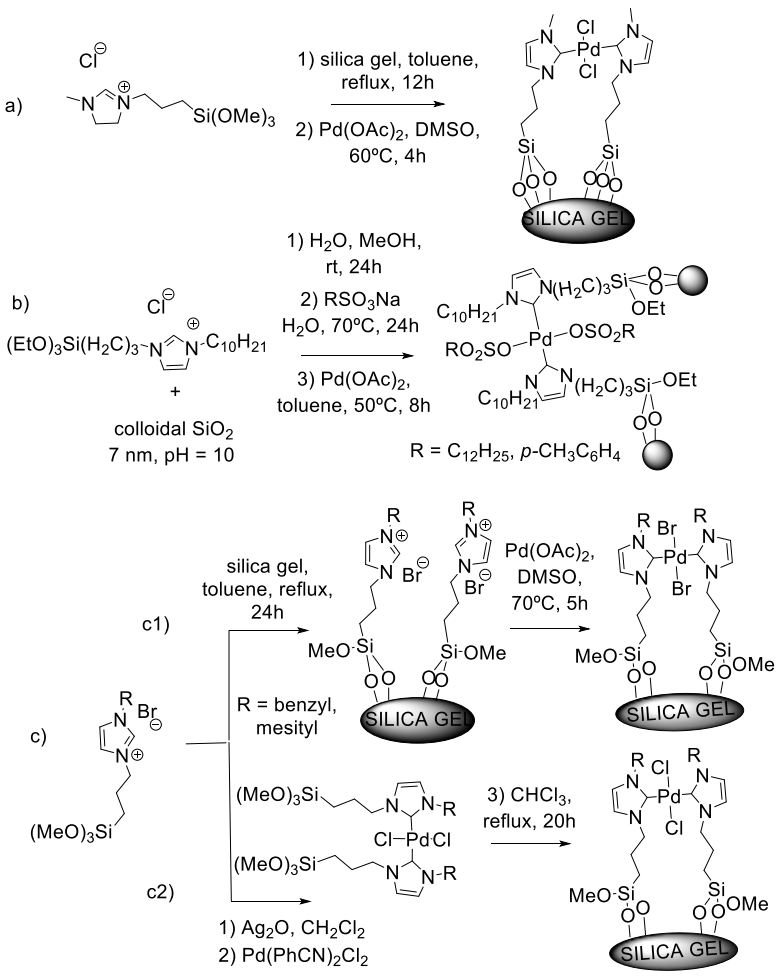

Scheme 3.6. Covalent immobilization of [Pd(NHC)] complexes onto silica supports by grafting methods; a), b) and c1) correspond to an immobilization of the ligand onto the support followed by metalation sequence; c2) immobilization of a preformed metal complex.

In this study the authors found that the catalysts prepared by immobilization of a preformed Pd complex were more active than the catalysts prepared by complexation of supported imidazolium salts. Interestingly, they also found that the catalytic activity increased with the steric bulk around the C2 (carbene donor atom), and N-2,6-diisopropylphenyl substitution on the imidazole wingtips provided the most active catalysts, a trend that is also observed in homogeneous systems.[52]The reported immobilization of [Pd(N-alkylimidazolylidene)] complexes, while yielding many successful catalytic systems, inherently

limits the steric bulk of the resulting NHC ligand in the vicinity of its imidazol-2-ylidene C2 (carbene) donor atom, a property which has proven very important for instance in cross-coupling reactions. Therefore the design of synthetic strategies for the preparation of solid-supported [(N,N'-diaryl NHC)Pd] is of great interest.

3.1.2.2. Supported [Pd(N,N'-diarylimidazolylidenes)]

Immobilization of the more sterically congested N,N'-diaryl NHC class has only been reported scarcely.[53,54] Immobilized versions of the 2nd generation Grubbs-Hoveyda Ru catalyst have been reported via the introduction of a suitably functionalized linker(s) in the C4 or/and C5 positions of the imidazole backbone in order to attach these complexes to polymers[55,56] or silica supports[54,55] (Figure 3.2 a)). A distinct synthetic strategy involves the introduction of functionality at the aryl wingtips (Figure 3.2 b)).

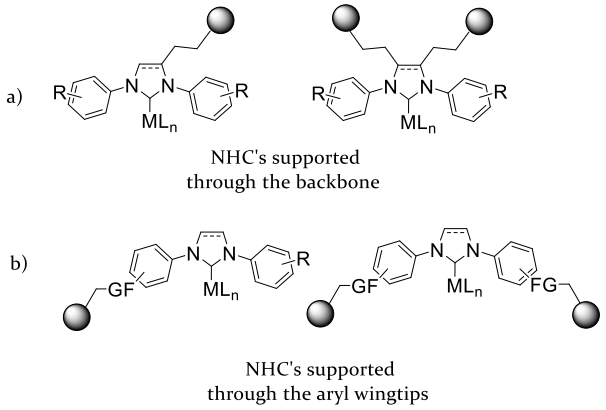

Figure 3.2. Strategies for the covalent immobilization of N,N'-diaryl imidazolylidene metal complexes onto inorganic supports.

Another method was described for the incorporation of the bulky IMes and IPr frameworks into the structure of PMO.[57,58] In this case, the introduction of the required anchoring functionality was achieved by means of Rh-catalyzed hydrosilylation of *p*-halogen functionalized N,N'-diarylimidazolium salts (Scheme 3.7). In this manner, hybrid materials with different degrees of functionalization were obtained (i.e. varying loadings of the built in NHC precursor). Subsequent metalation by

addition of various Pd precursors resulted in heterogeneous catalysts that were active in the Suzuki coupling of a wide range of activated and unactivated aryl chlorides with phenylboronic acids. Moreover, they showed good recyclability in several successive runs.[59,59]

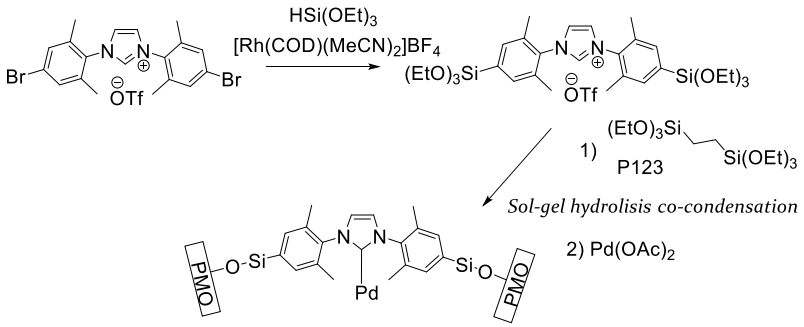

Scheme 3.7. Sol-gel synthesis of immobilized [Pd(N,N'-diarylimidazolylidenes)]

Recently, the group of Lu reported the grafting of an IPr·HCl analog onto the surface of mesoporous MCM-41 for its application as an organocatalyst (Scheme 3.8).[60] The imidazolium chloride salt was built up starting from 3,5-disubstituted p-alkenyl aniline. Thiol-ene click chemistry was subsequently used in order to introduce trimethoxysilyl groups.

To conclude, the functionalization of an NHC salt precursor by the introduction of alkoxysilyl groups constitutes a robust and straightforward protocol to establish a covalent bond with the inorganic oxides *via* condensation with the hydroxyl groups present on the surface of the support. The linker between the ligand and the support must be sufficiently long to grant good accessibility of the reactants to the metal center.

In principle, the immobilization of a preformed organometallic complex is desirable compared to the immobilization of a ligand followed by solid-phase metalation, since in the former case full characterization of the homogeneous Pd precatalyst can be performed prior to the anchoring reaction.

Covalent immobilization of [Pd(NHC)] complexes onto inorganic solid supports. Synthesis and characterization

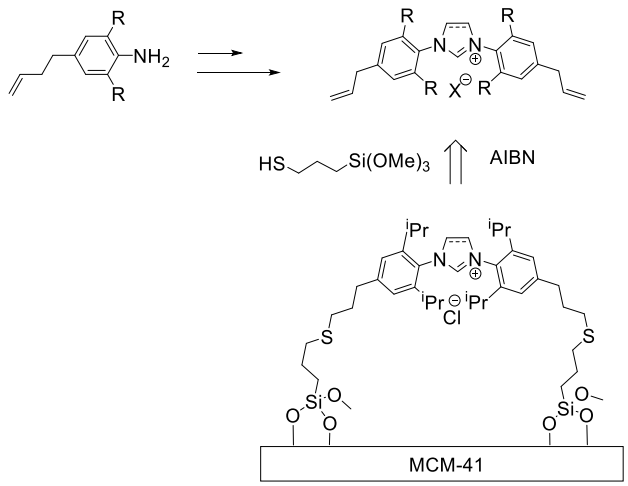

Scheme 3.8. Covalent immobilization of an IPr salt precursor onto a mesoporous MCM-41 support reported by Lu and co-workers.

The solid support immobilization of the more bulky N,N'-diaryl NHC class has been less studied compared with the solid support immobilization of N-alkylimidazolylidenes, due to the more challenging synthetic routes. However, the former class provides a more crowded environment in the proximity of the Pd center, a characteristic that has provided more active cross-coupling catalysts.[53] To the best of our knowledge the immobilization of [Pd(NHC)] complexes featuring the bulky IMes and IPr frameworks onto inorganic solid supports by grafting methods has not been reported to date.

In the following section the synthesis and characterization of inorganic oxide supported Pd catalysts bearing bulky N,N'-diaryl NHC will be described.

3.2. Results and discussion

Bulky NHC ligands featuring N,N'-diaryl substitution such as IMes or IPr (Scheme 3.9) have furnished excellent precatalysts in cross-coupling reactions.[34] More recently, work reported by Plenio indicated that substituting the alkyl groups at the aryl *para* positions by alkoxy groups does not greatly affect the ligand's donor characteristics.[61] Moreover, the group of Nolan reported the use of a *p*-methoxy functionalized NHC ligand, providing excellent activity in the Pd –catalyzed Büchwald-

Hartwig C-N cross-coupling.[62] Therefore we proposed that a ligand precursor bearing hydroxyl groups in the aryl *para* positions would provide a flexible method for attachment of various anchoring tethers through etherification (Scheme 3.10).

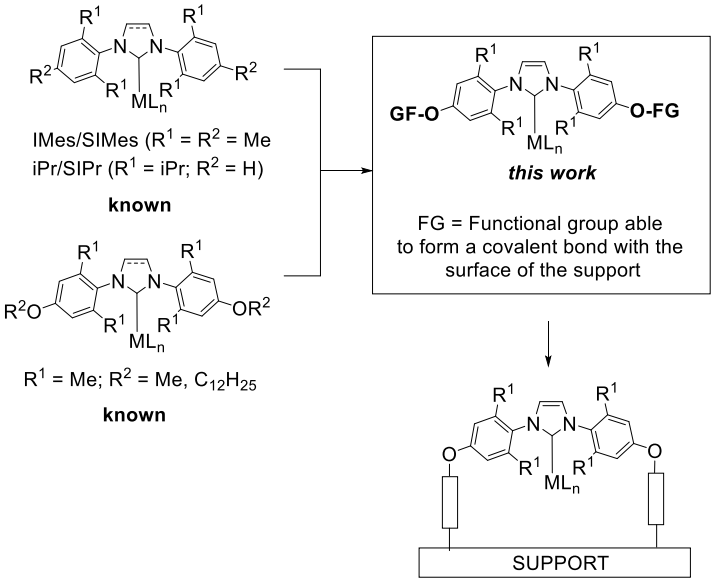

Scheme 3.9. Rationale for ligand design.

3.2.1. Synthesis of ligand salt precursors

At the beginning of the present study, all previously-reported syntheses of *p*-alkoxy-substituted IMes/SIMes analogs started with amination of 3,5-dimethylalkoxybenzenes, which does not allow facile variation of the alkoxy group or substitution with reactive functional groups.[63] It was therefore thought that for the purpose of this project, the use of a hydroxy-functionalized aniline as starting material would facilitate the installation of various functionalities later in the synthesis via etherification methodology (Scheme 3.10). Two groups reported a similar strategy for the synthesis of oligomer[55,64,] or bulky alkyl-decorated[65] Grubbs-Hoveyda metathesis catalysts bearing alkoxy-modified SIMes analogs. In both of these studies the commercially available 4-amino-3,5-dimethylphenol **4a** was employed as starting material.

Covalent immobilization of [Pd(NHC)] complexes onto inorganic solid supports. Synthesis and characterization

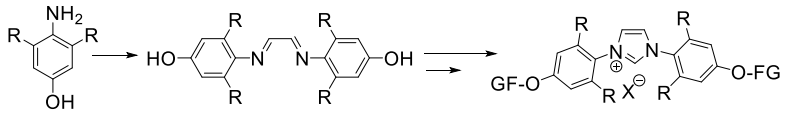

Scheme 3.10. Retrosynthetic approach starting with functionalized *p*-aminophenols.

Similar methodology can be envisioned for the formation of IPr analogs; however, to the best of our knowledge 4-amino-3,5-diisopropylphenol has not been reported outside the patent literature, and the reported synthesis is unattractive.[66,67] Therefore, it was necessary to develop an improved synthesis of this valuable intermediate using readily available materials (Scheme 3.11).

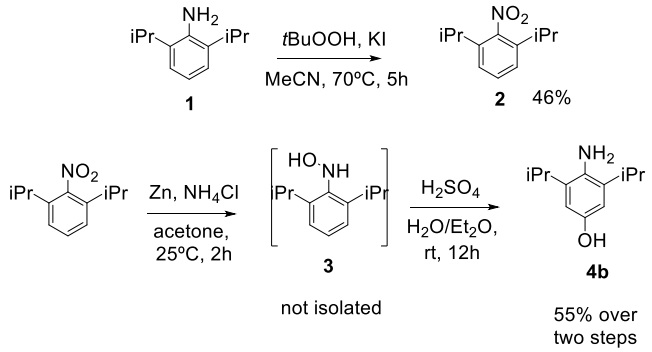

Scheme 3.11. Synthesis of 4-amino-3,5-diisopropylphenol.

First, 2,6-diisopropylaniline **1** was oxidized[68] to the corresponding nitrobenzene derivative **2** by using an excess of tert-butyl hydroperoxide. This product was obtained as an orange oil in 46% yield after purification by column chromatography. Subsequently compound **2** underwent partial reduction to the putative hydroxylamine **3** by using Zn powder as the reducing agent, a methodology based on literature precedent.[69] The crude hydroxylamine **3** was then directly treated with aqueous acid to effect a Bamberger rearrangement,[70] affording the *p*-aminophenol **4b** as a white solid in 55% yield over two steps. The ^{1}H NMR spectrum of this compound was in accordance with the presence of only two aromatic protons, according to integration of the corresponding signals.

Compounds **4a/b** were then condensed with 1,4-dioxane-2,3-diol, affording diazabutadienes **5a/b** in almost quantitative yield (Scheme 3.12). The formation of the expected reaction products was confirmed by the appearance of a singlet signal in the ^{1}H NMR spectra at δ 8,07 and 8,10 for compounds **5a** and **5b** respectively, corresponding to the imino protons which showed the expected integration values. The syntheses employing **4a** mentioned above required protection of the aminophenol before a Mitsunobu-type etherification in one case,[71] or direct etherification (in low yield) in the other.[68] We found that under the reaction conditions used here, *N*,*N*'-bis(hydroxyaryl)diazabutadienes **5a/b** could be used directly for etherification step to form the alkene-decorated species **6a/b** in 84-88% yield (Scheme 3.12).

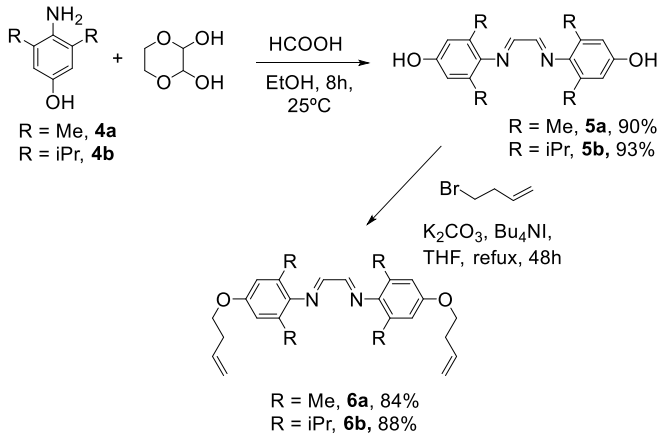

Scheme 3.12. Two step synthesis of the diazabutadienes **6a/b** from **4a/b**.

Formation of the desired bis-alkene tethered compounds **6** was confirmed by the appearance in the ^{1}H NMR spectra of the characteristic signals from the aryl ether methylene protons adjacent to the O atoms at δ 4,01 and 4,04 ppm, and also the signals from the alkene protons showing the right integration values. Further characterization of these compounds by elemental analysis and mass spectrometry was carried out.

It is worth noting that an alkene tether was employed here to facilitate our immobilization strategy, however, one can envision the introduction of a variety of functionality using this methodology.

Covalent immobilization of [Pd(NHC)] complexes onto inorganic solid supports. Synthesis and characterization

Alkene tethered diazabutadienes can then be converted to imidazolium salts by using para-formaldehyde as a C1-building block in the presence of one equivalent of acid.[72]For the case of IMes·HCl and IPr·HCl salts Nolan reported the use of HCl, 4M in dioxane,[31] but in our case this procedure yielded little of the desired product. Alternatively, we used TMSCl[73] as an acid equivalent, and in this way alkene tethered chloride salts **7** were obtained as white solids (Scheme 3.13).

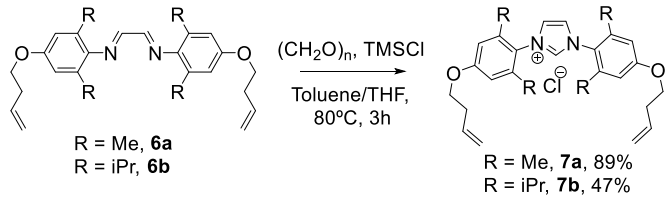

Scheme 3.13. Cyclization of diazabutadienes **6a/b** into the corresponding imidazolium chloride salts **7a/b**.

7a was obtained in 89% yield, whereas significantly lower yield was obtained for **7b**.The formation of the imidazolium chloride salts **7a/b** was clearly confirmed by ^{1}H NMR analysis, due to the appearance of a new signal at δ 10,43 and 9,77 ppm corresponding to the acidic NC*H*N proton in the imidazolium ring. The identities of **7a/b** were further confirmed by MS and elemental analysis.

As previously mentioned, the introduction of alkoxysilyl groups is one of the most reliable approaches to afford inorganic solid-heterogenized groups on the support.The group of Lu reported the introduction of such groups in an alkene tethered imidazolium chloride by using mild thiol-ene "click chemistry" methodology.[63] However, using the conditions reported by this group, the use of AIBN as a thermal initiator revealed ineffective in our case (Scheme 3.14).

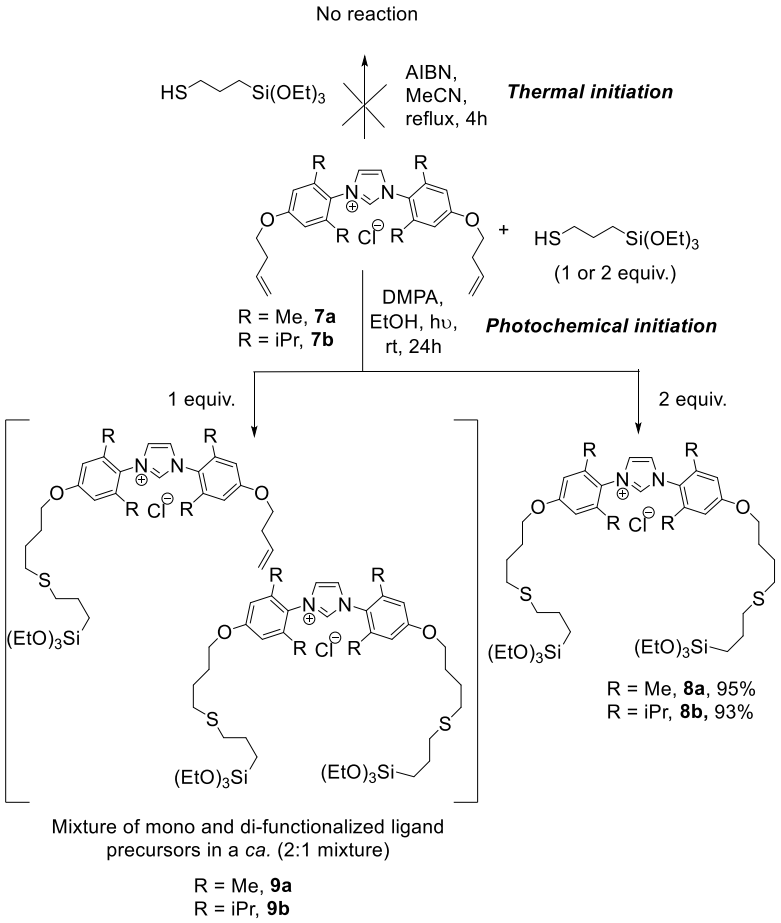

Scheme 3.14. Procedure for the introduction of alkoxysilyl groups in imidazolium chloride salts **7a**/**b** *via* thiol-ene click chemistry.

In contrast, under photochemical initiation in the presence of substoichiometric amounts of DMPA, the reaction proceeded smoothly and in the presence of 2 equivalents of mercaptopropyltriethoxysilane quantitative conversion of the starting materials was achieved as indicated by ^{1}H NMR analysis of the reaction mixtures, where the alkenic signals were no longer observed. Mass spectrometry and elemental analysis were used to further confirm the formation of preligands **8a** and **8b**.

Moreover, by adding one equivalent of the thiol reagent, the procedure resulted in a mixture of one- and two-tethered imidazolium preligands in a *ca.* 2:1 ratio. These mixtures were designated as **9a** and **9b**. Pre-

ligands **8** and **9** were isolated as moisture sensitive waxes. Pure compounds **8a/b** were obtained in 95% and 93% yield respectively.

3.2.2. Synthesis of heterogenized Pd(NHC) complexes

In order to explore the metal complexation of the new ligands before immobilization, the alkene tethered imidazolium chlorides **7a/b** were chosen for convenience. Complexes **10a/b** were synthesized by reaction of the chloride salts **7a/b** in the presence of Pd(acac)2. Performing the reaction in 1,2-dichloroethane (DCE) at 75°C for 48 hours. resulted in complete conversion of the starting materials according to NMR analysis, and the addition of an external base was not required (Scheme 3.15).

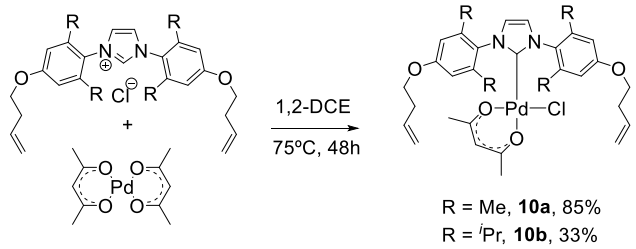

Scheme 3.15. Synthesis of complexes **10a** and **10b**.

Complexes **10a/b** are pale yellow, air- and moisture-stable solids. Complex 10a was obtained in 85% yield; in the case of complex **10b**, the pure compound could only be isolated in 33% yield owing to difficulties in the purification of the crude compound. Complexes **10a** and **10b** are analogs of [Pd(IMes)(acac)Cl] and [Pd(IPr)(acac)Cl] reported by Nolan[74] and exhibit very similar NMR features (Figure 3.3).

These [Pd(NHC)] species exhibited a typical ^{13}C NMR resonance shift downfield from 140 ppm to ca. 160 ppm relative to the imidazolium chlorides **7a/b.**

The same strategy was then used for the conversion of alkoxysilyl-functionalized pre-ligands **8a/b** into [Pd(NHC)(acac)Cl] complexes **11a/b.** Complexes **11a/b** could not be isolated, but reactions proceeded cleanly and to full conversion according to NMR analysis.

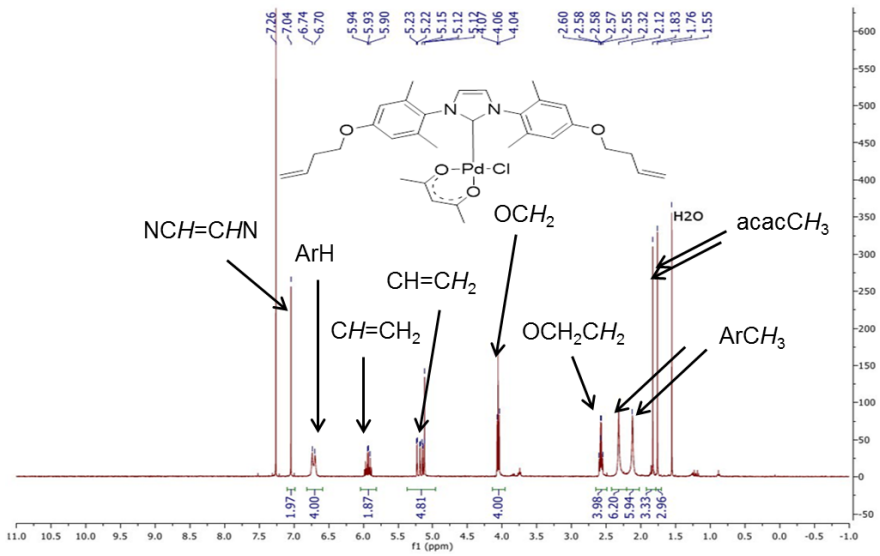

Figure 3.3. ^{1}H NMR spectrum of complex **10a**

For these species ^{1}H NMR resonances corresponding to the *meta* protons and C4-H and C5-H of the ligand appeared identical as in the case of complexes **10** (Figure 3.4).

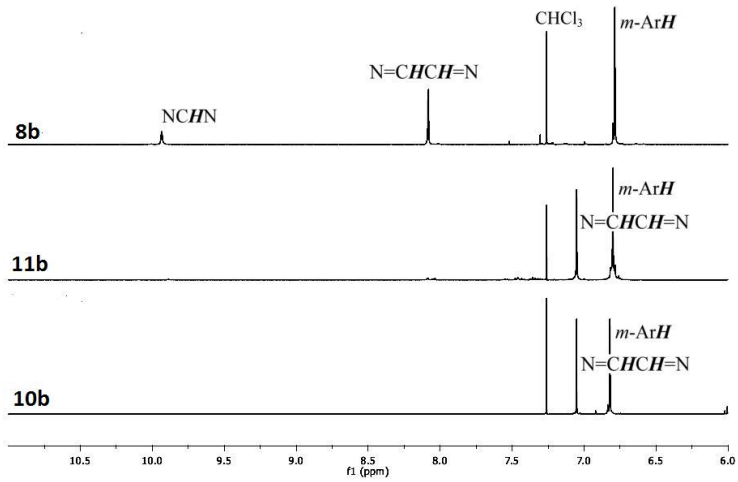

Figure 3.4. Imidazolium/imidazolylidene region of the ^{1}H NMR spectra of **8a**, **10b** and **11b**.

Covalent immobilization of [Pd(NHC)] complexes onto inorganic solid supports. Synthesis and characterization

Next, it was decided to perform the immobilization procedure in a one-pot, three step protocol, starting from the alkene tethered salts (Scheme 3.16).

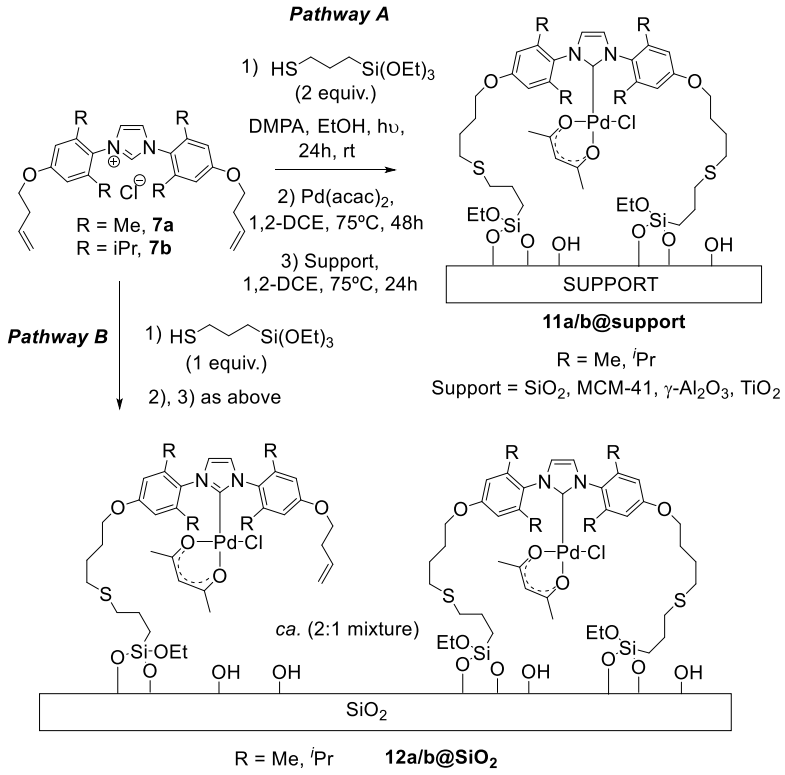

Scheme 3.16. One-pot protocol used for the formation of supported **11a/b@support** and **12a/b@support** from **7a/b.**

In the first step, the thiol-ene reaction was performed as previously described, in EtOH, at room temperature, for 24 hours. After removing the ethanol used as the reaction solvent the crude triethoxysilyl-functionalized imidazolium salts were concentrated, excluding these mixtures from moisture. Hexane was used to remove the remaining thiol reagent which was used in a small excess. Reaction of these preligands with $[Pd(acac)_2]$ in 1,2-DCE at 75°C afforded complexes **11a/b** in complete conversion after 2 days of reaction. The resulting solution containing the preformed Pd complex was directly transferred *via* cannula to a stirred suspension of the support (previously dried under vacuum) in 1,2-DCE, and after stirring at room temperature for 30

minutes, this mixture was heated at 75°C for 24h. After completion of the reaction, all the yellow color of the solution had been transferred to the solid, which was then hot-filtered, washed and dried under vacuum to yield the final supported product **11@support**, as pale yellow, air- and moisture-stable solids.

Notably, these one-pot protocol was not affected by the presence of impurities generated by DMPA used as photoinitiator in the thiol-ene reaction. The incorporation procedure was the same for all the supports used. Addition of only 1 equivalent of the alkoxysilyl thiol reagent in the first step yielded one-tethered enriched materials, in a statistical *ca.* 2:1 ratio (Scheme 3.16, Pathway B,). These one-tethered-enriched materials were only prepared using amorphous silica as the support and comparison in catalytic activity with the double tethered materials will be addressed in the next chapter.

Finally, in the case of silica materials, due to the larger population of surface hydroxyl groups compared to γ-Al_2O_3 and TiO_2 a post-immobilization treatment with methoxytrimethylsilane was carried out in order to cap the remaining accessible –OH groups (Scheme 3.17).

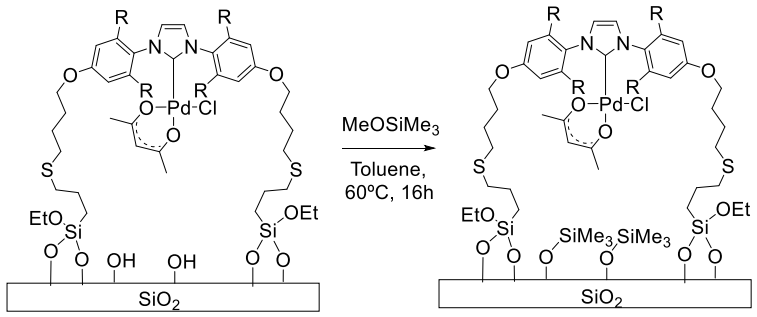

Scheme 3.17. End-capping treatment applied to the silica-supported materials **11@SiO_2** and **12@SiO_2**.

This end-capping treatment was also applied for the one-tethered enriched materials **12a/b**, but is not shown here for simplicity. Materials **13@SiO_2** and **14@SiO_2** were thus obtained.

As explained in the introduction of this chapter, immobilization of pre-formed metal complexes rather than immobilization of imidazolium

salts followed by treatment with a metal precursor is a better strategy in order to furnish heterogenized molecular catalysts with a well-defined configuration around the metal center. However, it is difficult to have a precise insight into the structure of the final functionalized solid materials. In order to track the ligand through the thiol-ene reaction, metallation, immobilization and post-immobilization modification, a ^{13}C-enriched sample was prepared by using ^{13}C-enriched paraformaldehyde earlier in the synthesis (Figure 3.5).

Going from the top to the bottom of Figure 3.5 the electronic environment around the pre- carbenic C2 carbon stays the same after the introduction of mercapto- triethoxysilyl linker with both chloride salts exhibiting resonances at 140 ppm; palladation results in a downfield shift to ca. 155 ppm corresponding to a soluble Pd-NHC species. Then CP-MAS analysis of the materials obtained after surface immobilization revealed a sharp resonance at the same chemical shift as observed in the homogeneous analog, therefore suggesting that at least the majority of the ligand is contained in the form of metal-carbene species.

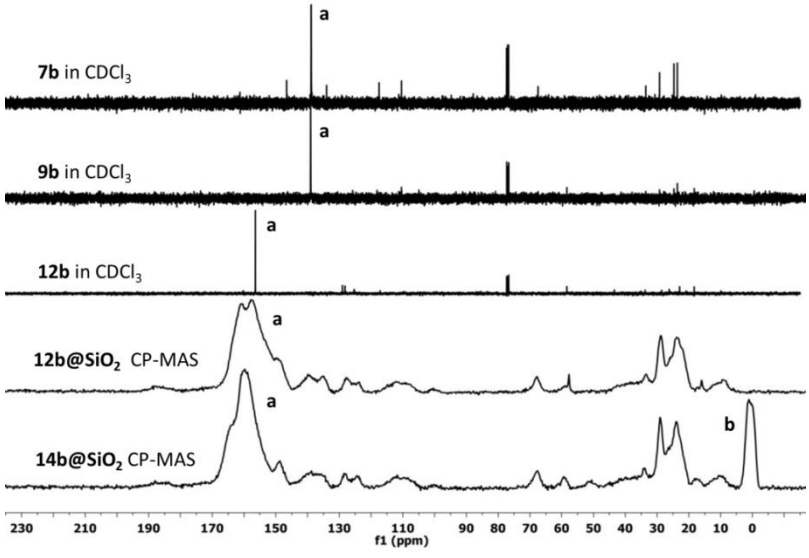

Figure 3.5. ^{13}C{^{1}H} NMR spectra of ^{13}C2-labeled **14b@SiO$_2$** and synthetic precursors. *a*. Imidazolium/ylidene C2 carbon. *b*. Peak corresponding to surface $SiMe_3$ groups.

This resonance does not seem to be shifted neither after the post-immobilization modification with $MeOSiMe_3$. For this latest reaction step, the appearance of a band at 0 ppm was indicative of the surface modification with trimethylsilyl groups.

Quantitative analysis of the catalyst loading in the functionalized solid materials was carried out by means of ICP-AES (Figure 3.6). Materials based on silica, either amorphous or mesoporous MCM-41, contained the highest Pd content of the series, followed by catalysts supported on γ-Al_2O_3. This is in agreement with the relative surface concentration of surface hydroxyl groups. Materials supported on titanium (II) oxide contained the lower amount of Pd, in agreement with the small surface area of this solid support (table 3.1).

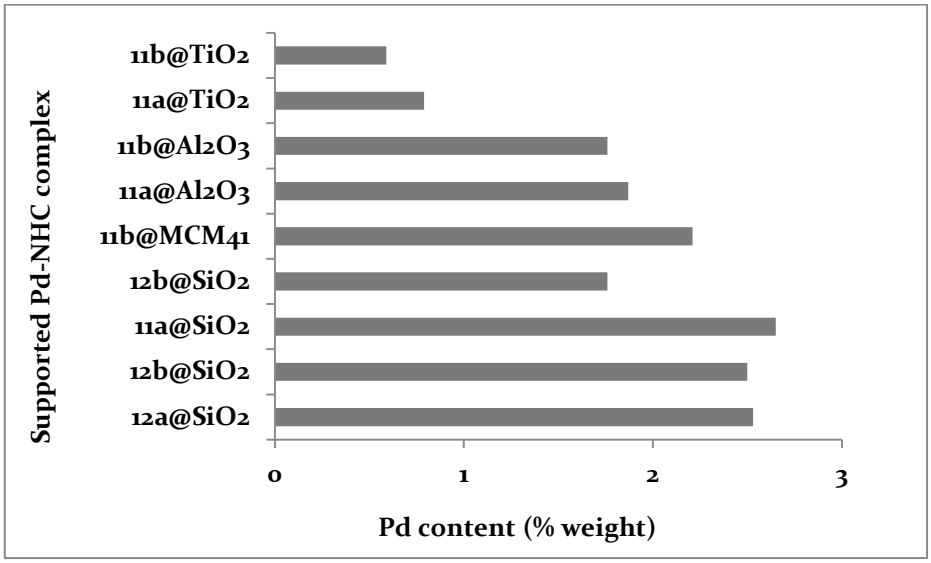

Figure 3.6. Pd content in the supported [Pd(NHC)] complexes.

Silica and alumina supports exhibited larger pore sizes compared to titania, as could be expected for mesoporous and microporous materials respectively. The R substitution on the NHC ligand only had very little influence, although less bulky Me groups on the aromatic wingtips generally resulted in slightly higher catalyst loadings. Finally, elemental analyses of C/H/N/S content for **11a/b@SiO_2** were in fair agreement with the ICP data, indicating that the majority of immobilized species are 1:1 NHC-Pd complexes. (Experimental Part).

Table 3.1. Surface area and mean pore size of the support materials.

Entry	Support	S_{BET} ($m^2 \cdot g^{-1}$)	$Ø_{pore}$ (Å)
1	SiO_2	473	61,2
2	γ-Al_2O_3	208	70,7
3	TiO_2	51	$2{,}03 \cdot 10^{-2}$

3.3. Conclusions

A reliable synthesis of the 4-amino-3,5-diisopropylphenol synthon **4b** has been described starting from commercially available 2,6-diisopropyl aniline (**1**), involving oxidation chemistry, then partial reduction to the putative hydroxylamine intermediate (**3**), and finally H^+(aq.) treatment yielding the desired analytically pure compound. Supporting our initial idea about the versatility of our synthetic route, alkene tethers were introduced into the ligand framework by simple etherification methodology. This is only one example of the various possibilities regarding the introduction of functionality through this methodology.

A one-pot immobilization procedure was also described starting from alkene-tethered imidazolium chloride salts **7a/b** involving "click chemistry", metalation, and immobilization to obtain the final air- and moisture-stable solid-supported [Pd(NHC)] complexes **11,12,13,14@support**. Moreover, the electronic environment of the ligand was tracked by ^{13}C NMR through the last stages in the synthetic sequence, that is "thiol-ene", formation of the Pd-NHC complex, immobilization and post-immobilization modification in order to gain more information about the nature of the final supported species. One-tethered enriched materials **12a/b@SiO_2** have also been synthesized. Finally, the Pd content in the final heterogenized materials was higher in the case of silica supports, due to the larger population of surface hydroxyl groups compared to titania and alumina.

In the following two chapters, the utilization of these materials in C-C coupling and hydrogenation/hydrogen transfer processes will be described.

3.4. Experimental part

General

Reactions were carried out using standard bench-top techniques unless the use of a Schlenk flask is specified, in which case Schlenk-line inert atmosphere techniques were used. Where stirring of the reaction mixture is indicated, magnetic stirring using a Teflon-coated stir bar was employed throughout. Commercially supplied compounds were used without further purification. Dry solvents were prepared by distillation from Na/benzophenone, CaH_2 or P_2O_5, or collected from a Braun SPS800 solvent purification system. Photochemical reactions were performed using a Philips HPL-N 125 W high-pressure mercury lamp, which can be purchased at most commercial lighting stores. Solution-state NMR spectra were obtained at the Servei de Recursos Científics i Tècnics (SRCiT), URV, with Varian (Agilent) Mercury VX400 or NMR System400 400 MHz spectrometers and calibrated to residual solvent peaks. CP-MAS spectra were recorded at the Servei de Ressonància Magnètica Nuclear (SeRMN), Universitat Autònoma de Barcelona on a 400 MHz spectrometer with a 12 kHz rotation speed (and calibrated to an external adamantane standard). Chemical shifts for ^{1}H and $^{13}C\{^{1}H\}$ NMR spectra are reported relative to TMS. ICP analyses were conducted at the SRCiT using an ICP-OES Spectro Arcos instrument. Samples were digested in concentrated HNO_3 under microwave irradiation before being diluted for analysis. HR-MS (ESI-TOF) analyses were also performed at the SRCiT, on an Agilent Time-of-Flight 6210 spectrometer. Elemental analyses were performed at the Centro de Microanálisis Elemental de la Universidad Complutense de Madrid or at the Unitat d'Anàlisi Química i Estructural-Serveis Tècnics de Recerca, Universitat de Girona. Other than solvents, reagents obtained from commercial sources were used without further purification. Silica used for catalyst immobilization was 60 mesh chromatography-grade (purchased from SDS), δ-Al_2O_3 was gamma-Alumina, 97% (purchased from Strem Chemicals), Titanium (IV) oxide nanopowder, ~21nm particle size was obtained from Aldrich, and mesoporous silica MCM-41 was prepared according to a modified literature procedure.[75] In each case, these materials were dried for 1 h at

80 °C, 10^{-3} mbar prior to use. $Pd(acac)_2$,[76] IPr·HCl[77] and IPrPd(acac)Cl[78] were prepared according to literature procedures.

Experimental procedures:

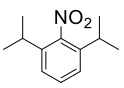

1,3-diisopropyl-2-nitrobenzene (2). In a round-bottom flask, 2,6-diisopropylaniline (20.0 g, 113 mmol, 1.0 equiv.) and potassium iodide (530 mg, 3.19 mmol, 0.03 equiv.) were added to acetonitrile (250 mL). While this mixture was stirred rapidly, 70% aqueous *tert*-butyl hydroperoxide (65 mL, 457 mmol, 4.1 equiv.) was added dropwise over 45 min. The reaction mixture was stirred at ambient temperature for 30 min, then heated at 70 °C for 5 h. The reaction vessel was allowed to cool, and the volatiles were removed using a rotatory evaporator (any unreacted hydroperoxide in the distillate was subsequently quenched with a saturated sodium thiosulfate solution). The resulting residue was directly chromatographed using hexane/ethyl acetate (50:1) as eluent. The desired product was the first colored band to elute; collection was stopped immediately prior to elution of the second colored band. The solvent was stripped from the collected eluent on a rotatory evaporator, affording an orange oil. Yield = 10.4 g (44%). **^{1}H NMR** (400 MHz, $CDCl_3$): δ 7.40 (t, J = 7.8 Hz, 1H, *p*-Ar*H*), 7.23 (d, J = 7.8 Hz, 2H, *m*-Ar*H*), 2.82 (sept, J = 6.8 Hz, 2H, C*H*Me$_2$), 1.25 (d, J = 6.8 Hz, 12H, CH*Me*$_2$). Peaks match the literature values.[79]

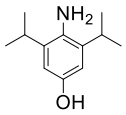

4-amino-3,5-diisopropylphenol (**4b**). Note: a previous (and very different) synthesis of this compound was reported in a patent, although no characterization data were given and the product sample was isolated as purple needles (the pure compound is colorless).[17] To our knowledge this is the first definitive report of the synthesis of this valuable intermediate. Nitrobenzene **2** (8.95 g, 43.2 mmol, 1.0 equiv.) and ammonium chloride (10.2 g, 190 mmol, 4.4 equiv.) were added to acetone (200 mL) in a 500 mL Schlenk flask, and N_2 gas was bubbled through the mixture for 30 min and the temperature of the bath was set at 25°C. Under rapid stirring, zinc dust (6.21 g, 95.0 mmol, 2.2 equiv.) was added in small portions over 2 h, sufficiently slowly to avoid a noticeable exotherm. The mixture was stirred for an additional 3 h, then filtered under N_2

atmosphere and evaporated under reduced pressure. The resulting residue was extracted with CH_2Cl_2 (100 mL) and the extract was filtered again. The CH_2Cl_2 was removed under reduced pressure, yielding an off-white semisolid crude (putative) hydroxylamine **3**, which was then dissolved in Et_2O (100 mL). Next, concentrated sulfuric acid (15 g) in deoxygenated water (100 mL) was added, and the biphasic mixture was stirred very rapidly. After about 10 min a flocculent white precipitate formed in the aqueous phase. The reaction mixture was stirred overnight after which time the resulting thick slurry was neutralized to pH 8 with a 2 N sodium hydroxide solution (Note: at this stage inert-atmosphere conditions were abandoned as the final product is air-stable). The organic phase was removed using a separatory funnel, and the aqueous phase was extracted three times with Et_2O (50 mL). The organic phases were combined, washed two times with brine (50 mL), and dried over magnesium sulfate. Finally, the Et_2O was removed on a rotatory evaporator to yield a purple oil which, upon trituration with pentane, became a white powder which was isolated by filtration and washed with cold pentane. Drying under reduced pressure afforded pure product. Yield = 4,56 g (55%). **^{1}H NMR** (400 MHz, $CDCl_3$): δ 6.55 (s, 2H, m-ArH), 2.94 (sept, J = 6.8 Hz, 2H, $CHMe_2$), 1.24 (d, J = 6.8 Hz, 12H, $CHMe_2$). **^{13}C {^{1}H} NMR** (100,6 MHz, $CDCl_3$): δ = 149,49, 135,44, 132,46, 110,33, 28,11, 22,66; HR-MS: m/z = 194,1558, calcd. for $C_{12}H_{20}NO$ [M+H+]: 194.1539, anal. calcd. for $C_{12}H_{19}NO$: C 74.57, H 9.91, N 7.25; found: C 74.84, H 10.14, N 7.31.

N,N'-bis(4-hydroxy-2,6-dimethylphenyl)-1,4-diazabutadiene (5a).4-amino-3,5-dimethylphenol 4a (4.00 g, 29.2 mmol, 1.0 equiv.) was combined with 1,4-dioxane-2,3-diol (1.75 g, 14.6 mmol, 0.5 equiv.) in a flame-dried Schlenk flask, and dry EtOH (40 mL) was added. With stirring, the mixture was gently heated with a hot-air gun until all material dissolved. Next, two drops of formic acid were added, resulting in the formation of precipitated product starting a few min after addition. The reaction mixture was stirred for 8 h, then cooled in an ice bath. After filtration, the solid yellow product was washed with cold CH_2Cl_2 (100 mL) until the filtrate exiting the filter frit was colorless, and dried under reduced pressure. Yield = 3.88 g (90%). **^{1}H NMR** (400 MHz, DMSO-d_6): δ = 9.19 (s, 2H, OH), 8.04 (s, 2H, N=CHCH=N), 6.52

(s, 4H, m-ArH), 2.07 (s, 12H, ArMe). **$^{13}C\{^1H\}$ NMR** (100,6 MHz, DMSO-d_6): δ = 162.91, 154.40, 141.57, 128.28, 115.00, 18.39; HR-MS: m/z = 297.1610, calcd. for $C_{18}H_{21}N_2O_2$ [M+H+]: 297.1597; anal. calcd. for $C_{18}H_{20}N_2O_2$: C 72.95, H 6.80, N 9.45; found: C 72.78, H 6.96, N 9.44.

N,N'-bis(4-hydroxy-2,6-diisopropylphenyl)-1,4-diazabutadiene (5b). Aminophenol **4b** (4.40 g, 22.8 mmol, 1.0 equiv.) was combined with 1,4-dioxane-2,3-diol (1.37 g, 11.4 mmol, 0.5 equiv.) in a flame-dried Schlenk flask, and dry EtOH (30 mL) was added. With stirring, the mixture was gently heated with a hot-air gun until all material dissolved. Next, two drops of formic acid were added, resulting in the formation of precipitated product starting a few min after addition. The reaction mixture was stirred for 8 h, then cooled in an ice bath. After filtration, the bright yellow product was washed with cold CH_2Cl_2 (100 mL) until the filtrate exiting the filter frit was very pale yellow in color, and dried under reduced pressure. The combined filtrates were concentrated, filtered and washed as above to yield additional product. Combined yield = 4,32 g (93%). **^{1}H NMR** (400 MHz, CD_3OD): *δ* = 7.99 (s, 2H, N=C*H*C*H*=N), 6.57 (s, 4H, *m*-Ar*H*), 2.85 (sept, *J* = 6.9 Hz, 4H, C*H*Me$_2$), 1.09 (d, *J* = 6.9 Hz, 24H, CH*Me*$_2$). **$^{13}C\{^1H\}$ NMR** (100,6 MHz, CD_3OD): *δ* = 165.32, 156.53, 141.70, 140.16, 111.33, 29.42, 23.95; HR-MS: m/z=409.2842, calcd. for $C_{26}H_{37}N_2O_2$ [M+H+]: 409.2850; anal. calcd. for $C_{26}H_{36}N_2O_2$:C 76.43, H 8.88, N 6.86; found: C 75.69, H 9.29, N 6.82.

N,N'-bis[4-(3-butenyloxy)-2,6-dimethylphenyl]-1,4-diazabutadiene (6a). Hydroxy-functionalized diazabutadiene **5a** (2.00 g, 6.75 mmol, 1.0 equiv.) was placed in a flame-dried Schlenk flask containing potassium carbonate (9.33 g, 67.5 mmol, 10 equiv.) and tetrabutylammonium iodide (248 mg, 0.671 mmol, 0.10 equiv.). *Via* syringe, 4-bromobutene (4.1 mL, 40 mmol, 6.0 equiv.) was added, followed by THF (40 mL). The mixture was heated at reflux for two days, during which time the initially-formed red/orange mixture turned bright yellow in color. After the vessel was allowed to cool, the solution was filtered from the solid waste products (which were then washed with 30 mL of THF) and the combined solutions evaporated

under reduced pressure. The residue was then placed in a Soxhlet apparatus and extracted with pentane (50 mL), until no yellow color was present in the extract exiting the extraction thimble. The extractant was allowed to cool, and the solid product was filtered off and subsequently washed with cold hexane. Yield = 2.28 g (84%). **^{1}H NMR** (400 MHz, $CDCl_3$): δ = 8.10 (s, 2H, N=C*H*C*H*=N), 6.66 (s, 4H, *m*-Ar*H*), 5.97-5.87 (m, 2H, C*H*=CH_2), 5.21-5.10 (m, 4H, CH=CH_2), 4.01 (t, *J* = 6.7 Hz, 4H, ArOCH_2), 2.58-2.52 (m, 4H, CH_2CH=CH_2), 2.20 (s, 12H, Ar*Me*). **^{13}C{^{1}H} NMR** (100,6 MHz, $CDCl_3$): δ = 163.62, 156.18, 143.52, 134.74, 128.78, 117.18, 114.53, 67.46, 33.94, 18.93; HR-MS: m/z = 405.2533, calcd. for $C_{26}H_{33}N_2O_2$ [M+H+]: 405.2538; anal. calcd. for $C_{26}H_{32}N_2O_2$: C 77.19, H 7.97, N 6.92; found: C 77.32, H 8.15, N 6.94.

N,N'-bis[4-(3-butenyloxy)-2,6-diisopropylphenyl]-1,4-diazabutadiene (6 b). Hydroxy-functionalized diazabutadiene **5b** (3.85 g, 9.42 mmol, 1.0 equiv.) was added to a flame-dried Schlenk flask containing potassium carbonate (13.0 g, 94.2 mmol, 10 equiv.) and tetrabutylammonium iodide (348 mg, 0.942 mmol, 0.10 equiv.). *Via* syringe, 4-bromobutene (7.6 mL, 75.0 mmol, 8.0 equiv.) was added, followed by of THF (60 mL). The mixture was heated at reflux for 48 h, during which time the initially-formed red mixture turned bright yellow in color. After the vessel was allowed to cool, the solution was filtered from the solid waste products (which were then washed with 30 mL of THF) and the combined solutions evaporated under reduced pressure. The residue was then placed in a Soxhlet apparatus and extracted with pentane (50 mL), until no yellow color was present in the extract exiting the extraction thimble. The pentane solution was then boiled down to about 20 mL and allowed to cool. After further cooling in an ice bath, the supernatant was decanted from the precipitated product, which was then quickly washed with cold pentane (15 mL). Yield = 4,27 g (88%). **^{1}H NMR** (400 MHz, $CDCl_3$): δ = 8.07 (s, 2H, N=C*H*C*H*=N), 6.73 (s, 4H, *m*-Ar*H*), 6.00-5.90 (m, 2H, C*H*=CH_2), 5.23-5.12 (m, 4H, CH=CH_2), 4.04 (t, *J* = 6.7 Hz, 4H, ArOCH_2), 2.97 (sept, *J* = 6.8 Hz, 4H, C*H*Me_2), 2.60-2.55 (m, 4H, CH_2CH=CH_2), 1.19 (d, *J* = 6.8 Hz, 24H, CH*Me*$_2$). **^{13}C{^{1}H} NMR** (100,6 MHz, $CDCl_3$): δ = 163.78, 156.76, 141.83, 138.89, 134.81, 117.24, 109.58, 67.45, 34.07, 28.39, 23.64; HR-MS: m/z = 517.3794, calcd. for $C_{34}H_{49}N_2O_2$

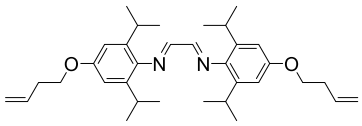

[M+H+]: 517.3788; anal. calcd. for $C_{34}H_{48}N_2O_2$: C 79.02, H 9.36, N 5.42; found: C 79.33, H 9.88, N 5.51.

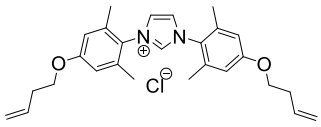

1,3-bis[4-(3-butenyloxy)-2,6-dimethylphenyl]imidazolium chloride *(7a)*. A flame-dried Schlenk flask was charged with **6a** (1.80 g, 4.45 mmol, 1.0 equiv.), paraformaldehyde (147 mg, 4.89 mmol, 1.1 equiv.) and toluene (30 mL). This mixture was heated to 80 °C with rapid stirring. To a separate flame-dried Schlenk flask was added TMSCl (620 µL, 4.89 mmol, 1.1 equiv.) and THF (15 mL). The TMSCl solution was then slowly added to the heated, stirred solution containing **7a** over a period of 45 min, during which time a white precipitate formed. The reaction mixture was heated for 2 h more, let cool to ambient temperature and then cooled further in an ice bath. The precipitate was collected by filtration and washed with toluene. Yield = 1.80 g (89%). **^{1}H NMR** (400 MHz, $CDCl_3$): δ = 10.43 (t, *J* = 1.4 Hz, 1H, NC*H*N), 7.55 (d, *J* = 1.4 Hz, 2H, N=C*H*C*H*=N), 6.72 (s, 4H, *m*-Ar*H*), 5.94-5.83 (m, 2H, C*H*=CH_2), 5.21-5.11 (m, 4H, CH=CH_2), 4.02 (t, *J* = 6.7 Hz, 4H, ArOCH_2), 2.57-2.52 (m, 4H, CH_2CH=CH_2), 2.19 (s, 12H, Ar*Me*). **^{13}C{^{1}H} NMR** (100,6 MHz, $CDCl_3$): δ = 160.17, 139.65 (NCHN), 135.94, 134.12, 125.98, 125.15, 117.40, 114.83, 67.46, 33.50, 18.10. HR-MS: m/z=417.2516, calcd. for $C_{27}H_{33}N_2O_2$ [M-Cl^-]: 417.2538; anal. calcd. for $C_{27}H_{33}ClN_2O_2$: C 71.58, H 7.34, N 6.18; found: C 70.97, H 7.49, N 6.07.

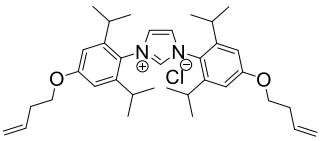

1,3-bis[4-(3-butenyloxy)-2,6-diisopropylphenyl]imidazolium chloride (7b). A flame-dried Schlenk flask was charged with **6b** (2.00 g, 3.87 mmol, 1.0 equiv.), paraformaldehyde (128 mg, 4.26 mmol, 1.1 equiv.) and toluene (20 mL). This mixture was heated to 80 °C with rapid stirring. To a separate flame-dried Schlenk flask was added TMSCl (565 µL, 4.26 mmol, 1.1 equiv.) and THF (10 mL). The TMSCl solution was then slowly added to the heated, stirred solution containing **7b** over a period of 45 min, during which time the reaction mixture developed a deep brown color. The vessel was heated for 2 h more and then, while hot, the reaction mixture was concentrated under reduced pressure to about 1/3 of its original volume. Hexane (30 mL) was added and the mixture was

allowed to cool to ambient temperature, and subsequently it was cooled in an ice bath. The supernatant was then decanted and the black/brown residue extracted with Et_2O until a while powder was obtained, which was collected by filtration and washed with more Et_2O. Yield = 1.03 g (47%). **^{1}H NMR** (400 MHz, $CDCl_3$): δ = 9.77 (t, *J* = 1.5 Hz, 1H, NC*H*N), 8.09 (d, *J* = 1.5 Hz, 2H, N=C*H*C*H*=N), 6.78 (s, 4H, *m*-Ar*H*), 5.97-5.87 (m, 2H, C*H*=CH_2), 5.24-5.13 (m, 4H, CH=CH_2), 4.06 (t, *J* = 6.7 Hz, 4H, ArOCH_2), 2.61-2.56 (m, 4H, CH_2CH=CH_2), 2.39 (sept, *J* = 6.8 Hz, 4H, C*H*Me_2), 1.24 (d, *J* = 6.8 Hz, 12H, CH*Me*$_2$), 1.20 (d, *J* = 6.8 Hz, 12H, CH*Me*$_2$). **^{13}C{^{1}H} NMR** (100,6 MHz, $CDCl_3$): δ = 161.49, 146.80, 139.17 (NCHN), 134.20, 127.43, 122.87, 117.69, 110.64, 67.66, 33.73, 29.43, 24.90, 23.81; HR-MS: m/z = 529.3860, calcd. for $C_{35}H_{49}N_2O_2$ [M-Cl^-]: 529.3787; anal. calcd. for $C_{35}H_{49}ClN_2O_2$: C 74.37, H 8.74, N 4.96; found: C 73.94, H 9.15, N 4.95.

The C2-labeled compound **^{13}7b** was synthesized following the same procedure (but at smaller scale) using 99% ^{13}C-enriched paraformaldehyde. The ^{1}H NMR spectrum exhibits a C2 proton $J_{C\text{-}H}$ of 222 Hz.

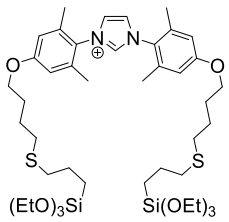

1,3-bis(2,6-dimethyl-4-(4-((3--triethoxysilyl)propyl)thio)butoxy)phenyl) imidazolium chloride (8a). A flame-dried Schlenk flask was charged with **7a** (400 mg, 0.883 mmol, 1.0 equiv.), 3-mercaptopropyl(triethoxy)silane (540 µL, 2.12 mmol, 2.4 equiv.) and 2,2-Dimethoxy-2-phenylacetophenone (DMPA, 45 mg, 0.18 mmol, 0.20 equiv.), followed by freshly-dried EtOH (2 mL). The reaction mixture was then stirred and irradiated with a 125 W high-pressure mercury lamp (8 cm of separation between the bulb and flask) at room temperature for 24 h. The solvent was removed under reduced pressure, and the residue was re-dissolved in CH_2Cl_2 and evaporated again in order to fully remove the EtOH. Eventually, excess of thiol reagent was removed by washing the residue with dry hexane (2 x 2 mL) and filtering this mixture with a cannula. The product thus obtained was dried under reduced pressure to yield a light yellow, moisture-sensitive wax. 673 mg (yield = 82%); **^{1}H NMR** (400 MHz, $CDCl_3$): δ = 10.64 (s, 1H, NCHN), 7.61 (s, 2H, N=CHCH=N), 6.59 (s, 4H, m-ArH), 3.89 (t, J = 5.9 Hz, 4H, $ArOCH_2$), 3.74 (q, J = 7.0 Hz, 12H, OCH_2CH_3), 2.50 (t, J

= 7.2 Hz, 4H, SCH_2), 2.47 (t, J = 7.5 Hz, 4H, SCH_2), 2.07 (s, 12H, ArMe), 1.84-1.77 (m, 4H, CH_2), 1.71-1.59 (m, 8H, CH_2), 1.14 (t, J = 7.0 Hz, 18H, OCH_2CH_3), 0.66 (t, J = 8.3 Hz, 4H, CH_2Si). **$^{13}C\{^1H\}$ NMR** (100,6 MHz, $CDCl_3$): δ = 160.18, 139.95 (NCN), 135.84, 125.89, 124.94, 114.71, 67.64, 58.37, 35.10, 31.56, 28.24, 26.10, 23.21, 18.32, 18.05, 9.88; HR-MS: m/z = 893.4662, calcd. for $C_{45}H_{77}N_2O_8S_2Si_2$ [M-Cl^-]: 893.4651; anal. calcd. for $C_{45}H_{77}ClN_2O_8S_2Si_2$: C 58.12, H 8.35, N 3.01, S 6.90; found: C 57.47, H 7.88, N 3.51, S 6.83.

1,3-bis(2,6-diisopropyl-4-(4-((3-(triethoxysilyl)propyl)thio)butoxy)phenyl) imidazolium chloride (8b). A flame-dried Schlenk flask was charged with **7b** (400 mg, 0.708 mmol, 1.0 equiv.), 3-mercaptopropyl(triethoxy) silane (431 µL, 1.70 mmol, 2.4 equiv.) and DMPA (36 mg, 0.14 mmol, 0.20 equiv.), followed by freshly-dried EtOH (3 mL). The reaction mixture was then stirred and irradiated with a 125 W high-pressure mercury lamp (8 cm of separation between the bulb and flask) for 24 h. The solvent was removed under reduced pressure, and the residue was re-dissolved in CH_2Cl_2 and evaporated again in order to fully remove the EtOH. The crude product was washed three times with hexane (3 mL), and finally dried under reduced pressure once again to yield 686 mg (yield = 93%) of colorless, moisture-sensitive wax **8b**. **^1H NMR** (400 MHz, $CDCl_3$): δ = 9.93 (s, 1H, NCHN), 8.08 (s, 2H, N=CHCH=N), 6.79 (s, 4H, m-ArH), 4.04 (t, J = 6.1 Hz, 4H, $ArOCH_2$), 3.82 (q, J = 7.0 Hz, 12H, OCH_2CH_3), 2.61 (t, J = 7.1 Hz, 4H, SCH_2), 2.57 (t, J = 7.3 Hz, 4H, SCH_2), 2.41 (sept, J = 6.8 Hz, 4H, $CHMe_2$), 1.98-1.91 (m, 4H, CH_2), 1.87-1.78 (m, 4H, CH_2), 1.76-1.69 (m, 4H, CH_2), 1.27 (d, J = 6.8 Hz, 12H, $CHMe_2$), 1.23 (t, J = 7.0 Hz, 18H, OCH_2CH_3), 1.22 (d, J = 6.9 Hz, 12H, $CHMe_2$), 0.75 (t, J = 8.3 Hz, 4H, CH_2Si). **$^{13}C\{^1H\}$ NMR** (100,6 MHz, $CDCl_3$): δ = 161.15, 146.41, 139.22 (NCHN), 126.98, 122.58, 110.15, 67.49, 58.34, 34.96, 31.47, 29.05, 28.15, 25.99, 24.52, 23.46, 23.09, 18.18, 9.75; HR-MS: m/z = 1005.5986, calcd. for $C_{53}H_{93}N_2O_8S_2Si_2$ [M-Cl^-]: 1005.5901; anal. calcd. for $C_{53}H_{93}ClN_2O_8S_2Si_2$: C 61.09, H 8.99, N 2.69, S 6.15; found: C 60.75, H 8.61, N 2.94, S 6.03.

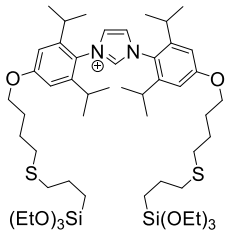

1,3-bis[4-(3-butenyloxy)-2,6-dimethylphenyl]imidazol-2-ylidenyl(acetylacetonato)palladium chloride *(10a)*. A flame-dried Schlenk flask was charged with **7a** (200 mg, 0.442 mmol, 1.0 equiv.) and $Pd(acac)_2$ (128 mg, 0.420 mmol, 0.95 equiv.), and 1,2-dichloroethane (1,2-DCE, 6 mL) was added. The reaction mixture was stirred at 75 °C for 24 h after which time the solvent was removed under reduced pressure. The residue was extracted with toluene (5 mL), and the extract was then heated at 60 °C while hexane was slowly added until turbidity remained for an instant after an additional drop was added. The mixture was allowed to cool to ambient temperature, and the precipitated product was collected by filtration and washed with Et_2O, yielding a very pale yellow powder. Yield = 235 mg (85%). **^{1}H NMR** (400 MHz, $CDCl_3$): δ 7.04 (s, 2H, N=C*H*C*H*=N), 6.74 (br s, 2H, *m*-Ar*H*), 6.70 (br s, 2H, *m*-Ar*H*), 5.97-5.88 (m, 2H, C*H*=CH_2), 5.23-5.12 (m, 4H, CH=CH_2), 5.12 (s, 1H, acac-CC*H*C) 4.06 (t, *J* = 6.7 Hz, 4H, ArOCH_2), 2.60-2.55 (m, 4H, CH_2CH=CH_2), 2.32 (br s, 6H, Ar*Me*), 2.12 (br s, 6H, Ar*Me*), 1.83 (s, 3H, acac-*Me*), 1.76 (s, 3H, acac-*Me*). **^{13}C{^{1}H} NMR** (100,6 MHz, CDCl3): δ = 187.22, 183.21, 159.13, 154.45 (NCHN), 138.27, 137.31, 134.57, 130.56, 124.10, 117.22, 114.36, 99.79, 67.32, 33.80, 27.24, 25.71, 19.39, 18.23. Anal. Calcd. for $C_{32}H_{40}ClN_2O_4Pd$: C, 58,4; H, 6,08; N, 4,26. Found: C, 57,98; H, 6,10; N, 4,15.

1,3-bis[4-(3-butenyloxy)-2,6-diisopropylphenyl]imidazol-2-ylidenyl(acetylacetonato)palladium chloride *(10b)*. A flame-dried Schlenk flask was charged with **7b** (200 mg, 0.354 mmol, 1.0 equiv.) and $Pd(acac)_2$ (102 mg, 0.336 mmol, 0.95 equiv.), and 1,2-dichloroethane (1,2-DCE, 6 mL) was added. The reaction mixture was stirred at 75 °C for 3 days after which time the solvent was removed under reduced pressure. The residue was extracted twice with Et_2O (10 mL) and the solvent was removed from the extracts. The evaporated extract was then chromatographed on silica under N_2 atmosphere using a 1:1 hexane:Et_2O mixture as eluent, collecting only the pure fractions. Yield = 85 mg (33%). **^{1}H NMR** (400 MHz, $CDCl_3$): δ 7.05 (s, 2H, N=C*H*C*H*=N), 6.82 (s, 4H, *m*-Ar*H*), 6.02-5.92 (m, 2H, C*H*=CH_2), 5.26-5.14 (m, 4H, CH=CH_2),

5.11 (s, 1H, acac-CC*H*C) 4.10 (t, *J* = 6.7 Hz, 4H, ArOCH_2), 2.88 (br s, 4H, C*H*Me$_2$), 2.64-2.58 (m, 4H, CH_2CH=CH$_2$), 1.83 (s, 3H, acac-*Me*), 1.82 (s, 3H, acac-*Me*), 1.29 (br s, 12H, CH*Me*$_2$), 1.07 (d, *J* = 6.9 Hz, 12H, CH*Me*$_2$). **^{13}C{^{1}H} NMR** (100,6 MHz, $CDCl_3$): δ 186.74, 183.65, 160.19, 156.58 (NCN), 148.43 (br), 148.21 (br), 134.66, 128.28, 125.58, 117.32, 110.06, 99.52, 67.39, 33.93, 28.80, 27.24, 26.33, 23.08. Anal. Calcd. for $C_{40}H_{56}ClN_2O_4Pd$: C, 62.33; H, 7.32; N, 3.63. Found: C, 60.91; H, 6.90; N, 3.81.

General procedure for the covalent immobilization of Pd-NHC complexes onto inorganic supports.

The experimental procedures will refer to the case of silica gel-supported Pd-NHC complexes but the same procedures were applied for the other solid materials, MCM-41, γ-Al_2O_3 and TiO_2.

***One-pot procedure for preparation of* 11b@SiO$_2$.** A flame-dried Schlenk flask was charged with **7b** (213 mg, 0.377 mmol, 1.0 equiv.), 3-mercaptopropyl(triethoxy)silane (190 µL, 0.754 mmol, 2.0 equiv.) and DMPA (19 mg, 0.08 mmol, 0.20 equiv.), followed by freshly-dried EtOH (1.5 mL). The reaction mixture was then stirred and irradiated with a 125 W high-pressure mercury lamp (8 cm of separation between the bulb and flask) for 24 h. The solvent was removed under reduced pressure, and the residue was re-dissolved in CH_2Cl_2 and evaporated again in order to fully remove the EtOH. Next, Pd(acac)$_2$ (115 mg, 0.377 mmol, 1.0 equiv.) was added along with 1,2-DCE (5 mL). After the reaction mixture was heated at 75 °C with stirring for 2 days and then allowed to cool, it was slowly transferred *via* cannula to another Schlenk flask containing a stirred (400 rpm) suspension of previously dried 60 mesh silica (1.71 g) in 1,2-DCE (3 mL). This suspension was stirred at 250 rpm for 30 min at ambient temperature, then the temperature was increased to 75 °C and stirring was continued for 24 h. During this time all of the yellow color in the supernatant was transferred to the silica. Finally, the material was hot-filtered and washed with copious amounts of CH_2Cl_2. The recovered yield of **11b@SiO$_2$** was 2.5 g. Pd content by ICP: 1.76 wt% (0.165 mmol / g). Anal.

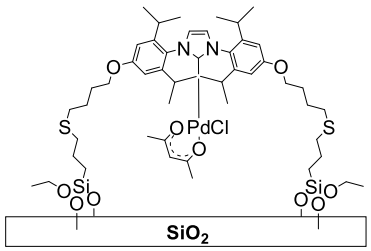

Calcd. for $C_{50}H_{80}ClN_2O_6PdS_2Si_2@SiO_2$ based on Pd loading: C, 9.91; H, 1.33; N, 0.46; S, 1.06. Found: C, 8.87; H, 1.94; N, 0.58; S, 0.97

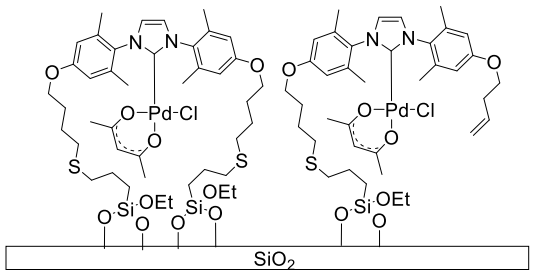

***One-pot procedure for preparation of* 12b@SiO$_2$.** A flame-dried Schlenk flask was charged with **7b** (875 mg, 1.54 mmol, 1.0 equiv.), 3-mercaptopropyl(triethoxy)silane (390 µL, 1.54 mmol, 1.0 equiv.) and DMPA (50 mg, 0.20 mmol, 0.13 equiv.), followed by freshly-dried EtOH (40 mL). The reaction mixture was then stirred and irradiated with a 125 W high-pressure mercury lamp (8 cm of separation between the bulb and flask) for 2 days. The solvent was removed under reduced pressure, and the residue was re-dissolved in CH_2Cl_2 and evaporated again in order to fully remove the EtOH. Next, $Pd(acac)_2$ (469 mg, 1.54 mmol, 1.0 equiv.) was added along with 1,2-DCE (20 mL). After the reaction mixture was heated at 75 °C with stirring for 2 days and then allowed to cool, it was slowly transferred *via* cannula to another Schlenk flask containing a stirred (400 rpm) suspension of previously dried 60 mesh silica (5.10 g) in 1,2-DCE (10 mL). This suspension was stirred at 250 rpm for 30 min at ambient temperature, then the temperature was increased to 75 °C and stirring was continued for 24 h. Finally, the material was hot-filtered and washed with copious amounts of CH_2Cl_2. The recovered yield of **12b@SiO$_2$** was 6.14 g. Pd content by ICP: 2.50 wt% (0.237 mmol / g).

11b@MCM-41. Pd content by ICP: 2,21 wt% (0.207 mmol/g). Anal. Calcd. for $C_{50}H_{80}ClN_2O_6PdS_2Si_2@MCM\text{-}41$ based on Pd loading: C, 12,51; H, 1.67; N, 0.58; S, 1.33. Found: C, 12,30; H, 2,54; N, 0,61; S, 0,40.

11a@γ-Al$_2$O$_3$. Pd content by ICP: 0,72 wt% (0.068 mmol/g). Anal. Calcd. for $C_{42}H_{64}ClN_2O_6PdS_2Si_2@\gamma\text{-}Al_2O_3$ based on Pd loading: C, 3,42; H, 0,43; N, 0,19; S, 0,43; Si, 0,38 Found: C, 2,85; H, 2,27; N, 0,19; S, 0,16; Si, 1,33.

11b@γ-Al$_2$O$_3$. Pd content by ICP: 1,73 wt% (0.163 mmol/g). Anal. Calcd. for $C_{50}H_{80}ClN_2O_6PdS_2Si_2@\ \gamma\text{-}Al_2O_3$ based on Pd loading: C, 9,79; H, 1,31; N, 0,45; S, 1.04. Found: C, 6,62; H, 1,78; N, 0,44; S, 1,08.

11a@TiO_2. Pd content by ICP: 0,90 wt% (0.085 mmol/g). Anal. Calcd. for $C_{42}H_{64}ClN_2O_6PdS_2Si_2@TiO_2$ based on Pd loading: C, 4,90; H, 0,54; N, 0.24; S, 0,54; Si, 0,475 Found: C, 2,69; H, 0,23; N, 0,24; S, 0,1; Si, 1,53.

11b@TiO_2. Pd content by ICP: 0,76 wt% (0.071 mmol/g). Anal. Calcd. for $C_{50}H_{80}ClN_2O_6PdS_2Si_2@TiO_2$ based on Pd loading: C, 4,30; H, 0,58; N, 0.20; S, 0,46. Found: C, 3,18; H, 0,53; N, 0,19; S, 0,50.

13,14@SiO_2. A Schlenk flask was charged with the appropriate supported Pd complex (1.00 g) and flushed with N_2. The solid was suspended in toluene (3 mL) and then stirred at 400 rpm while $MeOSiMe_3$ (1.5 mL) was added dropwise *via* syringe. After fastening the flask's stopper securely and closing the N_2 inlet, the reaction mixture was heated at 60 °C with stirring (150 rpm) overnight. Upon cooling, the product material was collected by filtration and washed with copious amounts of CH_2Cl_2. Note: the synthesis of **14b@SiO_2** was also carried out at a 3 g scale. **13b@SiO_2**: yield = 980 mg. Pd content by ICP: 1.67 wt% (0.157 mmol / g). **14a@SiO_2**: yield = 990 mg. Pd content by ICP: 1.97 wt% (0.185 mmol / g). **14b@SiO_2**: yield = 1.00 g. Pd content by ICP: 1.73 wt% (0.163 mmol / g).

3.5. References

[1] P. Diddams, *Inorganic supports and catalysts – an overview*. In: Solid supports and catalysts in organic synthesis, **1992**. Ed. K. Smith, Chichester, Ellis Horwood and Prentice Hall.
[2] From *Catalysis by metal complexes* **2010**, *33* (*Heterogenized Homogeneous Catalysts for Fine Chemicals Production)*. Ed. P. Barbaro, F. Liguori. Springer
[3] A. Corma, H. García, *Adv. Synth. Catal*. **2006**, *348*, 1391.
[4] N. Herron, *Inorg. Chem.*, **1986**, *25*, 4714.
[5] M. Poyatos, F. Márquez, E. Peris, C. Claver, E. Fernández, *New. J. Chem.* **2003**, *27*, 425.
[6] *Nanostructured Carbon Materials for Catalysis*, **2015**; eds. P. Serp, B. Machado, RSC, Cambridge.
[7] C. Vriamont, M. Devillers, O. Riant, S. Hermans, *Chem. Eur. J*. **2013**, *19*, 12009.
[8] S. Sabater, J.A. Mata, E. Peris, *ACS Catal*. **2014**, *4*, 2038.
[9] D. Didier, E. Schulz, *Tetrahedron: Asymmetry*, **2013**, *24*, 769.
[10] H. Yang, Y. Wang, Y. Qin, Y. Chong, Q. Yang, G. Li, L. Zhang, W. Li, *Green Chem*., **2011**, *13*, 1352.
[11] S. Tanielyan, R.L. Augustine, N. Marin, G. Alvez, *ACS Catalysis,* **2011**, *1(2)*, 159.
[12] C.E. Song, S.-G. Lee, *Chem. Rev*. **2002**, *102*, 3495.
[13] Z.-I. Lu, E. Lindner, H. A. Mayer, *Chem. Rev*. **2002**,*102*, 3543.
[14] A. P. Wight, M. E. Davis, *Chem. Rev*. **2002**, *102*, 3589.
[15] D. E. De Vos, M. Dams; B. F. Sels, P. A. Jacobs, *Chem.Rev*. **2002**, *102,* 3615.
[16] V. Polshettiwar, Á. Molnár, *Tetrahedron* **2007**, *63*, 6949.
[17] C.M. Crudden, M. Sateesh, R. Lewis, *J. Am. Chem. Soc*. **2005**, *127*, 10045.
[18] R. Chen, R. P. J. Bronger, P. C. J. Kamer, P. W. N. M. van Leeuwen, J. N. H. Reek, *J. Am. Chem. Soc*. **2004**, *126*, 14557.
[19] M. Bandini, R. Luque, V. Budarin, D. J. Macquarrie, *Tetrahedron* **2005**, *61*, 9860.
[20] C. Baleizao, A. Corma, H. García, A. Leyva, *J. Org. Chem.* **2004**, *69*, 439.
[21] R. Sayah, K. Glegola, E. Framery, V. Dufaud, *Adv. Synth. Catal.* **2007**, *349*, 373.
[22] K. Smith, *Solid supports and catalysts in organic reactions*, Ellis Horwood Ltd, Chichester, **1992.**
[23] B. Lin, Z. Liu, M. Liu, C. Pan, J. Ding, H. Wu, J. Cheng, *Catal. Commun*. **2007**, *8*, 2150.
[24] S. S. Soomro, C. Röhlich and K. Köhler, *Advanced Synthesis & Catalysis*, **2011**, *353*, 767.
[25] N.T. Lucas, J.M. Hook, A.M.McDonagh, S.B. Colbran, *Eur. J. Inorg. Chem.* **2005**, 496.
[26] G. Villaverde, A. Corma, M. Iglesias, F. Sánchez, *ChemCatChem*, **2011**, *3*, 1320.
[27] E. Tyrrell, L. Whiteman, N. Williams, *J. Organomet. Chem.*, **2011**, *696*, 3465.
[28] A. J. Arduengo, H. V. R. Dias, R. L. Harlow, M. Kline, *J. Am. Chem. Soc.* **1992**, *114*, 5530.
[29] C. M. Zhang, J. K. Huang, M. L. Trudell, S. P. Nolan, *J. Org. Chem.* **1999**, *64*, 3804.

[30] J. K. Huang, E. D. Stevens, S. P. Nolan, J. L. Petersen, *J. Am. Chem. Soc.* **1999**, *121*, 2674.
[31] V. P. W. Böhm, C. W. K. Gstöttmayr, T. Weskamp, W. A. Herrmann, *J. Organomet. Chem.* **2000**, *595*, 186.
[32] J. K. Huang, S. P. Nolan, *J. Am. Chem. Soc.* **1999**, *121*, 9889.
[33] J.K. Huang, G. Grasa, S. P. Nolan, *Org. Lett.* **1999**, *1*, 1307.
[34] L. Jafarpour, E. D. Stevens, S. P. Nolan, *J. Organomet. Chem.* **2000**, *606*, 49.
[35] O. Diebolt, P. Braunstein, S. P. Nolan, C. S. J. Cazin, *Chem. Commun.* **2008**, 3190.
[36] F. Glorius, G. Altenhoff, R. Goddard, C. Lehmann, *Chem. Commun.* **2002**, 2704.
[37] V. Lavallo, Y. Canac, C. Prasang, B. Donnadieu, G. Bertrand, *Angew. Chem. Int. Ed.* **2005**, *44*, 5705.
[38] M. G. Organ, S. Çalimsiz, M. Sayah, K. H. Hoi, A. J. Lough, *Angew. Chem. Int. Ed.* **2009**, *48*, 2383.
[39] L. Wu, E. Drinkel, F. Gaggia, S. Capolicchio, A. Linden, L. Falivene, L. Cavallo, R. Dorta, *Chem. Eur. J.* **2011**, *17*, 12886.
[40] G. C. Vougioukalakis, *Chem. Eur. J.* **2012**, *18*, 8868.
[41] N. Gürbüz, I. Özdemir, T. Seçkin, B. Çetinkaya, *J. Inorg. Organomet. Polym.* **2004**, *14*, 149.
[42] A. Monge-Marcet, R. Pleixats, X. Cattöen, M.W.C. Man, *Catal. Sci. Technol.*, **2011**, *1*, 1544.
[43] P. D. Stevens, G. F. Li, J. D. Fan, M. Yen, Y. Gao, *Chem. Commun.* **2005**, 4435.
[44] S. Tandukar, A. Sen, *J. Mol. Catal. A-Chem.* **2007**, *268*, 112.
[45] V. Polshettiwar, R. S. Varma, *Tetrahedron* **2008**, *64*, 4637.
[46] H. L. Qiu, S. M. Sarkar, D. H. Lee, M. J. Jin, *Green Chem.* **2008**, *10*, 37.
[47] S. Dastgir, K. S. Coleman, M. L. H. Green, *Dalton Trans.* **2011**, *40*, 661.
[48] L. Wang, S. Shylesh, D. Dehe, T. Philippi, G. Dörr, A. Seifert, Z. Zhou, M. Hartmann, R. N. Klupp Taylor, M. Jia, S. Ernst, W. R. Thiel, *ChemCatChem* **2012**, *4*, 395.
[49] G. Borja, A. Monge-Marcet, R. Pleixats, T. Parella, X. Cattoën, M. W. C. Man, *Eur. J. Org. Chem.* **2012**, 3625.
[50] J. Blummel, *Coord. Chem. Rev.*, **2008**, *252*, 2410.
[51] T. Posset, J. Blummel, *J. Am. Chem. Soc.*, **2006**, *128*, 8394
[52] G.A. Grassa, M.S. Viciu, J. Huang, C. Zhang, M.L. Trudell, S.P. Nolan, *Organometallics,* **2002**, *21*, 2866..
[53] D.P. Allen, M.M. van Wingerden, R. H. Grubbs, *Org. Lett.* **2009**, *11*, 1261.
[54] A. Monge-Marcet, R. Pleixats, X. Cattoën, M. W. C. Man, *J. Mol. Catal. A-Chem.* **2012**, *357*, 59.
[55] S.C. Schürer, S. Gessler, N. Buschmann, S. Blechert, *Angew. Chem. Int. Ed.*, **2000**, *39*, 3898.
[56] Y. Yang, N. Priyadarshani, T. Khamatnurova, J. Suriboot, D.E. Bergbreiter, *J. Am. Chem. Soc*. **2012**, *134*, 14714.
[57] T.P. Nguyen, P. Hesemann, P. Gaveau, J.J.E. Moreau, *J. Mater. Chem.*, **2009**, *19*, 4164.
[58] H. Yang, G. Li, Z. Ma, J. Chao, Z. Guo, *J. Catal.*, **2010,** *276*, 123.

[59] G. Lin, H. Yang, W. Li, G. Zhang, *Green Chem.*, **2011**, 13, 2939
[60] H. Zhou, Y. M. Wang, W. Z. Zhang, J. P. Qu, X.B. Lu, *Green Chem.* **2011**, *13*, 644.
[61] S. Wolf, H. Plenio, *J. Organomet. Chem.*, **2009**, 694, 1487.
[62] S. Meiries, K. Speck, D. B. Cordes, A. M. Z. Slawin, S. P. Nolan, *Organometallics*, **2013**, *32*, 330.
[63] S. Leuthäußer, D. Schwartz, H. Plenio, *Chem. Eur. J.*, **2007**, 13, 7195.
[64] C. Hongfa, H.L. Su, H. S. Bazzi, D.E. Bergbreiter, *Org. Lett.* **2009**, 11, 665.
[65] S. Shahane, L. Toupet, C. Fischmeister, C. Bruneau, *Eur. J. Inorg. Chem.* **2013**, *2013*, 54.
[66] D. A. Bansleben, E. F. Connor, R. H. Grubbs, J. I. Henderson, T. R. Younkin, A. R. Nadjadi, Jr. (Cryovac, Inc.), *US Patent* 6,197,714, **2001**; *Chem. Abstr.* **2000**, *133*, 267224.
[67] K. Shiboya, K. Kawamine, Y. Sato, T. Miura, C. Ozaki, T. Edano, M. Hirata (Kowa Company, Ltd.), *European Patent* 0,987,254, **2004**; *Chem. Abstr.* **1998**, *130*, 52439.
[68] K. R. Reddy, C. U. Maheswari, M. Venkateshwar, M. L. Kantam, *Adv. Synth. Catal.* **2009**, *351*, 93.
[69] S. Ung, A. Falguières, A. Guy, C. Ferroud, *Tetrahedron Lett.* **2005**, *46*, 5913.
[70] a) E. Bamberger, *Chem. Ber.* **1894**, *27*, 1347; b) E. Bamberger, *Chem. Ber.* **1894**, *27*, 1548; c) T. Sone, K. Hamamoto, Y. Seiji, S. Shinkai, O. Manabe, *J. Chem. Soc.-Perkin Trans. 2* **1981**, 1596.
[71] C. Hobbs, Y. C. Yang, J. Ling, S. Nicola, H. L. Su, H. S. Bazzi, D. E. Bergbreiter, *Org. Lett.* **2011**, *13*, 3904.
[72] L. Benhamou, E. Chardon, G. Lavigne, S. Bellemin-Laponnaz, V. César, *Chem. Rev.* **2011**, 111, 2705.
[73] L. Hintermann, *Beilstein J. Org. Chem.*, **2007**, 3, 22.
[74] O. Navarro, N. Marion, N. M. Scott, J. González, D. Amoroso, A. Bell, S. P. Nolan, *Tetrahedron* **2005**, *61*, 9716;
[75] W. Lin, Q. Cai, W. Pang, Y. Yue, *Chem. Commun.*, **1998**, 2473.
[76] G. Künstle, H. Siegl (Wacker-Chemie GmbH), *US Patent* 3,960,909, **1976**; *Chem. Abstr.* **1975**, *83*, 208102.
[77] J. Cooke, O. C. Lightbody, *J. Chem. Educ.* **2011**, *88*, 88.
[78] N. Marion, P. de Frémont, I. M. Puijk, E. C. Ecarnot, D. Amoroso, A. Bell, S. P. Nolan, *Adv. Synth. Catal.* **2007**, *349*, 2380.
[79] A. G. Giumanini, G. Verardo, P. Geatti, P. Strazzolini, *Tetrahedron* **1996**, *52*, 7137.

UNIVERSITAT ROVIRA I VIRGILI
HETEROGENIZED N-HETEROCYCLIC CARBENE METAL COMPLEXES FOR SELECTIVE CATALYSIS
Alberto Martínez Lombardía

UNIVERSITAT ROVIRA I VIRGILI
HETEROGENIZED N-HETEROCYCLIC CARBENE METAL COMPLEXES FOR SELECTIVE CATALYSIS
Alberto Martínez Lombardía

Chapter 4

"Application of solid-supported [Pd(NHC)] complexes in Suzuki-Miyaura, Heck and Sonogashira couplings. Studies under batch and continuous flow conditions."

UNIVERSITAT ROVIRA I VIRGILI
HETEROGENIZED N-HETEROCYCLIC CARBENE METAL COMPLEXES FOR SELECTIVE CATALYSIS
Alberto Martínez Lombardía

> Application of solid-supported [Pd(NHC)] complexes in Suzuki-Miyaura, Heck and Sonogashira couplings. Studies under batch and continuous flow conditions

4.1. Introduction

Palladium-catalyzed cross-coupling reactions constitute one of the most efficient methods for the construction of carbon-carbon bonds.[1,2,3] These cross-coupling methodologies have lead to a major improvement in synthetic organic chemistry, shifting paradigm from consecutive reaction steps using protected substrates to a direct C-C formation in one step. These remarkable advances were deservedly recognized with the award of the Nobel Prize in Chemistry in 2010 to the trio of Richard F. Heck, Ei-ichi Negishi[4] and Akira Suzuki[5]. This type of reactions consists in the carbon-carbon bond formation between a less reactive organic electrophile, R^1-X, and an organometallic nucleophile, R^2-m (m is a metal or a semi-metal), in the presence of a catalyst [M] (Scheme 4.1), except for the Heck-Mizoroki coupling where the organometallic reagent is substituted by an alkene. In some of these reactions, a base is required and plays different roles within the catalytic cycle.[6] C-C cross-coupling reactions are often classified depending on the metal or semi-metal present in the nucleophile. For instance, Suzuki-Miyaura[1] is boron-mediated, Stille[7] reaction is tin-mediated, Negishi[8] reaction zinc-mediated, etc... The catalysts most widely employed are transition metal complexes from groups 8-10, and particularly complexes of palladium.

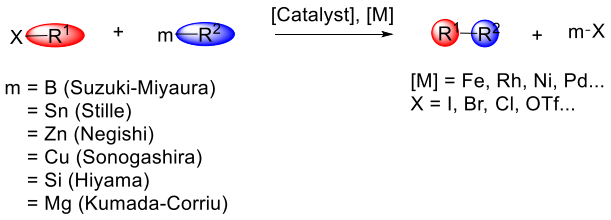

Scheme 4.1. General scheme of metal-catalyzed cross-coupling reactions.

These cross-coupling processes follow a reaction mechanism involving three main steps: an oxidative addition of the organic electrophile to an electron-rich coordinatively unsaturated Pd(0) complex, transmetalation of an organic fragment carried by a suitable organometallic reagent, and finally a C-C bond is formed from two Pd-bonded organic fragments via reductive elimination, thus regenerating

the active catalytic species (Scheme 4.2). Among these C-C bond-forming processes, Suzuki-Miyaura, Heck and Sonogashira have found very wide applicability in both industry and academia, and have thus been thoroughly studied.[9,10,11,12]

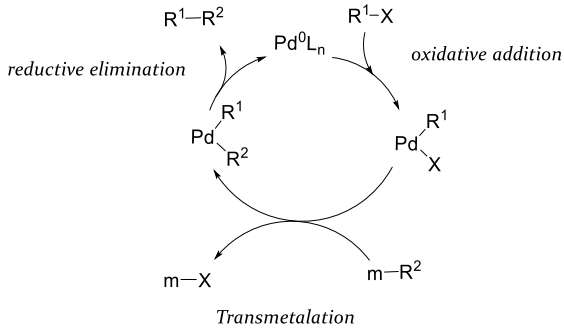

Scheme 4.2. General catalytic cycle for Pd-catalyzed cross-coupling reactions.

4.1.1. Suzuki-Miyaura, Heck and Sonogashira couplings under homogeneous reaction conditions

The work described in this chapter deals with the application of supported Pd catalysts in Suzuki-Miyaura, Heck and Sonogashira. In the next pages, fundamental concepts about these reactions will be addressed, as well as the type of substrates, the catalyst systems and the reaction mechanisms.

4.1.1.1. General aspects about substrate scope and catalyst systems for these cross-coupling reactions

The electrophiles used in these coupling reactions are either aryl or vinyl fragments connected to a halide or pseudohalide such as triflate or tosyl derivatives. In the first step of the catalytic cycle, the electrophile adds oxidatively to the catalytically active Pd species, where the Pd complex increases its coordination number, and its oxidation state by two units. The rate at which this elementary step may proceed depends upon the strength of the C-X bond in the substrate; the bond dissociation enthalpies for chloro-, bromo- and iodobenzene have been calculated and they range from X = Cl 95.5 ± 1.5 kcal mol^{-1}; X

= Br 80,4 ± 1.5 kcal mol^{-1} to X = I 65,0 ± 1 kcal mol^{-1}.[13] Therefore, iodide substrates are the easiest to couple, whereas chorides represent the most challenging type. Yet from the standpoints of cost and availability, chloride substrates are more attractive than the corresponding iodides, bromides or triflates, and thus much effort has been put forth to design catalysts able to activate C-Cl bonds.[14]

Historically, Pd catalysts bearing phosphorus-based ligands, and particularly triarylphosphines, such as triphenylphosphine have been employed for the coupling of iodo- and bromoaryl substrates, due to their superior stability compared to trialkylphosphines.[15] Most of the systems able to activate iodides and bromides were also effective in the coupling of electron-poor aryl chlorides (Figure 4.1).

Activated aryl chlorides can be classified in two subclasses, heteroaryl chlorides and substrates where the aromatic ring is functionalized with an electron-withdrawing group, such as nitro, cyano, carboxy, fluoro, trifluoromethane... Most of the systems studied are formed in situ by combining a Pd precursor that can be a Pd(0) such as $Pd_2(dba)_3$ or a Pd(II) species such as $Pd(OAc)_2$ with a phosphorus-based ligand.[16] Phosphines have been most widely employed,[17] but bulky phosphites are also effective.[18] In addition to P ligands, other options have been successfully applied such as diazabutadienes,[19] *N*-heterocyclic carbenes[20] or even ligandless Pd,[21] but applying these catalysts in the coupling of unactivated electron-neutral or electron-rich chlorides led to poor results (Figure 4.1).[22,23,24]

The efficient coupling of unactivated aryl chlorides was not achieved until 1998 (Figure 4.2).[25] Büchwald proved that the use of dialkyl aryl phosphines bearing a biphenyl aryl substituent were able to couple deactivated aryl chlorides even at room temperature. Fu et al. reported that bulky electron rich trialkyl phosphines such as tri(tert-butyl) phosphine and tricyclohexyl phosphine efficiently coupled a wide array of deactivated chlorides.[26]

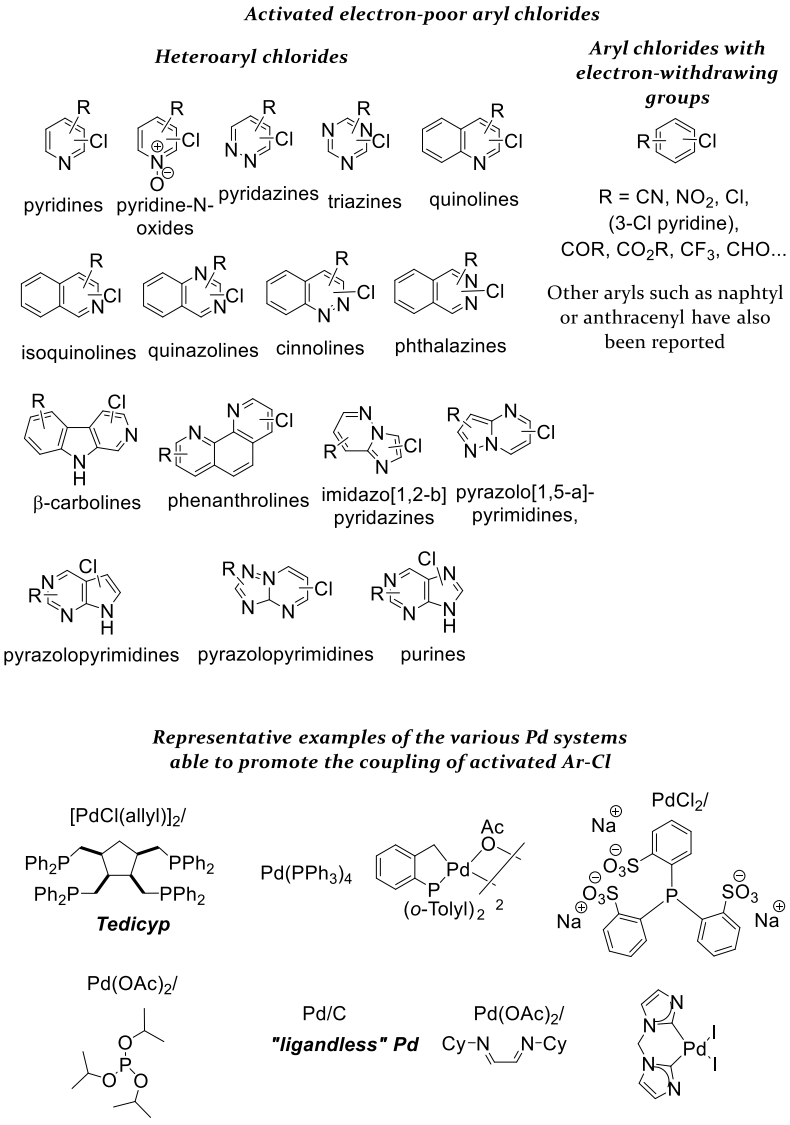

Figure 4.1. Examples of activated electron-poor aryl chlorides and some of the catalyst systems reported for their conversion into coupling products.

Alternatively to P based ligands, Nolan reported the Suzuki coupling of deactivated aryl chlorides using a [Pd(IMes)] catalyst generated in situ from $Pd_2(dba)_3$ and IMes·HCl in the presence of a base.[27] Compared to the air-sensitive alkyl phosphines, the advantage of this system is to use the air and moisture-stable IMes·HCl to generate the carbene ligand in situ.

Application of solid-supported [Pd(NHC)] complexes in Suzuki-Miyaura, Heck and Sonogashira couplings. Studies under batch and continuous flow conditions

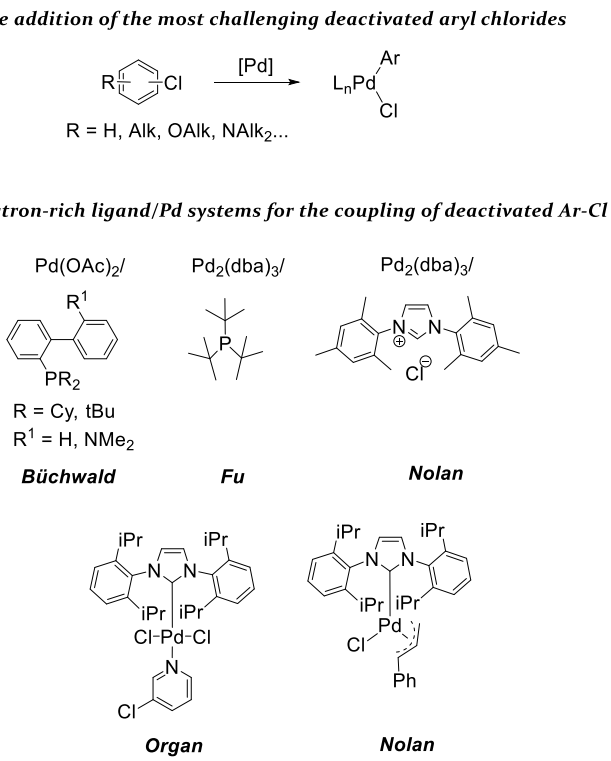

Figure 4.2. Relevant examples of catalysts systems reported for the coupling of deactivated aryl chlorides.

The efficiency of these ligands has mostly been attributed to their electron-rich character thus facilitating the oxidative addition of the Ar-Cl bond. Their high steric demand also favors the reductive elimination step, yielding the coupling product and regenerating the highly reactive monoligated Pd species.[28,29] Nowadays, NHCs stand as an ideal ligand class for this type of cross coupling reactions, owing to their stronger donor capacity compared to phosphines and the possibility to tune the steric and electronic environment of the ligand.[14] Various preformed [Pd(NHC)] precatalysts have displayed outstanding efficiency, coupling deactivated, and sterically hindered aryl chlorides at room temperature at low catalyst loadings.[30,31,32]

4.1.1.2. Reaction mechanism

In the case of Suzuki-Miyaura and Sonogashira reactions, the general reaction mechanism is closely resembled to the general catalytic cycle shown in Scheme 4.2, although some remarks can be pointed out. In the Suzuki coupling an external base is used to promote the reaction. Indeed theoretical calculations have shown a high energy barrier for the endothermic Suzuki.[6] The added base may act as depicted in Scheme 4.3. In the basic reaction medium OH^- can be generated from traces of water (if non-aqueous reaction conditions are employed), and it binds to the boronic acid, generating an organoboronate species that transmetalates the organic group to Pd (Pathway A, Scheme 4.3).

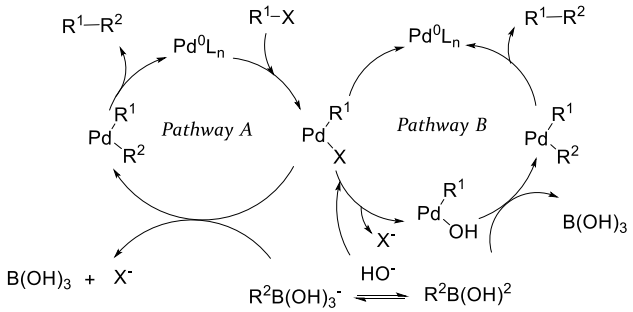

Scheme 4.3. Catalytic cycles for the Pd-catalyzed Suzuki-Miyaura coupling.[6]

In some cases, alternative pathway B has been proposed involving halide exchange by OH^- followed by transmetalation[33]. The other steps in the cycle are common to other cross-coupling reactions.

Typically, the Sonogashira reaction starts with an oxidative addition of the aryl halide or triflate to the Pd complex (Scheme 4.4). The most classical reaction conditions involve the use of a Cu(I) salt as a cocatalyst and a base which is usually a tertiary amine. The base assists the formation of a copper-acetylide complex, which is the actual transmetalating agent. The copper is not reduced in the process, so only a catalytic amount is required, whereas the base is used in stoichiometric amounts. In some cases, the presence of Cu(I) salts revealed an inhibitory effect in the Sonogashira reaction,[34,35] and consequently copper-free protocols have been developed. Thus, the

alternative copper-free Sonogashira reaction proceeds through the deprotonation of the π-bound alkyne in the presence of a base[36] forming a σ-bound Pd-alkynyl intermediate that undergoes reductive elimination with the other R group attached to the metal to yield the disubstituted alkyne product.

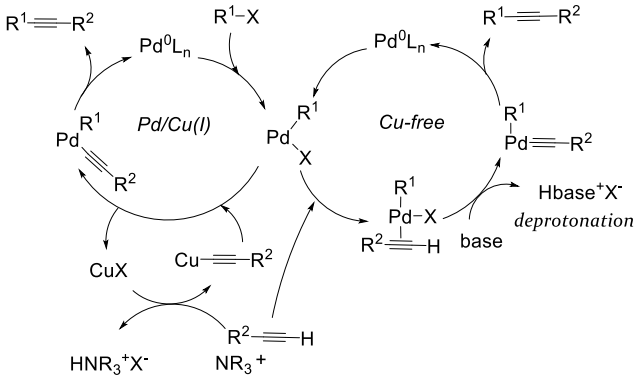

Scheme 4.4. Mechanistic picture of the Sonogashira reaction. Pd(0)/Cu(I) (left) and Pd/Cu-free variants.[6]

The Heck reaction proceeds in a slightly different manner, since the electrophile is coupled with an alkene instead of a metal/semi-metal containing nucleophile (Scheme 4.5).[2]

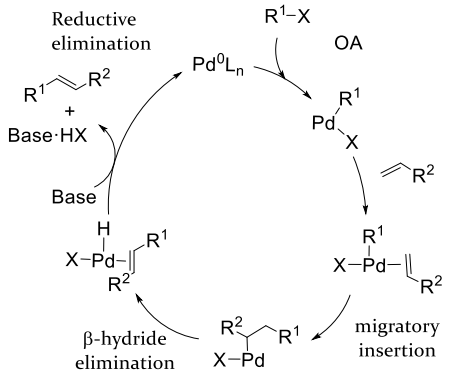

Scheme 4.5. Catalytic cycle for the Heck-Mizoroki coupling.[2]

The olefin coordinates to the Pd(II) intermediate, and undergoes subsequent migratory insertion into the Pd-Ar[1] bond to generate a Pd-

alkyl species, thus forming the new C-C bond. From this intermediate, ß-hydride elimination results in the formation of a Pd(II)-hydride with a π-bound olefin product. The Heck coupling product is released and the Pd-hydride reductively eliminates in the presence of a base to regenerate the catalytically active Pd(0) species.

4.1.1.3. Exploiting the potential of Pd-catalyzed C-C couplings

To highlight the relevance of these Pd-mediated transformations some examples of complex organic molecules which are currently synthesized at industrial scale through a synthetic route involving at least one metal-catalyzed cross-couplings step are displayed (Figure 4.3).[37,38,39]

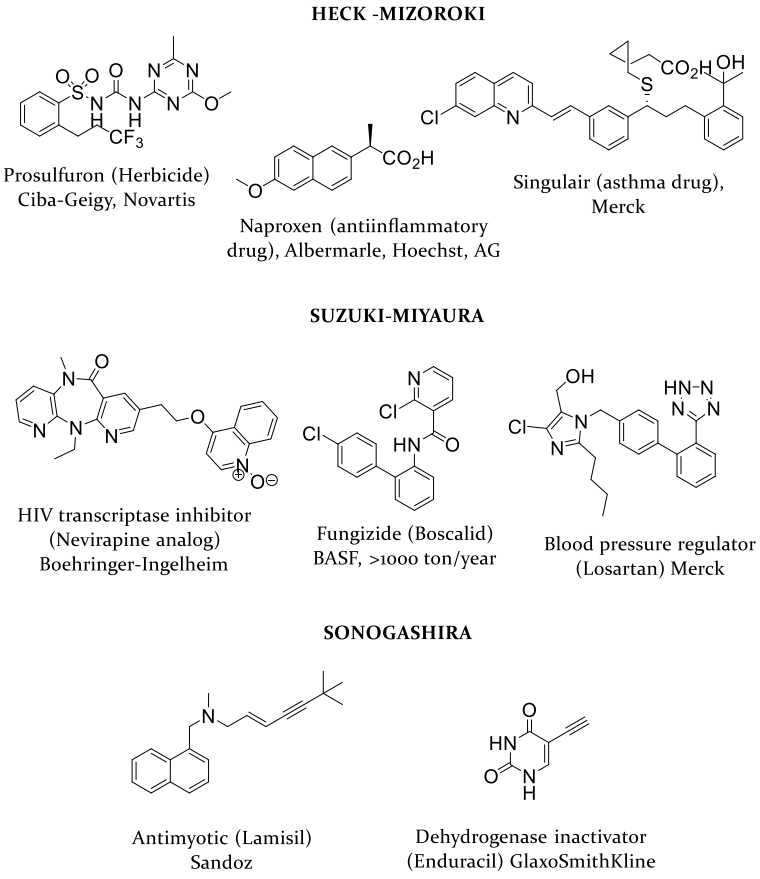

Figure 4.3. Examples of industrially relevant products involving a metal-catalyzed cross-coupling step in the synthetic route.[38]

> Application of solid-supported [Pd(NHC)] complexes in Suzuki-Miyaura, Heck and Sonogashira couplings. Studies under batch and continuous flow conditions

The synthesis of multikilogram quantities of high added value products principally from the pharmaceutical, fine chemicals and agrochemicals sectors relies upon these transformations and the catalysts that make them possible. In spite of their high efficiency there's still room for improvement since several drawbacks can be pointed out.

When Pd-catalysis is applied to the synthesis of biologically active compounds at meso- or industrial scale, several factors need to be considered: due to its elevated cost, the TON achieved needs to be sufficiently high to be cost-effective compared to other (non-catalytic) synthetic routes; moreover, there's an important issue of product contamination with residual metal and ligands. This is of special concern in the case of pharmaceuticals, where stringent regulations apply and usually the heavy metal content in API's (Active Pharmaceutical Ingredients) has to be controlled to levels below 10 ppm.[40]

Scavenging methods are effective especially when ligand-less or colloidal Pd(0) is used,[41,42,43,44]However, complications arise for the case of less reactive substrates such as aryl chlorides or alkyl halides for instance which require the presence of Pd in combination with sophisticated "state of the art" ligands such as bulky, electron-rich monophosphines,[45,46,47] which are sometimes even more expensive than the metal itself. In these cases, Pd may remain ligated to the phosphine or interacting with some additives and it may remain in solution, thus difficulting its adsorption by the scavenger.

Several approaches may help to improve the efficiency of these catalytic processes (Scheme 4.6). Much effort has been devoted to the design of improved catalysts able to activate the most challenging substrates, achieving high TON and working under mild reaction conditions.[33,31] Catalysts based on cost-effective non-precious metals such as copper,[48] nickel or iron[49] have been developed, although they do not constitute an alternative to Pd catalysts to date. A lot of work has been carried out to develop recyclable catalysts with the aim of combining great efficiency and building up high cumulative TON by recovering and reusing the catalyst in successive operations.

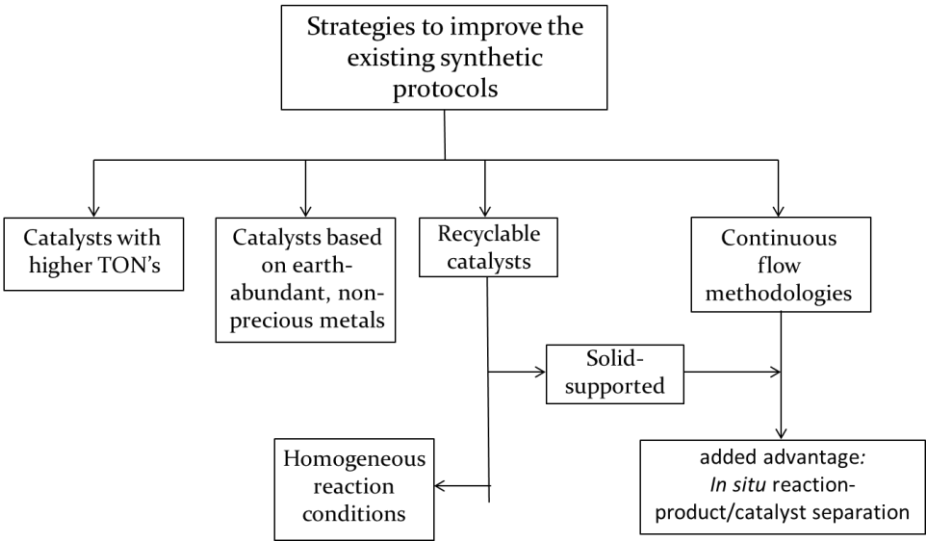

Scheme 4.6. Strategies to improve the synthesis of complex organic molecules such as API's.

Homogeneous (or liquid-liquid biphasic) reaction conditions have been applied, showing great potential. The most important systems are based on Pd catalysts stabilized by ionic liquids.[50,51,52] Clearly, the vast majority of the work on recyclable catalysts has been devoted to solid-supported (heterogeneous) catalysts due to the ease of recovery and reuse by filtration or centrifugation.[53]

Finally, though it cannot strictly be considered as a mean of catalyst recycling, operation in continuous flow reactors provides various appealing advantages[54] (already commented in Chapter 1), and especially the combination of continuous flow reactors with heterogenized catalysts constitutes a very desirable synthetic strategy since it allows for the recovery and reuse of the catalysts while obtaining the desired products with minimal cost in terms of time and waste.[55]

Application of solid-supported [Pd(NHC)] complexes in Suzuki-Miyaura, Heck and Sonogashira couplings. Studies under batch and continuous flow conditions

4.1.2. Heterogeneous catalysts for Suzuki-Miyaura, Heck and Sonogashira couplings

A plethora of heterogeneous Pd catalysts have been developed and applied in C-C cross coupling processes over the recent years, and they have been comprehensively reviewed.[36,56] The reported catalysts mainly differ in i) chemical nature (organic, inorganic, or hybrid organic-inorganic) of the solid matrix containing the Pd catalyst, and ii) the nature of the catalyst attachment (chemical or physical entrapment), which, in turn, is related to the nature of the attached catalyst (a Pd organometallic complex or Pd nanoparticles[57]). Due to the vast amount of reports in this area, and the lack of uniform criteria to present the collected data a direct comparison between the different catalysts types is practically not feasible. However, the big efforts undertaken to date have certainly helped to expand the knowledge in this field of research and to shed light on the challenges, and requirements which should guide the development of improved heterogeneous catalysts.

When using heterogeneous, supported Pd catalysts in cross-coupling chemistry, several mechanistic pictures need to be considered (Scheme 4.7).[58] Three main cycles may contribute to a certain extent in the formation of the coupling product. On one hand, the supported catalyst may act as a truly heterogeneous system providing a stable linkage with the support. This possibility is applicable to either heterogenized complexes or supported Pd NPs. Another possibility is that “naked” Pd atoms leave the surface of the support by dissociation from the original catalyst precursor. Finally, in the case of particulate catalysts, the presence of the substrate may be responsible to oxidatively add to a surface Pd atom, thus facilitating its release into the reaction medium. The last two cycles actually involve homogeneous catalysis. A completely heterogeneous cycle is the most desirable scenario, as it grants the absence of contaminating metal in the reaction products, and moreover, enables the use of the heterogeneous phase catalyst under continuous flow conditions.

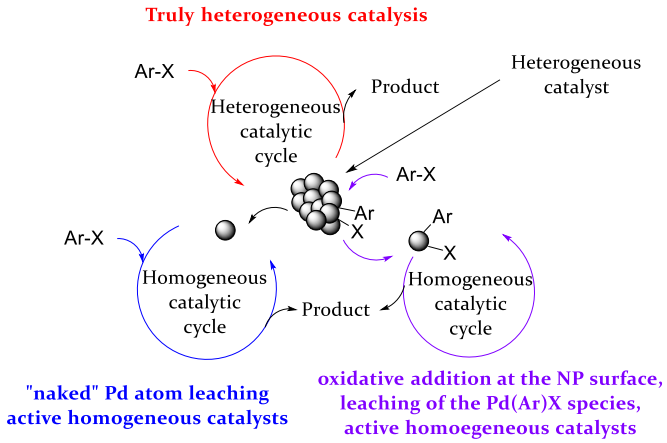

Scheme 4.7. Catalytic cycles that may be in operation when using supported Pd catalysts in cross-coupling reactions.

Since most of the reported heterogeneous catalysts have been typically tested in various cross-couplings with satisfactory results, in the following, observations, comments and explanations about the distinct catalyst materials will be made regardless of which particular cross-coupling they have been successfully applied in.

4.1.2.1. Recyclable supported catalysts applied in C-C cross couplings.

The first commercially available heterogeneous Pd catalysts for C-C cross couplings were based on Pd particles supported on inorganic materials such as Pd/C, Pd/SiO_2 or Pd/Al_2O_3. They were effective in the Suzuki, Heck and Sonogashira couplings providing up to 36000 TON upon successive reuses.[59,60] Whilst these catalysts performed well for the coupling of the more reactive aryl iodides, activation of challenging substrates was elusive. Therefore there was a need to develop more sophisticated catalyst materials.[36]

In response to this need, many efficient catalysts have been developed. Nanoparticles (preformed or *in situ* generated) as well as Pd complexes or even Pd salts immobilized on organic, or inorganic (or hybrid) supports have been described in this respect. Organic support materials can roughly be classified in polymeric beads, or fibers, encapsulated catalysts... etc.[65] The structure of this polymeric materials can be

tailored by varying the synthetic route, and different types of ligands or functional groups can be introduced. Among inorganic supports besides the use of silica or alumina materials, many other types have been explored: metal organic frameworks (MOFs),[61] Pd embedded in polyoxometalates and supported on a carrier, [62] Pd incorporated in perovskite type structures,[63] or materials prepared by sol-gel techniques,[64] only to cite some of the most relevant.

Criteria to assess the performance of a supported catalyst applied in C-C coupling reactions

In many cases, leached Pd from the heterogeneous phase contributes to some extent to the catalytic cycle.[65] However, this does not necessarily limit the practical synthetic advantages of these materials, although the cases for which the catalyst is recyclable and leaching is limited must be distinguished from options for which the catalyst is strongly modified and the original activity is dramatically reduced after one run. Pagliaro addressed this issue and introduced some criteria in order to assess the performance of a supported catalyst and to grant comparison between the different catalyst types. According to his criteria, hot filtration tests should be performed, to tell if there's any "homogeneous" contribution from leached Pd. However, inactive leached species may lead to an erroneous interpretation of this test, and therefore actual values of leached Pd should be measured. Then, the activity of the catalyst in further recycles may show if any deactivation is occurring. Nonetheless these data may not be completely reliable since excessive reaction times are sometimes used, and therefore, catalyst deactivation upon recycling can be masked. Another point is that new catalysts should be tested in the coupling of challenging substrates, because even traces of Pd in the ppb or ppm level can promote the coupling of aryl iodides and bromides.[65]

Various tools have been applied to evaluate the nature of the catalytically active species, for instance the mercury drop test (mercury is known to amalgamate metallic Pd but not homogeneous Pd complexes), [66] and the three-phase test,[74] where one of the reagents is bound to a solid support, therefore, a true heterogeneous catalyst would

be inactive due to limitations in diffusion and accessibility to (and of) the active sites. Addition of solid or soluble poisons, such as thiol- or urea-containing resins which can trap Pd clusters or particles has been used to assess hetereogeneity of a supported catalyst.

However, from a practical perspective, what really matters most when evaluating a supported catalyst is the total TON that can be achieved, and the related TOF. That should be the ultimate goal, for productivity and environmental reasons.[36,67] In this respect, the two highest TON displayed by any supported catalysts in any cross-coupling reaction involving bromide substrates were achieved using catalysts **15** and **16** (Figure 4.4).[53]

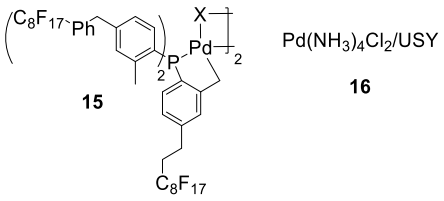

Figure 4.4. Most active catalysts reported for cross-coupling reactions involving aryl bromides.

Catalyst **15** could be reused 5 times without noticeable decrease in activity, achieving a total TON of 530000 in the Suzuki coupling between 4-bromomandelic acid with phenylboronic acid.[68] Catalyst **16**, consists in *in situ* generated Pd nanoclustes in the nanocages of zeolite USY.[69] This catalyst provided TON of 5300000 in the Suzuki coupling between 4-bromoacetophenone and phenylboronic acid. However, these results compare unfavorably to the use of $Pd(OAc)_2$ in the Heck coupling between bromobenzene and styrene, for which TON 47000000 was reported by Köhler et al.[70]

The main conclusion that can be drawn from these examples is that in most cases, the supported systems have not reached the TON achieved when using homogeneous catalysts.[55] Indeed, in industry, very often, the use of ligand-less systems, such as $Pd(OAc)_2$ is preferred for the cross-coupling of aryl iodides and bromides. [71,38]

> Application of solid-supported [Pd(NHC)] complexes in Suzuki-Miyaura, Heck and Sonogashira couplings. Studies under batch and continuous flow conditions

Supported Pd catalysts for the C-C coupling of aryl chlorides

Because of the intrinsic advantages of heterogeneous catalysis regarding separation of the catalyst from the products and avoiding metal contamination, efforts continue towards the design of more active heterogeneous catalysts. In this regard, the development of supported catalysts able to promote the coupling of the least reactive aryl chlorides represents an important challenge. It is well-known that coordination of a ligand modifies the reactivity of a metal catalyst.[72,73] With a few exceptions[62,74,75] activation of aryl chlorides has mostly been achieved by the use of immobilized Pd complexes featuring electron-donating ligands such as phosphines or NHC's (Figure 4.5).

Catalysts **19**[76] and **21**[77] were shown to be truly heterogeneous according to hot filtration tests and Pd analysis on the reaction mixtures; moreover, catalyst **22** could be recycled up to 10 times without observable decrease in activity for the coupling of 4-chloroanisole with phenylboronic acid. Catalyst **21** showed the highest level of activity, very close indeed to that of unsupported catalyst **22** which is one of the most active catalysts reported for the Suzuki coupling.[31] However, recycling and reusing this catalyst was unsuccessful. Catalyst **17** promoted the Suzuki coupling between 2-methylchlorobenzene and phenylboronic acid.[78] However, recycling of deactivated aryl chlorides was not reported. Hybrid organic-inorganic silica material **21** developed by Yang could be recycled up to three times in the Suzuki coupling between 4-chloroacetophenone and phenylboronic acid before activity started to drop.[79]

In view of the published results, evaluation of the maximum TON that can be reached with these systems is lacking, and therefore the long-term stability of these catalysts remains uncertain. While the presented examples refer to the Suzuki coupling, literature reports on recyclable catalysts able to promote the Sonogashira coupling of aryl chlorides are much scarcer.[76,80]

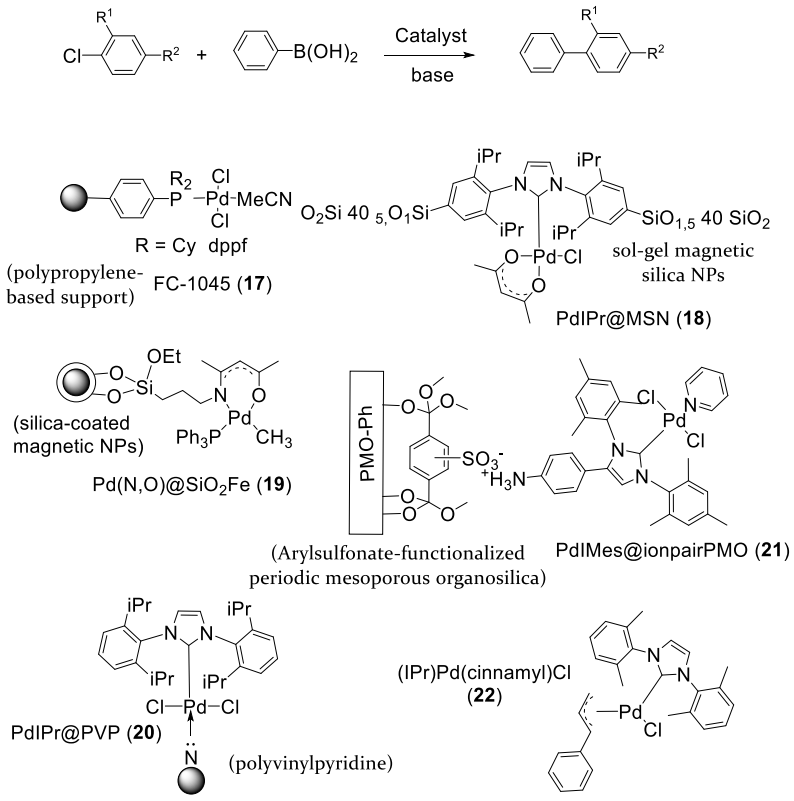

Figure 4.5. Supported Pd complexes active in the Suzuki coupling of aryl chlorides.

On the contrary, extensive reports have been made on the application of heterogeneous catalysts in the Heck reaction,[36] but very few of them could promote the Heck coupling of unreactive aryl chlorides in repeated runs.[81,82,83,84] In the Heck reaction, catalysts decomposition to generate catalytically active Pd NP's has been reported for many homogeneous systems, including Pd pincers,[85] palladacycles[86,87] and [Pd(NHC)][66], this phenomenon is favored when the reaction is performed at higher temperatures,[88] and may explain the fast loss of activity of the recyclable catalysts due to the progressive agglomeration of Pd particles. Therefore, the development of supported catalysts with improved stability remains challenging.

Application of solid-supported [Pd(NHC)] complexes in Suzuki-Miyaura, Heck and Sonogashira couplings. Studies under batch and continuous flow conditions

4.1.2.2. Immobilized catalysts applied in C-C cross couplings under continuous flow conditions

In the recent years, a number of heterogeneous catalysts have been applied in various C-C cross coupling reactions under continuous flow conditions. Most of them were based on Pd and were recently reviewed.[89] The main requirements for a catalyst system to be implemented in a flow process are high activity, robustness, and high resistance to leaching. To cope with the issue of Pd leaching, several strategies have been developed[89] such as the use of scavengers after the catalyst bed[90] or performing the reactions in cyclic flow set-ups.[82] As also encountered in the case of heterogeneous Pd catalysts tested in batch experiments, most of the reported continuous flow tests refer to the more reactive aryl iodides,[91,92,93,94] and very often small scale tests are reported.[95]

Among the most robust systems reported[96] catalyst **23** (Figure 4.6) achieved a TON of 3800 in the Suzuki coupling of 4-bromotoluene with phenylboronic acid and only marginal Pd leaching was observed in the products thanks to the cyclic design of the flow system. [43] Importantly, a much lower E-factor (defined as Kg of waste per Kg of product manufactured) was calculated by the authors for the flow experiment compared with the corresponding batch process due to the need of a purification step and the difficulty in recovering the mix of solvents used when the reaction was performed under batch operation.

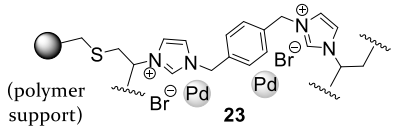

Figure 4.6. Pd NPs supported stabilized by a cross-linked matrix of IL, **23**.

Pagliaro and Béland reported on the application of commercially available SiliaCat-dPP-Pd in the Suzuki coupling between 2-chlorobenzonitrile and *p*-tolylboronic acid.[97] A rate enhancement was demonstrated when the optimum reaction conditions were transferred from batch to continuous flow experiments.

Many heterogeneous Pd systems have appeared in the last decades, yet truly heterogeneous catalysts able to efficiently couple challenging chloride substrates and having sufficient stability for prolonged use are lacking.

In the next section the results obtained in the application of supported Pd catalysts bearing bulky electron-rich NHC ligands in Suzuki, Heck and Sonogashira couplings will be presented and discussed.

4.2. Results and discussion

4.2.1. Application of solid-supported [Pd(NHC)] complexes in the Suzuki-Miyaura coupling of aryl bromides and chlorides with phenylboronic acids

In this section the heterogenized [Pd(NHC)] complexes described in Chapter 3 are used as catalysts in the Suzuki-Miyaura reaction with the objective of recycling and reusing the catalysts as well as applying them under continuous flow conditions. The application of catalysts supported on amorphous silica will be described. Subsequently, the influence of catalysts support material on the catalysts' performance will be studied, both in batch and in continuous flow experiments.

4.2.1.1. Studies on SiO_2-supported Pd-NHC catalysts; from batch tests to a continuous flow application

4.2.1.1.1. Optimization tests, substrate scope and recycling studies

Optimization of reaction conditions, and comparison between catalysts

Initial studies on SiO_2-immobilized [Pd(NHC)] complexes **11-14@SiO_2** (Chapter 3, Scheme 3.16 and Scheme 3.17) aimed at evaluating the impact of reaction parameters on the catalysts' performance in the coupling of 1-bromo-2,4-dimethylbenzene with 4-phenylboronic acid (Table 4.1). Entries 1-8 correspond to the application of catalysts **11a-14a@SiO_2** (Figure 4.7).

Application of solid-supported [Pd(NHC)] complexes in Suzuki-Miyaura, Heck and Sonogashira couplings. Studies under batch and continuous flow conditions

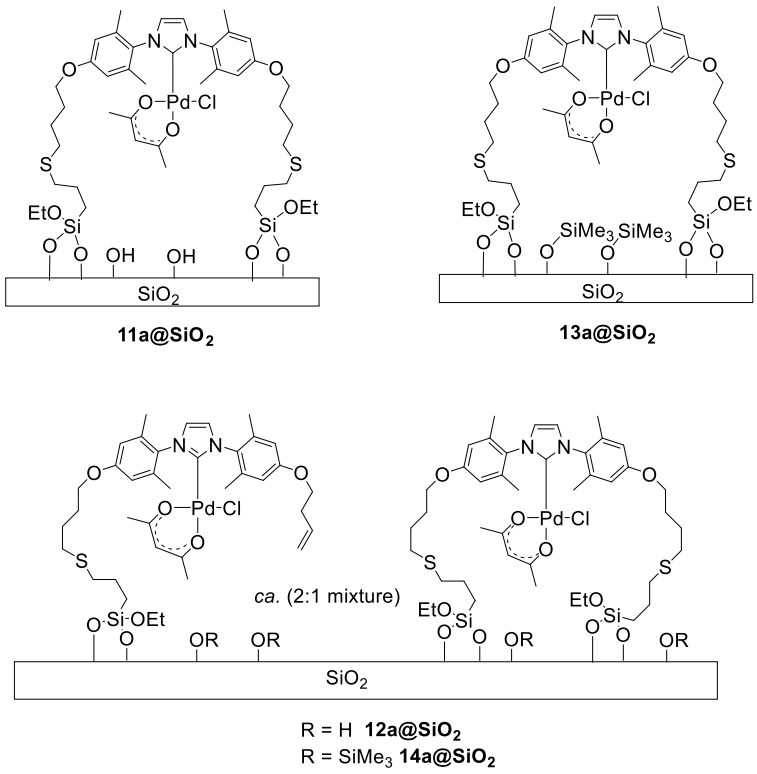

Figure 4.7. Molecular structure of catalysts **11a-14a@SiO$_2$**.

In contrast with other [Pd(NHC)] catalysts, where optimal reaction conditions comprised alkoxide bases in non-aqueous solvents such as iPrOH[98] or dioxane,[27] herein the best results were obtained when the reaction was carried out in a biphasic toluene/water mixture in the presence of carbonate bases (entries 1, 2, 4 vs entries 5, 6).[99] These conditions provide the added advantage of increased solubility of base and boronic acid partner. Moreover, the use of a mild base at relatively low temperatures (60°C) is highly desirable regarding the coupling of thermally sensitive or unstable substrates.[99] Next, the influence of a double (**11a@SiO$_2$**), or single linkage (**12a@SiO$_2$**) of the Pd complex with the support in the catalytic activity was evaluated (entry 2 vs entry 4), and similar results were obtained, indicating that the different linking mode does not have a large effect on catalysts activity for this particular ligand scaffold.

Table 4.1. Optimization of reaction conditions for the Suzuki Miyaura coupling of 1-bromo-2,4-dimethylbenzene (**24a**) with 4-methoxyphenylboronic acid (**25a**).

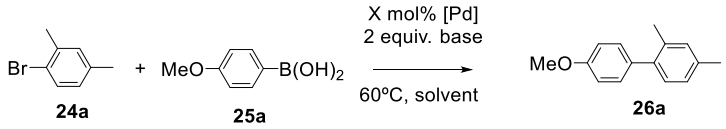

24a **25a** **26a**

E.	Cat.	Solv.	Base	t (h)	Yield(%)[a]
1	**11a@SiO$_2$** 2.5 mol% Pd	toluene/ H_2O	Na_2CO_3	20	69(1)
2	**11a@SiO$_2$** 1.5 mol% Pd	toluene/ H_2O	Cs_2CO_3	20	40(0)
3	**12a@SiO$_2$** 2.4 mol% Pd	toluene/ H_2O	Na_2CO_3	16	46(36)
4	**12a@SiO$_2$** 1.5 mol% Pd	toluene/ H_2O	Cs_2CO_3	20	35(1)
5	**12a@SiO$_2$** 2.4 mol% Pd	dioxane	KO^tBu	20	21(16)
6	**12a@SiO$_2$** 2.4 mol% Pd	dioxane	NaOMe	20	8(<1)
7	**12a@SiO$_2$** 2.4 mol% Pd	MeCN/H_2O	Na_2CO_3	20	49(44)
8	**14a@SiO$_2$** 1.8 mol% Pd	toluene/ H_2O	Na_2CO_3	20	35(56)
9	**11b@SiO$_2$** 1.8 mol% Pd	toluene/ H_2O	Na_2CO_3	20	52(0)
10	**11b@SiO$_2$** 2.0 mol% Pd	toluene/ H_2O	Cs_2CO_3	20	85(0)
11	**13b@SiO$_2$** 2.0 mol% Pd	toluene/ H_2O	Cs_2CO_3	5	87(0)
12	**12b@SiO$_2$** 1.5 mol% Pd	toluene/ H_2O	Cs_2CO_3	20	85(0)
13	**14b@SiO$_2$** 2.0 mol% Pd	toluene/ H_2O	Na_2CO_3	5	81(0)
14	**14b@SiO$_2$** 2.0 mol% Pd	toluene/ H_2O	K_2CO_3	5	81(0)
15	**14b@SiO$_2$** 2.0 mol% Pd	toluene/ H_2O	K_3PO_4	5	>95(0)
16	**14b@SiO$_2$** 2.0 mol% Pd	toluene/ H_2O	Cs_2CO_3	5	>95(0)
17	**14b@SiO$_2$**	toluene/	Cs_2CO_3	5	77(0)

Application of solid-supported [Pd(NHC)] complexes in Suzuki-Miyaura, Heck and Sonogashira couplings. Studies under batch and continuous flow conditions

	2.0 mol% Pd	H_2O			
18	**14b@SiO$_2$**	toluene/	Cs_2CO_3	5	88(0)
	1.0 mol% Pd	H_2O			

Conditions: 0,5 mmol 1-bromo-2,4-dimethylbenzene, 0,6 mmol 4-methoxyphenylboronic acid, 2 mL organic solvent or 1,5 mL organic solvent/0,75 mL H2O; reactions were run under Ar atmosphere, using degassed solvents. [a]Determined by GC-FID, yield based on ArBr, average of two runs; In parenthesis percent of 0.5 mmol ArB(OH)2 needed for C–C coupling converted to deboronation product

The selectivity of the reaction is influenced by the choice of the carbonate base; cesium carbonate was more efficient than sodium carbonate and no deboronation byproducts were formed with the former base (entry 4 vs entries 3, 7, 8).

In entries 8-18, results obtained in the application of materials bearing the bulkier 2,6-diisopropylphenyl motif (**11b-14b@SiO$_2$**) are displayed (Figure 4.8). Catalytic precursors based on this motif displayed higher activity in the coupling of **24a** with **25a** compared to catalysts bearing 2,6-dimethylphenyl substitution (entry 2 vs entry 10), a trend that is also observed in the case of unsupported [Pd(NHC)].[100] Capping the remaining silanol groups on the surface of amorphous silica-based materials resulted in enhanced activity compared to non-capped catalysts, and the former achieved the same conversions at much shorter reaction time (entry 10 vs entry 11). Finally, among end-capped catalysts bearing diisopropylphenyl substitution, catalysts containing a single-tethered-enriched mixture performed better than double-tethered materials (entry 12 vs entry 10 and entry 16 vs entry 11). The best results were obtained by using end-capped-one-tethered **14b@SiO$_2$** in combination with either Cs_2CO_3 or K_3PO_4 (entries 15, 16).

Importantly, the use of biphasic reaction conditions may provide the benefit of complete dissolution of all reagents, base and also products and byproduct salts, thus preventing clogging of the microreactor channel during a continuous flow process.[101]

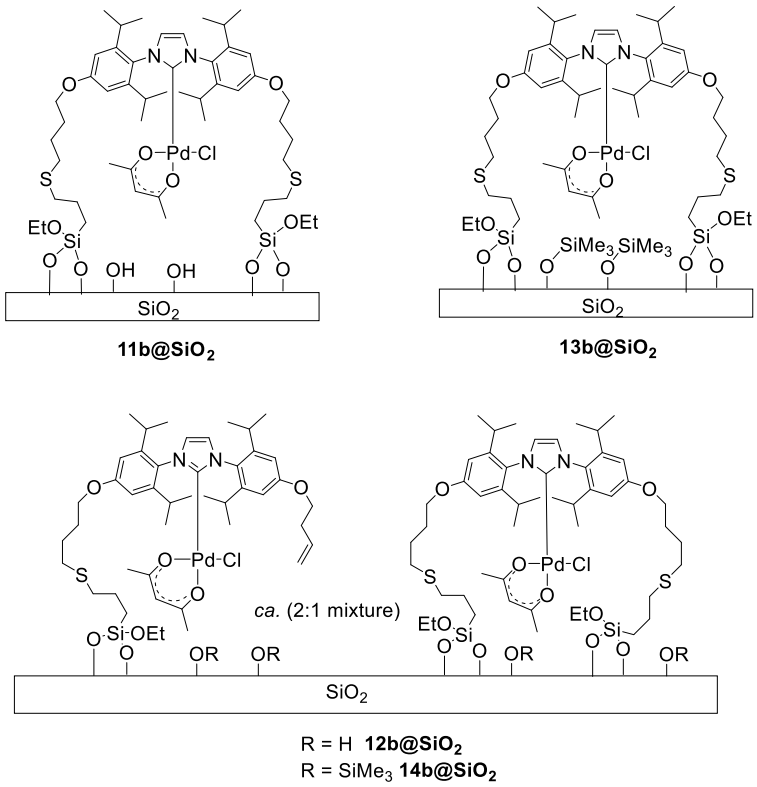

Figure 4.8. Molecular structure of catalysts **11b-14b@SiO₂**

Substrate scope

The most active catalyst formulation **14b@SiO₂** was used to briefly explore the substrate scope possible with this system (Table 4.2). Ortho-substitution is tolerated in both coupling partners, yielding the di-*ortho* substituted biphenhyl product in 79% isolated yield (entry 1). Heteroaromatic bromides can be coupled in up to 92% isolated yield (entry 2); switching the boronic acid partner from **16c** to 4-methoxyphenyl boronic acid **16b** resulted in lower reaction rates, yielding the corresponding biaryl in 50% yield. Activated bromide **15f** bearing the electron-withdrawing cyano group at the *para* position was coupled with **16b** in 92% yield, indicating that coupling of this substrate proceeded slightly faster compared to bromide **15d** (entry 1), very likely due to more favorable electronic and steric effects in this substrate.

Application of solid-supported [Pd(NHC)] complexes in Suzuki-Miyaura, Heck and Sonogashira couplings. Studies under batch and continuous flow conditions

Table 4.2. Scope of aryl halides and phenylboronic acids tested in the Pd-catalyzed Suzuki-Miyaura reaction using **14b@SiO$_2$** as catalyst.

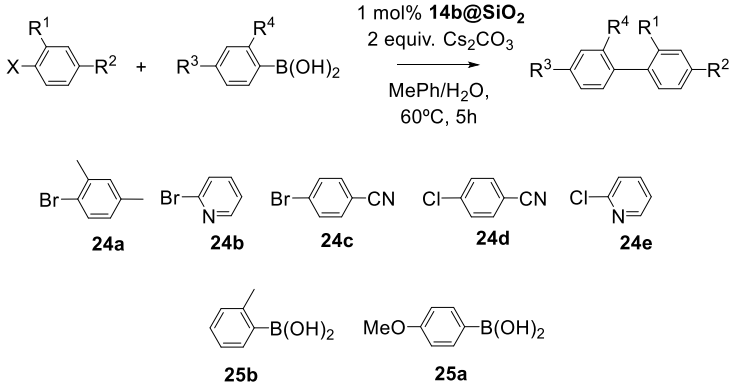

Entry	ArX	ArB(OH)$_2$	Isolated yield (%)[a]
1	**24a**	25b	79
2	**24b**	25b	92
3	**24b**	25a	50
4	**24c**	25a	94[b]
5	**24d**	25a	84
6	**24e**	25b	45

[a] Conditions: 0,5 mmol ArX, 0,6 mmol ArB(OH)$_2$, 1,0 mmol Cs_2CO_3, 1,5 mL toluene, 0,75 mL H_2O, 60°C, 5h. [b] No starting material or by-products observed by GC-FID, yield indicates loss during workup.

Activated chlorides **24d** was also coupled in high yield (84%) (entry 5). The coupling of the heteroaryl chloride **24e** represented a more challenging substrate for this catalyst and 45% yield was obtained after 5 hours, posing some limitations on the catalyst system under the present reaction conditions (60°C).

On the basis of these results, catalyst **14b@SiO$_2$** can couple moderately difficult deactivated and sterically hindered aryl bromides, and also activated chlorides at relatively low reaction temperatures; related supported catalysts bearing phosphine[68] or NHC[99] ligands frequently operate at higher temperatures (80-110°C) for the coupling of bromide substrates. However, they are much less efficient than homogeneous [Pd(NHC)] systems containing the bulky IPr ligand[32] which quickly couple aryl chlorides at room temperature, using much lower catalyst loadings.

Recycling tests and investigations on catalyst's instability

Material **14b@SiO$_2$** was applied as catalyst in the coupling of 1-bromo-2,4-dimethylbenzene **24a** with 4-methoxyphenylboronic acid **25a** and its recyclability was tested. In the first run, the cross-coupling product was obtained in 97% yield with perfect selectivity; the supernatant was filtered and the solid catalyst was successively washed with H_2O, EtOH and Et_2O, and it was dried under vacuum before being used in the next reaction run. However, successive catalyst's recyclings resulted in a rapid drop in product yield, and no conversion was observed in the 4th run (Figure 4.9). During these experiments, the formation of a black residue was observed within the solid catalyst material, which was pointed out as Pd black formed upon catalyst degradation. This was surprising given the relatively mild reaction conditions employed (60°C), and the stable nature of the NHC-Pd bond. Therefore, the origin of such instability was investigated.

In order to facilitate analysis and also to obtain a direct comparison with the homogeneous [Pd(IPr)(acac)Cl] catalyst, an experiment was performed where unsupported alkene-tethered Pd complexes **10a** and **10b**, and parent [Pd(IPr)(acac)Cl] were tested as precatalysts in the Suzuki coupling between **24a** and **25a** under the reaction conditions previously used for the supported catalysts (Table 4.3). When [Pd(IPr)(acac)Cl] was employed, full conversion to the desired product was obtained within two hours (entry 1). Furthermore, the reaction mixture did not darken noticeably. However, when **10a** or **10b** were used as precatalysts, a black precipitate formed shortly after the sample was brought to temperature.

Application of solid-supported [Pd(NHC)] complexes in Suzuki-Miyaura, Heck and Sonogashira couplings. Studies under batch and continuous flow conditions

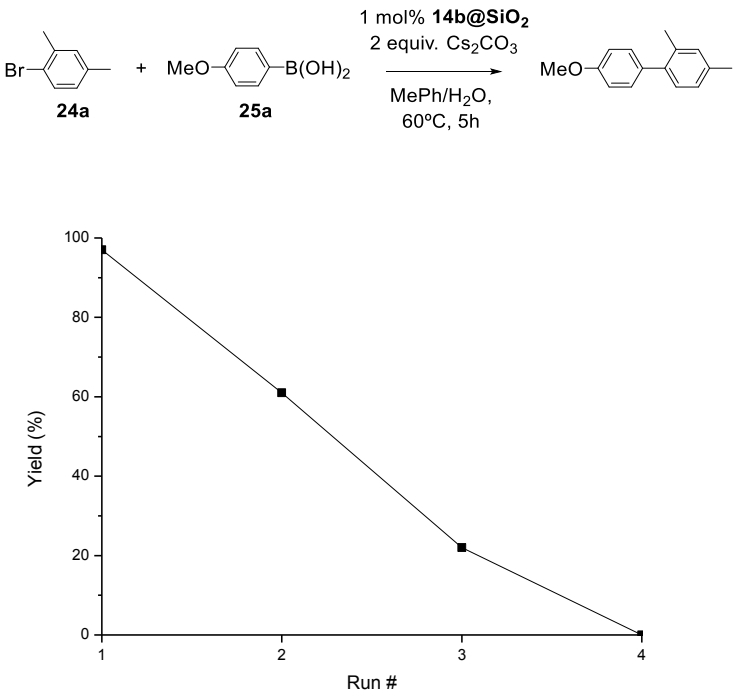

Figure 4.9. Recycling tests for the Suzuki-Miyaura coupling between **24a** and **25a** using catalyst **14b@SiO$_2$** under optimized reaction conditions. Conditions: 0,5 mmol ArX, 0,6 mmol ArB(OH)2, 1,0 mmol Cs2CO3, 1,5 mL toluene, 0,75 mL H2O, 60°C, 5h.

This difference in aspect was accompanied by poor product yields after 2 h of reaction time for both catalysts (entries 2, 4). Tripling the reaction time resulted in only modest increases in yield (entries 3, 5) which indicated that, by that time, most of the catalyst had decomposed. Therefore, it was concluded that deactivation of the supported catalysts presented above is due to an intrinsic instability of the (NHC)Pd core complexes and not to "external" factors such as interactions with the solid support or the thioether tether linkages.

A simple explanation for the instability of these catalysts would be that the (NHC)-Pd bond is somehow weakened by the changes made to the ligand architecture, although prior studies using other metals do not indicate that this should be the case.[102,103,104]

Application of solid-supported [Pd(NHC)] complexes in Suzuki-Miyaura, Heck and Sonogashira couplings. Studies under batch and continuous flow conditions

Table 4.3. Activity comparison between [Pd(IPr)(acac)Cl] and **10a/b** in the Suzuki coupling between **24a** and **25a** under biphasic reaction conditions.

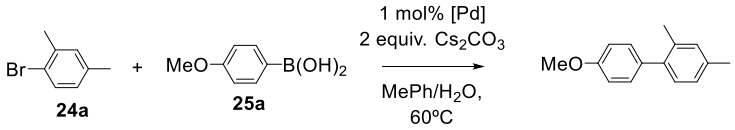

24a 25a

Entry	Catalyst	Time (h)	Yield[a] (%)
1	[Pd(IPr)(acac)Cl]	2	>95
2	(**10a**)	2	39
3		6	46
4	(**10b**)	2	55
5		6	73

Conditions: 0.5 mmol ArBr, 0.6 mmol $ArB(OH)_2$, 1.0 mmol Cs_2CO_3, 1.5 mL MePh, 0.75 mL H2O, 60 °C. a By GC-FID, average of two runs.

Nevertheless, this issue was investigated computationally (Scheme 4.8) (see footnote).

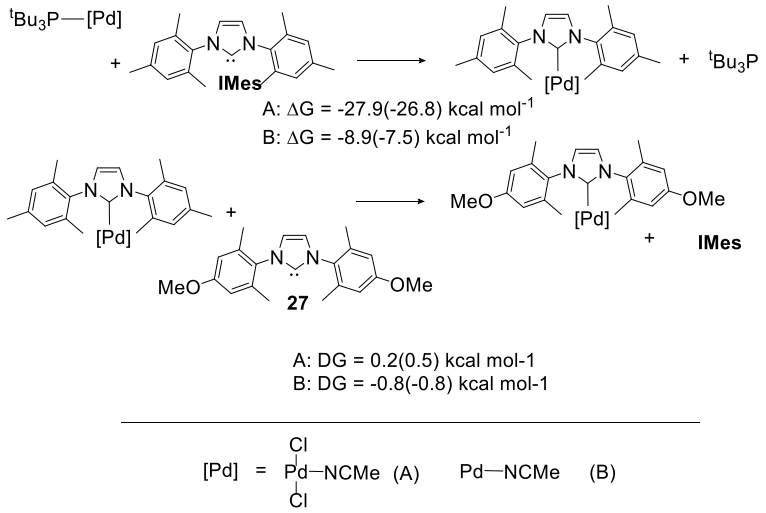

Scheme 4.8. Comparison of B_3LYP-d_3/LACVP* ligand exchange energies for Pd(II) and Pd(0) complexes of P^tBu_3, IMes and **27**. Gibbs free energies incorporate PBF benzene and DMF (in parentheses) solvent corrections.

Theoretical calculations were carried out by P.-O Norrby et al. at University of Gothemburg, Sweden

The relative binding energies of tBu$_3$P, IMes and ligand **27** bearing 2,6-dimethyl-4-methoxyphenyl substitution at the N wingtips (ligand **27** was chosen due to its steric and electronic similarities with the NHC ligand obtained from deprotonation of **7a**). As shown in Scheme 4.8, the IMes ligand was correctly predicted to displace tBu$_3$P in complexes of both Pd(II) and Pd(0). As could be expected, the substitution reaction was calculated to be much less exothermic for the Pd(0) system than for that containing divalent palladium. Conversely, no significant difference between Pd(0) and Pd(II) was predicted for the IMes/**27** substitution reaction. More importantly, the reaction is predicted to be thermoneutral in both cases, that is, negligible differences in binding energy between IMes and **27** were found. These data are in agreement with the experimental findings concerning other NHC-metal complexes[95,103,104] for predicting NHC-palladium bonding properties, and cast further doubt on an unstable NHC-Pd bond as a culprit for catalyst decomposition in this case.

In light of the findings presented above, additional experiments were performed to rule out other possible modes of catalyst decomposition. While the catalytic reaction conditions reported here are relatively mild, the ligands ether linkages could conceivably be susceptible to cleavage by base and/or halide ions present in the reaction medium. To check for such reactivity, complex **10a** was treated with 12 equivalents each of Cs_2CO_3 and KBr in toluene/H_2O solvent in the absence of substrate (Scheme 4.9, compare with optimized catalytic reaction conditions).

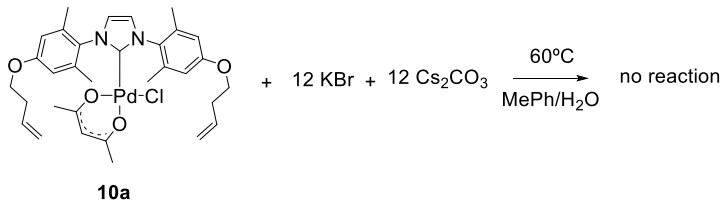

10a

Scheme 4.9. Reactivity of precatalyst **10a** when treated with potassium bromide and cesium carbonate under the reaction conditions but in the absence of substrate.

After 20 hours at 60 °C, no precipitates formed and no change to **10a** was observed by ^{1}H NMR spectroscopy. Three conclusions can be derived: a) direct attack by base or Br^- ion on the ligand's ether linkage is not operative; b) more generally, catalyst decomposition does not occur by base/halide-mediated decomposition of precatalyst **10a**; c) if catalyst activation to [Pd(0)(NHC)] occurs by attack of the base on the precatalyst's acac ligand, as proposed for Nolan's system using alkoxide bases,[105] then this process is very slow under the conditions employed here.

A second set of experiments involved direct observation of the catalysts' behavior at high loading under the full set of reaction conditions, using 6 equivalents of 4-methoxyphenylboronic acid and 4-bromo-*m*-xylene substrates in addition to the 12 equivalents of Cs_2CO_3 used in the experiment outlined above (Scheme 4.10).

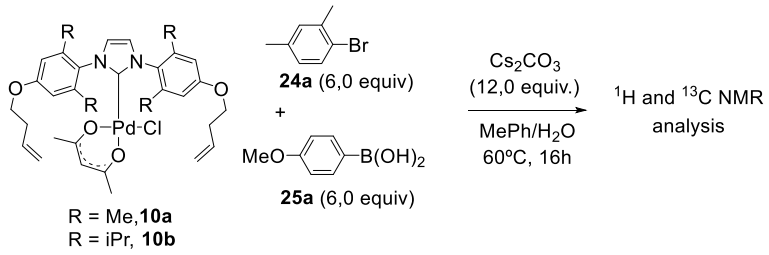

Scheme 4.10. Suzuki-Miyaura coupling between **24a** and **25a** using **10a** and **10b** at high catalyst loadings.

When **10a** or **10b** were used as precatalyst, a noticeable quantity of black precipitate was observed after heating the reaction mixture at 60 °C for 3 hours (**10b** generated this precipitate after a few minutes). However, little more precipitate had formed after 16 additional hours at this temperature. After 19 h, the volatiles were removed and the remaining organic-soluble material analyzed by ^{1}H NMR spectroscopy. The spectral region corresponding to the OC*H*$_2$R protons of the NHC ether linkages exhibited peaks arising from three major species containing that fragment, the most abundant being unreacted **10a/b** or a very closely related species (characteristic signals arising from the NHC backbone and acac methyl groups were retained). Combined peak integrations (relative to substrate signals) indicated that at least the vast majority of

added ligand was present as soluble species. Furthermore, no signals corresponding to the imidazolium salts were detected.

A ^{13}C C2-labeled sample of **10b** was prepared in order to facilitate the use of $^{13}C\{^1H\}$ NMR spectroscopy as an additional analysis tool. Precatalyst **10b** displays a resonance at 156.7 ppm corresponding to the imidazol-2-ylidene (C2) carbon nucleus, whereas in the imidazolium pre-ligand this carbon nucleus resonates at 139 ppm. After the catalytic reaction, three peaks with large intensity (due to the ^{13}C label) were observed at 155.7, 156.1 and 156.7 ppm, in agreement with the identification of three major NHC-containing species from the above analysis. Their extremely similar C2 chemical shifts, and the fact that one of those signals is due to, or overlaps that of **10b** supports the assignment of all three species as intact [Pd(NHC)] complexes.

All data from the catalytic experiments discussed above indicate that, at high precatalyst loadings, very little of the [PdL(acac)Cl] complex is activated and thus only a small fraction yields a highly active, yet unstable catalyst. Furthermore, the remaining precatalyst was not catalytically degraded by the active species. Therefore, the only forthcoming explanation for catalyst decomposition in this system is that a reactive intermediate in the catalytic cycle (or a side product arising from the activated catalyst) is susceptible to decomposition *via* a stoichiometric pathway.

An obvious candidate for this catalytic intermediate is the 1-coordinate [Pd(0)(NHC)] complex proposed as the active catalyst in such systems. A bulky phosphine-containing Pd(0) complex has been shown to cleave O–CH_3 bonds of aryl methyl ethers.[106] According to this proposal the highly unsaturated [Pd(0)(NHC)] compounds would attack the O–R bond of a neighboring [Pd(NHC)] complex. Under the catalytic reaction conditions, the initially-formed [Pd(NHC)(OAr)R] then presumably decomposes to precipitate palladium metal (Scheme 4.11).

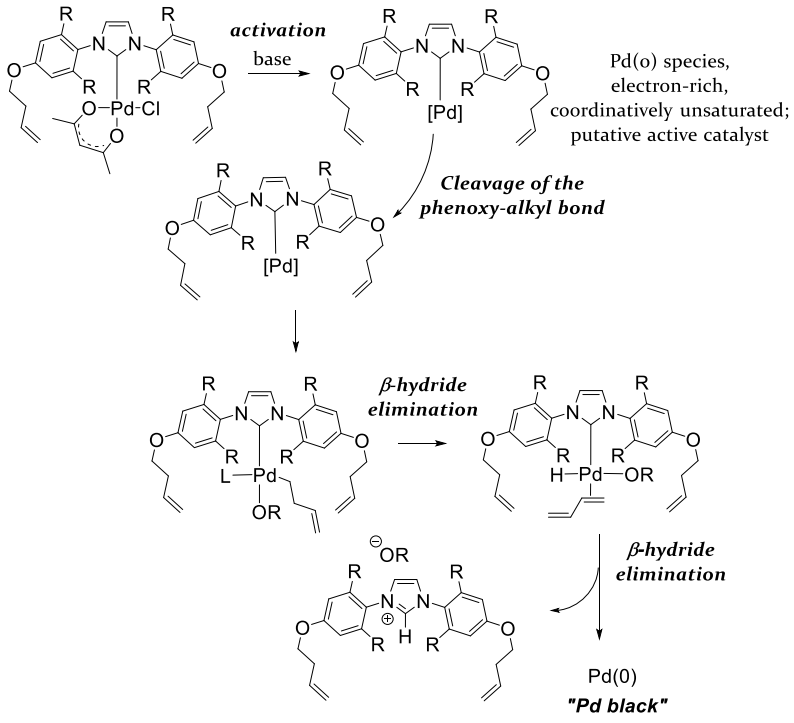

Scheme 4.11. Proposed deactivation pathway involving cleavage of ArO-R bond in the ligand framework by highly reactive Pd(0) species.

However, it is not clear how this mechanism would operate when the ligands are immobilized on a solid support, wherein each catalytic site is fairly distant. Moreover, formation of imidazolium salt was not detected in the above described experiments. An alternative explanation would be occasional, reversible dissociation of an unsaturated Pd(0) fragment from the NHC ligand, which might go unnoticed in systems employing non-functionalized NHCs but which in this case could result in intramolecular O–R activation. It is often stated that the NHC-Pd bond is sufficiently strong that dissociation should not occur. However, mechanisms involving IPr dissociation from palladium have been proposed.[107]

Application of solid-supported [Pd(NHC)] complexes in Suzuki-Miyaura, Heck and Sonogashira couplings. Studies under batch and continuous flow conditions

4.2.1.1.2. Alternative conditions for improving catalyst's stability. Batch and continuous flow studies

Suzuki-Miyaura reaction in the absence of water

Although initial optimization of the reaction conditions for these systems (Table 4.1) had pointed out to an optimal reaction medium involving a biphasic toluene/water mixture, several [Pd(NHC)]-based heterogenized catalysts have been applied under non-aqueous reaction conditions, displaying enhanced recyclability compared to their use under aqueous/organic biphasic conditions.[90] Moreover, the Pd-catalyzed Suzuki-Miyaura reaction has been described in toluene, in the absence of any other solvent.[91] Thus, alternative reaction conditions were used involving the use of anhydrous toluene, and the reaction temperature was rised from 60°C to 80°C. Under these conditions, longer reaction times were needed (compared to the use of biphasic toluene/water medium) to achieve high conversions, in spite of the higher temperature. However, the robustness of supported [Pd(NHC)] catalysts **13b@SiO$_2$** and **14b@SiO$_2$** (Figure 4.8 page 110) under these conditions was evaluated in the Suzuki-Miyaura coupling between **24a** and **25a** (Figure 4.10).

In the first reaction run, catalyst **14b@SiO$_2$** achieved 95% conversion compared to 80% for catalyst **13b@SiO$_2$**. Both catalysts displayed perfect selectivity under these conditions, and undesired deboronation and homocoupling were not observed. The catalysts were washed and recycled as described before, and used in successive runs. In the second run, lower yields were obtained with both catalysts; for catalyst **14b@SiO$_2$** a drop of more than 50% of the initial yield was found, whereas for catalyst **13b@SiO$_2$** a smaller drop of 25% compared to the first run was quantified (from 81% to 60% yield). Further recycling the catalysts resulted in similar performance over the next two runs for catalyst **13b@SiO$_2$**, or three runs for catalyst **14b@SiO$_2$** before a large drop in yield observed in the 5th and 6th runs respectively.

Therefore, under these conditions, double tethered catalyst **13b@SiO$_2$** displayed superior robustness compared to single-tethered enriched **14b@SiO$_2$**.

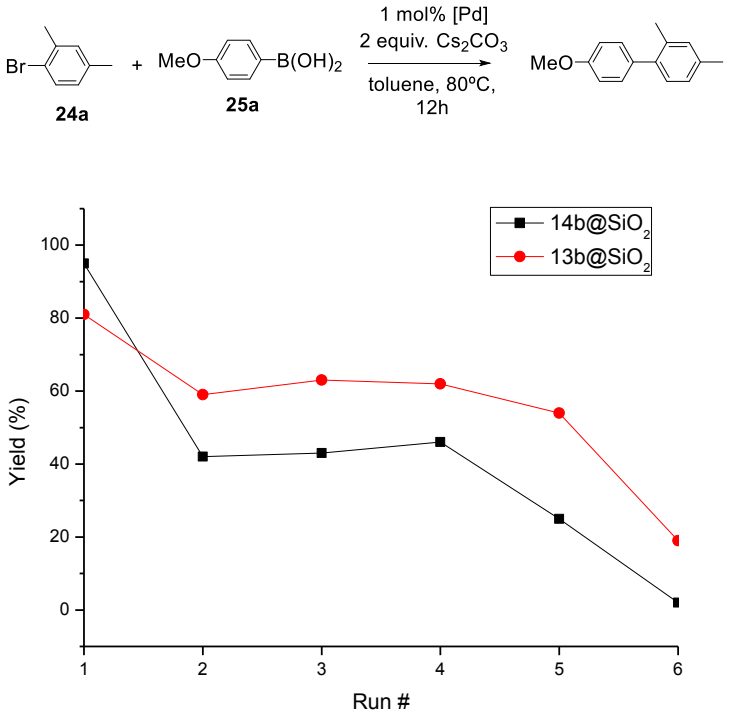

Figure 4.10. Recyclability studies on catalysts **13b@SiO$_2$** and **14b@SiO$_2$** in the Suzuki coupling between **24a** and **25a** under anhydrous reaction conditions.

Conditions: 0.5 mmol ArBr, 0.6 mmol ArB(OH)$_2$, 1.0 mmol Cs_2CO_3, 2,0 mL toluene, 80 °C, 12h. Yields obtained by GC-FID, average of two runs.

To know whether the observed decrease in catalyst activity maight be attributed to catalyst degradation or to Pd leaching, the reaction mixtures were analyzed by ICP-OES (Table 4.4).

Table 4.4. Values of leached % Pd leached with respect to initial Pd content in each reaction run.

Entry	1	2	3	4	5	6
Run	1	2	3	4	5	6
13b@SiO$_2$	0,58	0,67	0,78	0,82	0,98	0,88
14b@SiO$_2$	0,87	0,88	0,9	0,87	0,88	0,89

A non-negligible amount of Pd was present after every single run, however the observed values are too small to solely explain the drop in activity. Therefore, partial deactivation of the catalysts under these conditions might still be occurring, although formation of Pd black was not evident.

Continuous flow experiments for Suzuki-Miyaura

The most active silica-supported catalysts **13b@SiO$_2$** and **14b@SiO$_2$** were selected for their application in the Suzuki-Miyaura coupling between **24a** and **25a** under continuous flow conditions, in order to evaluate the benefits of this technique over conventional batch operation. The continuous flow experiments were carried out at University of Cambridge in collaboration with the group of Prof. Dr. A. Lapkin. Representation of a continuous flow microreactor is illustrated in figure 4.11.

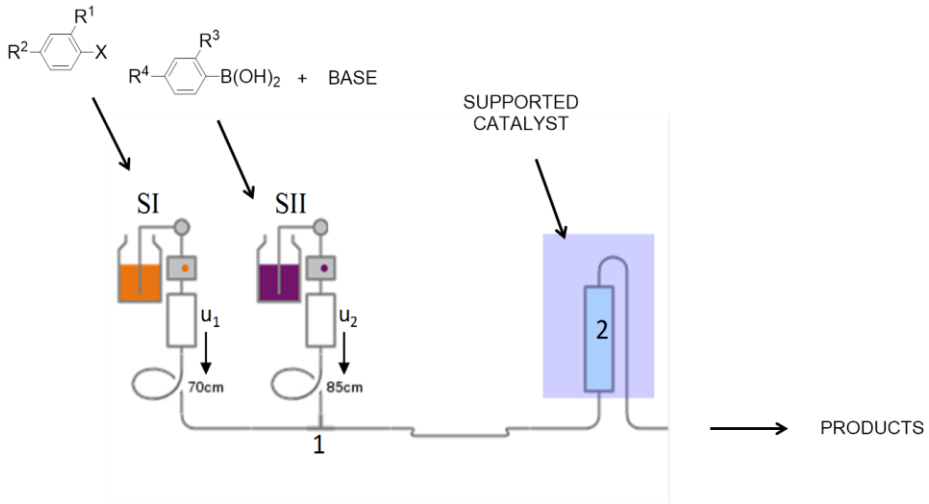

Figure 4.11. General scheme of a continuous flow reactor. SI is Solution I containing the aryl halide; SII is Solution II, containing the arylboronic acid and the base; (1) is called T connection; (2) is the packed bed containing the supported catalyst.

A solution of the substrate (SI) and a second solution containing the arylboronic acid and the base (SII) are fed into the flow reactor at equal

flow rates by menans of an HPLC pump. These two solutions mix when they get into the T-connection (1). The merged flow is then introduced to the inlet of the packed bed column assembly (2) containing the solid catalyst. The reaction takes place in the packed bed and the products flow out of the flow reactor and are collected.

To carry out the continuous flow Suzuki reactions, needed to be adjusted, because base, boronic acid and byproduct halide salts are poorly soluble in toluene, which could lead to clogging of the microreactor. Among the different alternatives tested in batch, methanol was chosen to run the continuous flow tests because it offered the best option for the solubility of the reactants and byproduct salts. (See table S4.1 in the experimental part for details).

Two continuous flow experiments were carried out, in order to compare the performance of one-tethered and two-tethered catalysts under these conditions (Table 4.5).

Table 4.5. Reaction conditions for the Suzuki coupling between **24a** and **25b** under continuous flow conditions.

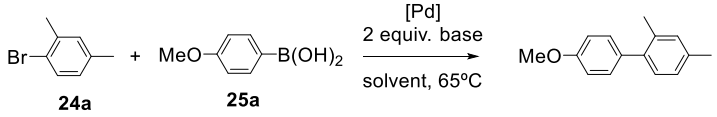

24a **25a**

Exp	Sol. I		Sol. II			Catalyst	
	Solv.	[ArBr] M	Solv.	Base/ C(M)	[ArB] (M)	Title	Pd. mmol
1	MeOH	0,2	MeOH	Cs_2CO_3 /0,4	0,2	**14b@SiO₂**	0,07
2	MeOH	0,2	MeOH	Cs_2CO_3 /0,4	0,2	**13b@SiO₂**	0,07

Conditions: 65°C, $\mu_1 = \mu_2 = 0{,}15$ mL/min. Aliquots were analysed using GC, mesitylene was used as the internal standard.

In the case of single-tethered **14b@SiO₂** an initial activation period was observed under flow conditions, and the highest conversion (94%) was achieved after 40 minutes on stream (Figure 4.12, black filled circles). In contrast, catalyst **13@SiO₂** (red filled circles) achieved its maximum

activity after 15 minutes on stream. initial activities were observed compared to double tethered.

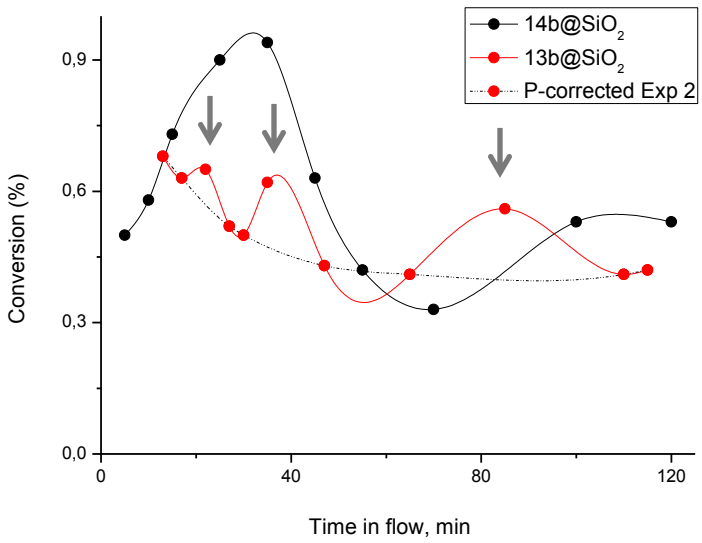

Figure 4.12. Conversion vs time on stream for the Suzuki coupling between **24a** and **25a** catalyzed by **13b@SiO$_2$** and **14b@SiO$_2$** under continuous flow; reaction conditions shown in Table 4.11.

A maximum 94% conversion was obtained with the former system after 40 minutes on stream. After this initial activation for catalyst **14b@SiO$_2$**, a similar deactivation trend to that previously observed for batch experiments was also detected under flow conditions, and conversion decreased rapidly over the next 40 minutes. After two hours conversion was in the 50% range. For the analogous two-tethered catalyst, a small decrease in activity was also evident, although to a lesser extent, going from 68% maximum conversion down to 45% after 2 hours on stream, and remained stable until t = 120 minutes. Although initial concentration of the reagents were selected to always generate the byproduct bromide salt below its solubility limit, during the course of the experiment, at some points, the local concentration of the salt at the catalytic centers may exceed this value during the experiment, due to faster reaction compared to the dissolution rate, thus resulting in

temporary constriction/blockage of the flow paths. These phenomena caused a change in the flow rate/residence time and hence oscillations of the conversion (see arrows in Figure 4.12). At the same time the catalytic activity (and therefore the rate of formation of CsBr) dropped due to the blockage of the Pd centres.The "shells" of CsBr are then partially dissolved by the unsaturated reaction mixture during the period of lower reaction rate/prolonged residence time, which in turn increases the conversion and decreases the residence time and so on. In spite of the differences in reaction conditions applied due to the solubility restrictions in the case of continuous flow operation, the productivity in terms of space-time yields can still be compared with the batch process. Considering the results obtained by using the double-tethered **14b@SiO$_2$** catalyst in batch and in continuous mode, the TOF was *ca* 4 times higher (Table 4.6) for the latter mode, even when non optimal reaction conditions and lower temperature (65°C vs 80°C) were used. The criterion used for comparing results obtained under batch with those obtained under continuous flow conditions is that reliable comparison between TOF's must be done at closely similar TON's.

Table 4.6. Comparison of the performance of catalyst **13b@SiO$_2$** in the Suzuki coupling between **24a** and **25a** by operating under batch or continuous flow conditions.

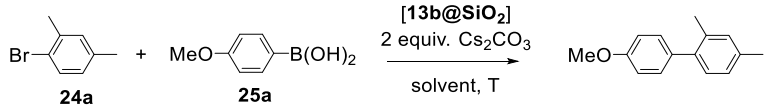

24a **25a**

Mode	mmol conv.	mmol Pd	T(°C)	Operation Time (h)	TON[a]	TOF[a] (h^{-1})
Batch[b]	0,405	0,005	80	12	81	6,75
Cont. flow	3,6[c]	0,07	65	2	51	25,5

[a] TON and TOF data refer to the overall continuous flow process and to the 1st run of the corresponding batch process (under anhydrous conditions). [b] for the exact reaction conditions in the batch experiments see Table 4.11. . [c] A constant conversion of 45% during 2 hours flow run was considered to calculate the amount of cross-coupling product.

The results presented, although involving only small scale tests provide some evidence of the enhanced productivity achieved when the Suzuki

reaction was performed in the confined channels of a continuous flow microreactor.[54]

4.2.1.2. γ-Al_2O_3- and TiO_2-supported [Pd(NHC)], materials for continuous flow applications

After studying the recycling and the evaluation of [Pd(NHC)] immobilized on silica, and in view of the results obtained, it was considered of interest to evaluate the influence of other supports on catalysts performance and stability. Therefore, the protocols developed for the silica-immobilized catalysts were then extended to the application of catalysts heterogenized onto MCM-41, γ-Al_2O_3 and TiO_2 in the Suzuki-Miyaura coupling.

4.2.1.2.1. Influence of the support material on the robustness of the heterogenized catalysts

In order to allow for a comparison between the different catalyst formulations regarding the solid support, the two-tethered materials based on the 2,6-diisopropylphenyl scaffold were chosen; end-capped SiO_2- and MCM-41-based materials were used. These catalysts were first tested in the Suzuki coupling between **24a** and **25a** under batch conditions (Figure 4.13).

A very similar activity was found for the TiO_2-, γ-Al_2O_3- and MCM-41-supported [Pd(NHC)] in the first reaction run, the three of them reaching conversions above 95%, outperforming the SiO_2-supported catalyst. SiO_2-supported **13b@SiO_2** and γ-Al_2O_3-supported **11b@γ-Al_2O_3** displayed a similar recycling profile, and some deactivation was observed after the 1st run. This deactivation was more pronounced for the silica-tethered catalyst, but then both materials yielded the desired cross-coupling product in over 50% yield after 5 runs. Microporous TiO_2-supported material **11b@TiO_2** proved the most robust of the four, and conversions were maintained above 80% during 4 successive runs before ultimately showing signs of deactivation in the 5th run. The use of MCM-41 as support led to a rapid and constant decline in activity, which might be associated to the rather thin pore walls in this material with low (hydro)thermal stability which may lead to structure collapse.[108]

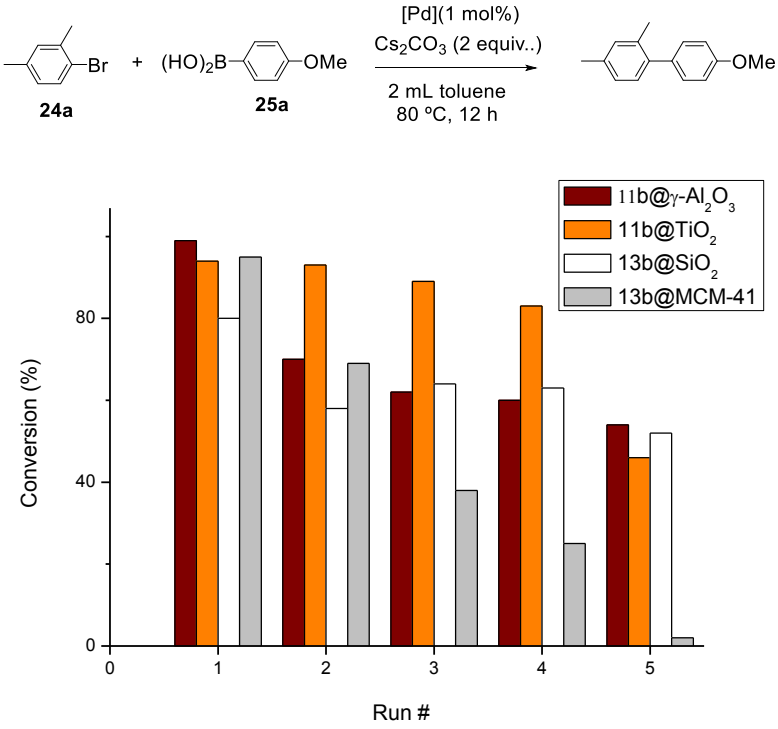

Figure 4.13. Influence of the support material on the catalysts' performance on successive reaction runs for the Suzuki-Miyaura reaction between **24a** and **25a**.

Conditions: 0,5 mmol 1-bromo-2,4-dimethylbenzene, 0,6 mmol 4-methoxyphenylboronic acid. Conversions determined by GC-FID relative to calibration curves.

In view of these results MCM-41 was discarded due to its lower long-term stability and TiO_2-, γ-Al_2O_3-supported **11b@TiO₂** and **11b@γ-Al₂O₃** were taken up for evaluation under continuous flow operation.

4.2.1.2.2. Performance of γ-Al₂O₃- and TiO₂-supported [Pd(NHC)] as catalysts in the Suzuki reaction under continuous flow conditions

Two continuous flow experiments were carried out using **11b@TiO₂** and **11@γ-Al₂O₃** (Figure 4.14). Conditions are detailed in Table 4.7.

Application of solid-supported [Pd(NHC)] complexes in Suzuki-Miyaura, Heck and Sonogashira couplings. Studies under batch and continuous flow conditions

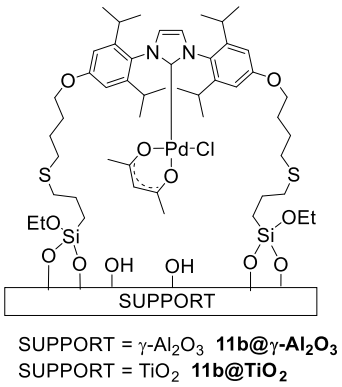

Figure 4.14. Molecular structure of catalysts **11b@γ-Al_2O_3** and **11b@TiO_2**.

Table 4.7. Reaction conditions for the continuous flow experiments involving the Suzuki coupling between **25a** and **25a** catalyzed by **11b@TiO_2** and **11b@γ-Al_2O_3** .

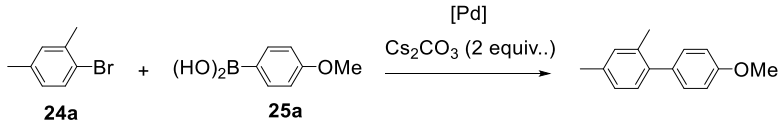

Exp	Sol. I		Sol. II			Catalyst	
	Solv.	[ArBr] M	Solv.	Base/ C(M)	[ArB] (M)	Title	Pd. mmol
1	MeOH	0,2	MeOH	Cs_2CO_3 /0,4	0,2	**11b@TiO_2**	0,020
2	MeOH	0,2	MeOH	Cs_2CO_3 /0,4	0,2	**11b@γ-Al_2O_3**	0,045

Conditions: 65°C, $\mu_1 = \mu_2 = 0{,}2$ mL/min. Aliquots were analysed using GC, mesitylene was used as the internal standard

Compared to the previous flow experiments using silica-supported catalysts the catalyst loadings are lower due to the minor content of Pd in catalysts **13b@TiO_2** and **11b@γ-Al_2O_3** compared to catalyst **13b@SiO_2**. Moreover, the applied flow rate is slightly higher (0,4 mL/min vs 0,3 mL/min referred to the merged flow), thus implying a shorter residence time. The best conversions over time in flow were observed for **11b@γ-Al_2O_3** (Figure 4.15, black curve);

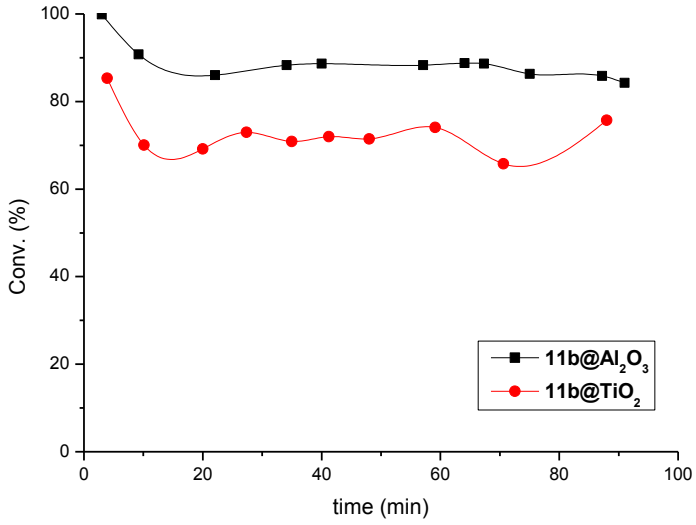

Figure 4.15. Performance of **11b@γ-Al_2O_3** and **11b@TiO_2** in the Suzuki coupling between **24a** and **25a** under continuous flow conditions; reaction conditions shown in Table 4.13.

the initial 100% conversion dropped to 89% during the first 20 minutes on stream, clearly showing the better performance over its silica counterpart, where lower conversions were achieved in spite of the higher amount of Pd in the packed bed of the reactor, and the longer residence time. Morover, no significant deactivation was observed, and no Pd black was observed in the outlet of the flow reactor. Lower conversions were measured for **11b@TiO_2**. A drop in activity was observed within the first 10 minutes (from 85% to 70%) but then this level of conversion slightly above 70% was maintained for the rest of the experiment up to 88 minutes. In the case of **11b@TiO_2** the activity is remarkable given its lower Pd content (Table 4.7). Therefore, a more logical comparison between the two materials would be according to the TON and TOF achieved by the end of the flow experiment (Table 4.14). The higher values in TON and TOF displayed by catalyst **11b@TiO_2** correlate with the superior performance of this catalyst in the previously described batch studies (Figure 4.8). Under continuous flow conditions, TiO_2-supported **11b@TiO_2** more markedly outperforms **11b@γ-Al_2O_3** (Table 4.8). Under continuous flow conditions, both

catalysts display increased activity and stability compared to silica-supported **13b@SiO$_2$** (Figure 4.12). Consequently, catalyst **13b@SiO$_2$** bearing the largest surface area and the highest Pd loading (see Table 3.1) displayed the poorest performance, whereas catalyst **11b@TiO$_2$** bearing microporous titania as support, and having the lowest surface area and Pd loading, displayed the best results of the series in the Suzuki-Miyaura coupling between **24a** and **25a** both under batch and continuous flow operation.

Finally, with the collected data in hand a comparison is possible between the productivity of batch and continuous processes in terms of space-time yields (Table 4.14). As in the previous case for silica-supported catalysts, TOF values obtained in flow experiments and in batch reactions, are presented at similar TON to obtain a more reliable comparison. For the case of **11b@TiO$_2$**, the TOF was improved by more than one order of magnitude, and a 6-fold rate enhancement was achieved for catalyst **11b@γ-Al$_2$O$_3$**. These results highlight the potential of the continuous flow techniques in organic synthesis.

Table 4.8. Comparison in activity and productivity of catalysts **11b@γ-Al$_2$O$_3$** and **11b@TiO$_2$** in the Suzuki coupling between **24a** and **25a** in relation to the mode of operation (batch or continuous flow).

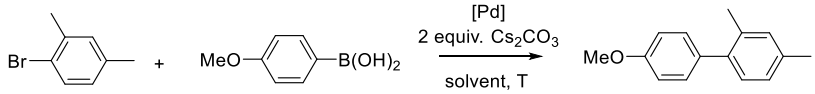

24a **25a**

Mode	Cat.[a]	mmol conv.	mmol Pd	T(°C)	Operation Time (h)	TON[b]	TOF[b] (h^{-1})
Batch[c]	Ti	0,47	0,005	80	60	94	7,83
	Al	0,49	0,005	80	60	98	8,17
Cont. flow	Ti	2,52[e]	0,045	65	1,5	126	84
	Al	3,24[e]	0,045	65	1,5	72	48

[a] Ti = **11b@TiO$_2$**, Al = **11b@γ-Al$_2$O$_3$**; [b] TON and TOF data refer to the overall continuous flow experiment and to results obtained in the first run of the batch tests. [c] For the exact reaction conditions in the batch experiments see Figure 4.6. [e] total cross-coupling product obtained after 90 minutes in flow, by GC analysis using mesitylene as standard.

4.2.2. Application of solid-supported [Pd(NHC)] complexes in related Pd-mediated cross-coupling processes

Besides the application of the heterogenized Pd-NHC complexes in continuous Suzuki couplings, it was considered of interest to study their performance in related Pd-catalyzed Sonogashira and Heck couplings. In view of their higher activity in the Suzuki-Miyaura reaction, precatalysts containing NHC ligands with the more bulky 2,6-diisopropylphenyl motif were chosen for these studies.

4.2.2.1. Application of supported [Pd(NHC)] complexes in the Cu-free Sonogashira coupling

4.2.2.1.1. Evaluation of catalyst performance in batch mode

Taking into account the previous results on the use of these supported catalysts in the Suzuki-Miyaura reaction it was considered of interest to explore their activity, recovery and reuse in the Sonogashira reaction, since this transformation offers a convenient access to substituted alkynes.[109] Initial tests focused on optimizing the reaction conditions for this transformation bearing in mind the improved stability of the catalysts under anhydrous conditions (see results on the Suzuki coupling)(Table 4.9).

Table 4.9. Screening of various solvents for the Sonogashira coupling between **24f** and **28a** catalyzed by **11b@γ-Al_2O_3**.

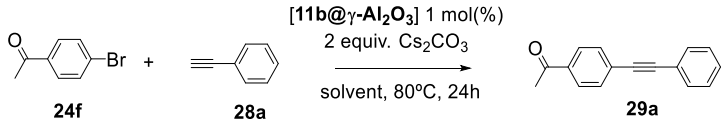

Entry	Solvent	Yield (%)[a]
1	Toluene	traces
2	1,4-dioxane	33
3	DME	26
4	DMF	99[b]

Conditions: 0,5 mmol ArBr, 0,75 mmol phenylacetylene, 2 mL dry and degassed solvent. [a] GC yield using mesitylene as internal standard and correlated to a calibration curve. [b] the reaction was completed after 16h.

When toluene was used as the solvent in combination with Cs_2CO_3 (Table 4.9, entry 1), only traces of the coupling product were detected. Better results were obtained using more polar solvents such as dioxane (entry 2) or DME (entry 3), but only partial conversion was obtained. However, running the reaction in DMF afforded complete conversion and perfect cross-coupling selectivity after 16 hours at 80°C. Next, the Sonogashira reaction was examined for various alkynes and the results are gathered in Table 4.10. Reaction of 4-acetophenone (**24f**) with phenylacetylene (**28a**) led to the corresponding coupling product **29a** in 98% isolated yield. Good-to-excellent yield was obtained in the coupling of *p*-bromoacetophenone **28a** with electron rich alkynes **28b** and **28c** (entries 2 and 3, respectively) and finally *ortho*-substitution in the alkyne was tolerated providing the final product **29d** in excellent yield (entry 4). Thus this results showed that precatalyst **11b@γ-Al_2O_3** is active in the Sonogashira coupling of aryl bromides with *ortho*-substituted and electron rich aromatic alkynes.

Table 4.10. Alkyne scope in the Sonogashira coupling between *p*-bromoacetophenone **24f** and various aromatic alkynes using catalyst **11b@ γ-Al_2O_3**.

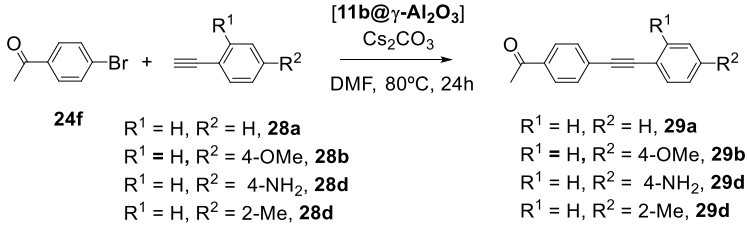

Entry	Alkyne	Product	Yield (%)[a]
1	28a	29a	98
2	28b	29b	80
3	28c	29c	96
4	28d	29d	95

Conditions: 1,0 mmol ArBr, 1,5 mmol alkyne, 2,0 mmol Cs_2CO_3, 1 mol% [Pd]. [a] Isolated yield after column chromatography

The recyclability of these materials was tested in batch mode in successive reaction runs for the coupling of 4-bromoacetophenone **15b** with phenylacetylene **28a** (Figure 4.16).

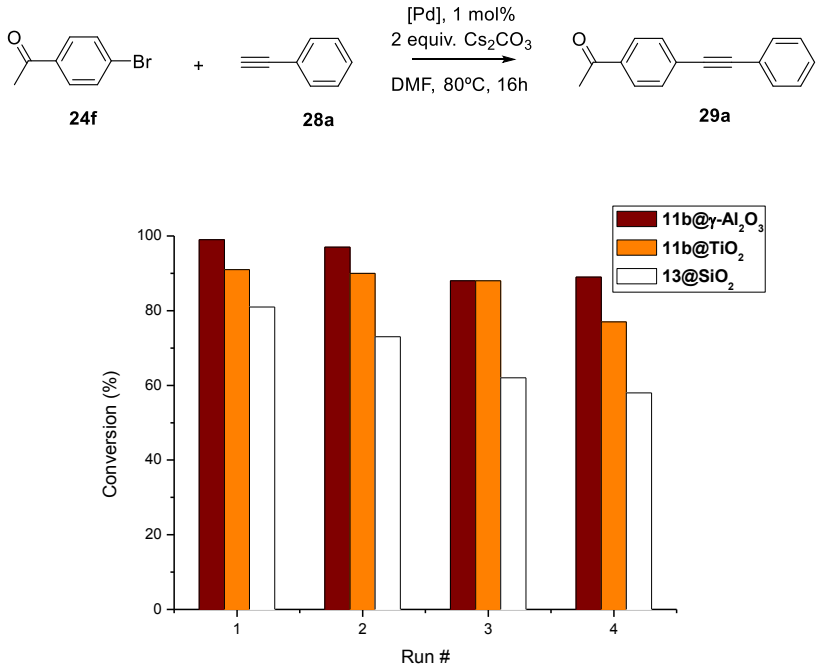

Figure 4.16. Influence of the support material on the catalysts recyclability in the Cu-free Sonogashira coupling of **24f** with **28a**.

Conditions: 0,5 mmol 4-bromoacetophenone, 0,75 mmol phenylacetylene, 1 mol% [Pd], 2 mL dry and deoxygenated DMF

Catalysts immobilized onto mesoporous MCM-41 were not included in the study. Under these conditions **11b@γ-Al_2O_3** exhibited higher activity than the other materials, providing product **29a** in more than 95% yield over the first two runs, and then only slightly decreasing its activity to 88% in the 4th run. Catalyst **11b@TiO_2** afforded **29a** in yields above 85% over the first three runs before a slight decrease in activity was observed in the fourth run (76%). The silica-supported **13b@SiO_2** afforded 80% of the coupling product in the 1st run and then gradually dropped its activity to 56% in the 4th run. In any of these experiments formation of Pd black was evident. As observed in the study of the Suzuki-Miyaura

coupling, catalysts **11b@ γ-Al_2O_3** and **11b@TiO_2** provided better reusability compared to silica supported **13b@SiO_2**.

Due to their increased robustness **11b@ γ-Al_2O_3** and **11b@TiO_2** were selected for application under continuous flow conditions.

4.2.2.1.2. Evaluation of catalyts performance in continuous flow operation

Catalysts **11b@γ-Al_2O_3** and **11b@TiO_2** were evaluated in the continuous Sonogashira coupling of *p*-bromoacetophenone **24f** with phenylacetylene **28a** (Table 4.11). Both systems displayed excellent activity in flow mode (Figure 4.17). Whereas Sonogashira couplings of aryl iodides have been reported,[89] very few works have reported the Sonogashira coupling of the more challenging aryl bromides under continuous flow operation.[89]

Table 4.11. Reaction conditions for the continuous Sonogashira couplingsbetween **24f** and **28a**

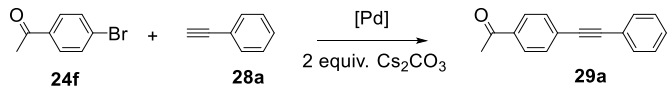

24f **28a** **29a**

Exp	Sol. I		Sol. II			Catalyst	
	Solv.	[15b] M	Solv.	Base/ C(M)	[28a] (M)	Title	Pd. mmol
1	MeOH	0,2	MeOH	Cs_2CO_3 /0,4	0,3	**11b@γ-Al_2O_3**	0,047
2	MeOH	0,2	MeOH	Cs_2CO_3 /0,4	0,3	**11b@TiO_2**	0,028
3[a]	MeOH	0,2	MeOH	Cs_2CO_3 /0,4	0,3	**11b@TiO_2**	0,028
4[ab]	MeOH	0,2	MeOH	Cs_2CO_3 /0,4	0,3	**11b@TiO_2**	0,028

Conditions: 65°C, $\mu_1 = \mu_2 = 0{,}05$ mL/min. [a] $\mu_1 = \mu_2 = 0{,}1$ mL/min. [b] Long term experiment. Aliquots were analysed using GC, mesitylene as the internal standard

For this reaction, an initial incubation period was observed in both experiments, which could indicate the possible generation of palladium

nanoclusters,[110] although no decomposition was apparent during the experiments.

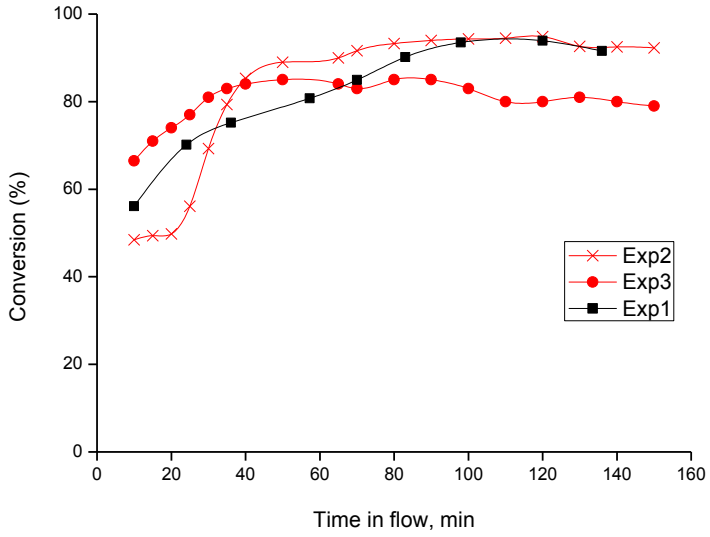

Figure 4.17. Performance of catalysts **11b@γ-Al_2O_3** and **11b@TiO_2** in the Sonogashira coupling between **24f** and **28a** under continuous flow conditions; reaction conditions are shown in Table 4.17.

Under these conditions, the reaction reached the steady state after 70 minutes on stream for **11b@γ-Al_2O_3** and after 80 min for **11b@TiO_2**. Again, as in the case of the Suzuki reaction, remarkably high activity was exhibited by **11b@TiO_2** which contains lower amount of Pd. In Exp 3 (Table 4.11) the performance of **11b@TiO_2** was assessed by increasing the flow rate by a factor of two compared to Exp 2 while maintaining the same substrate concentration, therefore reducing the mean residence time also by a factor of two. At these reaction times, the conversion afforded by both catalytic systems was higher than 92%.These high levels of conversion were maintained during the following 70 minutes under the continuous flow process and no by-products could be detected by GC. The vast majority of supported catalysts applied in the copper-free Sonogashira reaction under continuous flow conditions involve particulate catalysts,[118] and not well-defined organometallic complexes.[111] In the most cases only the coupling of aryl iodides is described,[112,113] and reactions usually take place at rather high

temperatures (110°C-170°C).[114] Moreover, leaching is observed in some cases, which requires the installation of a scavenging column at the end of the reactor.[118] Under these conditions the steady state was reached more rapidly, 40 minutes after the start of the experiment. Over the next 60 minutes, 85% conversion was achieved, after which time conversion slowly dropped to 79% after 160 minutes under continuous flow.

As in the case of the Suzuki reaction, with the data collected from batch and continuous flow experiments the overall TOF can be used as a measure of the space-time productivity. Again, a rate enhancement was found when the cross-coupling reaction was performed inside the flow microreactor; in the case of the **11b@γ-Al_2O_3** the reaction rate gain was rather small (Table 4.12), whereas for the case of **11b@TiO_2** the reaction was *ca* 5 times faster compared to the corresponding batch process.

Table 4.12. Comparison in activity and productivity of catalysts **11b@γ-Al_2O_3** and **11b@TiO_2** in the Sonogashira coupling between **24f** and **28a** in relation to the mode of operation (batch or continuous flow).

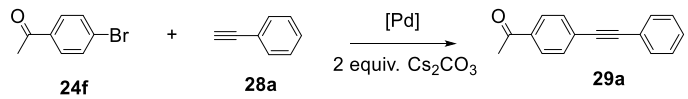

24f **28a** **29a**

Mode	Cat.[a]	mmol conv.	mmol Pd	T(°C)	Operation Time (h)	TON[b]	TOF[b] (h^{-1})
Batch[c]	Ti	0,46	0,005	80	64	91	5,69
	Al	0,49	0,005	80	64	99	6,19
Cont.	Ti	1,938[e f]	0,028	65	2,33	69,21	29,7
flow	Al	1,06[e]	0,045	65	2,33	24	10,11

[a] Ti = **11b@TiO_2**, Al = **11b@γ-Al_2O_3**; [b] TON and TOF data refer to the overall flow experiment and to results obtained in the first run of the batch tests; (the first 140 minutes were considered for the flow experiment). [c] For the exact reaction conditions in the batch experiments see Figure 4.10.[d] Sum of the total cross-coupling product obtained after 5 successive runs. [e] total cross-coupling product obtained after 140 minutes in flow, by GC analysis using mesitylene as standard. [f] Refers to Exp 3.

Next, a long term Sonogashira experiment employing the titania supported catalyst **11b@TiO_2** was carried out (Figure 4.18). The reaction

was carried out employing the same conditions as previously (Table 4.11, entry 4,). Again, an incubation period was observed, after which a maximum of 82 % of conversion was achieved. This conversion was maintained for 4 hours under continuous flow. At longer reaction times, the conversion started to decrease, before apparently settling down again at 57% conversion during the last hour of the experiment.

Despite this deactivation, the results obtained using **11b@TiO$_2$** represent the first example of the application of a heterogenized Pd complex in the Sonogashira coupling of aryl bromides under continuous flow conditions.

Under flow conditions catalyst **11b@TiO$_2$** displayed significantly higher TOF compared to the corresponding batch process, demonstrating the potential of catalytic flow synthesis.

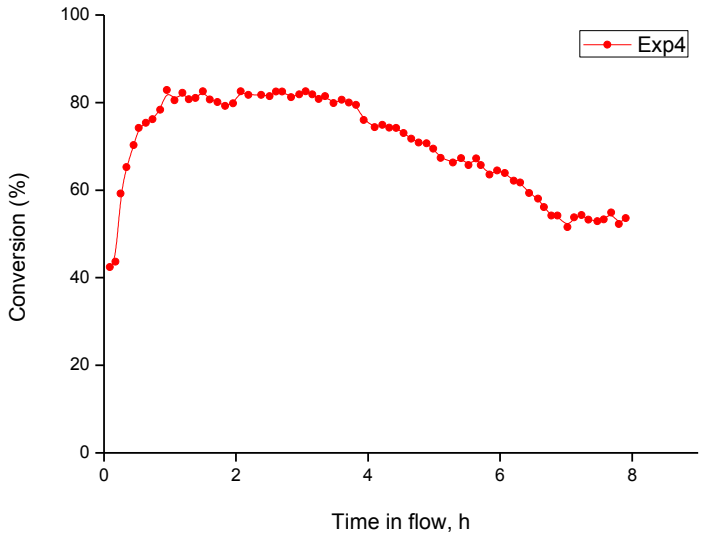

Figure 4.18. Performance of **11b@TiO$_2$** in the Sonogashira coupling between **24f** and **28a** in a long continuous flow run.

4.2.2.2. Application of heterogenized [Pd(NHC)] complexes in the Heck coupling

The Heck reaction is a very convenient methodology for the synthesis of vinylarenes and the construction of

conjugated double bonds.[2] For this reason the previously described solid-supported [Pd(NHC)] complexes were applied in this useful transformation. In view of the detrimental effect of the presence of water on catalyst's stability in related C-C processes, the supported catlaysts were tested in the reaction between 4-bromoacetophenone (**24f**) and ethyl acrylate (**30**) using various combinations of bases and solvents under non-aqueous reaction conditions (Table 4.13). When Cs_2CO_3 was used as the base, in combination with polar and non polar solvents, very little of the desired Heck product was obtained (entries 1-4). In contrast, high yield was obtained by using K_2CO_3 instead, yielding **31a** in up to 88% yield when the reaction was run in DMF (entry 5). The use of organic bases such as trimethylamine is interesting regarding its higher solubility in organic solvents, and also the better solubility of byproduct ammonium salts compared to the very low solubility of alkali halides in DMF for instance. However only low product yields were obtained using this base in combination with either DMF (Table 4.13, entry 7) or MeOH (entry 8).

Table 4.13. Optimization of reaction conditions for the Heck coupling between **24f** with **30** catalyzed by **13b@MCM-41**.

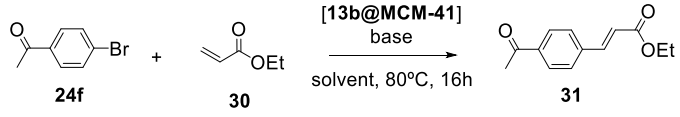

Entry	Solvent	Base	Yield(%)[a]
1	toluene	Cs_2CO_3	trace
2	DMF	Cs_2CO_3	trace
3	MeOH[b]	Cs_2CO_3	5
4	dioxane	Cs_2CO_3	trace
5	DMF	K_2CO_3	88
6	MeOH[b]	K_2CO_3	60
7	DMF	NEt_3	22
8	MeOH	NEt_3	19

Conditions: 0,5 mmol 4-bromoacetophenone, 0,75 mmol ethyl acrylate, 2,0 equiv base, 1 mol % **13b@MCM-41**; [a] GC-FID using mesitylene as standard, and referred to calibration curves. [b] the reaction mixture was heated to reflux.

Next, the most successful reaction conditions (entry 5) were used to evaluate the robustness of this system by recycling and reusing the catalysts. In view of the better performance of TiO_2- and γ-Al_2O_3-supported catalysts in related C-C coupling processes only these two materials were included in the study (Figure 4.19). **11b@TiO$_2$** showed higher activity in the first cycle, affording the coupling product **31** in 98% yield to 78% for **11b@γ-Al$_2$O$_3$**. However, a marked, constant decrease in activity was observed for both catalysts, ultimately resulting in zero conversion after the 4th run for both systems. ICP-OES analysis of the reaction mixtures after each run revealed a total amount of leached Pd representing 10,11% of the total Pd in the fresh catalyst.

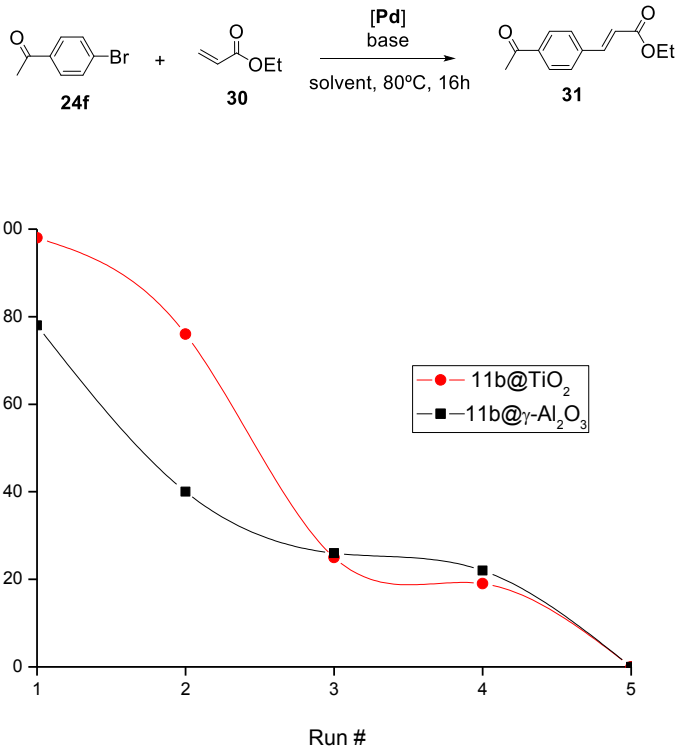

Figure 4.19. Recycling of catalysts **11b@γ-Al$_2$O$_3$** and **11b@TiO$_2$** in the Heck coupling between **24f** and **30** under batch conditions.

Conditions: 0,5 mmol 4-bromoacetophenone, 0,75 mmol phenylacetylene, 1 mol% [Pd], 2 mL dry and deoxygenated DMF.

These results indicate that some of the catalyst is lost during the reaction under these conditions and a contribution from *in situ* formed NPs or Pd clusters on the results must be considered. The leaching values observed in the recycling experiments for the Heck reaction between **24f** and **30** are slightly higher than those measured in the Suzuki coupling of **24a** with **25a** (Table 4.4), but the quantified leached Pd does not entirely explain the drop in catalyst activity, and other phenomena may also be contributing to the activity decay.

4.3. Conclusions

The heterogenized [Pd(NHC)] complexes were active in three different C-C bond forming processes. In the Suzuki-Miyaura reaction, various SiO_2-supported materials were tested, and compared. The results highlighted the importance of bulky *ortho*-substitution on the aromatic wingtips of the ligand for high catalytic activity. The end-capping of the silica surface with apolar groups resulted in more active/stable materials. Activation of challenging aryl chlorides was achieved, and bromide substrates with varying steric and electronic effects or having an heteroaromatic structure were coupled with efficiency under relatively mild conditions. However, under optimized reaction conditions, degradation of the catalyst occurred, resulting in the leaching of Pd species into the product. Running the Suzuki coupling under non-aqueous conditions resulted in improved catalyst stability, and degradation of the catalyst occurred more slowly, and without visible formation of Pd black. This enhanced stability allowed for the application of **13b@SiO_2** and **14b@SiO_2** in the Suzuki coupling under continuous flow conditions, maintaining a moderate conversion after two hours on stream.

Heterogenized [Pd(NHC)] precatalysts were also applied in the Sonogashira coupling of aryl bromides with various alkynes, obtaining high to excellent yields in batch mode. Furthermore catalytic materials based on SiO_2, γ-Al_2O_3 and TiO_2 could be recycled for at least four consecutive runs; again **11b@γ-Al_2O_3** and **11b@TiO_2** were the most robust under the applied reaction conditions. Performing the Sonogashira coupling under continuous flow conditions revealed that

both catalytic materials remained active after more than two hours on stream without significant loss in catalytic activity.

An induction period of *ca* 40 minutes was observed, in contrast with what was observed during the Suzuki reaction, and could be due to the *in situ* formation of catalytically active clusters, although no Pd black was found in the outlet flow in any of the anhydrous experiments. Finally the **11b@TiO$_2$** material was applied in a long-term continuous experiment, and catalyst deactivation was detected after 4 hours on stream. Again, the TOF's obtained in the continuous flow experiments were compared with those obtained for the corresponding batch process, and the reaction rates were increased up to 5 times, confirming the increased space-time yields that can be achieved by operating a synthetic process in a continuous manner.

Lastly, **11b@TiO$_2$** and **11b@Al$_2$O$_3$** were active in the Heck coupling of aryl bromides with electron-poor olefins. However, under the most optimal reaction conditions (excluding the presence of water) poor recyclability was observed.

4.4. Experimental part

General

Reactions were carried out using standard bench-top techniques unless the use of a Schlenk flask is specified, in which case Schlenk-line inert atmosphere techniques were used. Where stirring of the reaction mixture is indicated, magnetic stirring using a Teflon-coated stir bar was employed throughout. Commercially supplied compounds were used without further purification. Dry solvents were prepared by distillation from Na/benzophenone, CaH_2 or P_2O_5, or collected from a Braun SPS800 solvent purification system. Solution-state NMR spectra were obtained at the Servei de Recursos Científics i Tècnics (SRCiT), URV, with Varian (Agilent) Mercury VX400 or NMR System400 400 MHz spectrometers and calibrated to residual solvent peaks. Chemical shifts for ^{1}H and ^{13}C{^{1}H} NMR spectra are reported relative to TMS. ICP analyses were conducted at the SRCiT using an ICP-OES Spectro Arcos instrument. Samples were digested in concentrated HNO_3 under microwave irradiation before being diluted for analysis. Other than

solvents, reagents obtained from commercial sources were used without further purification.

General procedure for catalytic Suzuki–Miyaura reaction runs.

A small Schlenk flask or a 5 mL screw topped vial was charged with the catalyst, base, boronic acid, and the aryl halide (if solid). The flask or the vial was capped with a septum and flushed with N_2, and then the aryl halide was added using a microsyringe if liquid. The solvent was added using a syringe (2 mL of organic solvent or 1.5 mL of organic solvent and 0.75 mL of water) and, in the case of the Schlenk flask runs, the septum was replaced with a glass stopper. The reaction mixture was then stirred at 400 rpm and heated at the indicated temperature. After the indicated reaction time, the vessel was cooled in an ice bath. Next, the organic fraction was filtered through a small plug of silica. In the case of the biphasic aqueous runs, the aqueous layer was then extracted with toluene (2 × 0.5 mL) and the extracts were filtered through the same silica plug. The silica plug was then washed with toluene (1 mL). The product mixture was analyzed by GC-FID at this stage, and then it was evaporated under reduced pressure and purified by silica gel chromatography using hexane/EtOAc as the eluent.

General procedure for catalytic Sonogashira reaction runs. A small Schlenk flask was charged with the catalyst, base, alkyne and *p*-bromoacetophenone. 2 mL of solvent were added and the septum was replaced with a glass stopper. The reaction mixture was then stirred at 400 rpm and heated at the indicated temperature. After the indicated reaction time, the vessel was cooled in an ice bath. Next, the organic fraction was filtered through a small plug of silica. The silica plug was then washed with toluene (1 mL). The product mixture was analyzed by GC-FID at this stage, and then it was evaporated under reduced pressure and purified by silica gel chromatography using hexane/EtOAc as the eluent.

General procedure for catalytic Heck reaction runs. A small Schlenk flask was charged with the catalyst, *p*-bromoacetophenone and ethyl acrylate. 2 mL of solvent were added and the reaction was brought

to the indicated temperature. Inmediately, the base was added and the reaction mixture was maintained at the indicated temperature while stirring. After the reaction time, the vessel was cooled in an ice bath. The supernatant was decanted and additional solvent was added to collect any remaining substrate Next, the organic fraction was filtered through a small plug of silica. The silica plug was then washed with toluene (1 mL). The product mixture was analyzed by GC-FID at this stage, and then it was evaporated under reduced pressure and purified by silica gel chromatography using hexane/EtOAc as the eluent.

Coupling products obtained by SM reactions

4-methoxy-2 ,4´ -dimethylbiphenyl. The reagents 4-bromo-*m*-xylene (136 µL, 1.0 mmol, 1.0 equiv.), 4-methoxyphenylboronic acid (182 mg, 1.2 mmol, 1.2 equiv.), Cs_2CO_3 (652 mg, 2.0 mmol, 2.0 equiv.), (**14b@SiO$_2$**) (60 mg, 0.01 equiv.) were used as described in the general procedure for catalytic SM reaction runs. Purified by column chromatography using 25:1 n-hexane/EtOAc as the eluant. **^{1}H NMR** (400 MHz, $CDCl_3$): δ 7.24 (d, J = 8.8 Hz, 2H), 7.12 (d, J = 7.7 Hz, 1H), 7.09 (s, 1H), 7.05 (d, J = 7.7 Hz, 1H), 6.94 (d, J = 8.8 Hz, 2H), 3.85 (s, 3H), 2.36 (s, 3H), 2.25 (s, 3H). NMR data match literature values. MS (EI): m/z = 212 (H+), 197, 181.

2,4-dimethyl-2'-methylbiphenyl. The reagents 4-bromo-*m*-xylene (136 µL, 1.0 mmol, 1.0 equiv.), 2-methylphenylboronic acid (164 mg, 1.2 mmol, 1.2 equiv.), Cs_2CO_3 (652 mg, 2.0 mmol, 2.0 equiv.), (**14b@SiO$_2$**) (60 mg, 0.01 equiv.) were used as described in the general procedure for catalytic SM reaction runs. Purified by column chromatography using n-hexane as the eluant. **^{1}H NMR** (400 MHz, $CDCl_3$): δ 7.26–7.19 (m, 3H), 7.11–7.09 (m, 2H), 7.04 (br d, J = 7.6 Hz, 1H), 7.00 (d, J = 7.6 Hz, 1H), 2.37 (s, 3H), 2.06 (s, 3H), 2.03 (s, 3H). MS (EI): m/z = 196 (M+), 181, 165, 152. NMR and MS peaks match literature values.

2-(2-methylphenyl)pyridine. The reagents 2-bromopyridine (96 µL, 1.0 mmol, 1.0 equiv.), 2-methylphenylboronic acid (164 mg, 1.2 mmol, 1.2 equiv.), Cs_2CO_3 (652 mg, 1.0 mmol, 2.0 equiv.), (**14b@SiO$_2$**) (30 mg, 0.01 equiv.) were used as described in the general procedure for catalytic SM reaction runs. Purified by column chromatography using 10 : 1 n-hexane/EtOAc as the eluant. **^{1}H NMR** (400 MHz, $CDCl_3$): δ 8.71 (d d d, J^1 = 4.9 Hz, J^2 = 1.8 Hz, J^3 = 0.9 Hz, 1H), 7.78 (d d d, J^1 = 7.7 Hz, J^2 = 7.7 Hz, J^3

= 1.8 Hz, 1H), 7.43 (d d d, J^1 = 7.8 Hz, J^2 = 1.1 Hz, J^3 = 1.0 Hz, 1H), 7.41–7.39 (m, 1H), 7.32–7.26 (m, 4H), 2.03 (s, 3H). HR-MS: m/z = 170.1000, calcd. for $C_{12}H_{12}N$ [M–H+]: 170.0966.

2-(4-methoxyphenyl)pyridine. The reagents 2-bromopyridine (96 µL, 1.0 mmol, 1.0 equiv.), 4-methoxyphenylboronic acid (182 mg, 1.2 mmol, 1.2 equiv.), Cs2CO_3 (652 mg, 1.0 mmol, 2.0 equiv.), (**14b@SiO_2**) (30 mg, 0.01 equiv.) were used as described in the general procedure for catalytic SM reaction runs. Purified by column chromatography using 10 : 1 n-hexane/EtOAc as the eluant. **^{1}H NMR** (400 MHz, CDCl3): δ 8.65 (ddd, J^1 = 4.9 Hz, J^2 = 1.8 Hz, J^3 = 1.0 Hz, 1H), 7.95 (d, J = 9.0 Hz, 2H), 7.75–7.66 (m, 2H), 7.18 (ddd, J^1 = 7.2 Hz, J^2 = 4.9 Hz, J^3 = 1.3 Hz, 1H), 7.00 (d, J = 9.0 Hz, 2H), 3.87 (s, 3H). HR-MS: m/z = 186.0889, calcd. for $C_{12}H_{12}NO$ [M–H+]: 186.0915.

4-(4-methoxyphenyl)benzonitrile. The reagents 4-bromobenzonitrile (91 mg, 0.5 mmol, 1.0 equiv.), 4-methoxyphenylboronic acid (91 mg, 0.6 mmol, 1.2 equiv.), Cs_2CO_3 (326 mg, 1.0 mmol, 2.0 equiv.), (**14b@SiO_2**) (30 mg, 0.01 equiv.) were used as described in the general procedure for catalytic SM reaction runs. Chromatographed with 5:1 *n*-hexane/EtOAc. **^{1}H NMR** (400 MHz, $CDCl_3$): *δ* 7.70 (d, *J* = 8.7 Hz, 2H), 7.64 (d, *J* = 8.7 Hz, 2H), 7.54 (d, *J* = 8.9 Hz, 2H), 7.01 (d, *J* = 8.9 Hz, 2H), 3.87 (s, 3H). HR-MS: *m*/*z* = 232.0712, calcd. for $C_{14}H_{11}NNaO$ [M-Na^+]: 232.0735.

Coupling products obtained by Sonogashira reactions

1-(4-((4-methoxyphenyl)ehtynyl)phenyl)ethanone. 4'-bromoacetophenone (203 mg, 1.0 mmol, 1.0 equiv.), ethynylanisole (200 µL, 1.5 mmol, 1.5 equiv.), Cs_2CO_3 (652 mg, 2.0 mmol, 2.0 equiv.), (**11b@Al_2O_3**) (60.4 mg, 0.01 equiv.). Chromatographed with 5:1 n-hexane/EtOAc. **^{1}H NMR** (400 MHz, $CDCl_3$): δ 2.59 (s, 3H), 3.81 (s, 3H), 6.88 (d, 2H, J = 8.8 Hz), 7.48 (d, 2H, J = 9.2 Hz), 7.56 (d, 2H, J = 8.8 Hz), 7.91 (d, 2H, J = 8.8 Hz); NMR and MS peaks match literature values. MS (EI): m/z = 212 (H+), 197, 181.

1-(4-o-Tolylethynylphenyl)ethanone. 4'-bromoacetophenone (203 mg, 1.0 mmol, 1.0 equiv.), 2-ethynyltoluene (195 µL, 1.5 mmol, 1.5 equiv.), Cs_2CO_3 (652 mg, 2.0 mmol, 2.0 equiv.), (**11b@Al_2O_3**) (60.4 mg, 0.01

equiv.). Chromatographed with n-hexane. **^{1}H NMR** (400 MHz, $CDCl_3$): δ 2.53 (s, 3H), 2.62 (s, 3H), 7.18-7.27 (m, 3H), 7.51 (d, 2H, J = 8.4 Hz), 7.61 (d, 2H, J = 8.4 Hz), 7.94 (d, 2H, J = 8.8 Hz); m/z = 196 (M+), 181, 165, 152. NMR and MS peaks match literature values.[115]

***1-(4-(Phenylethynyl)phenyl)ethanone*.** 4'-bromoacetophenone (203 mg, 1.0 mmol, 1.0 equiv.), 2-phenylacethylene (170 µL, 1.5 mmol, 1.5 equiv.), Cs_2CO_3 (652 mg, 2.0 mmol, 2.0 equiv.), (**11b@Al_2O_3**) (60.4 mg, 0.01 equiv.). Chromatographed with n-hexane. **^{1}H NMR** (400 MHz, $CDCl_3$): δ 2.62 (s, 3H), 7.36-7.39 (m, 3H), 7.54-7.57 (m, 2H), 7.60-7.63 (m, 2H), 7.95 (d, 2H, J = 8.0 Hz); m/z = 196 (M+), 181, 165, 152. NMR and MS peaks match literature values.[116]

***1-(4-((4-aminophenyl)ethynyl)phenyl)ethanone*.** 4'-bromoacetophenone (203 mg, 1.0 mmol, 1.0 equiv.), 4-ethynylaniline (182 µL, 1.5 mmol, 1.5 equiv.), Cs_2CO_3 (652 mg, 2.0 mmol, 2.0 equiv.), (**11b@Al_2O_3**) (60.4 mg, 0.01 equiv.). Chromatographed with n-hexane. **^{1}H NMR** (400 MHz, $CDCl_3$): δ 2.60 (s, 3H), 7.64 (d, 2H, J = 8.0 Hz), 7.35 (d, 2H, J = 8.0 Hz), 7.55 (d, 2H, J = 8.0 Hz), 7.91 (d, 2H, J = 8.0 Hz); m/z = 196 (M+), 181, 165, 152. HR-MS: m/z = 186.0889, calcd. for $C_{12}H_{12}NO$ [M-H+]: 186.0915.

Coupling products obtained by Heck reactions

(E)-Ethyl 3-phenylacrylate: The reagents 4-bromoacetophenone (99,5 mg, 0,5 mmol, 1.0 equiv.), ethyl acrylate (80 µL, 0,75 mmol, 1.5 equiv.), K_2CO_3 (138 mg, 1.0 mmol, 2.0 equiv.), (**11b@γ-Al_2O_3**) (31 mg, 1 mol%.) were used as described in the general procedure for catalytic SM reaction runs. Chromatographed with 6:1 *n*-hexane/EtOAc. . **^{1}H NMR** (400 MHz, $CDCl_3$): *δ* 7.68 (d, J = 16.03 Hz, 1H), 7.52–7.36 (m, 5H), 6.43 (d, J = 16.01 Hz, 1H), 4.26 (q, J = 7.16 Hz, 2H), 1.33 (t, J = 7.10 Hz, 3H). Peaks match literature values.[117]

General procedure for recycling of the supported catalysts under batch operation.

In the cases where catalyst recycling was performed, an internal standard (undecane) was added after cooling the reaction mixture in an ice bath; the supported catalyst was separated from the organic phase by decantation, filtration and washing with toluene (2 × 1 mL), which was

then combined with the organic phase of the reaction. The supported catalyst was then successively washed with water, EtOH and Et_2O, then dried under vacuum and directly reused in the next cycle.

Experimental procedure for continuous flow tests. The catalytic activity and stability of the supported catalysts were studied under flow conditions using a Vapourtec system with an R2 pump module and an R4 reactor module. Two feed solutions were deoxygenated by bubbling N_2 for 1 h prior to reactions and then were pumped by two HPLC pumps into the T-connection (PTFE, 0.5 mm through holes, Upchurch Scientific) via PFA tubing (1.6 mm in OD, 1.2 mm in ID) at equal flow rates (u1 = u2 = 0.15 mL min− 1). The merged flow was then introduced to the inlet of the packed bed column assembly (borosilicate glass with PTFE end pieces, 6.6 mm in ID × 100 mm in length, OmniFit). The column was packed with a catalyst and has a catalytic bed length of 2.3 cm, which corresponds to a packed bed volume of 0.787 mL. The measured amount of the catalyst was diluted with QuadraSil AP (Johnson Matthey) spherical silica beads. The void volume in the catalytic bed in the approximation of random close packing of ideal spheres is 0.295 mL (the void fraction is about 0.375, neglecting the porosity of the support). The mean residence times in the packed bed were found to be 3.5 and 1.9 minutes in the cases of organic and aqueous–organic flow, respectively (calculated from the residence time distribution curves measured for the QuadraSil AP using a standard tracer technique). For the loadings of the catalysts used in this study this void corresponds to an initial molar ratio of Ar–Br : Pd ≈ 2.1 in the reactor in the case of the aqueous–organic flow experiment or 0.4 in the case of the organic anhydrous conditions. The catalytic loadings in the reactor are still quite high even if we assume the porosity of the support to be about 60% (ArBr : Pd ≈ 4.2 or 0.9 for the aqueous-organic and anhydrous conditions, respectively).

Table S4.1. Screening of polar solvents for the Suzuki-Miyaura coupling between **24a** and **25a** under batch conditions.

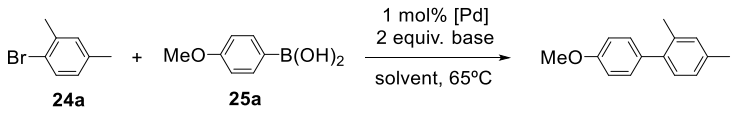

24a **25a**

Entry	Base	Solv.	Conv. (%)	[Base]$_S$ (M)[b]	[Byprod.]$_S$ (M)[b]	[Subst.]$_S$ (M)[b]
1	Cs_2CO_3	Toluene	95	0,002	CsBr (low)	0,0005
2		Dioxane	4	0,005	CsBr (low)	0,00025
3		MeOH	74	1,2	CsBr (0,11)	0,055
4		EtOH	16	0,3	CsBr (<0,11)	<0,05
5		DMF	N/T	0,4	CsBr (0,024)	0,012
6		DMSO	0	1,1	N/A	N/A
7		NMP	N/T	2,2	N/A	N/A
8	CsF	MeOH	23	6	CsBr (0,11)	0,055
9		EtOH	44	<6	CsBr (<0,11)	<0,05
10		DMF	17	0,0006	CsBr (0,024)	0,012
11	K_3PO_4	MeOH	70	0,09	KBr (0,17)	0,045
12		EtOH	71	<0,09	KBr (0,04)	0,02
13		DMF	41	N/A	KBr (0,008)	0,004

Conditions: 0.5 mmol ArBr, 0.6 mmol ArB(OH)2, 1.0 mmol base, 2,0 mL solvent, 60 °C. [a] Conversions obtained by GC-FID, average of two runs.[b] Solubilities at 25°C; N/T = Not tested; N/A = Not available.

4.5. References

[1] N. Miyaura, A. Suzuki, *Chem. Rev.* **1995**, *95*, 2457.
[2] I.P. Beletskaya, A.V. Cheprakov, *Chem. Rev.* **2000**, *100*, 3009.
[3] R. Chinchilla, C. Nájera, *Chem. Soc. Rev.* **2011**, *40*, 5084.
[4] E.-I. Negishi, *Angew. Chem. Int. Ed.* **2011**, *50*, 6738.
[5] A. Suzuki, *Angew. Chem. Int. Ed.* **2011**, *50*, 6722.
[6] M. García-Melchor, A.A.C. Braga, A. Lledós, G. Ujaque, F. Maseras, *Acc. Chem. Res.*, **2013**, *46*, 2626.
[7] J.K. Stille, *Angew. Chem. Int. Ed*. **1986**, *25*, 508.
[8] E.-I. Negishi, A.O. King, N. Okukado, *J. Org. Chem.* **1977**, *42*, 1821.
[9] A. de Meijere, F. Diderich, *Metal-catalyzed cross-coupling reactions*, 2nd ed.; Wiley-VCH: Weinheim **2008**
[10] K. Tamao, N. Miyaura, *Top. Curr. Chem.* **2002**, *219*, 1.
[11] A. Zapf, M. Beller, *Chem. Commun.* **2005**, 431.
[12] J. Tsuji, *Pd reagents and catalysts*, Wiley: New York, **2004**, Chapter 3, p 105.
[13] Y.-R. Lou, *Comprehensive Handbook of Chemical Bond Energies,* CRC Press, London, **2007**.
[14] G.C. Fortman, S.P. Nolan, *Chem. Soc. Rev*., **2011**, *40*, 5151.
[15] J. Tsuji, *Palladium Reagents and Catalysts, Innovations in Organic Synthesis*, Wiley, New York, **1995**.
[16] K. Inada, N. Miyaura, *Tetrahedron*, **2000**, *56*, 8661.
[17] S. Saito, M. Sakai, N. Miyaura, *Tetrahedron Lett*. **1996**, *37*, 2993.
[18] A. Zapf, M. Beller, *Chem. Eur. J*., **2000**, *6*, 1830.
[19] G. A. Grassa, A. C. Hillier, S. P. Nolan, *Org. Lett*., **2001**, *3*, 1077.
[20] W. A. Herrmann, C.-P. Reisinger, M. Spiegler, *J. Organomet. Chem*., **1998**, *557*, 93.
[21] C. R. LeBlond, A. T. Andrews, Y. Sun, J. R. Sowa, Jr., *Org. Lett*., **2001**, *3*, 1555.
[22] M. Feuerstein, H. Doucet, M. Santelli, *Synlett*, **2001**, 1458
[23] C. Amatore, A. Jutand, *Acc. Chem. Res*., **2000**, *33*, 314.
[24] F. Firooznia, C. Gude, K. Chan, Y. Satoh, *Tetrahedron Lett*. **1998**, *39*, 3985.
[25] D. W. Old, J. P. Wolfe, S. L. Buchwald, *J. Am. Chem. Soc*., **1998**, *120*, 9722
[26] A. F. Littke, G. C. Fu, *Angew. Chem. Int. Ed*. **1998**, *37*, 3387.
[27] C. Zhang, J. Huang, M. L. Trudell, S. P. Nolan, *J. Org. Chem*. **1999**, 64, 3804.
[28] J. F. Hartwig, F. Paul, *J. Am. Chem. Soc*., **1995**, *117*, 5373.
[29] J. F. Hartwig, *Pure Appl. Chem*., **1999**, *71*, 1417.
[30] C. J. O'Brien, E. A. B. Kantchev, C. Valente, N. Hadei, G. A. Chass, A. Lough, A. C. Hopkinson and M. G. Organ, *Chem.–Eur. J*., **2006**, *12*, 4743.
[31] N. Marion, O. Navarro, J. Mei, E. D. Stevens, N. M. Scott and S. P. Nolan, *J. Am. Chem. Soc*., **2006**, *128*, 4101.
[32] O. Diebolt, P. Braunstein, S.P. Nolan, C.S.J. Cazin, *Chem. Commun*., **2008**, 3190.
[33] A.J.J. Lennox, G.C. Lloyd-Jones, *Angew. Chem. Int. Ed.*, **2013**, 52, 7362.
[34] D. Gelman, S.L. Buchwald, *Angew. Chem. Int. Ed.*, **2003**, *42*, 5993.

[35] M. Aufiero, F. Proutiere, F. Schoenebeck, *Angew. Chem. Int. Ed.*, **2012**, *51*, 7226.
[36] T. Ljungdahl, T. Bennur, A. Dallas, H. Emtenäs, J. Martensson, *Organometallics,* **2008**, *27*, 2490.
[37] C. Torborg, M. Beller, *Adv. Synth. Catal.*, **2009**, 351, 3027.
[38] J. Magano, J.R. Dunetz, *Chem. Rev.*, **2011**, *111*, 2177.
[39] A.F.P. Biajoli, C.S. Schwalm, J. Limberger, T.S. Claudino, A.L. Monteiro, *J. Braz. Chem. Soc.*, **2014**, 25, 2186.
[40] The European Agency for the Evaluation of Medicinal Products. http://www.emea.europa.eu/pdfs/human/swp/44460oen.pdf, August **2007**.
[41] Y. Urawa, M. Miyazawa, N. Ozeki, K. Ogura, *Org. Process Res. Dev.* **2003**, *7*, 191.
[42] C. E. Garrett, K. Prasad, *Adv. Synth. Catal*. **2004**, *346*, 889.
[43] SiliCycle, www.silicycle.com; April **2003**
[44] C.J. Pink, H. Wong, F. C. Ferreira, A. G. Livingston, *Org. Process Res. Dev*. **2008**, *12*, 589.
[45] K. Azyat, E. Jahnke, T. Rankin, R. R. Tykwinski, *Chem. Commun*. **2009**, 433.
[46] T. Schulz, C. Torborg, B. Schäffner, J. Huang, A. Zapf, R. Kadyrov, A. Börner, M. Beller, *Angew. Chem. Int. Ed*. **2009**, *48*, 918.
[47] S. Hayashi, H. Yorimitsu, K. Oshima *J. Am. Chem. Soc*. **2009**, *131*, 2052.
[48] S. L. Büchwald, C. Bolm, *Angew. Chem. Int. Ed*. **2009**, *48*, 5586.
[49] A. Correa, O. G. Mancheno, C. Bolm, *Chem. Soc. Rev.* **2008**, *37*, 1108.
[50] Y. Liu, S.-S. Wang, W. Liu, Q.-X. Wan, H.-H. Wu, G.-H. Gao, *Curr. Org. Chem.* **2009**, *13*, 1322.
[51] S. Liu, J. Xiao, *J. Mol. Catal. A: Chem*. **2007**, *270*, 1.
[52] H. Wong, S. Han, A.G. Livingston, *Chem. Eng. Sci.* **2006**, *61*, 1338.
[53] Á. Molnár, *Chem. Rev*. **2011**, *111*, 2251.
[54] R. Porta, M. Benaglia, A, Puglisi, *Org. Process Res. Dev*. **2016**, *20*, 2.
[55] C. Pavia, E. Ballerini, L. A. Vilona, F. Fiacalone, C. Aprile, L. Vaccaro and M. Gruttadauria, *Adv. Synth. Catal.,***2013**, *355*, 2007.
[56] L. Yin, J. Liebscher, *Chem. Rev.*, **2007**, *107*, 133.
[57] A. Balanta, C. Godard, C. Claver, *Chem. Soc. Rev.,* **2011**, *40*, 4973.
[58] M. Pagliaro, V. Pandarus, R. Ciriminna, F. Béland, P.D. Carà, C*hemCatChem* **2012**, *4*, 432.
[59] R. G. Heidenreich, K. Köchler, J. G. E. Krauterb, J. Pietsch*, Synlett,* **2002**, 1118.
[60] A. Biffis, M. Zecca, M. Basato, *Eur. J. Inorg. Chem.* **2001**, 1131.
[61] B. Yuan, Y. Pan, Y. Li, B. Yin, H. Jiang, *Angew. Chem. Int. Ed*. **2010**, *49*, 4054.
[62] V. Kogan, Z. Aizenshtat, R. Popovitz-Biro, R. Neumann, *Org. Lett*., **2002**, *4*, 3529.
[63] S. Lohmann, S. P. Andrews, B. J. Burke, M. D. Smith, J. P. Attfield, H. Tanaka, K. Kaneko, S. V. Ley, *Synlett*, **2005**, 1291.
[64] R. Ciriminna, L. M. Ilharco, A. Fidalgo, S. Campestrini, M. Pagliaro, *Soft Matter,* **2005**, *1*, 231.
[65] R. K. Arvela, N. E. Leadbeater, M. S. Sangi, V. A. Williams, P. Granados, R. D. Singer, *J. Org. Chem*. **2005**, *70*, 161.
[66] M. Weck, C. W. Jones, *Inorg. Chem*., **2007**, *46*, 1865.
[67] S. Hübner, J.G. de Vries, V. Farina, *Adv. Synth. Catal.* **2016**, *358*, 3.

---

[68] C.C. Tzschucke, V. Andrushko, W. Bannwarth,, *Eur. J. Org. Chem.*, **2005**, 5248.
[69] K. Okuruma, T. Tomiyama, S. Okuda, H. Yoshida, M. Niwa, *J. Catal.*, **2009**, *265*, 89.
[70] K. Köhler, S.S. Pröckl, W. Kleist, *Catal. Lett.*, **2008**, *125*, 197.
[71] M. T. Reetz, E. Westermann, *Angew. Chem. Int. Ed,.* **2000**, *39*, 165
[72] D. J. Berrisford, C. Bolm, K. B. Sharpless, *Angew. Chem. Int. Ed. Engl*., **1995**, *34*, 1059.
[73] R. J. Lundgren, M. Stradiotto, *Chem. Eur. J.* **2012**, *18*, 9758.
[74] B. Yuan, Y. Pan, Y. Li, B. Yin, H. Jiang, *Angew. Chem. Int. Ed*. **2010**, *49*, 4054.
[75] M. D. Smith, A. F. Stepan, C. Ramarao, P. E. Brennan, S. V. Ley, *Chem. Commun*., **2003**, 2652.
[76] M.-J. Jin, D.-H. Lee, *Angew. Chem. Int. Ed*. **2010**, *49*, 1119.
[77] F. Rajabi, D. Shaffner, S. Follmann, C. Wilhelm, S. Ernst, W.R. Thiel, *ChemCatChem,* **2015**, *7*, 3513.
[78] T.J. Colacot, W.A. Carole, B.A. Neide, A. Harad, *Organometallics* **2008,** *27,* 5605.
[79] G. Li, H. Yang, W. Li, G. Zhang, *Green Chem.*, **2011**, *13*, 2939.
[80] H. Remmele, A. Köllhofer, H. Plenio, *Organometallics*, **2003**, *22*, 4098.
[81] M.L. Kantam, S. Roy, M. Roy, M.S. Subhas, P.R. Likhar, B. Sreedhar, *Synlett*, **2006**, 2747.
[82] B.M. Choudary, S. Madhi, N.S. Chowdari, M.L. Kantam, B. Sreedhar, *J. Am. Chem. Soc.*, **2002**, *124*, 14127.
[83] Y. Wan, H. Wang, Q. Zhao, M. Klingstedt, O. Terasaki, D. Zhao, *J. Am. Chem. Soc.*, **2009**, *131*, 4541.
[84] J.-C. Xiao, B. Twamley, J.M. Shreeve, *Org. Lett.*, **2004**, *6*, 3845.
[85] K.Q. Yu, W. Sommer, M. Weck, C.W. Jones, *J. Catal.,* **2004**, 226, 101.
[86] E. Alacid, D.A. Alonso, L. Botella, C. Nájera, M.C. Pacheco, *Chem. Rev.* **2006**, *6*, 117.
[87] A. Corma, H. García, A. Leyva, *J. Catal.* **2006**, *240*, 87.
[88] J. de Vries, *Dalton Trans.* **2006**, 421.
[89] D. Cantillo, C.O. Kappe, *ChemCatChem*, **2014**, *6*, 3286.
[90] A. Kirschning, C. Altwicker, G. Dröger, J. Harders, N. Hoffmann, U. Hoffmann, H. Schçnfeld, W. Solodenko, U. Kunz, *Angew. Chem. Int. Ed.,* **2001**, *40*, 3995.
[91] S. C. Stouten, Q. Wang, T. Noel, V. Hessel, *Tetrahedron Lett.* **2013**, *54*, 2194.
[92] C. Battilocchio, B. N. Bhawal, R. Chorghade, B. J. Deadman, J. M. Hawkins, S. V. Ley, *Isr. J. Chem.* **2014**, *54*, 371.
[93] C. Mateos, J. A. Rincon, B. Martn-Hidalgo, J. Villanueva, *Tetrahedron Lett.* **2014**, 55, 3701.
[94] N. Nikbin, M. Ladlow, S. V. Ley, *Org. Process Res. Dev*. **2007**, 11, 458- 462.
[95] N. T. S. Phan, J. Khan, P. Styring, *Tetrahedron* **2005**, *61*, 12065.
[96] M. Irfan, T.N. Glasnov, C.O. Kappe, *ChemSusChem,* **2011**, *4*, 300.
[97] V. Pandarus, G. Gingras, F. Béland, R. Ciriminna, M. Pagliaro, *Org. Process Res. Dev.,* **2014**, *18*, 1550.

[98] H. Yang, Y. Wang, Y. Qin, Y. Chong, Q. Yang, G. Li, L. Zhang, W. Li, *Green Chem.*, **2011**, *13*, 1352.
[99] G. Borja, A. Monge-Marcet, R. Pleixats, T. Parella, X. Cattoën, M. W. C. Man, *Eur. J. Org. Chem.* **2012**, 3625.
[100] J. Huang, S.P. Nolan, *J. Am. Chem. Soc.* **1999,** *121,* 9889.
[101] J.M. Muñoz, J. Alcázar, A. de la Hoz, A. Díaz-Ortiz, *Adv. Synth. Catal*. **2012**, *354,* 3456.
[102] S. Leuthäußer, D. Schwarz, H. Plenio, *Chem. Eur. J.* **2007**, *13*, 7195.
[103] S. Leuthäußer, V. Schmidts, C. M. Thiele, H. Plenio, *Chem. Eur. J.,* **2008**, *14*, 5465.
[104] S. Wolf, H. Plenio, *J. Organomet. Chem.* **2009**, *694*, 1487.
[105] O. Navarro, N. Marion, N. M. Scott, J. González, D. Amoroso, A. Bell, S. P. Nolan, *Tetrahedron* **2005**, *61*, 9716.
[106] H. Weissman, L. J. W. Shimon, D. Milstein, *Organometallics* **2004**, *23*, 3931.
[107] S. Fantasia, S. P. Nolan, *Chem. Eur. J.* **2008**, *14*, 6987.
[108] W. Lin, Q. Cai, W. Pang, Y. Yue, *Chem. Commun.*, **1998**, 2473.
[109] *Comprehensive Organic Synthesis,* ed. K. Sonogashira, Pergamon Press, Oxford, **1991**.
[110] J. Oliver-Meseguer, J. R. Cabrero Antonino, I. Dominguez, A. Leyva-Perez, A. Corma, *Science*, 2012, **238**, 1452.
[111] A. Gçmann, J. A. Deverell, K. F. Munting, R. C. Jones, T. Rodemann, A. J. Canty, J. A. Smith, R. M. Guijt, *Tetrahedron*, **2009**, *65*, 1450.
[112] S. Voltrova, J. Srogl, *Org. Chem. Front.*, **2014**, *1*, 1067.
[113] W. Solodenko, H. Wen, S. Leue, F. Stuhlmann, G. Sourkouni-Argirusi, G. Jas, H. Schçnfeld, U. Kunz, A. Kirschning, *Eur. J. Org. Chem*., **2004**, 3601.
[114] Y. Zhang, T. F. Jamison, S. Patel, N. Mainolfi, *Org. Lett.,* **2011**, *13*, 280.
[115] T. T. Hung, C. M. Huang and F. Y. Tsai, *ChemCatChem*, **2012**, *4*, 540.
[116] E. Buxaderas, D. A. Alonso and C. Najera, *Eur. J. Org. Chem.* **2013**, 5864.
[117] R. Imashiro, M. Seki, *J. Org. Chem*. **2004**, *69*, 4216.

UNIVERSITAT ROVIRA I VIRGILI
HETEROGENIZED N-HETEROCYCLIC CARBENE METAL COMPLEXES FOR SELECTIVE CATALYSIS
Alberto Martínez Lombardía

UNIVERSITAT ROVIRA I VIRGILI
HETEROGENIZED N-HETEROCYCLIC CARBENE METAL COMPLEXES FOR SELECTIVE CATALYSIS
Alberto Martínez Lombardía

Chapter 5

"Application of supported [Pd(NHC)] complexes in the semi-reduction of alkynes and alkynols."

UNIVERSITAT ROVIRA I VIRGILI
HETEROGENIZED N-HETEROCYCLIC CARBENE METAL COMPLEXES FOR SELECTIVE CATALYSIS
Alberto Martínez Lombardía

Application of supported [Pd(NHC)] complexes in the semi-reduction of alkynes and alkynols

5.1. Introduction

5.1.1. Background

The catalytic reduction by partial hydrogenation (semi-hydrogenation) of alkynes is an efficient method for the production of olefins, and palladium catalysts have been the most effective achieving this transformation.[1,2,3,4] In the bulk chemical industry, this reaction is used in the polymerization of ethylene to polyethylene to purify the feedstock from acetylene, which would otherwise poison the polymerization catalyst.[5,6] Thus, research on new palladium species for the catalytic semi-hydrogenation of acetylene to ethylene is a subject of present industrial interest.[7,8] The catalytic reduction of alkynes is also relevant to the fine chemicals sector. Many biologically active molecules incorporate carbon–carbon double bond(s) with well-defined configurations (E or Z), such as β-carotene,[9] polyene antifungal drugs,[10,11] crocacine,[12] but also polyunsaturated fatty acids (PUFAs), pheromones,[13,14,15] and cruentaren.[16]

In this context, various methodologies have been developed to synthesize alkenes with high regio- and stereocontrol of the resulting double bond. Several of these methods imply the construction of a C-C double bond, namely Wittig,[17,18] Horner–Emmons–Wadsworth,[19] Julia–Kocienski,[20] Peterson,[21] Takai olefination,[22] olefin metathesis[23,24] and cross-couplings.[25] Alternative methods for the stereoselective access to alkenes are elimination of halides[26] and reduction of alkynes.[27,28,13] While most of the above-mentioned reactions afford selectively (E)-alkenes, Pd-catalyzed semi-reduction of internal alkynes leads selectively to (Z)-alkenes (Scheme 5.1).

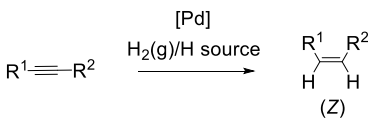

Scheme 5.1. Pd-catalyzed (Z)-selective semireduction of alkynes.

Over the last six decades, Lindlar's catalyst has been the benchmark for the selective semi-hydrogenation of internal alkynes to *cis*-alkenes.[29] This

heterogeneous catalyst is composed by Pd (5% weight) deposited on $CaCO_3$ and partially poisoned with $Pb(OAc)_2$ and quinoline.[30] This catalyst is commercially available, cheap, easy to handle, insensitive to air, and works under mild reaction conditions, usually room temperature and atmospheric H_2 pressure. Moreover, it tolerates the presence of other reducible functional groups, for instance free[31] and protected[32] alcohols, epoxide,[33] ketones[34] esters,[35] allylic chloride,[36] cyclopropane,[37] and dihydrooxazole.[38] However, it also presents some important limitations. In the semi-reduction of terminal alkynes, low alkene selectivity is sometimes obtained due to overhydrogenation of terminal alkenes to alkanes. Furthermore, for internal alkynes, careful monitoring of the reaction is required in order to avoid undesired isomerization/overreduction processes, Finally, a more environmentally friendly hydrogenation protocol, avoiding the use of toxic lead is highly desirable.

To overcome these drawbacks, improved transition metal catalysts have been developed, based on Ni,[39,40] Cu,[41] Ru,[42] Au,[43] but especially on Pd. Besides the use of heterogeneous palladium catalysts,[13,4] many publications have appeared on the development of nanoparticles[44,45,46] or supported nanoparticles.[47,48,49] Finally, homogeneous catalyst systems were also developed, which are more suitable for establishing quantitative structure-activity relationships, and thus rational catalyst design. Two methodologies have been applied for the catalytic semi-reduction of alkynes: semi-hydrogenation, in which the reductant is hydrogen gas, or transfer semi-hydrogenation, where organic molecules are used as hydrogen donors.

To test the efficiency of new catalysts in the semireduction of alkynes, and to compare them with other existing catalysts several benchmark alkyne substrates are employed including terminal and internal alkynes and alkynols (Figure 5.1).

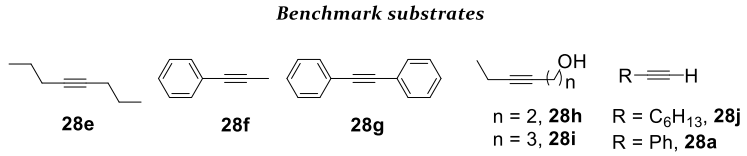

Figure 5.1. Internal alkyne substrates frequently used to test new semihydrogenation catalysts.

5.1.2. Catalytic semi-hydrogenation of alkynes using molecular Pd catalysts

Only a few homogeneous Pd catalysts have been reported for the (*Z*)-selective alkyne semihydrogenation. Some of these catalysts were Pd(II) complexes[50,5152] and other reports involved the use of Pd(0) precatalysts.[53,54,55] One of the most successful examples reported used the Pd(0) complex **32** (Scheme 5.2). Besides benchmark substrates shown in Figure 5.1, catalyst **32** efficiently semi-hydrogenates a broad substrate scope including internal and terminal alkynes and alkynols, enynes and substrates bearing reducible functional groups such as nitro, carboxylic acids, or carboxylic esters. All these substrates were converted to the corresponding (*Z*)-alkenes in 87-99% selectivity measured at 99,5% alkyne conversion.

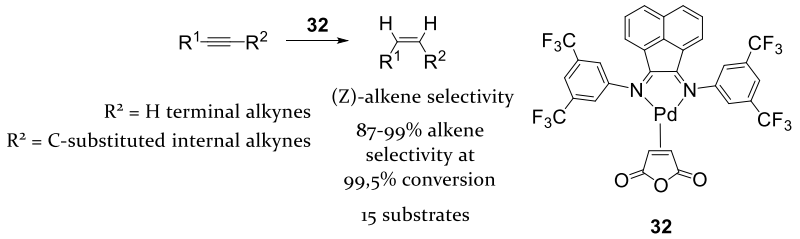

Scheme 5.2. Structure of [Pd{(3, 5'-$(CF_3)_2C_6H_3$)-bian}(ma)] (**32**); (bian = bis(imino)acenaphthene; ma = maleic anhydride).

Kinetic studies PHIP, ^{1}H NMR and ^{2}H NMR experiments helped to clarify the mechanism behind the high selectivity displayed by the complex **32**, which is one of the most selective homogeneous catalysts reported for this transformation (Scheme 5.2).[56] The high reactivity of this system precluded the isolation of any intermediate from the catalytic cycle. According to the collected data from kinetic measurements, PHIP ^{1}H

NMR studies and ^2H NMR studies, the authors proposed the catalytic cycle shown in Scheme 5.3.

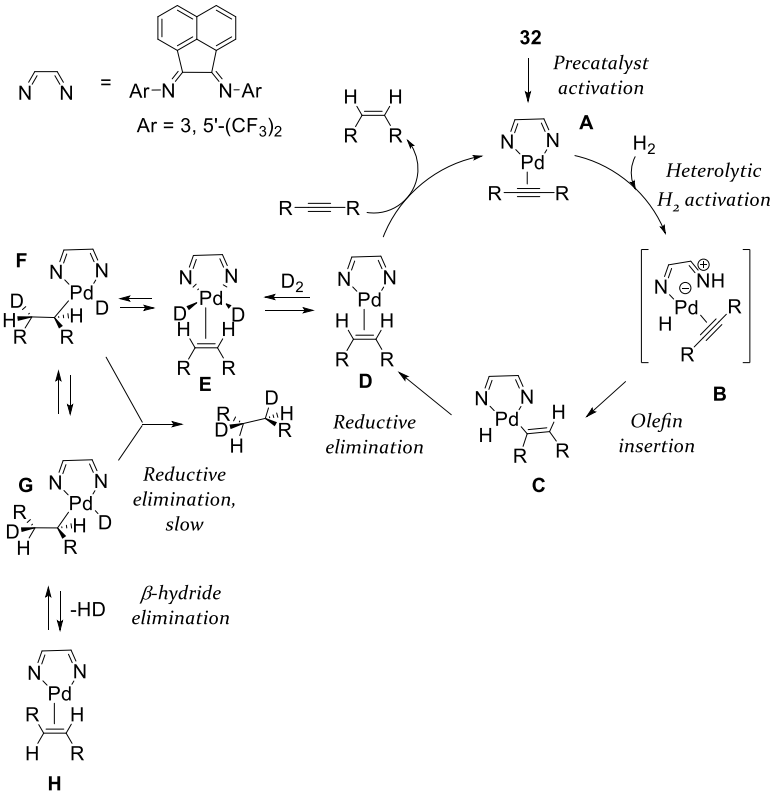

Scheme 5.3. Proposed catalytic cycle for the semihydrogenation of 4-octyne (**28e**) using **32**.[56]

The preactivation of complex **32** occurs in the presence of hydrogen; as the maleic anhydride ligand is hydrogenated, thus generating a vacant site that is occupied by the alkyne substrate, to form the catalytically active species **A**. Theoretical calculations in related catalyst systems indicated that heterolytic activation of H_2 has a lower energy barrier with respect to activation through oxidative addition,[57] therefore, protonolysis of the Pd-N bond very likely occurs to generate a Pd(alkyne)-hydride species **B**. From species **B**, rapid insertion of the alkyne into the Pd-H bond, and addition of the N-H bond to Pd generates the Pd(alkenyl)-hydride species **C**. Then, reductive elimination generates the (η^2-alkene)-

Pd intermediate **D** where the (Z)-alkene product remains coordinated to the Pd(0) fragment. From this intermediate, the (*Z*)-alkene product is displaced by a molecule of alkyne which regenerates the catalytically active species **A**. Moreover, experiments using deuterium demonstrated that alkenes undergo isomerization. From species **D**, in the presence of H_2 (or D_2), a dihydride species **E** is formed, and rapid insertion of the alkene into the Pd-H(or D) bond leads to Pd(alkyl)-hydride **F**. Then, the Pd-bonded alkyl fragment can rotate around the C-C bond generating **F** which undergoes ß-hydride elimination to give the (*E*)-alkene.

It is remarkable that in this system, the selectivity does not depend neither on the H_2 pressure, nor on the substrate concentration, nor on the concentration of the precatalyst. In the study, the semihydrogenation of 4-octyne led to a 95% yield of the *cis*-alkene, with formation of 5% *trans*-alkene and no overreduction. This high chemoselectivity is explained due to the much stronger binding of alkynes compared to the alkene products. Whereas cis/trans isomerization only occurs to a very small extent, overreduction is completely prevented, although a [Pd(hydrido)(alkyl)] species is assumed during the isomerization process (**F**, **G**). Apparently, the *β*-elimination, which is known to be a very low-barrier process in the case of palladium,[58] is much faster than the reductive elimination of the alkane from [Pd(H)(alkyl)] species. For this catalyst, the reaction rate showed a first order dependence on the concentration of palladium, indicating that only mononuclear species are involved in the product formation.

[Pd(NHC)] complexes shown in Scheme 5.4 have also been applied in the semihydrogenation of alkynes.[59,57] The [Pd(0)(NHC)] catalysts **33** provided higher selectivity in the hydrogenation of substrate **28f** compared to the preformed Pd(0) complex **34**. For this substrate, the complex **34d** displayed the best selectivity of the series yielding the (*Z*)-alkene in 95% selectivity, whereas the undesired (*E*)-alkene and alkane products were only obtained in 2% and 3% respectively, measured at 99% alkyne conversion.

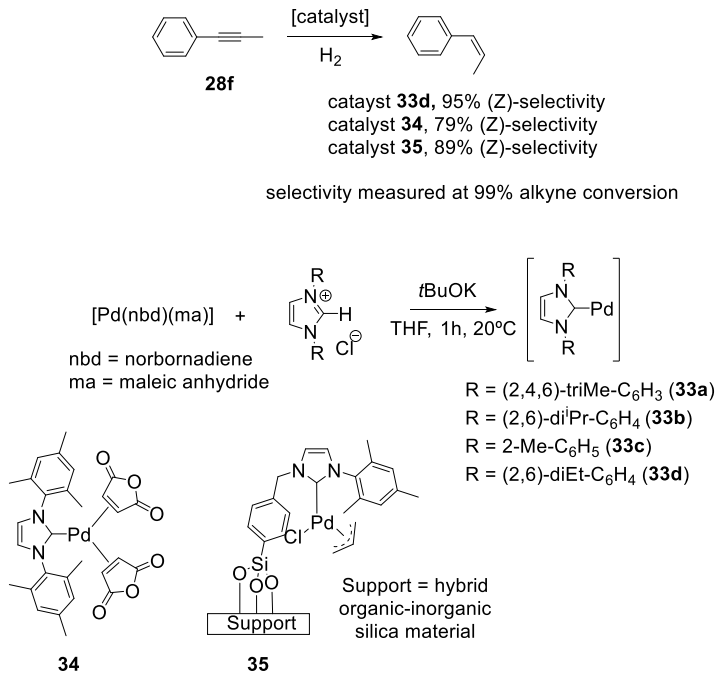

Scheme 5.4. Molecular (homogeneous and supported) Pd catalysts applied in the semihydrogenation of alkynes.

Other substrates such as diphenylacetylene (**28g**) were semi-hydrogenated in lower selectivity and the possible products ((*Z*)-stilbene/(*E*)-stilbene/diphenylethane) were obtained in a (88/5/7) ratio, which is a similar selectivity to that obtained using catalyst **32**. Surprisingly, the catalyst **33d** could not hydrogenate 4-octyne (**28e**). In spite of the good selectivity towards the (Z)-alkenes, overhydrogenation to the corresponding alkane products was difficult to control at high alkyne conversions. Moreover, the semihydrogenation reaction proceeded at rather slow rates, with the fastest TOF of 49,9 h^{-1} for the semi-hydrogenation of **28f** using catalyst **33d**.

A significant difference between the catalyst **32** and [Pd(NHC)] catalysts concerns the mechanism for hydrogen activation. For catalyst **32**, the diazabutadiene ligand assists the heterolytic splitting of hydrogen (**B**, Scheme 5.3), which is not an option for the [Pd(0)(NHC)] complexes where the hydride has to be formed through oxidative addition. This oxidative addition is proposed to have a large energy barrier which makes the reaction relatively slow. Hence, the application of an alternative

hydrogen source should improve this system. An ionic hydrogen source would transfer a hydridic type of hydrogen and a proton-like hydrogen to the catalyst and would provide a route that is similar to the BIAN system (**32**).

The [Pd(II)(NHC)] complexes are also active catalysts in this reaction. The supported catalyst **35** was much faster than catalysts **33**, achieving a maximum TOF of 13200 h^{-1} in the semihydrogenation of 4-octyne **28e**. With this catalyst the substrates **28e**, **28f** and alkynol **28i** were converted to the corresponding (*Z*)-alkenes in 87%-92% selectivity at 99% alkyne conversion. However, the more challenging diphenylacetylene was semihydrogenated to (*Z*)-stilbene in lower selectivity (56%) due to overreduction at high alkyne conversion.

5.1.3. Catalytic transfer semi-hydrogenation of alkynes using molecular Pd catalysts

The catalytic transfer hydrogenation consists in the reduction of an unsaturated organic substrate in the presence of a catalyst and a hydrogen donor (Scheme 5.5).[60]

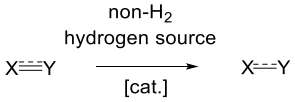

Scheme 5.5. General scheme of a transfer hydrogenation reaction.

This reaction has been widely studied for the case of substrates with polarized multiple bonds, such as carbonyls or imines.[61,62,63] According to theoretical calculations, activation barriers for the transfer hydrogenation of non-polar substrates are *ca.* 10 kcal mol^{-1} higher than for polar substrates,[64] and because of this, the transfer hydrogenation of C-C multiple bonds is more challenging, and fewer examples have been reported,[65,66,67] especially in the case of alkynes.[68,69,70,71,72]

Compared with semi-hydrogenations conducted under hydrogen atmosphere, the transfer semi-hydrogenation of alkynes is an attractive method due to its operational simplicity, the environmental friendly properties of the hydrogen donors and the safer, non flammable

operation conditions. Various metals have been used to promote this reaction, for instance Ru, Rh, Fe or Ni, but usually Pd has provided the most effective catalysts.[73] Various hydrogen donors have been reported, such as triethylammonium formate,[69] sodium methoxide,[74] KOH/DMF,[71] silanes (monohydrosilanes[75] and dihydrosilanes[76])/acetic acid, or Hantzsch ester 1,4-dihydropyridine.[77]

Since the earlier reports by Sato[78] and Trost[75] on the use of Pd(0)/PR_3 catalyst systems for the transfer semi-hydrogenation of alkynes a variety of homogeneous, and also supported Pd complexes have been applied in this reaction.[73] Among the various types of reported Pd complexes, [Pd(*N*-Heterocyclic carbene)] complexes have displayed enhanced chemo- and stereoselectivity.[65,79]

5.1.3.1. [Pd(NHC)] complexes for the selective transfer semi-hydrogenation of alkynes

Elsevier et al. synthesized a [Pd(0)(NHC)] complex (**36**) (Scheme 5.6) that was applied in the semi-hydrogenation of terminal and internal alkynes and alkynols using NEt_3/HCOOH as the hydrogen donor.[69] For substrates **28e**, **28f**, **28g** and **28h** product distribution ((*Z*)-alkene/(*E*)-alkene/alkane) at >99% alkyne conversion was (93/3/4), (96/4/1), (>99/-/-) and (>99/-/-). Moreover, substrates bearing carbonyl functionalities could be reduced without affecting the C=O double bond. Remarkably, the catalyst **36** did not lead to significant overreduction after complete consumption of the alkyne substrates .

The mechanism of this highly selective reaction was investigated in detail.[54] Kinetic experiments, measurement of kinetic isotope effect and NMR analysis, including studies with deuterium labeled formic acid led to the proposal of the reaction mechanism as shown in Scheme 5.6. Compared with the reaction mechanism shown in Scheme 5.3 for the semi-hydrogenation using dihydrogen, **II** is generated by exchange of the MeCN molecule by an incoming substrate molecule.

NMR studies provided evidence for the coordination of a formate anion to Pd, as in species **III**. Then, carbon dioxide is released by decarboxylation that generates a Pd(alkyne)-hydride species **IV**, that undergoes migratory

insertion followed by protonolysis assisted by the base to generate the (*Z*)-alkene product.

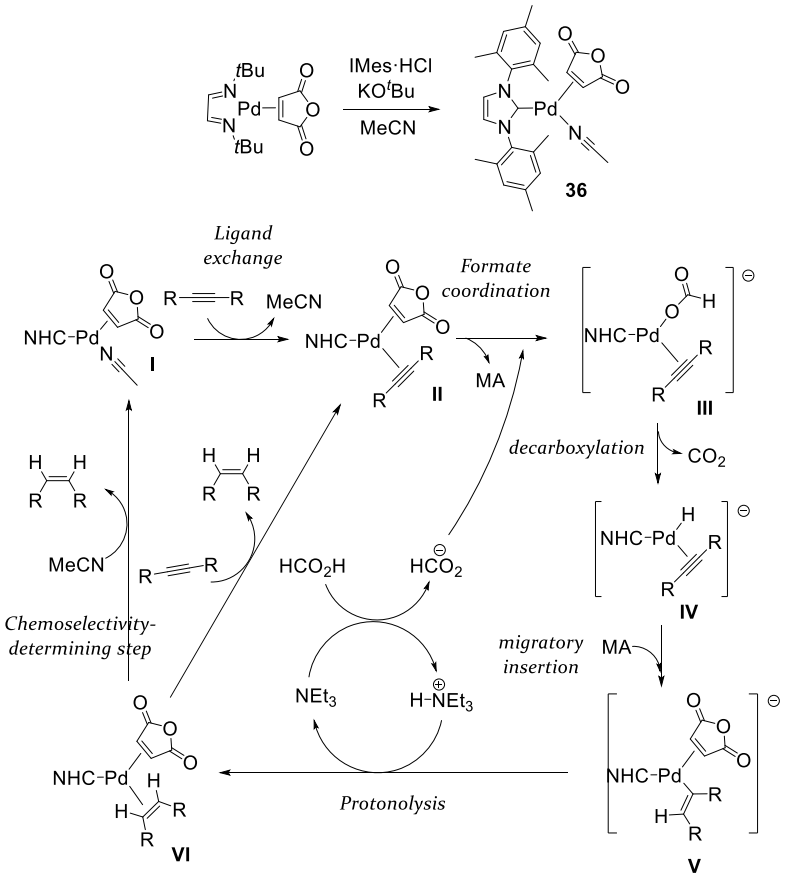

Scheme 5.6. Proposed mechanism for the selective transfer semihydrogenation of alkynes catalyzed by **37**.[69]

The stability of species **VI**, where the already formed *cis*-alkene remains coordinated to Pd has a tremendous importance for the selectivity of the reaction. Ideally, the alkene should be easily and rapidly displaced by a molecule of solvent or substrate. The longer the alkene stays coordinated to Pd, the more chances to undergo overhydrogenation to the alkane. Experimental findings on this system told that the use of a coordinating solvent such as MeCN is essential, not only to improve the chemoselectivity, but also to prevent stabilization of the Pd(0) complex. In comparison, when the reaction was performed in THF, faster reaction

rates were observed (probably due to the lack of competition for the alkyne to bind to Pd), but the chemoselectivity was worse, and some overhydrogenation occurred. Additionally, when higher catalyst loadings were applied (lower [alkyne]/[Pd] ratio), lower selectivities were observed, which was accompanied by decomposition of part of the catalyst to Pd black. This is in agreement with the fact that at higher Pd loadings, there is less alkyne available to stabilize the unsaturated Pd(0) species, which tend to aggregate into particles and ultimately into Pd black.

While this system is highly selective, practical limitations arise from the fact that it needs to be generated *in situ* shortly before being used, and it needs to be kept under inert atmosphere. Therefore, a more user friendly protocol would be desirable. Recently, the application of bench stable [Pd(II)(NHC)] complexes **37** and **38** in the selective transfer semi-hydrogenation of alkynes was reported (Scheme 5.7).[79] Reactions were performed in acetonitrile, a this coordinating solvent plays a role both in stabilizing the Pd(0) active species and in preventing overreduction and isomerization by displacing the *cis*-alkene product (see Scheme 5.6).

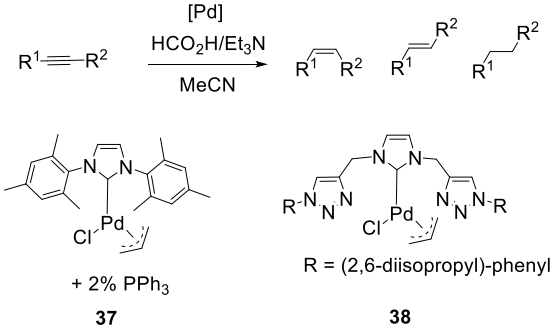

Scheme 5.7. [Pd(II)(NHC)] catalyst systems reported for the selective transfer semihydrogenation of alkynes.[59,52]

In the complex **38** two 1,2,3-triazole moieties were introduced in the ligand structure, under the premise that they would act as hemilabile ligands, allowing for the coordination of the alkyne, and then upon formation of the alkene product the triazoles would coordinate to Pd, displacing the alkene, and preventing isomerization and overreduction. However, the reaction rate was greatly reduced, probably due to a strong coordination of the triazole arms, which blocks the binding of the alkyne substrates.

The use of precatalyst **37** provided excellent selectivities for both internal and terminal alkynes with negligible isomerization and overreduction in the most cases. Benchmark substrates **28f**, **28h** and **28j** were converted into the corresponding (*Z*)-alkenes (or terminal alkenes) with selectivities ranging from 92% to 99% at alkyne conversions above 93% in all cases. Numerous substrates bearing various functional groups were used to demonstrate the usefulness of this catalyst system.

Importantly, the high selectivity achieved with catalyst **37**, required the addition of a small amount of PPh_3 (2,0 equiv. of PPh_3 with respect to the Pd complex). The role of PPh_3 was to displace the Pd-bound *cis*-alkene product especially at high alkyne conversions (see Scheme 5.6). A decrease in the reaction rate was observed due to the competition between the alkyne and PPh_3 in binding to the Pd center; however the reaction is not inhibited, and complete conversions were achieved with excellent chemo- and stereoselectivities.

In the next section, the results obtained in the semi-reduction of alkynes catalyzed by heterogenized [Pd(NHC)] complexes described in Chapter 3 will be presented and discussed.

5.2. Results and discussion

The objective of this chapter is to use the supported [Pd(NHC)] complexes previously described in Chapter 3 as catalysts in the semi-reduction of alkynes to alkenes. In view of the superior performance of γ-Al_2O_3- and TiO_2-supported catalysts under flow conditions in comparison with the silica-supported analogs in the C-C bond formation reactions, the former materials were selected for their application in the semi-reduction of alkynes.

5.2.1. Semihydrogenation of internal alkynes to (Z)-alkenes

First, the supported catalysts **11a@γ-Al_2O_3**, **11b@ γ-Al_2O_3**, **11a@TiO_2** and **11b@TiO_2** (Chapter 3, Scheme 3.16) were evaluated in the (*Z*)-selective semi-hydrogenation of internal alkynes under H_2 atmosphere. Diphenylacetylene (**28g**) was selected as the benchmark

substrate to explore the potential of the supported catalysts in the semihydrogenation reaction (see Figure 5.1).

5.2.1.1. *Optimization of the reaction conditions in the semi-hydrogenation of internal alkynes under batch conditions*

The material **11a@γ-Al_2O_3** was used as the in the screening of the optimal reaction conditions for these systems in the semi-hydrogenation of **28g** (Table 5.1). Pd catalysts are usually active enough to perform this transformation, and in many cases they operate at room temperature and under atmospheric H_2 pressure.[30] Nevertheless, incomplete conversion was observed in the semihydrogenation of diphenylacetylene (**28g**) at 25°C and under 10 bars of H_2(g), but with very good selectivity, only marginal isomerization and overreduction (entry 1). When the reaction was run for a longer time (entry 2), complete conversion was observed after 9 hours, but under these conditions the major reaction product was 1,2-diphenylethane. Then, the reaction time was shortened and the temperature was risen from 25°C to 40°C (entry 3).

Table 5.1. Optimization of the reaction conditions for the semi-hydrogenation of internal alkynes using **11a@γ-Al_2O_3**.

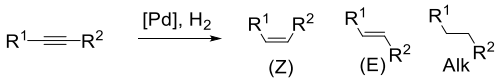

E.	Alkyne	R¹,R²	P(H_2) (bar)	T °C	t(h)	Conv.%[a]	(Z)/(E)/alk [a, b]
1	28g	Ph, Ph	10	25	5h	78	93/3/3(86%)
2	28g	Ph, Ph	10	25	9h	100	39/5/56(95%)
3	28g	Ph, Ph	3	40	2h	100	69/4/27(97%)
4[c]	28g	Ph, Ph	3	40	2h	0	-
5[d]	28g	Ph, Ph	3	40	2h	76	93/1/6
6	28f	Ph, Me	3	40	2h	69	93/0/7
7	28l	Ph, CH_2OH	3	40	2h	0	-

1 mol % **11a@γ-Al_2O_3**, 3 mL degassed MeCN. [(a)] conversion and selectivity determined by ^{1}H NMR by correlation to mesitylene as external standard [(b)] mass balances are expressed in parentheses if they are not 100%;. [c] 1,5% PPh_3 was added; [d] the reaction was run in degassed AcOEt.

Under these conditions, full conversion of **28g** was achieved, yielding (*Z*)-stilbene in 69% selectivity along with 4% of (*E*)-stilbene and 27% of 1,2-diphenylethane. As reported for other Pd catalysts, overreduction of the alkene to the alkane was difficult to avoid at high alkyne conversions.[51] The use of additives is a widely used strategy to improve the catalyst selectivity, either for heterogeneous[80] or homogeneous systems.[89] Therefore, the semi-hydrogenation of **28g** was carried out in the presence of 1,5 mol% of PPh_3. Under these conditions the activity of the catalyst was completely inhibited (entry 4). Running the reaction in ethyl acetate as solvent provided *cis*-stilbene in 93% selectivity at 76% conversion (Entry 5). Lastly, good selectivity was achieved for 1-phenyl-1-propyne (**28f**) at 69% conversion (entry 6). 3-phenyl-2-propyn-1-ol (**28l**) could not be hydrogenated under these conditions (entry 7).

1-phenyl-1-propyne (**28f**) was used to test the performance of other catalysts under the above optimized conditions (Table 5.2).

Table 5.2. Comparison in the performance of supported catalysts **11a@γ-Al_2O_3**, **11b@ γ-Al_2O_3**, **11a@TiO_2** in the semihydrogenation of **28f** under optimized reaction conditions.

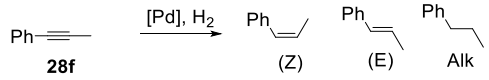

Entry	Catalyst	Conversion(%)	Z/E/Alkane
1	**11a@γ-Al_2O_3**	69	93/0/7
2	**11b@γ-Al_2O_3**	34	33/0/1
3	**11a@TiO_2**	30	30/0/0

Conditions: 1 mol % [Pd], 3 mL degassed MeCN, 40°C, 2 bars H_2, 2 hours; conversion and selectivity were determined by ^1H NMR by correlation to mesitylene as external standard.

Faster reactions were achieved by catalysts bearing 2,6-dimethylphenyl substitution motif on the NHC wingtips in comparison with bulkier 2,6-diisopropylphenyl substitution (entry 1 vs entry 2)(see Chapter 3, Scheme 3.16 for the molecular structure of the supported Pd complexes). Furthermore, materials supported onto γ-Al_2O_3 provided higher conversions than catalysts supported onto TiO_2 (entry 1 vs entry 3).

Since the supported systems tested showed promising activity in the semi-hydrogenation of internal alkynes under batch reaction conditions,

following experiments were aimed at testing the performance of the supported catalysts under continuous flow conditions. For these tests, the catalysts **11a@γ-Al_2O_3** and **11a@TiO_2**, bearing the 2,6-dimethylphenyl motif were selected, since they had shown superior performance in the batch experiments compared with the catalysts bearing the 2,6-diisopropylphenyl motif.

5.2.1.2. Preliminary studies on the continuous semi-hydrogenation of diphenylacetylene

Continuous operation provides the opportunity to better control reaction parameters,[81] and therefore to improve the selectivity obtained under batch reaction conditions. The experiments carried out under continuous flow conditions presented in this chapter were performed in collaboration with the group of Prof. W. Leitner, under the supervision of Dr. G. Franciò, at RWTH University of Aachen. An initial test was conducted in a continuous flow microreactor to look for the best reaction conditions for the semi-hydrogenation of **28g** under continuous flow operation, using catalyst **11a@γ-Al_2O_3**. In this initial experiment, various reaction parameters were systematically modified, namely temperature, flow rate and flow of H_2 (the whole continuous flow experiment was operated at a constant $P(H_2)$ = 3 bar). The results obtained are collected in Table 5.3. Importantly, the flow microreactor used did not provide the opportunity to perform an online analysis of the samples, therefore, the samples were only analyzed after the experiment.

Initially, the reaction temperature was set at 40°C, in accordance with the optimized conditions used in the batch experiments, and the substrate solution was injected into the reactor at a flow rate of 1 mL/min. Under these conditions complete conversion of diphenylacetylene (**28g**) was achieved together with 73% selectivity towards *cis*-stilbene (Entry 1). Decreasing the flow rate from 1 mL/min to 0,5 mL/min implies an increase of the mean residence time.

Table 5.3. Study of the influence of various reaction parameters in the semihydrogenation of **28g** under continuous flow conditions using catalyst **11a@γ-Al_2O_3.**

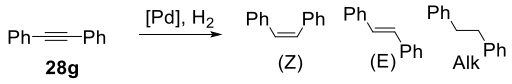

E.	P(H_2) (bar)	T (°C)	Flow rate (mL/min)	Flow(H_2) (mL/min)	Conv. (%)	Z/E/alk (%)
1	3	40	1,0	15	100	73/8/19
2	3	40	0,5	15	100	59/11/30
3	3	40	0,5	30	100	56/10/34
4	3	40	0,5	45	100	49/13/39
5	3	50	0,5	45	100	4/12/84
6	3	50	1,0	45	100	34/12/54
7	3	50	1,0	15	100	33/10/57
8	3	60	1,0	15	100	10/12/78
9	3	60	1,0	45	100	12/11/77

Conditions: 0,05M substrate stock solution in AcOEt, not degassed; conversion and yield determined by ^{1}H NMR analysis, relative to mesitylene. Note: for each entry, which represents a variation in one of the reaction parameters, the system was allowed to settle (until "stable" was read on the display screen of the apparatus) and then 5 minutes later the sample to be analyzed was collected. Online analysis was not possible, so "blind samples" were taken which were not analyzed until the end of the experiment.

Under these conditions (Entry 2), full conversion was observed, but the selectivity towards (Z)-stilbene decreased due to an increase in the formation of undesired overhydrogenation product 1,2-diphenylethane (entry 2). Increasing the flow of H_2, (at constant P) resulted in a slight increase in overreduction (entries 3, 4, vs entry 2). At 50°C almost total hydrogenation was observed (84% selectivity towards 1,2-diphenylethane) (entry 5). Increasing the flow rate at this temperature, thus reducing the residence time, reduced the selectivity towards the overreduced product to 54% (entry 6). Finally, at 60°C up to 78% of the starting material was fully hydrogenated to the alkane (entry 8).

A comparison between Table 5.3, entry 1 vs Table 5.1, entry 3 indicates that similar activity and selectivity were observed under batch and continuous flow conditions.

Additional continuous flow experiments are presented (Table 5.4) using the catalyst **11a@TiO$_2$** in which MeCN was used as the reaction solvent. In these experiments, the solution of the substrate was twice as concentrated as in the continuous flow experiment shown in Table 5.3.

Table 5.4. Study of the robustness of catalyst **11a@TiO$_2$** in the semi-hydrogenation of **28g** under continuous flow conditions.

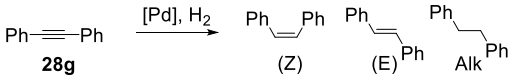

E.	P(H_2) (bar)	T (°C)	Flow rate (mL/min)	Flow(H_2) (mL/min)	Conv. (%)	Z/E/alk
1	2	25	0,5	15	47%	93/5/2
2	2	25	1,5	15	37%	90/6/4
3	2	25	2,5	15	35%	84/9/7
4	2	30	1,0	15	100%	69/10/21
5	2	30	2,0	15	91%	80/8/12
6	2	35	1,0	15	100%	29/8/63
7	2	35	2,0	15	97%	55/10/35
8	2	35	2,5	15	91%	59/9/32
9	2	25	1,0	15	100%	20/7/73
10	2	30	2,0	15	100%	43/11/46

Conditions: 0,1M substrate stock solution in deoxygenated MeCN; conversion and yield determined by ^{1}H NMR analysis, relative to mesitylene. Note: for each entry, which represents a variation in one of the reaction parameters, the system was allowed to settle (until "stable" was read on the display screen of the apparatus) and then 5 minutes later, the sample to be analyzed was collected. Online analysis was not possible, so "blind samples" were taken which were not analyzed until the end of the experiment.

At the longest possible residence time (0,5 mL/min flow rate) (entry 1) nearly half of the substrate was converted with 93% selectivity to *cis*-stilbene. Increasing the flow rate to 1,0 mL/min and then to 2,5 mL/min (hence decreasing the residence time) resulted in lower conversions as could be expected (entries 2, 3). However, these results deserve careful analysis. When increasing the flow rate from 1,0 mL/min to 2,5 mL/min (entry 2 vs entry 3) conversion is practically unaffected (from 37% to 35%), whereas selectivity to (*Z*)-alkene dropped from 90% to 84%. This very likely points out to an alteration of the original active species, and its conversion into more reactive but less selective species under the reaction conditions.[79]

Increasing the temperature to 30°C and applying a flow rate of 2,0 mL/min resulted in 91% conversion and 80% selectivity to (*Z*)-stilbene (entry 5). When the temperature was further increased to 35°C (entries 6-8) lower chemoselectivity was observed, and the alkane was formed in over 30% selectivity.

Importantly, resetting the initial reaction conditions, led to a different conversion and selectivity (entry 9, vs entries 1, 2). Again, this observation gives a hint that the nature of the active species changed during the course of the experiment.

Unfortunately, a single continuous flow experiment carried out entirely under the same reaction conditions could not be realized. Under all tested conditions, initial semi-reduction of internal alkyne substrates proceeded with good chemo- and stereoselectivity to the (*Z*)-alkenes. However, at high alkyne conversions (over 70%) the supported catalysts displayed low chemoselectivity, and significant amounts of isomerized and overreduced byproducts were detected. Apparently catalyst decomposition to Pd black did not occur under these conditions, and the visual aspect of the catalyst did not change during these experiments.

In an attempt to improve the selectivity of the semi-reduction of alkynes to (*Z*)-alkenes, the catalysts **11a@γ-Al_2O_3**, and **11a@TiO_2** were tested in the transfer semi-hydrogenation of alkynes.

5.2.2. Transfer semi-hydrogenation of internal and terminal alkynes

There are some precedents on the application of homogeneous [Pd(II)(NHC)] catalyst precursors in this type of transformation,[89,82] In most cases, triethylammonium formate has been used as the hydrogen donor.[78,83,84,] However, to the best of our knowledge, the application of supported molecular Pd complexes as catalysts for the reduction of alkynes under transfer hydrogenation conditions has not yet been reported.

5.2.2.1. *Transfer semi-hydrogenation of internal alkynes to (Z)-alkenes.*

Optimization of the reaction conditions

Initial experiments were conducted using the catalyst **11a@γ-Al_2O_3** to explore the most suitable reaction conditions for the chemo- and stereoselective transfer semi-hydrogenation (TSH) of internal alkynes (Table 5.5). Among disubstituted alkynes, diphenylacetylene (**28g**) was chosen as a model to optimize the reaction conditions. Acetonitrile, due to its coordination capability plays a role in stabilizing the active catalytic species, and preventing decomposition into elemental Pd and hence was the solvent of choice in these experiments.[82] The presence of an excess of H-donor (5,0 equiv.) was thought to be important to assess the *true* selectivity of the catalyst, and not a selectivity imposed by stoichiometry. Generally, transfer hydrogenation reactions require higher temperatures compared to typical hydrogenations in the presence of H_2(g).[60]

Table 5.5. Optimization of the reaction conditions in the transfer semihydrogenation of **28g** employing catalyst **11a@γ-Al_2O_3**.

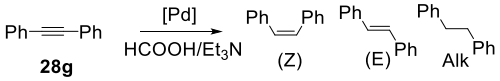

Entry	Additive	Solv.	T (°C)	t (h)	Conv. (%)	(Z)/(E)/alk (%)
1	-	MeCN	70	16	94%	90/10/0
2[(a)]	-	MeCN	70	16	0%	-
3	-	MeCN	70	24	100%	3/77/20
4	-	MeCN	82	16	100%	0/65/35
5[(b)]	-	MeCN	70	16	100%	13/57/30
6[(c)]	-	MeCN	70	16	100%	4/45/51
7	-	AcOEt	70	24	85%	86/12/0
8	2% PPh_3	MeCN	82	16	94%	96/4/0
9	5% PPh_3	MeCN	82	16	55%	97/3/0

Conditions: 1 mol% **11a@γ-Al_2O_3**., 0,5 mmol diphenylacetylene, HCOOH/Et_3N (5.0 equiv.), 3 mL solvent.[(a)]Control experiment in the absence of any catalyst or additive. [(b)] 10.0 equiv. of HCOOH/Et_3N. [(c)] 20.0 equiv. HCOOH/Et_3N.

Performing the TSH at 70°C (entry 1) afforded 94% conversion and 90% selectivity towards *cis*-stilbene, although 10% *trans*-stilbene was formed. A blank experiment was performed in the absence of the Pd catalyst (entry 2) but no reaction occurred.Running the reaction for a longer time (entry 3) provided full conversion of the starting material, although a mixture of *cis*- and *trans*-stilbene and 1,2-diphenylethane was obtained, with the (E)-isomer being the major product and the (Z)-stereoisomer the minor product. This is a different situation to the previous results obtained in the semihydrogenation of **28g** using H_2 gas, where the *trans*-alkene was only observed in small amounts (below 10%) whereas the major byproduct was always 1,2-diphenylethane due to overhydrogenation. Maintaining the same reaction time as in entry 1, and increasing the temperature to reflux had a similar negative effect on the selectivity (entry 4). An increase in the concentration of H donor also yielded an unselective mixture of the (*Z*), (*E*) and alkane products (entries 5, 6). The solvent AcOEt did not provide better results than MeCN (entry 7 vs entry 1).

In order to enhance the selectivity of the system and to prevent isomerization and overreduction after reaching complete conversion, a small amount (2%) of PPh_3 was added to the system (entries 8, 9).[79] With this modified system, at 80°C 96% selectivity was obtained towards *cis*-stilbene at 94% conversion (entry 8). This result compares favorably with the results obtained using other [Pd(NHC)] catalysts in the semi-reduction of this challenging substrate.[79,52] When a higher amount of PPh_3 (entry 9) was added the reaction became slower, but the selectivity remained unaltered. Using these reaction conditions, the substrate scope was briefly explored (Table 5.6).

Besides the excellent selectivity obtained with the difficult substrate **28g**, replacing one of the phenyl groups of diphenylacetylene by an alkyl group resulted in only a small loss in selectivity, achieving 87% and 88% selectivity towards the *cis*-alkene products in the TSH of 1-phenyl-1-propyne (**28f**) and 1-phenyl-1-butyne (**28m**), at full conversion (entries 2 and 3). Replacement of the two aromatic rings by alkyl groups such as in 4-octyne (**28e**) had a more pronounced effect, and overreduction occurred more rapidly, thus addition of an extra amount of PPh_3 (5 mol% vs 2 mol% for the rest of the substrates) was necessary in order to

maintain the selectivity in good levels, (92% selectivity at 82%. conversion after 72 hours, entry 4). Finally 3-phenyl-2-propyn-1-ol (**28l**) (entry 5) was fully converted after 3 days. Overreduction was not an issue although the selectivity was compromised by isomerization to the (*E*)-alkene and by the competitive formation of elimination products, which were detected by GC-MS.

Table 5.6. Substrate scope possible for the transfer semi-hydrogenation of internal alkynes and alkynols catalyzed by **11a@γ-Al_2O_3**.

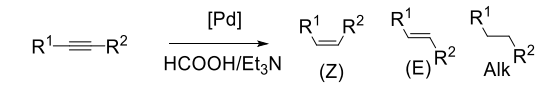

$R^1 = R^2$ = Ph, **28g**
R^1 = Ph, R^2 = Me, **28f**
R^1 = Ph, R^2 = Et, **28m**
$R^1 = R^2$ = Pr, **28e**
R^1 = Ph, R^2 = CH_2OH, **28l**

Entry	Alkyne	Time(h)	Conv.(%)	Z/E/Alk
1	**28g**	**16**	**94**	**96/4/0**
2	**28f**	**16**	**100**	**87/9/4**
3	**28m**	**16**	**100**	**88/12/0**
4[a]	**28e**	**72**	**82**	**92/8/0**
5[b]	**28l**	**72**	**100**	**84/16/0**

Conditions: 1 mol% **11a@γ-Al_2O_3**, HCOOH/Et_3N (5.0 equiv.), T = 82°C, 3 mL deoxygenated MeCN (d^3), 2 mol% PPh_3.[(a)] 5 mol% PPh_3 was used. [(b)] 76% selectivity towards hydrogenation products. Products coming from elimination side reactions were observed by NMR and GC-MS. Conversions and yields determined by ^{1}H NMR and by GC-MS. Mesitylene was used as the standard

In summary, the catalytic system formed by **11a@γ-Al_2O_3 + 2% PPh_3** could be applied in the TSH of internal alkynes and alkynols, and the corresponding (Z)-alkene products were obtained in high selectivity, especially comparing these results with the lower selectivities achieved in the semihydrogenation reaction presented in the previous section.

5.2.2.2. Transfer semi-hydrogenation of terminal alkynes

In view of the results achieved in the TSH of internal alkynes and alkynols using the catalyst **11a@γ-Al_2O_3**, the application of

this methodology was extended to the TSH of terminal alkynes and alkynols (Table 5.7).

Table 5.7. Transfer semi-hydrogenation of terminal alkynes and alkynols catalyzed by **11a@γ-Al_2O_3**.

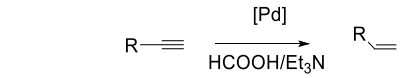

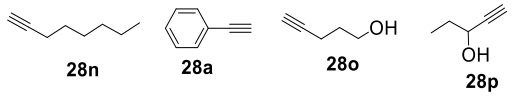

28n 28a 28o 28p

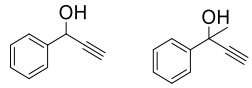

28q 28r

Entry	Alkyne	Conv.(%)	Alkene(%)	Byproducts
1	**28a**	100	40	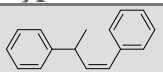
2	**28n**	100	0	C16
3	**28o**	100	99	-
4	**28p**	100	95	-
5	**28q**	100	0	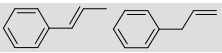
6	**28r**	100	80	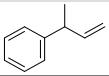

Conditions: 1 mol% **11a@γ-Al_2O_3**, HCOOH/Et_3N (5.0 equiv.), T = 82°C, t = 16h, 3 mL deoxygenated MeCN (d^3), 2 mol% PPh_3. Conversions and yields determined by ^1H NMR and by GC-MS. Mesitylene was used as the standard.

For alkyne substrates without hydroxy groups, poor performances were obtained. Phenylacetylene (**28a**) was fully converted after 16 hours, but the yield of styrene was only 40% and products arising from the dimerization of styrene product were observed by GC-MS analysis (entry 1). Oligomerisation and polymerization products can also be formed from styrene, although they could not be detected by GC-MS analysis due to their high molecular weight. Such selectivity was also observed in related catalyst systems.[79] 1-octyne (**28n**) was also fully converted, although 1-octene was not observed (entry 2). C16 products were observed by GC-MS, which could come from homocoupling of two alkyne molecules, or from oxidative coupling. Similar Pd catalysts also give rise to these C16 products at high alkene concentrations.[52]

On the contrary, the reduction of terminal alkynols provided much better selectivity. Isomeric pentynols (**28o** and **28p**) were cleanly converted to terminal alkenes (entries 3, 4). 1-phenyl-2-propyn-1-ol (**28q**) was fully converted, but the desired alkene could not be detected and the only observed products came from dehydration reactions (entry 5). Better selectivity was obtained for 2-phenyl-3-butyn-2-ol (**28r**) (entry 6) yielding 80% of the semi-hydrogenation alkene product, and 20% of dehydration product.The described results indicate that terminal alkynes without hydroxyl functionalization were converted into various products, but their selective transformation into terminal alkenes proved difficult mainly due to in situ dimerization or oligomerization processes. In the case of terminal alkynols much better selectivities towards the terminal alkenes were generally obtained, except for substrate **28q** for which the only observed products arised from the competitive dehydration reaction.

5.2.2.3. Insights in the role of PPh_3 in the catalyst system

In view of the results obtained using catalyst **11a@γ-Al_2O_3** in the absence of the phosphine additive, it was reasoned that isomerization was occurring leading to subsequent overreduction to the alkane byproduct. Generally, the expected route for (Z) to (E) isomerization of an alkene should involve a metal-hydride species, to effect the "1 hydrogen atom half-hydrogenation" to generate a metal-ligated alkyl species, which could now rotate around the single C-C bond, and then subsequent β-hydride elimination can produce the more thermodynamically stable *trans*-alkene.[85]

In Scheme 5.8 the isomerization of to *trans*-stilbene under TSH conditions catalyzed by **11a@γ-Al_2O_3** is demonstrated. In the absence of a H source, catalyst **11a@γ-Al_2O_3** did not convert *cis*-stilbene (**39a**) (Scheme 5.8, a); the signals corresponding to the alkenic protons and to the aromatic protons of **39a** or **39b** is highlighted in each case). However, when a substoichiometric amount (10%) of HCOOH/Et_3N was added (Scheme 5.8, b)), complete conversion of (*Z*)-stilbene (**39a**) into (*E*)-stilbene (**39b**) was observed by ^{1}H NMR.

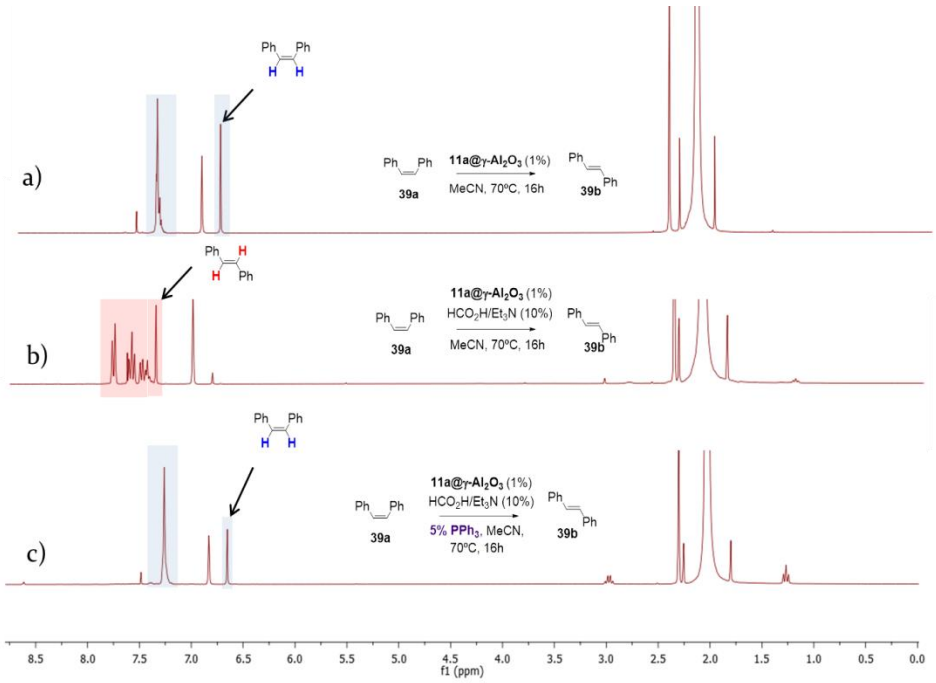

Conditions: 0,5 mmol **40a**, 1 mol% **11a@γ-Al_2O_3**, , T = 70°C, t = 16h, 3 mL deoxygenated MeCN,. Conversions and yields determined by ^{1}H NMR using mesitylene was used as the standard.

Scheme 5.8. Isomerization of **39a** catalyzed by **11a@γ-Al_2O_3**.

Finally, performing the isomerization reaction under the reaction conditions used in Scheme 5.8 b) but adding a substoichiometric amount of PPh_3 (5 mol%) resulted in no conversion.

A very similar effect of the addition of PPh_3 was reported by Elsevier et al. in a related [Pd(NHC)]-based catalyst system.[79] Their proposed explanation for the observed results is consistent with the experimental results presented here (Scheme 5.9).[79]

The [Pd(II)(NHC)] precatalyst **A** is in situ converted into the active Pd(0) species **B**; an activation pathway was proposed (not shown in the scheme above) involving exchange of the chloride ligand by a formate anion, which then generates a hydride species by liberating one molecule of CO_2.

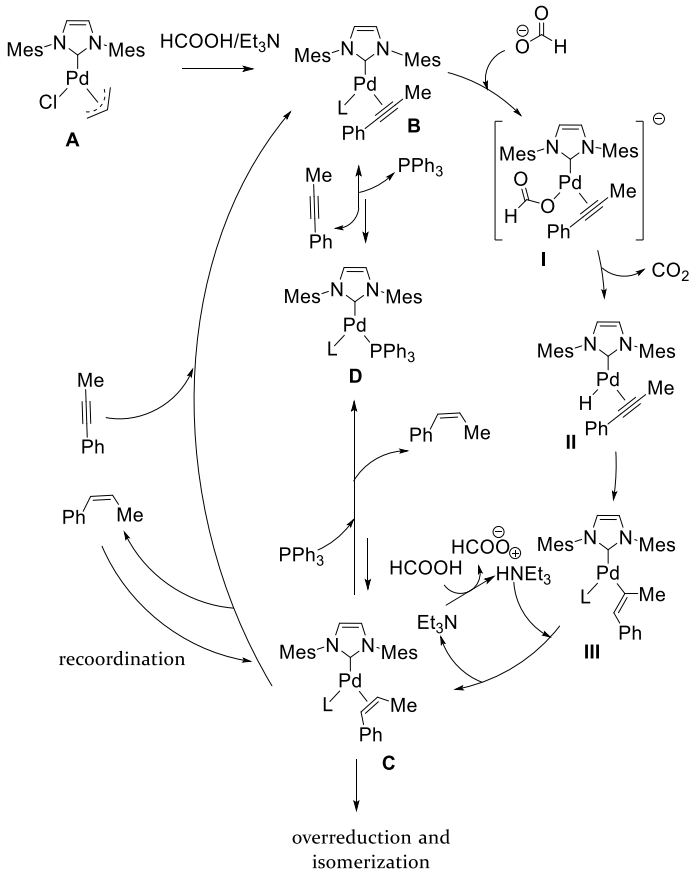

Scheme 5.9. Proposed mechanism for the transfer semihydrogenation of substrate **28f** using catalyst system **37** reported by Elsevier et al.[79]

Reductive elimination of propene generates a Pd(0) species, in which two molecules of either a coordinating solvent (MeCN) or alkyne substrate (or PPh_3) are occupying the available coordination positions and stabilizing this compound. This was supported by the detection of propene and CO_2 in the gas phase of the reaction and also by trapping a [Pd(0)(IMes)] species with CS_2 and characterizing the resulting complex. The main difference (not considering the presence of the support) between the system reported by Elsevier et al. and the system under study here is the substitution of an η^2-allyl by a η^2-acetylacetonato ligand. Nonetheless a similar route could well be in operation, since reductive elimination in related [Pd(II)-η^2-(acac)] complexes yielding Pd(0) species has been demonstrated.[86]

From species **B** the catalytic cycle proceeds via intermediates **I**, **II** and **III** obtained after formation of a Pd-hydride species **II** which undergoes migratory insertion to the alkenyl species **III**; then protonolysis by tryethylammonium results in the formation of intermediate **C**.Ideally, the *cis*-alkene in η^2-alkene species **C** should be readily replaced by a new molecule of the alkyne substrate, regenerating species **B** and starting a new catalytic cycle. However, as the conversion increases there are less alkyne molecules available and this can compromise the liberation of the *cis*-alkene in **C**, leading to undesired isomerization and overreduction processes. The presence of PPh_3 as an additional ligand helps displacing the cis-alkene from **C**, resulting in formation of intermediate **D**, which can be viewed as a protected catalyst dormant state, which can eventually give rise to **B** again if there's still any alkyne left in the reaction medium. To summarize, the phosphine binds much stronger than the *Z*-alkene, and hence, the additive slows down the overreduction and isomerization steps by substituting the alkene and preventing its recoordination. The semihydrogenation steps are also slowed down but to a lesser extent because the binding affinity of the alkyne and PPh_3 are competitive.

Since the results obtained demonstrate that catalyst **11a@γ-Al_2O_3** is active in the TSH reaction and also in the isomerization of (Z)-alkenes to (E)-alkenes it was decided to explore the possibility of converting diphenylacetylene (**28g)** into *trans*-stilbene (**39b**) in a one-pot protocol. Catalytic (*E*)-selective synthesis of alkenes has been reported for homogeneous Pd catalysts, operating via (*Z*)-selective alkyne semihydrogenation, then isomerization, which can also be referred to as indirect (*E*)-selective semihydrogenation,[87] in contrast to direct (*E*)-selective semihydrogenation, which has been reported with Ru catalysts.[88] Thus, under carefully controlled reaction conditions, in the absence of any additive *trans*-stibene was obtained in 90% yield from diphenylacetylene, with only 10% overreduction (Scheme 5.10). Extended studies on other substrates have not been carried out yet.

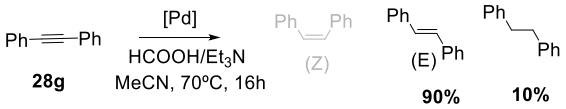

Scheme 5.10. Indirect (*E*)-selective transfer semihydrogenation of **28g** catalyzed by **11a@γ-Al_2O_3**.

Conditions: 0,5 mmol substrate, 1 mol%, 5,0 equiv HCOOH/Et_3N, 3,0 mL deoxygenated MeCN. Yields determined by ^1H NMR analysis relative to mesitylene.

5.2.2.4. Recycling experiments

Recycling of catalysts **11a@γ-Al_2O_3** and **11a@TiO_2** in the TSH reaction was studied under batch conditions. These catalysts were applied in the TSH of diphenylacetylene (**28g**) under the conditions previously described in Table 5.5, entry 8. Both catalysts, **11a@γ-Al_2O_3** and **11a@TiO_2** yielded (*Z*)-stilbene in more than 90% yield in the first reaction run. After the reaction, the supernatant was filtered and the solid catalyst was washed with dichloromethane and allowed to dry under vacuum before the addition of fresh reagents (see experimental part for detailed recycling procedure). However, complete loss of activity was observed for both catalysts in the next reaction run.

To understand the reasons behind this rapid deactivation, the reaction mixtures were analyzed by ICP-AES. Pd leaching was found for both catalysts, accounting for a total 5% of the initial Pd in the case of catalyst **11a@γ-Al_2O_3**, and a higher 19% Pd leaching was found for catalyst **11a@TiO_2**. This constitutes a very serious concern by itself, but it doesn't explain the complete loss in catalytic activity observed.

Another possible explanation for the observed results could be the agglomeration of Pd atoms resulting in the formation of clusters, nanoparticles and ultimately in inactive bulk Pd.[89] The greyish colour of the recovered catalyst after the reaction could be an indication of this process. Therefore, the recovered catalyst was analyzed by TEM, but the presence of NP's or Pd agglomerates was not detected, probably due to the low Pd loading in both materials. XRD analysis of the catalysts after the reaction runs was carried out but metallic Pd could not be found, and the only relevant diffraction peaks were those coming from the ordered structure of the titania support.

Under the present reaction conditions, the issue of Pd leaching, and the total loss of activity observed in the second reaction run prevented further studies regarding long term reusability and application of this system under continuous flow conditions.

5.3. Conclusions

Supported catalysts **11a@γ-Al_2O_3**, **11b@ γ-Al_2O_3** and **11a@TiO_2** were shown to be active in the semihydrogenation of internal alkynes using H_2(g), although selectivity was difficult to control at high alkyne conversion, and rapid overreduction to the alkane occurred. Promising results were found when the reaction was run under continuous flow conditions. The most influencing parameters in the selectivity of this system were the residence time (reaction time) and the temperature. Only a slight increase in the temperature resulted in a pronounced enhancement in activity, but selectivity was negatively affected. Regarding the performance of the catalyst distinct results were obtained over time even under the same reaction conditions. This can be an indication of a change in the nature of the catalytically active species over time, possibly generating clusters or nanoparticles under hydrogenation conditions.

Alternatively to the use of a H_2 atmosphere, the use of triethylammonium formate as H-donor in combination with PPh_3 as additive provided higher chemo- and stereo-selectivity. With this methodology various internal alkynes were reduced to the corresponding (*Z*)-alkenes in high yields and selectivities. The system is also effective for the semihydrogenation of terminal alkynols. Due to a slower overreduction reaction compared to the case of hydrogenations with H_2(g) a one-pot semihydrogenation-isomerization protocol allowed for the obtention of the stereocomplementary *trans*-stilbene in 90% yield under appropriate reaction conditions.

However, recycling studies showed complete loss of activity in the second reaction run. This deactivation could be due to the agglomeration of Pd atoms into bulk metal, although experimental evidence supporting this hypothesis could not be obtained. Pd leaching was encountered, ranging

from 5% for catalyst **11a@γ-Al_2O_3** and 19% for catalyst **11a@TiO_2** referred to the initial Pd content in both catalysts.

5.4. Experimental Part

General

Schlenk-line and other inert atmosphere techniques were used. Teflon-coated stir bars were used for magnetic stirring. Commercially supplied alkyne substrates as well as *cis*-stilbene were used without further purification. Et_3N was distilled over CaH_2 prior to use, and HCOOH was 95% reagent grade from Aldrich. 99,5% MeCN-as received was used. AcOEt was distilled under vacuum prior to use. Solution-state NMR experiments were carried out at the Servei de Recursos Científics i Tècnics (SRCiT), URV, with Varian (Agilent) Mercury VX400 or NMR System400 400 MHz or at the Institut für Technische und Makromolekulare Chemie, RWTH Aachen University with Bruker AV 400 (400 MHz) or Bruker AV 300 (300 MHz). In all cases, spectra were calibrated to residual solvent peaks. Chemical shifts for ^1H and $^{13}C\{^1H\}$ NMR spectra are reported relative to TMS. ICP analyses were conducted at the SRCiT using an ICP-OES Spectro Arcos instrument. Samples for measuring the leached Pd were prepared by refluxing in concentrated HNO_3 before being diluted for analysis. GC-MS (ESI-TOF) analyses were performed at the CTQ, on an Agilent 7980A GC System connected to a 5975C MSD spectrometer. TEM analysis of the supported catalyst after the transfer semihydrogenation runs was carried out at the SRCiT, using a JEOL JEM-1011 electronic microscope. XRD of the used catalysts was also carried out at SRCiT using a Siemens D 5000 Diffraktometer apparatus.

General procedure for the semi-hydrogenation reactions

An appropriate vessel, fitted with a teflon coated stirring bar was charged with the supported catalyst. Then, this vessel was placed in a 20 mL autoclave. After securely tightening all the valves and screws, the reactor was connected to the line, and three cycles of vacuum/Argon were applied, and the autoclave was left under an Argon atmosphere. Separately, in a small schlenk flask, 3 mL of AR-grade MeCN were added, and Argon was bubbled in for 3 minutes through a needle and a septum. Then, under a flow of Argon, the alkyne substrate was added and

dissolved by shaking. This substrate solution was then transferred via cannula to the vessel inside the autoclave containing the catalyst. Then all connections within the autoclave were securely closed, and this equipment connected to the high-pressure end for pressurizing. When small H_2 pressures were applied, an external manometer ranging from 0-25 bar was installed in between the high pressure end and the autoclave. After charging the autoclave with the indicated H_2 pressure, stirring was set to 500 rpm.

Experimental set-up for the continuous semihydrogenation of diphenylacetylene using the H-Cube Pro Reactor

Preparation of the substrate stock solution:

In a 250 mL schlenk flask, a concentration of 0,05 M or 0,1M of diphenylacetylene was built up by exactly weighing the added amount of each the substrate and the solvent. After complete dissolution of diphenylacetylene, this mixture was deoxygenated by bubbling through Argon for 15 minutes. The exact weight of the schlenk flask plus the whole reaction mixture was written down. The schlenk flask was connected to Argon, and the screw lid was replaced by a screw stopper fitted with a pierced septum.

Packing of the supported catalyst in the CatCart®:

The small size 30 x 0,4 mm CatCart® cartridge which is the exchangeable part of the H-Cube Pro reactor was charged with the supported catalyst ensuring the appropriate packing using the H-Cube Pro filling station provided for this purpose. This resulted in a catalyst loading of *ca*. 320 mg.

Setting reaction parameters, sample collection and sample analysis:

First, an empty but yet sealed cartridge was fixed, and solvent was pumped into the system through both “reactant” and “solvent” tubing inlets at a flow rate of 1,0 mL/min; this procedure was carried out for 10 minutes. The solvent was pumped out through the “product” tubing outlet and afterwards through the “waste” outlet. Then, quickly the “reactant” inlet was placed inside the substrate stock solution through the

pierced septum, and the "product" outlet was fixed at the mouth of an Erlenmeyer flask of exactly known weight. The desired reaction parameters were set at the main display menu in the H-Cube Pro. Then pressing the "Start" button results in the set parameters being applied After a few minutes, the "stable" state can be read on the main display. From this moment 10 minutes were counted. After this time, samples were collected in vials of exactly known weight. After the reaction run, "reactant" inlet was moved back into the flask containing clean MeCN, and the "product" outlet was fixed into the mouth of the Erlenmeyer flask of known weight. MeCN was pumped into the system for 15 minutes to ensure that no reaction products neither starting materials remained inside the capillaries. From each sample, an aliquot was taken, and its exact weight was measured. A known weight of external standard mesitylene (for NMR analysis) and dodecane (for GC analysis) was added to each aliquot. 1,2 mL from this aliquot was placed in a GC vial, and 12 drops were pippeted into an NMR tube, which was brought to 0,6 mL with CDCl3. The results thus obtained after GC and NMR analysis of these aliquots were extrapolated to the original sample. Finally the schlenk flask containing the substrate stock solution was weighed and the difference in weight compared with the starting solution was calculated. An aliquot was taken from the Erlenmeyer flask containing the initial and the final fractions coming out of the reactor, and after adding a known amount of external standards, they were also analyzed by GC and NMR, and the results were extrapolated to the total sample volume. With these data in hand, the percentage recovery for each reaction run could be calculated.

General procedure for the transfer semihydrogenation of internal and terminal alkynes

In a small schlenk flask fitted with a teflon coated stirring bar, 3 mL of AR-grade MeCN were added (or AcOEt when indicated). NEt_3 (352 µL; 2,5 mmol) was dissolved and then HCOOH (94 µL; 2,5 mmol) was added to the mixture. A septum lid was placed on top, and Argon was bubbled in this solution through a needle for 2 minutes. After this time 0,5 mmol of the alkyne substrate were added, the vessel was capped with a Teflon screw stopper and it was placed in the heating bath with stirring at 500 rpm, and brought to the reaction temperature. After reaching the reaction temperature, the catalyst and the additive (when indicated) were added

under a flow of Argon, and this reaction mixture was left with heating and stirring for the indicated reaction time. After the reaction time, this mixture was allowed to cool, and then external standard mesitylene (70 µL; 0,5 mmol) was added. After ensuring homogeneous mixing of the liquid phase, and letting the solid decant during a few minutes 12 drops were pippeted out to an NMR tube, and $CDCl_3$ was added for a total volume of 0,6 mL. Quantitative analysis of these samples was carried out using a 300 MHz spectrometer.

General procedure for the isomerization experiments

In a schlenk flask Et_3N/HCOOH (10% or 25% as indicated) were dissolved in 3 mL MeCN. Argon was bubbled in this solution for 2 minutes through a needle, and right after *cis*-stilbene (93 µL, 0,5 mmol, 1,0 equiv.) was added. This solution was heated to the 70°C and upon reaching the reaction temperature (the additive and) the catalyst (1 mol%) were added. After the reaction time, the vessel was allowed to cool and external standard mesitylene was added (70 µL; 0,5 mmol). After decanting of the solid, 12 drops were pippeted out to an NMR tube, and $CDCl_3$ was added to a total volume of 0,6 mL for ^{1}H NMR analysis.

General procedure for the recovery and reuse of the catalyst in consecutive reaction runs

After running the transfer semihydrogenation reaction (following the same procedure as described above), the reaction vessel was removed from the heating bath and it was allowed to cool down to room temperature. Mesitylene (71 µL, 0,5 mmol, 1,0 equiv.) were added, with shaking to ensure homogeneous mixture. The reaction mixture was allowed to stand for a few minutes, after which time it was filtered *via* cannula. The solid catalyst was washed with CH_2Cl_2 (3 x 2 mL) and filtered with a cannula each time. Then it was dried for 2 hours under vacuum, before it was recharged with PPh_3 (2,6 mg, 2 mol%), MeCN (3 mL) and HCOOH/Et_3N (5,0 equiv). This mixture was heated to reflux and then diphenylacetylene (91 mg, 0,5 mmol, 1,0 equiv.) was added.

Products obtained by Transfer semi-hydrogenation of internal and terminal alkynes and alkynols

Cis-stilbene. The reagents diphenylacetylene (89 mg, 0,5 mmol, 1,0 equiv), Et_3N (349 µL, 2,5 mmol, 5,0 equiv.), HCOOH (94 µL, 2,5 mmol, 5,0 equiv.), additive PPh_3 (2,62 mg, 0,01 mmol, 0,02 equiv.) and catalyst **11a@γ-Al_2O_3** (71 mg, 0,005 mmol, 0,01 equiv.) were used as described in the general procedure for catalytic TSH reaction runs. Not purified. Quantification by ^{1}H NMR analysis of a dilution of the reaction mixture in $CDCl_3$. Mesitylene was used as external standard. **^{1}H NMR** (400 MHz, $CDCl_3$): δ 7,26 (m, 10H), 6,64 (s, 2H). Peaks match the literature values.[90] Identity of *cis*-stilbene was further confirmed by GC-MS analysis.

(*Z*)-1-phenyl-1-propene. The reagents 1-phenyl-1-propyne (63 µL 0,5 mmol, 1,0 equiv), Et_3N (349 µL, 2,5 mmol, 5,0 equiv.), HCOOH (94 µL, 2,5 mmol, 5,0 equiv.), additive PPh_3 (2,62 mg, 0,01 mmol, 0,02 equiv.) and catalyst **11a@γ-Al_2O_3** (71 mg, 0,005 mmol, 0,01 equiv.) were used as described in the general procedure for catalytic TSH reaction runs. Not purified. Quantification was carried out by ^{1}H NMR analysis of the reaction mixture. Mesitylene was used as external standard. **^{1}H NMR** (400 MHz, MeCN(d_3)): δ 7,33 (m, 4H), 7,12 (m, 1H), 6,45 (dq, J = 11,6 Hz, 1,8 Hz, 1H), 5,84 (dq, J = 11, Hz, 7,2 Hz), 1,91 (dd, J = 7,2 Hz, 1,9 Hz, 3H). Peaks match the literature values.[90] Identity of (*Z*)-1-phenyl-1-propene was further confirmed by GC-MS analysis.

(*Z*)-1-phenyl-1-butene. The reagents 1-phenyl-1-butyne (71 µL 0,5 mmol, 1,0 equiv), Et_3N (349 µL, 2,5 mmol, 5,0 equiv.), HCOOH (94 µL, 2,5 mmol, 5,0 equiv.), additive PPh_3 (2,62 mg, 0,01 mmol, 0,02 equiv.) and catalyst **11a@γ-Al_2O_3** (71 mg, 0,005 mmol, 0,01 equiv.) were used as described in the general procedure for catalytic TSH reaction runs. Not purified. Quantification was carried out by ^{1}H NMR analysis of the reaction mixture. Mesitylene was used as external standard. **^{1}H NMR** (400 MHz, MeCN(d_3)): δ 7,38-7,29 (m, 4H), 7,24 (m, 1H), 6,41 (dq, J = 11,7 Hz, 1,9 Hz, 1H), 5,69 (dt, J = 11,7, Hz, 7,3 Hz), 2,33 (m, 2H), 1,06 (t, J = 7,5 Hz, 3H). Peaks match the literature values.[91] Identity of (*Z*)-1-phenyl-1-butene was further confirmed by GC-MS analysis.

(*Z*)-4-octene. The reagents 4-octyne (73 µL 0,5 mmol, 1,0 equiv), Et_3N (349 µL, 2,5 mmol, 5,0 equiv.), HCOOH (94 µL, 2,5 mmol, 5,0 equiv.),

additive PPh_3 (6,6 mg, 0,025 mmol, 0,05 equiv.) and catalyst **11a@γ-Al_2O_3** (71 mg, 0,005 mmol, 0,01 equiv.) were used as described in the general procedure for catalytic TSH reaction runs. Not purified. Quantification was carried out by **^{1}H NMR** analysis of the reaction mixture. Mesitylene was used as external standard. ^{1}H NMR (400 MHz, MeCN(d_3)): δ 5,38 (m, 2H), 2,05-1,96 (m, 4H), 1,40-1,31 (m, 4H), 0,90 (t, J = 7,3 Hz, 6 Hz). Peaks match the literature values.[92] Identity of (*Z*)-4-octene was further confirmed by GC-MS analysis.

(*Z*)-3-phenyl-2-propen-1-ol. The reagents 3-phenyl-2-propyn-1-ol (62 µL 0,5 mmol, 1,0 equiv), Et_3N (349 µL, 2,5 mmol, 5,0 equiv.), HCOOH (94 µL, 2,5 mmol, 5,0 equiv.), additive PPh_3 (2,62 mg, 0,01 mmol, 0,02 equiv.) and catalyst **11a@γ-Al_2O_3** (71 mg, 0,005 mmol, 0,01 equiv.) were used as described in the general procedure for catalytic TSH reaction runs. Not purified. Quantification was carried out by ^{1}H NMR analysis of the reaction mixture. Mesitylene was used as external standard**. ^{1}H NMR** (400 MHz, MeCN(d_3)): δ 7,45-7,26 (m, 5H), 6,51 (dt, J = 11,9 Hz, 1,7 Hz, 1H), 5,89 (dt, J = 12,1 Hz, 6,2 Hz, 1H), 4,35 (dd, J = 6,2 Hz, 1,9 Hz, 2H), 2,16 (m, 2H), 1,6 (m, 2H) . Identity of (*Z*)-3-phenyl-2-propen-1-ol was further confirmed by GC-MS analysis.

4-penten-1-ol. The reagents 4-pentyn-1-ol (47 µL 0,5 mmol, 1,0 equiv), Et_3N (349 µL, 2,5 mmol, 5,0 equiv.), HCOOH (94 µL, 2,5 mmol, 5,0 equiv.), additive PPh_3 (2,62 mg, 0,01 mmol, 0,02 equiv.) and catalyst **11a@γ-Al_2O_3** (71 mg, 0,005 mmol, 0,01 equiv.) were used as described in the general procedure for catalytic TSH reaction runs. Not purified. Quantification was carried out by ^{1}H NMR analysis of the reaction mixture. Mesitylene was used as external standard. **^{1}H NMR** (400 MHz, MeCN(d_3)): δ 5,90 (ddt, J = 17 Hz, 10,2 Hz, 6,7 Hz, 1H), 5,06 (ddt, J = 17,2 Hz, 2,2 Hz, 1,6 Hz, 1H), 4,98 (ddt, J = 10,8 Hz, 2,2 Hz, 1,6 Hz, 1H), 3,53 (7, J = 6,6 Hz, 2H). Peaks match the literature values.[93] Identity of 4-penten-1-ol was further confirmed by GC-MS analysis.

1-penten-3-ol. The reagents 1-pentyn-3-ol (43 µL 0,5 mmol, 1,0 equiv), Et_3N (349 µL, 2,5 mmol, 5,0 equiv.), HCOOH (94 µL, 2,5 mmol, 5,0 equiv.), additive PPh_3 (2,62 mg, 0,01 mmol, 0,02 equiv.) and catalyst **11a@γ-Al_2O_3** (71 mg, 0,005 mmol, 0,01 equiv.) were used as described in the general procedure for catalytic TSH reaction runs. Not purified.

Quantification was carried out by **^{1}H NMR** analysis of the reaction mixture. Mesitylene was used as external standard. ^{1}H NMR (400 MHz, MeCN(d_3)): δ 5,87 (ddt, J = 17,3 Hz, 10,5 Hz, 5,9 Hz, 1H), 5,19 (ddd, J = 17,3 Hz, 2,1 Hz, 1,4 Hz, 1H), 5,04 (ddd, J = 10,5 Hz, 2,1 Hz, 1,63 Hz, 1H), 3,99 (m, 1H), 2,19 (s, 1H (OH)), 1,57-1,46 (m, 2H), 0,90 (t, J = 7,4 Hz, 3H). Peaks match the literature values.[94] Identity of 1-penten-3-ol was further confirmed by GC-MS analysis.

2-phenylbut-3-en-2-ol. The reagents 2-phenyl-3-butyn-2-ol (73 mg 0,5 mmol, 1,0 equiv), Et_3N (349 µL, 2,5 mmol, 5,0 equiv.), HCOOH (94 µL, 2,5 mmol, 5,0 equiv.), additive PPh_3 (2,62 mg, 0,01 mmol, 0,02 equiv.) and catalyst **11a@γ-Al_2O_3** (71 mg, 0,005 mmol, 0,01 equiv.) were used as described in the general procedure for catalytic TSH reaction runs. Not purified. Quantification was carried out by ^{1}H NMR analysis of the reaction mixture. Mesitylene was used as external standard. **^{1}H NMR** (400 MHz, MeCN(d_3)): δ 7,53 (m, 1H), 7,34 (m, 2H), 7,25 (m, 2H), 6,17 (dd, J = 17,3 Hz, 10,6 Hz, 1H), 5,28 (dd, J = 17,3 Hz, 1,6 Hz, 1H), 5,06 (dd, J = 10,6 Hz, 1,6 Hz, 1H), 1,59 (s, 3H). Peaks match the literature values.[95] Identity of 2-phenylbut-3-en-2-ol was further confirmed by GC-MS analysis.

Trans-stilbene. The reagents diphenylacetylene (89 mg, 0,5 mmol, 1,0 equiv), Et_3N (349 µL, 2,5 mmol, 5,0 equiv.), HCOOH (94 µL, 2,5 mmol, 5,0 equiv.) and catalyst **11a@γ-Al_2O_3** (71 mg, 0,005 mmol, 0,01 equiv.) were used as described in the general procedure for catalytic TSH reaction runs. Not purified. Quantification by ^{1}H NMR analysis of a dilution of the reaction mixture in $CDCl_3$. Mesitylene was used as external standard. **^{1}H NMR** (400 MHz, $CDCl_3$): δ 7,57 (m, 4H), 7,40 (m, 4H), 7,31 (m, 2H), 7,17 (2H). Peaks match the literature values.[90] Identity of *trans*-stilbene was further confirmed by GC-MS analysis.

5.5. References

[1] Á. Molnár, A. Sárkány, M. Varga, *J. Mol. Catal. A: Chem.,* **2001**, 173, 185.
[2] A.M. Kluwer, C.J. Elsevier, Homogeneous Hydrogenation of Alkynes and Dienes. In *The Handbook of Homogeneous Hydrogenation*; Eds. J. G. de Vries, C. J. Elsevier; Wiley-VCH: Weinheim, **2007**; p 375.
[3] I.J. Munslow, Alkyne Reductions. In *Modern Reduction Methods*; Eds. P. G. Andersson, I. J. Munslow; Wiley-VCH: Weinheim, **2008**; p 363.
[4] H. Arnold, F. Döbert, J. Gaube, Selective Hydrogenation of Hydrocarbons. In *Handbook of Heterogeneous Catalysis*; Eds. G. Ertl, H. Knözinger, F. Schüth, J. Weitkamp; Wiley-VCH: Weinheim, **2008**; Vol. 7, p 3266.
[5] A. Borodzinski, G.C. Bond, *Catal. Rev.: Sci. Eng*. **2006**, *48*, 91.
[6] A. Borodzinski, G.C. Bond, *Catal. Rev.: Sci. Eng.* **2008**, 50, 379.
[7] J. Osswald, R. Giedigkeit, R.E. Jentoft, M. Armbrüster, F. Girgsdies, K. Kovnir, T. Ressler, Y. Grin, R. Schlögl, *J. Catal.* **2008**, 258, 210.
[8] M. Armbrüster, K. Kovnir, M. Behrens, D. Teschner, Y. Grin, R. Schlögl, *J. Am. Chem. Soc.* **2010**, *132*, 14745.
[9] J. Paust, M. John, U.S. Patent US5689022, **1997**.
[10] K.C. Nicolaou, R.A. Daines, T.K. Chakraborty, Y. Ogawa, *J. Am. Chem. Soc*. **1987**, *109*, 2821.
[11] V.V. Semenov, A.S. Kyseliov, I.Y. Titov, I.K. Sagamanova, N.N. Ikizalp, N.B. Chernysheva, D.V. Tsyganov, L.D. Konyushkin, S.I. Firgang, R.V. Semenov, I.B. Karmanova, M.M. Raihstat, M.N. Semenova, *J. Nat. Prod.* **2010**, *73*, 1796.
[12] M. Chen, W.R. Roush, *Org. Lett*. **2012**, *14*, 1880.
[13] K. Mori, In *The total synthesis of natural products*; Ed. J. Apsimon; Wiley Interscience: New York, **1992**; Vol. 9.
[14] K. Mori, *Top. Curr. Chem*. **2004**, *239*, 1.
[15] V.N. Odinokov, *Chem. Nat. Compd.* **2000**, *36*, 11.
[16] M. Fouché, L. Rooney, A.G.M. Barrett, *J. Org. Chem.* **2012**, *77*, 3060.
[17] G. Wittig, U. Schollkopf, *Chem. Ber*. **1954**, *87*, 1318.
[18] B.E. Maryanoff, A.B. Reitz, *Chem. Rev.* **1989**, *89*, 863.
[19] W. Wadsworth, W.D. Emmons, *J. Am. Chem. Soc.* **1961**, 83, 1733.
[20] P.R. Blakemore, *J. Chem. Soc., Perkin Trans. 1* **2002**, 2563.
[21] D.J. Peterson, *J. Org. Chem.* **1968**, *33*, 780.
[22] K. Takai, K. Nitta, K. Utimoto, *J. Am. Chem. Soc.* **1986**, 108, 7408.
[23] B.K. Keitz, K. Endo, P.R. Patel, M.B. Herbert, R.H. Grubbs, *J. Am. Chem. Soc.* **2012**, *134*, 693.
[24] *Handbook of metathesis*; Ed. R.H. Grubbs; Wiley-CH: Weinheim, Germany, **2003**.
[25] B.M. Trost, Z.T. Ball, T. Joge, *J. Am. Chem. Soc.* **2002**, *124*, 7922.
[26] *March's advanced organic chemistry: reactions: mechanisms, and structure,* 5th ed.; Eds. M.B. Smith, J. March; Wiley-Interscience: New York, **2001**.
[27] *Metal-catalyzed cross-coupling reactions*; Eds. A. De Meijere, F. Diederich; Wiley-VCH: Weinheim, **2004**.
[28] A. Fürstner, K. Radkowski, *Chem. Commun.* **2002**, 2182.

[29] H. Lindlar, *Helv. Chim. Acta* **1952**, 35, 446 –450.
[30] H. Lindlar, R. Dubuis, *Org. Synth*. **1966**, *46*, 89.
[31] J.E. McMurry, N.O. Siemers, *Tetrahedron Lett.* **1994**, *35*, 4505.
[32] S.V. Naidu, P. Gupta, P. Kumar, *Tetrahedron* **2007**, *63*, 7624.
[33] Z.B. Zhang, Z.M. Wang, Y.X. Wang, H.Q. Liu, G.X. Lei, M. Shi, *Tetrahedron: Asymmetry* **1999**, *10*, 837.
[34] C. Guo, X.Y. Lu, *Tetrahedron Lett.* **1991**, *32*, 7549.
[35] D.A. Evans, D.M. Fitch, 2000, 39, 2536. *Angew. Chem. Int. Ed. Engl.* **2000**, *39*, 2536.
[36] J.M. Gaudin, C. Morel, *Tetrahedron Lett.* **1990**, *31*, 5749.
[37] G. McGaffin, A. de Meijere, *Synthesis*, **1994**, 583.
[38] P.A. Wade, S.G. D'Ambrosio, J.A. Rao, S. ShahPatel, D.T. Cole, J.K. Murray, P.J. Carroll, *J. Org. Chem*. **1997**, *62*, 3671.
[39] C.A. Brown, V.K. Ahuja, *J. Chem. Soc., Chem. Commun*. **1973**, *15*, 553.
[40] F. Studt, F. Albild-Pedersen, T. Bligaard, R.Z. Sørensen, C.H. Christensen, J.K. Nørskov, *Science* **2008**, *320*, 1320.
[41] K. Semba, T. Fujihara, T. Xu, J. Terao, Y. Tsuji, *Adv. Synth. Catal*. **2012**, *354*, 1542.
[42] M. Niu, Y. Wang, W. Li, J. Jiang, Z. Jin, *Catal. Commun*. **2013**, *38*, 77.
[43] L. Shao, X. Huang, D. Teschner, W. Zhang, *ACS Catal.* **2014**, *4*, 2369.
[44] T. Mitsudome, Y. Takahashi, S. Ichikawa, T. Mizugaki, K. Jitsukawa and K. Kaneda, *Angew. Chem., Int. Ed*., **2013**, 52, 1481.
[45] Y. Yabe, T. Yamada, S. Nagata, Y. Sawama, Y. Monguchi and H. Sajiki, *Adv. Synth. Catal.*, **2012**, *354*, 1264.
[46] P.T. Witte, S. Boland, F. Kirby, R. van Maanen, B.F. Bleeker, D.A. Matthijs de Winter, J.A. Post, J.W. Geus, P.H. Berben, *ChemCatChem,* **2013**, *5(2)*, 582.
[47] C.R. Lederhos, M.J. Maccarrone, J.M. Badano, G. Torres, F. Coloma-Pascual, J.C. Yori, M.E. Quiroga, *Appl. Catal., A*, **2011**, *396*, 170.
[48] M.W. Tew, H. Emerich, J.A. van Bokhoven, *J. Phys. Chem. C*, **2011**, *115*, 8457.
[49] Y. Takahashi, N. Hashimoto, T. Hara, S. Shimazu, T. Mitsudome, T. Mizugaki, K. Jitsukawa, K. Kaneda, *Chem. Lett.* **2011**, *40*, 405.
[50] P. Pelagatti, A. Venturini, A. Leporati, M. Carcelli, M. Costa, A. Bacchi, G. Pelizze, C. Pelizzi, *J. Chem. Soc., Dalton Trans.* **1998**, 2715.
[51] M. Costa, P. Pelagatti, C. Pelizze, D. Rogolino, *J. Mol. Catal. A* **2002**, *178*, 21.
[52] M.P. Conley, R.M. Drost, M. Baffert, D. Gajan, C.J. Elsevier, W.T. Franks, H. Oschkinat, L. Veyre, A. Zagdoun, A. Rossini, M. Lelli, A. Lesage, G. Casano, O. Ouari, P. Tordo, L. Emsley, C. Copéret, C. Thieuleux, *Chem. Eur. J*. **2013**, *19*, 12234.
[53] M.W. van Laren, C.J. Elsevier, *Angew. Chem., Int. Ed.* **1999**, *38*, 3715.
[54] E. Sulman, C. Deibele, J. Bargon, *React. Kinet. Catal. Lett*. **1999**, *67*, 112.
[55] M.W. van Laren, M.A. Duin, C. Klerk, M. Naglia, D. Rogolino, P. Pelagatti, A. Bacchi, C. Pelizzi, C.J. Elsevier, *Organometallics* **2002**, *21*, 1546.
[56] A.M. Kluwer, T.S. Koblenz, T. Jonischkeit, K. Woelk, C.J. Elsevier, *J. Am. Chem. Soc.*, **2005**, *127*, 15470.
[57] A. Dedieu, S. Humbel, C.J. Elsevier, C. Grauffel, *Theor. Chem. Acc.* **2004**, *112*, 305.
[58] N. Koga, S. Obara, K. Kitaura, K. Morokuma, *J. Am. Chem. Soc.* **1985**, *107*, 7109.

[59] J. W. Sprengers, J. Wassenaar, N. D. Clement, K. J. Cavell, C. J. Elsevier, *Angew. Chem. Int. Ed*. **2005**, 44, 2026.
[60] D. Wang and D. Astruc, *Chem. Rev.*, **2015**, *115*, 6621.
[61] A.J. Blacker, *In Handbook for Homogeneous Hydrogenation*, 1st ed.; Eds. J.G. de Vries, C.J. Elsevier; Wiley-VCH: Weinheim, **2007**, Vol. 3, pp 1215.
[62] S. Gladiali, E. Alberico, *Chem. Soc. Rev.* **2006**, *35*, 226.
[63] J.S. Samec, J.-E. Bäckvall, P.G. Andersson, P. Brandt, *Chem. Soc. Rev.* **2006**, *35*, 237.
[64] A. Comas-Vives, G. Ujaque, A. Lledós, *J. Mol. Struct: THEOCHEM,* **2009**, *903*, 123.
[65] D. Gnanamgari, A. Moores, E. Rajaseelan, R.H. Crabtree, *Organometallics* **2007**, *26*, 1226.
[66] J. P. Black, G. Cami-Kobeci, M.G. Edwards, P.A. Slatford, M.K. Whittlesey, J.M. Williams, J. *Org. Biomol. Chem.* **2006**, *4*, 116.
[67] D. Xue, Y.C. Chen, X. Cui, Q.W. Wang, J. Zhu, G.J. Deng, *J. Org. Chem.* **2005**, *70*, 3584.
[68] Y. Gao, M.C. Jennings, R.J. Puddephatt, *Can. J. Chem.* **2001**, *79*, 915.
[69] P. Hauwert, G. Maestri, J.W. Sprengers, M. Catellani, C.J. Elsevier, *Angew. Chem. Int. Ed*. **2008**, 47, 3223.
[70] S. Warsink, P. Hauwert, M.A. Siegler, A.L. Spek, C.J. Elsevier, *Appl. Organomet. Chem.* **2009**, *23*, 225.
[71] J. Li, R. M. Hua, T. Liu, *J. Org. Chem.* **2010**, *75*, 2966.
[72] R. Barrios-Francisco, J.J. García, *Appl. Catal., A* **2010**, *385*, 108.
[73] C. Oger, L. Balas, T. Durand, J.-M. Galano, *Chem. Rev*. **2013**, *113*, 1313.
[74] L.L. Wei, L.M. Wei, W.B. Pan, S.P. Leou, M.J. Wu, *Tetrahedron Lett*. **2003**, *44*, 1979.
[75] B.M. Trost, R. Braslau, *Tetrahedron Lett*. **1989**, 30, 4657.
[76] H. Yamada, S. Aoyagi, C. Kibayashi, *Tetrahedron Lett*. **1996**, *37*, 8787.
[77] Y.K. Zhao, Q.A. Liu, J. Li, Z.Q. Liu, B. Zhou, *Synlett,* **2010**, 1870.
[78] K. Tani, N. Ono, S. Okamoto, F. Sato, *J. Chem. Soc., Chem. Commun*. **1993**, 386.
[79] R.M. Drost, T. Bouwens, N.P. van Leest, B. de Bruin, C.J. Elsevier, *ACS Catal*. **2014**, *4*, 1349.
[80] N.M. Yoon, K.B. Park, H.J. Lee, J. Choi, *Tetrahedron Lett*. **1996**, 37, 8527.
[81] R. Porta, M. Benaglia, A. Puglisi, *Org. Process Res. Dev*., **2016**, *20*, 2.
[82] R.M. Drost, D.L.J. Broere, J. Hoogenboom, S.N. de Baan, M. Lutz, B. de Bruin, C.J. Elsevier, *Eur. J. Inorg. Chem.* **2015**, 982.
[83] R. Shen, T. Chen, Y. Zhao, R. Qiu, Y. Zhou, S. Yin, X. Guan, M. Goto, L. Han, *J. Am. Chem. Soc*. **2011**, 133, 17037.
[84] J. Broggi, V. Jurcik, O. Songis, A. Poater, L. Cavallo, A.M.Z. Slawin, C.S.J. Cazin, *J. Am. Chem. Soc*. **2013**, 135, 4588.
[85] J. Horiuti, M. Polanyi, *Trans. Faraday Soc.* **1934**, 30, 1164.
[86] J.P. Wolkowski, J.F. Hartwig, *Angew. Chem. Int. Ed*. **2002**, 41, 4289.
[87] F. Luo, C. Pan, W. Wang, Z. Ye, J. Cheng, *Tetrahedron*, **2010**, 66, 1399
[88] K. Radkowski, B. Sundararaju, A. Fürstner, *Angew. Chem. Int. Ed*. **2013**, 52, 355.
[89] R.M. Drost, V. Rosar, S.D. Marta, M. Lutz, N. Demitri, B. Milani, B. de Bruin, C.J. Elsevier, *ChemCatChem* **2015**, 7, 2095.

[90] C. Belger, N.M. Neusius, B. Plietker, *Chem. Eur. J.* **2010**, *16*, 12214
[91] Y. Moussaoui, K. Saïd, R.B. Salem, *Arkivoc*, **2006**, *12*, 1.
[92] J. Hori, K. Murata, T. Sugai, H. Shinohara, R. Noyori, N. Arai, N. Kurono, T. Ohkuma, *Adv. Synth. Catal.*, **2009**, *351*, 3143.
[93] D.S. Helfer, D.S. Phaho, J.D. Atwood, *Organometallics*, **2006**, *25*, 410.
[94] R.N. Shakhmaev, A.U. Ishbaeva, I.S. Shayakhmetova, *Russ. J. Gen. Chem.*, **2009**, *79*, 1171.
[95] C. Morrill, R.H. Grubbs, *J. Am. Chem. Soc.*, **2005**, *127*, 2842.

UNIVERSITAT ROVIRA I VIRGILI
HETEROGENIZED N-HETEROCYCLIC CARBENE METAL COMPLEXES FOR SELECTIVE CATALYSIS
Alberto Martínez Lombardía

UNIVERSITAT ROVIRA I VIRGILI
HETEROGENIZED N-HETEROCYCLIC CARBENE METAL COMPLEXES FOR SELECTIVE CATALYSIS
Alberto Martínez Lombardía

Chapter 6

"Pyrene-tagged chiral [Rh(bis(NHC))] complexes. Synthesis, characterization and immobilization onto MWCNTs. Preliminary studies in asymmetric catalysis."

UNIVERSITAT ROVIRA I VIRGILI
HETEROGENIZED N-HETEROCYCLIC CARBENE METAL COMPLEXES FOR SELECTIVE CATALYSIS
Alberto Martínez Lombardía

> Pyrene tagged chiral [Rh(bis(NHC))] complexes. Synthesis, characterization and immobilization onto MWCNTs. Preliminary studies in asymmetric catalysis

6.1. Introduction

Chemical stability and coordination versatility are two of the many properties of NHCs that may have helped their great development. The easy preparation of NHC-precursors has allowed an almost infinite access to new organometallic topologies.[1,2,3] Among NHCs, poly(N-heterocyclic carbene)s have attracted great attention because they allow the preparation of organometallic compounds with a variety of geometries.[4] Many poly(NHC)s have been developed and their structural and electronic properties have been related to their catalytic properties.[5,4] Among poly(NHC)s architectures, bis(NHC)s are by far the most abundant ones, and tris- and tetra(NHC)s are much less abundant, probably due to their usually complicated multi-step syntheses and the fact that the resulting tris- and tetra-cationic imidazolium salts are often difficult to purify due to their low solubility in most organic solvents.[6,7] In the next sections some important aspects about the coordination chemistry of bis(NHC)s will be addressed.

6.1.1. Topological properties of [M(bis(NHC))]

6.1.1.1. Bidentate [M(bis(NHC))]s and polydentate [M(bis(NHC))]s

Bis(NHC) feature two NHC fragments bound through a linker (Scheme 6.1.). The nature of the linker has important implications in the coordination ability of the bis(NHC) ligand and in the reactivity of the corresponding [M(NHC)] complex.[4]

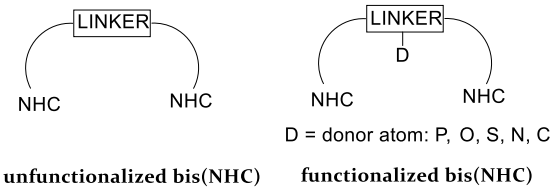

Scheme 6.1. General representation of bis(NHC) ligands, where the linker can provide additional donor functionality.

Two main groups of bis(NHC) ligands can be distinguished: those which are "unfunctionalized" and those carrying additional donor

functionalities, such as a pyridine, amino, phosphino, alkoxy, aryl, or any other coordinating group. This additional donor functionality is usually installed in the linker.[8] The latter group of bis(NHC)s are able to bind to the metal through the two NHCs and additionally through the donor atom, in a tridentate fashion, giving rise to tripodal[9] or pincer[10] geometries. In this work, the focus will be on "unfunctionalized" bis(NHC)s.

6.1.1.2. Bridging vs chelating coordination of bidentate bis(NHC)s

Bidentate bis(NHC)s may bind to one metal center (chelating coordination) or to two metal centers (bridging coordination). The preference for one or the other can be rationalized and depends on steric considerations (Scheme 6.2).[4,11]

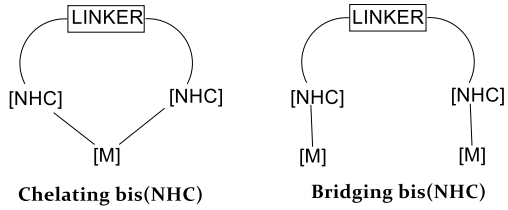

Scheme 6.2. Chelating vs bridging coordination of a bis(NHC) ligand.

In order to predict whether a chelating or bridging coordination will be adopted, several parameters need to be considered such as the geometry of the complex (square planar, or octahedral bearing apical ligands), the steric hindrance of the coligands and of the R substituents on the azole rings, or the nature of the linker.[4] The length and the rigidity of the linker greatly influence the conformation of the azole rings within the equatorial plane of the complex and the preference for a chelating or bridging coordination. When the two NHC fragments are bound by short linkers, the azole rings lie close to the sterically congested plane of the complex (plane *xy*) (Scheme 6.3 a). The steric interaction between the R substituents on the NHC with the other ligands in the complex (L) will determine the preference for a chelating (small coligands) or a bridging coordination (bulky coligands).

Pyrene-tagged chiral [Rh(bis(NHC))] complexes. Synthesis, characterization and immobilization onto MWCNTs. Preliminary studies in asymmetric catalysis

Bis(NHC) ligands bridged by longer linkers possess more flexibility, and the azole rings can align close to the *z* axis in order to avoid unfavorable interactions between the R substituents on the NHC and the other coligands in the complex (L) (Scheme 6.3 b). This situation resembles the case of monodentate NHC complexes, where rotation around the M-NHC bond is less restricted than in [M(bis(NHC))] and the azole plane is perpendicular to the *xy* plane. Compared to the previous case, now the R substituents of the two NHC fragments are much closer to each other; in this situation, bulky R groups may lead to a steric clash, so that a bridging coordination would be preferred.

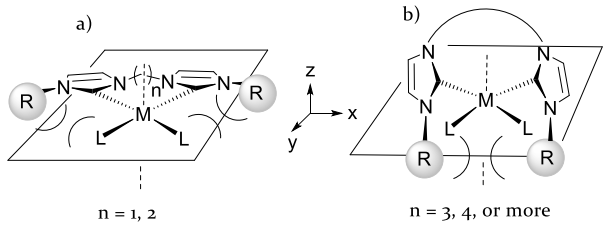

Scheme 6.3. Effect of the length of the linker on the structure of the [M(bis(NHC))] complex.

Several parameters have been defined for the quantification of the conformational and structural properties of chelating bis(NHC) metal complexes. The conformation of the azole rings relative to the plane of the complex *xy* can be measured by the α angle (mean dihedral angle between the azole planes and the *xy* plane), which theoretical values range between 0° (for short linkers) and 90° (for long linkers). The bite angle is an indication of the flexibility of the ligand, and values approaching the most favorable angle of 90° imply a flexible ligand structure. Another parameter to be defined is the θ (yaw angle)[11] which measures the "*in* plane" distortion, due to the steric constraints imposed by the formation of a metalacycle.

In addition to these considerations, some other factors have been recognized to play a role in the coordination mode of bis(NHC)s such as the counteranion.[11,12] Crabtree et al. showed that the absence of halide anions in the reaction medium tends to favor the formation of cationic chelate complexes instead of 2:1 metal ligand ones. Besides the length, the

rigidity of the linker can dictate the coordination mode of the bis(NHC). Very rigid linkers between the two NHC fragments have been used to specifically design non-chelating bis(NHC) (Scheme 6.4). In this regard, triazolylidenes[13,14] and benzobis(imidazolylidene)s[15] have appeared as interesting scaffolds that can bridge transition metals and provide enhanced electronic and catalytic properties.

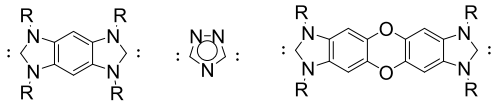

Scheme 6.4. Examples of linearly opposed bis(NHC)s specifically designed to display a non-chelating coordination mode.

6.1.1.3. [M(bis(NHC))] complexes. Chelate effect

Organometallic compounds bearing chelating bis(NHC) complexes exhibit superior stability over complexes bearing monodentate NHCs due to the chelate effect. In consequence, [M(bis(NHC))] complexes are more robust, and have superior thermal and chemical stability and this has allowed their use as catalysts under pretty harsh reaction conditions, involving high temperatures (170°C),[16] in the presence of air,[17] or strong oxidants.[18] This advantageous properties have resulted in numerous catalytic applications of [M(bis(NHC))] such as C-C couplings,[19] transfer hydrogenation of ketones and imines,[20,21] hydrosilylation of ketones[22] and terminal alkynes,[17] hydrogenation,[23] or hydroamination[24] to cite some of them.

Besides their superior stability compared with [M(mono(NHC))], bis(NHC) ligands allow a better control over the coordination sphere and the fine tuning of properties such as steric hindrance, bite angles, chirality, and fluxional behavior.[25] These features are attractive regarding the development of asymmetric catalysts based on bis(NHC) architectures. However, the application of [M(bis(NHC))] catalysts in asymmetric transformations has only been reported scarcely, and has only met with limited success.[26]

Pyrene-tagged chiral [Rh(bis(NHC))] complexes. Synthesis, characterization and immobilization onto MWCNTs. Preliminary studies in asymmetric catalysis

6.1.2. Chiral chelating [M(bis(NHC))]. Application in asymmetric catalysis

Due to the resemblance in their coordination properties with phosphorus-donor ligands, NHCs have the potential to promote any reaction catalyzed by traditional tertiary phosphine- and phosphite-based catalysts.[27] In this regard, the popular and highly successful motif of chiral chelating diphosphorus ligands[28] has prompted researchers to extend this type of geometry to bidentate NHC-based ligands. The most widely studied type of bidentate NHC-based chiral ligands include mixed NHC/heterodonor scaffolds, featuring one NHC fragment in combination with phosphine, thioether, sulfone, oxazole, oxazoline, imine or amine donor groups.[29]

In contrast, the type of chiral bis(NHC) ligand scaffold has been much less explored, and only a few unique chiral bis(NHC) architectures exist.[30,31,32,33,34,35,36,37,38,39] In accordance with the limited number of chiral bis(NHC) ligand architectures, applications of this type of ligands in asymmetric metal-catalyzed transformations are scarce. Poor enantioselectivities have been reported in many cases.[40,41,37,38,42] For some of these bis(NHC) ligands, application in enantioselective catalysis is not reported,[30,31,43] or metalation was not achieved.[44,45]

In the majority of these ligands the chirality is located at the backbone, with a few exceptions that incorporate a chiral center on the N-alkyl wingtips.[46,39,47] Introduction of chirality in both the backbone and on the N-alkyl arms has also been reported.[48] Selected examples are shown in Figure 6.1.

Chelating [M(bis(NHC))] complexes bearing ligands **42-45** in Figure 6.1, where the chirality is situated at the ligand backbone displayed the highest levels of enantioinduction compared with the rest of chiral bis(NHC) reported (see references above). Incorporation of additional chiral centers at the N-wingtips, as in the case of **41** was studied by Veige et al., and they found that it only had a minor effect on enantioinduction.

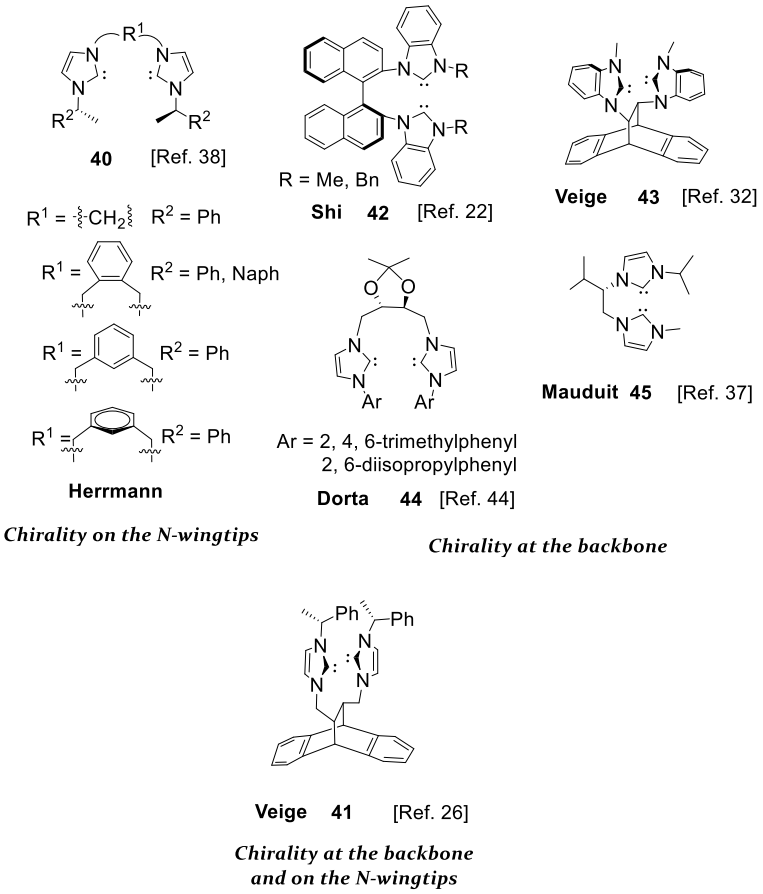

Figure 6.1. Representative examples of chiral bis(NHC) ligands where the chirality is located at the N-wingtips, at the ligand backbone, or both. For those carrying chirality at the backbone, some of the most successful ligand frameworks are shown with respect to their application in enantioselective processes.

In contrast, some studies were carried out by Veige et al. indicating that modification of the linker had a much greater effect on the enantiodiscrimination.[48,49] Ligands where the linker forces a more rigid coordination environment around the metal center have a better spatial definition of the chiral pocket, and better enantioselectivities are obtained compared to more flexible ligand structures.

The best results reported so far in the application of a chiral bis(NHC) ligand in any enantioselective process correspond to ligand framework **42** (Figure 6.1). [22] Rhodium (III) complex **46** (Scheme 6.5) was applied in the enantioselective hydrosilylation of methyl ketones. Aryl and alkyl methyl ketones were reduced to the corresponding secondary alcohols in high

conversions and in 90-98% ee for the majority of the substrates. This complex also catalyzed the enantioselective hydrosilylation of 3-oxo-3-arylpropionic acid methyl or ethyl esters, affording the corresponding 3-hydroxy esters in high yields and enantiomeric excesses above 90% for most of the substrates.[50]

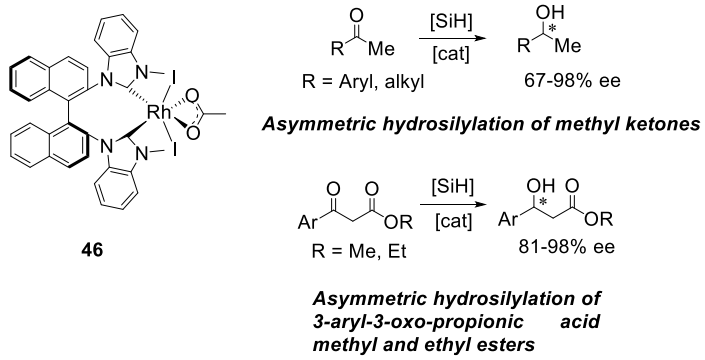

Scheme 6.5. Application of Rh complex **46** in the hydrosilylation of metyl ketones and 3-aryl-3-oxo propionic acid methyl and ethyl esters.

Besides Rh-catalyzed hydrosilylation Shi et al. have also reported the coordination of this ligand framework to Pd(II) precursors yielding complexes **47-49** where the coordination sphere of the metal is completed with iodide, aqua and acetate ligands (Figure 6.2). These complexes have been applied in a variety of transformations with notable success in terms of yields and high enantioinductions.[41,51,52]

These results may not be as surprising, given that these ligand framework is derived from the 1,1'-binaphtyl-2,2'-diamine (BINAM) backbone. BINAM belongs to the "privileged" ligand class defined by Jacobson and Yoon.[53] The privileged term arises from the fact that these ligands typically provide high enantio-discrimination across a number of reactions. BINAM is *C*2-symmetric (effectively halving the possible diastereotopic transition states) and exploits the restricted rotation about the biaryl bond providing a rigid backbone.

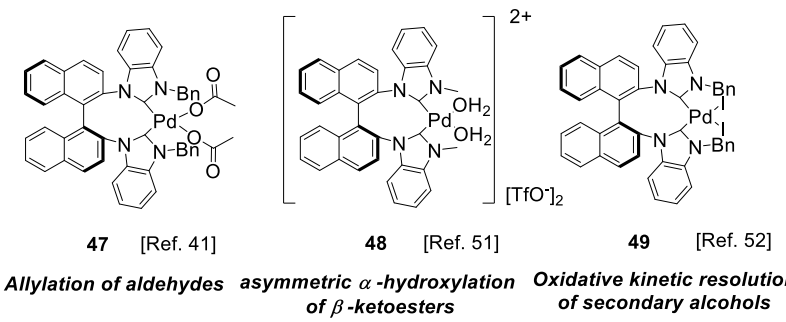

Figure 6.2. Application of Pd(II) complexes **47-49** in various asymmetric transformations.

Very recently Elsevier et al. have reported the synthesis of a BINAM-derived bis(NHC) ligand **53** bearing 2 "click" 1,2,3-triazol-5-ylidene fragments (Scheme 6.6).[54]

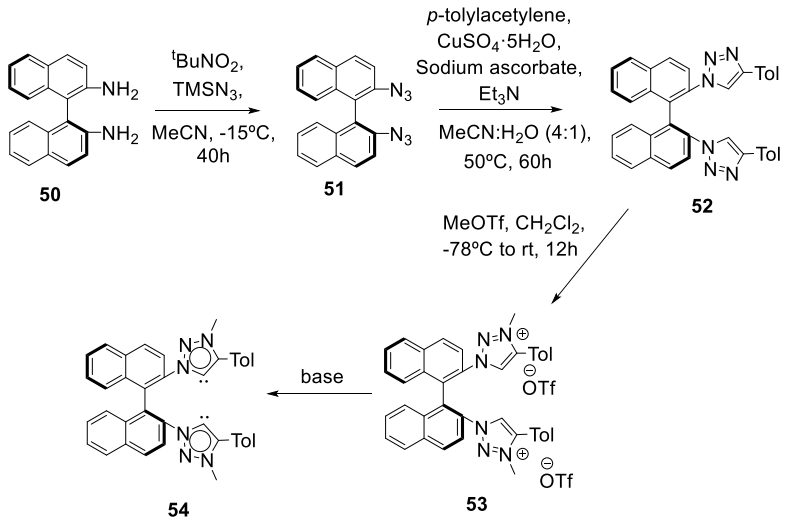

Scheme 6.6. BINAM-based bis(1,2,3-triazolylidene) ligand framework reported by Elsevier et al.

This ligand can be obtained by deprotonation of the diquaternary bistriazolium ditriflate salt **53**. This carbene salt precursor was synthesized in three steps, involving azidation to obtain compound **51**, then, by reaction with p-tolylacetylene using a copper salt as the catalyst CuAAC "click chemistry" bistriazole **52** wa obtained, and this compound was methylated using methyl triflate to yield **53** in an overall yield of 91%

starting from **50**. Therefore, bis(1,2,3-triazole-5-ylidene) ligand **54** combines the well-known successful BINAM chiral motif with the unexplored coordination and reactivity of the bis(1,2,3-triazol-5-ylidene) scaffold. 1,2,3-triazol-5-ylidenes have attracted a great deal of attention since their first appearance in the literature in 2008.[55] For the preparation of 1,2,3-triazol-5-ylidenes, 1,2,3-triazolium salts were rapidly identified as ideal precursors, by analogy to the classical deprotonation route used in the preparation of NHCs and related species.[56] In turn, triazoles are conveniently prepared by the Cu-catalyzed alkyne-azide cycloaddition (CuAAC, "click chemistry")[57] and are readily alkylated at N3 to yield the target triazolium salts (Scheme 6.7).

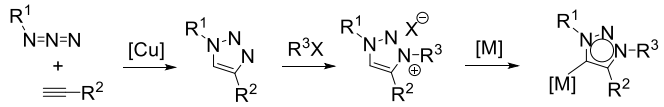

Scheme 6.7. Most common synthetic route to [M(1,2,3-triazol-4-ylidene)] complexes involving "click reaction", alkylation and metalation.

Another interesting feature of 1,2,3-triazol-5-ylidenes is that they belong to the group of abnormal or mesoionic carbenes (MIC), along with imidazol-4-ylidenes, for which no uncharged resonance structure can be drawn. Therefore, the lone pair of electrons on the carbene atom is less stabilized across the conjugate system compared to the case of more classic imidazol-2-ylidenes, and this reduced stabilization results in higher basicity and increased σ-donation.

In Table 6.1 the σ-donor properties of classic 1,3-imidazol-2-ylidenes are compared with that of abnormal carbenes 1,2,3-triazol-5-ylidenes and 1,3-imidazol-4-ylidenes by measuring the stretching frequencies of CO (υ(CO)) in the corresponding [Ir(NHC)Cl(CO)$_2$]. By comparing the υ(CO) it can be seen that for all 1,2,3-triazol-5-ylidenes displayed (entries 1-6) the υ(CO) in the corresponding Ir complexes are slightly lower than even in the case of the most basic 1,3-imidazol-4-ylidene (entry 10). This means that 1,2,3-triazole-5-ylidenes are stronger σ donors than classic 1,3-imidazol-2-ylidenes. Their donor capacity, though, is not as high as in the case of abnormal carbenes based on the 1,3-imidazol-4-ylidene scaffold (entry 11). The presence of three nitrogens in the azole ring in the case of

1,2,3-triazolylidenes reduces the electron density of the ligand and may thus explain their lower donor ability relative to 4-imidazolylidenes.

Table 6.1. Comparison of the υ(CO) stretching frequencies between imidazole-2-ylidenes, 1,2,3-triazol-5-ylidenes and imidazole-4-ylidenes in Ir complexes of the type [Ir(NHC)Cl(CO)$_2$].

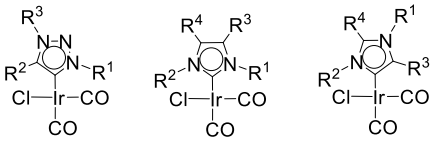

55 **56** **57**

Entry	Complex	R^1	R^2	R^3	R^4	υ(CO) (cm^{-1})
1	**55a**	Dipp	Dipp	Me	-	2019
2	**55b**	Mes	Mes	Me	-	2019
3	**55c**	Ph	Et	Me	-	2021
4	**55d**	Dipp	Ph	Me	-	2019
5	**55e**	Dipp	OEt	Dipp	-	2018
6	**55f**	Dipp	Dipp	Dipp	-	2020
7	**56a**	Dipp	Dipp	H	H	2024
8	**56b**	Mes	Mes	H	H	2024
9	**56c**	Cy	Cy	H	H	2023
10	**56d**	Ad	Ad	H	H	2021
11	**57a**	Me	iPr	Ph	Ph	2003

Dipp = 2,6-diisopropylphenyl. Data taken from Ref. 56 and references therein.

To assess the electron donating ability of ligand **54** the υ(CO) of the corresponding [Rh(**54**)(CO)$_2$Cl] (in analogy to the case of Ir complexes introduced in Table 6.1) were measured and they were compared with the values obtained for analogous Rh complexes bearing bidentate [2,2'-bis(diphenylphosphanyl)-1,1'-binaphthyl] (BINAP),[58] and chiral bis(imidazolylidene) and bis(benzimidazolylidene) ligands.[59] The same trend pointed out in Table 6.1 was observed and ligand **54** displayed stronger donor ability, due to the reduced electronic stabilization by the mesoionic 1,2,3-triazolylidene scaffolds. Metalation of ligand **54** with Ag, Pd, Rh and Ir was achieved, and these complexes were evaluated as precatalysts in various reactions (Scheme 6.8).[54] Pd complex **58** was tested

in the allylic alkylation of 1,3-diphenylprop-3-enyl acetate and dimethyl malonate, but no conversion was noted at room temperature. This might be due to an inhibiting effect of the strongly coordinated allyl ligand, preventing formation of the active Pd species. Rh(I) complex **59** was active in the hydrogenation of methyl (*Z*)-2-acetamido-3-phenylacrylate, and also in the transfer hydrogenation of acetophenone in iPrOH, but in both cases the racemic product was obtained. Better results were obtained in the hydrosilylation of aryl ketones. Enhanced enantioselectivities, up to 51% were obtained for bulkier substrates.

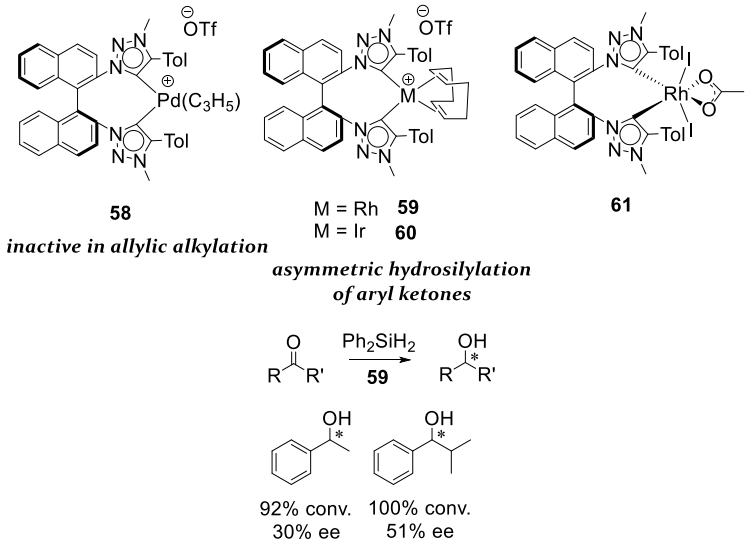

Scheme 6.8. Pd, Rh and Ir complexes **58-61** bearing ligand **54**, and pertinent catalytic applications.[54]

Octahedral Rh(III) complex **61** which has more similarities with successful catalyst **46** was less active and afforded the product as a racemate. A possible explanation for the inferior results with this system compared to Shi's Rh(III) complex **46** could be the superior rigidity and steric effects provided by the benzimidazol scaffold, as it has been pointed out in related [Rh(I)bis(NHC)] systems.[48] Considering the facile, modular and high yielding synthesis of ligand **54** through "click chemistry", the promising results obtained by this ligand scaffold deserve further exploration.

6.1.3. Heterogenization of molecular catalysts onto CNTs through π-π stacking interactions

As introduced in Chapter 1, the intrinsic limitations of homogeneous catalysts in separating the catalyst from the products and in catalyst recycling and reuse can be circumvented by immobilizing the homogeneous catalyst onto a solid support, which may allow an easy separation by simple filtration or centrifugation.[60,61] The most widely used method for the immobilization of homogeneous catalysts onto solid supports is the formation of covalent bonds between the ligands and the support.[62] By doing so, the supported catalyst is expected to be robust enough to withstand the harsh reaction conditions needed for some catalytic processes. However, this immobilization method has two important drawbacks. First, arising from the need for an additional functionalization of the ligand, thus adding additional effort to the catalyst synthesis. And a second drawback, arises from the possible changes in chemical reactivity (and therefore in catalytic activity), derived from the formation of the covalent bond between the support and the catalyst. As an alternative, immobilization of homogeneous catalysts onto solid supports through non-covalent interactions is a growing area of research owing to the fact that no chemical modification neither of the catalyst nor of the support is required. In this context, several groups have reported the immobilization of homogeneous catalysts onto carbonaceous supports through π-π stacking interactions.[63,64,65,66,67] In the next section, some important aspects about the immobilization of homogeneous catalysts onto carbon surfaces through this type of interaction will be introduced.

6.1.3.1. Carbon nanotubes (CNTs). General properties and functionalization

Among the various carbon supports available,[68] CNTs possess attractive properties such as high thermal and chemical stability, conductivity, and resistance to acid and basic media, which have enabled their application in fields such as nanoelectronics, nanomaterials science, drug delivery and catalysis.[69,70,71,72]

CNTs were first described by Iijima in 1991,[73] and are essentially sheets of graphene rolled up in the form of cylinders or tubes. According to the

number of sheets forming the cylinder, nanotubes can be either single-walled (SWCNTs) or multi-walled (MWCNTs). The length of the CNTs is in the micrometers range, and the diameters are up to 100 nm.[74] Their main properties can be summarized as following:

a. electronic properties such as capacity to transfer electrons between adsorbents molecules and molecules in solution.[75]

b. mechanical properties such as high flexibility, strength and low density.[76]

c. structural properties such as varying diameter and helicity.[77]

These properties, in combination with their lack of solubility in any solvents make them ideal candidates for the immobilization of organometallic catalysts. Indeed, the surface of CNTs can be functionalized with a variety of reagents either covalently[78] or non-covalently[79] (Scheme 6.9)

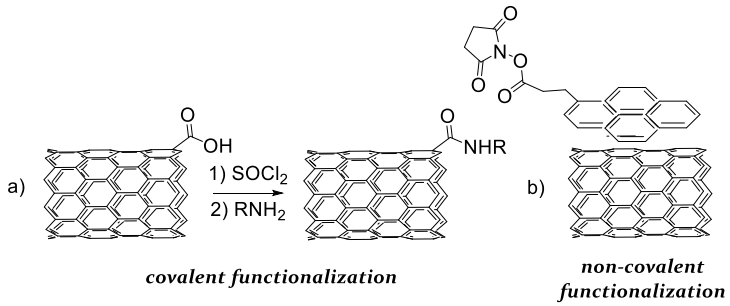

Scheme 6.9. Covalent and non covalent functionalization of CNTs.

From the point of view of the support, covalent functionalization strategies modify the carbon hybridization from sp^2 to sp^3 and therefore lead to a partial or total loss of the intrinsic properties of the pristine carbon nanotubes, which is in contrast to non-covalent functionalization. Pristine CNTs can interact with π systems via π-π stacking interactions. These type of non-covalent interactions are based on Van der Waals forces and take place between the π electron densities of planar, stacked aromatic systems and delocalized electron densities in the carbon network of CNTs.[80]

6.1.3.2. Immobilization of organometallic catalysts onto carbon surfaces through π-π stacking interactions

Factors influencing the strength of the π-π stacking interactions

The magnitude of these interactions depend on various factors but most notably on the size of the aromatic system. This was demonstrated by studying the π-π stacking interactions between organic molecules such as benzene, 2,3-dichloro-dichloro-5,6-dicyano-1,4-benzoquinone (DDQ), azulene, and pyrene with CNTs. The results obtained indicated that the stacking interactions between the pyrene moiety and CNTs (9.69 kcal/mol) is *ca.* twice stronger than in the case of benzene (4.61 kcal/mol).[81] Therefore, in order to obtain a stable heterogenized catalyst via such interactions, the presence of either a pyrene or coronene moiety within the structure of the ligand is required.

In addition to the arene size, the solvent and the temperature have also been identified to influence the strength of π-π stacking the interactions.[63,64] A significant example showing the influence of these parameters was reported by Hermans et al.[63] The gold complex **62** bearing a pyrene-tagged phosphine ligand was prepared and immobilized onto MWCNT's through π-π stacking to afford the supported complex **63** (Scheme 6.10). The immobilization of **62** onto MWCNTs was tested in various solvents, and depending on the solvent used, different loadings of **62** were obtained in the hybrid material **63**. For instance, among the solvents tested, acetone provided the highest loadings, followed by dichloromethane and acetonitrile. The gold content was measured by ICP and it ranged between 0,12 and 0,22 mmol of **62** per g of MWCNTs.

The choice of the solvent was also found to be critical when the hybrid material **63** was applied as a catalyst in the intramolecular cyclization of enynes. When the reaction was run at room temperature, in dichloromethane, a homogeneous reaction pathway was demonstrated by performing a hot filtration test (left hand side of Scheme 6.10). After the reaction, the temperature was brought down to -40°C, which allowed for the redeposition of the leached gold species onto the MWCNTs.

Pyrene-tagged chiral [Rh(bis(NHC))] complexes. Synthesis, characterization and immobilization onto MWCNTs. Preliminary studies in asymmetric catalysis

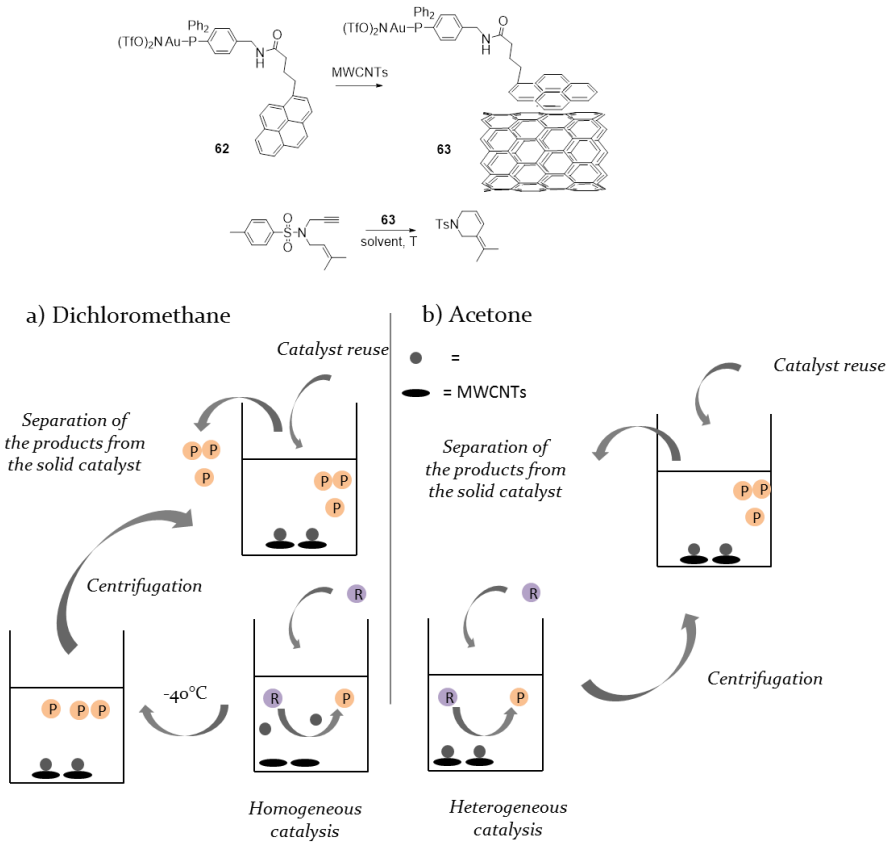

Scheme 6.10. Illustration of the effect of the solvent and the temperature on the strength of π-π stacking interactions in catalyst **63**. Heterogeneous catalysis vs "boomerang effect".

The authors referred to this mode of operation where the catalysis is carried out by homogeneous species as "boomerang effect". Alternatively,[63] switching the reaction solvent to acetone resulted in a heterogeneous reaction mechanism. This system could be efficiently recycled up to four reaction runs, although activity gradually dropped afterwards.

In Scheme 6.11 some remarkable examples of organometallic catalysts immobilized onto CNT's or related carbon surfaces through π-π stacking interactions are displayed. Asymmetric catalysis has been reported as in the case of materials **64**[82] and **65**,[66] which could be recycled up to 9 or 7

runs respectively maintaining the same same enantioselectivity during all the catalytic runs.

The last two examples correspond to NHC-based complexes **66**[64] and **67** bearing a pyrene tag and immobilized onto SWCNT's and reduced graphene oxide respectively (rGO). Especially, material **67** proved very robust and no significant decrease in catalyst activity was detected after 10 reaction runs in the hydrogenation of styrene.

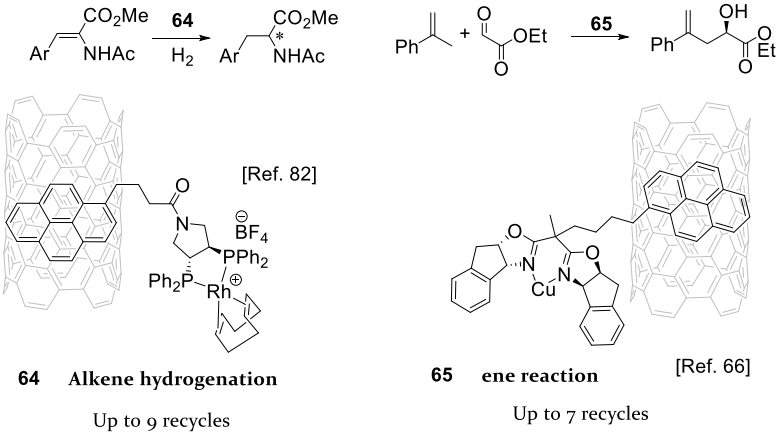

64 **Alkene hydrogenation**

Up to 9 recycles

65 **ene reaction**

Up to 7 recycles

NHC-based catalysts heterogenized onto carbon surfaces through π-π interactions

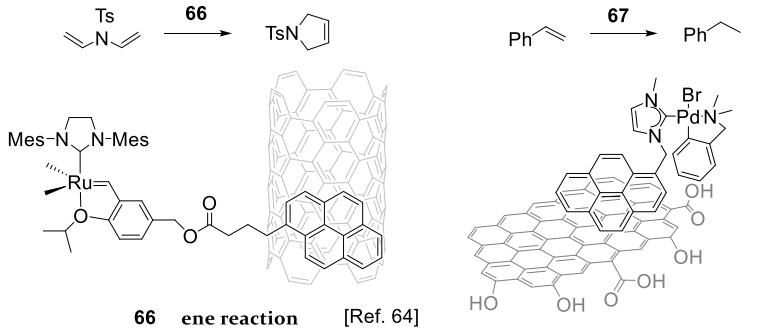

66 **ene reaction** [Ref. 64]

Up to 8 recycles

67 **alkene hydrogenation**

Up to 10 recycles [Ref. 67]

Scheme 6.11. Representative examples of transition metal complexes immobilized onto carbon surfaces through π-π stacking interactions.

Only few examples have been reported yet on the immobilization of molecular organometallic catalysts onto the surface of carbon materials through π-π stacking, but the number of reports is increasing due to the

promising results obtained so far. In the next section, the work carried out in this PhD Thesis regarding the synthesis and characterization of pyrene-tagged [Rh(bis(NHC))] complexes and their immobilization onto MWCNT's through π-π stacking interactions will be presented.

6.2. Results and discussion

This part of the work was done in collaboration with the group of Prof. Dr. X. Sala, from Universitat Autònoma de Barcelona. In view of the handful of successful applications of BINAM-based bisbenzimidazoldiylidenes as ligands in asymmetric catalysis we got interested in exploring the potential of the related BINAM-based bistriazoldiylidenes as strongly electron-donating ligands for their application in metal-catalyzed asymmetric processes. In our group we aimed at evaluating the catalytic potential of metal complexes bound to this novel ligand architecture, and also to study the introduction of pyrene tags in order to be able to immobilize the resulting complexes onto carbon surfaces *via* π-π stacking interactions (Figure 6.7).

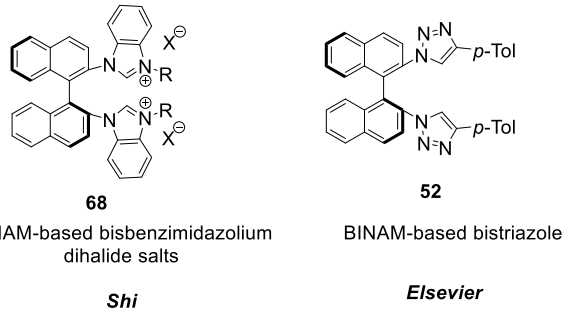

Figure 6.7. Two classes of atropisomeric carbene precursors derived from BINAM, containing respectively a bisbenzimidazolium or a bistriazolium scaffold.

The synthesis of bistriazole **52** was carried out *via* copper-catalyzed alkyne-azide [3+2] cycloaddition, a transformation which is included in the list of "click" reactions (Scheme 6.12). The first step consisted on the preparation of BINAM-diazide. For the synthesis of this key intermediate we have used the conditions optimized by Sala et al.,[83] although they

differ from the conditions recently reported by Elsevier for a very similar compound.[54]

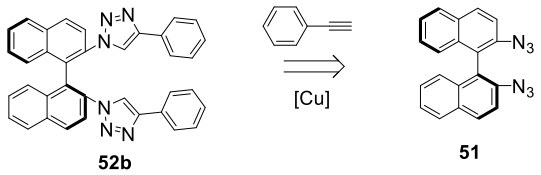

52b 51

Scheme 6.12. Retrosynthetic analysis of compound **52b**, synthesized from key diazide precursor **51**.

For comparison, the synthesis of **51** was also performed under the conditions reported by Elsevier (Scheme 6.13).

Formation of the diazide proceeds through the intermediate formation of a bis(diazonium) salt species which is usually very reactive and in the presence of an azide source a substitution reaction takes place releasing N_2 gas and yielding the diazide product. In the case of Elsevier synthesis a low temperature is used -15°C. It was reasoned that the substitution of the diazonium intermediate **69** proceeds *via* an S_N1 mechanism, and therefore a carbocation is generated which may decrease the steric interaction between the 2 and 2' positions thus possibly causing racemization of the binaphtyl backbone.

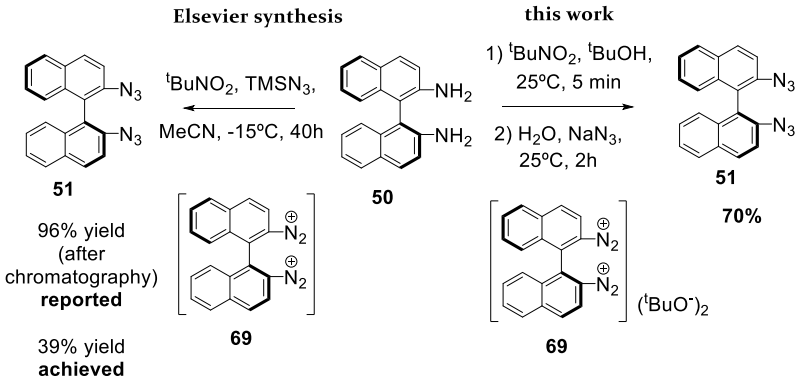

Scheme 6.13. Comparison of the distinct reaction conditions used by Elsevier, and in this work.

In our synthesis, bisdiazonium salt species **69** is formed first by addition of tert-butyl nitrite to a suspension of BINAM in ^{t}BuOH, and after five

minutes water is added followed by sodium azide. Immediate evolution of nitrogen gas from the mixture after addition of sodium azide is indicative of the reaction progress. To rule out the formation of a racemic mixture under our reaction conditions we carried out the synthesis of BINAM-diazide starting from both enantiomers of BINAM. Analysis by HPLC showed only one signal for the case of pure compounds, whereas two well resolved signals one next to the other were observed when a mixture of the two pure compounds was prepared on purpose for analysis Figure S6.1, Exp. Part). Under our reaction conditions, BINAM-diazide **51** was obtained as an air- and moisture-stable orange solid and this compound can be stored without any special protection for several weeks. Diazide **51** was used in the next step without the need of chromatographic purification.

6.2.1. Synthesis of pyrene-tagged BINAM-bistriazolium ditriflate salts

During the course of our work we came up with two different strategies for the introduction of a unit in the framework of the BINAM-based bistriazolic scaffold (Scheme 6.14). In pathway A, diazide **51** was used to obtain bistriazole **52b** by reaction with an alkyne partner, and later, one, or two pyrene moieties were introduced into this framework through an alkylation reaction with a suitable pyrene-containing electrophile. In pathway B, diazide **51** was reacted with a pyrene-derived alkyne partner obtaining bistriazoles functionalized with two pyrene groups. Results will be discussed separately according to the two different strategies followed.

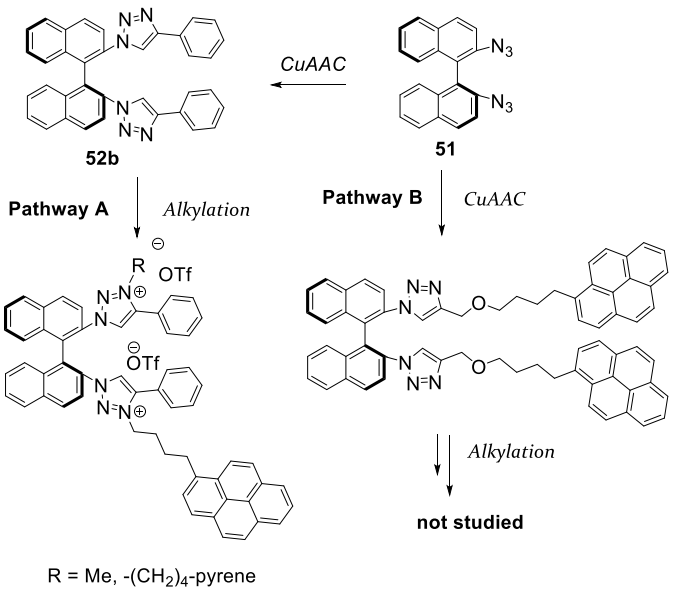

Scheme 6.14. Synthetic strategies studied for the introduction of a pyrene moiety in the BINAM-bistriazole framework.

6.2.1.1. Introduction of pyrene moieties via an alkylation reaction (Pathway A).

The first step in this strategy consisted on the synthesis of BINAM-based bistriazole **52b** (Scheme 6.15). Reaction conditions involved the use of a polar THF/water mixture and the presence of a Cu(II) salt.

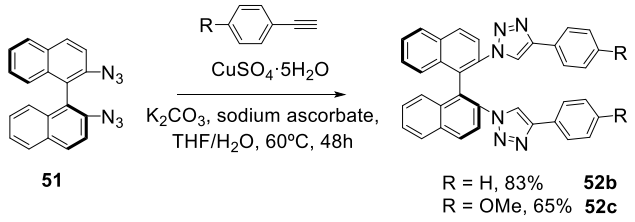

Scheme 6.15. Cu-catalyzed cycloaddition to transform diazide **51** into bistriazolic compounds **52b** and **52c**.

Heating this mixture at 60°C for two days afforded compound **52b** in 83% yield. By using 4-methoxy phenylacetylene as the alkyne partner under otherwise the same reaction conditions compound **52c** bearing two electron rich methoxy groups on the triazole rings was obtained in 65% yield. Both compounds were characterized by ^{1}H and ^{13}C NMR and by MS.

Pyrene-tagged chiral [Rh(bis(NHC))] complexes. Synthesis, characterization and immobilization onto MWCNTs. Preliminary studies in asymmetric catalysis

6.2.1.1.1. Early tests

Differently to the case of imidazolium based salts which can usually be obtained in perfect yields by alkylation of 1,3-imidazole compounds, the presence of an extra N atom in the structure of triazoles significantly reduces the electron density available, and consequently, stronger alkylating agents are usually required.[84,85] In an initial alkylation test, **52c** bearing more electron-rich methoxy groups was reacted with 1-(bromomethyl)-pyrene. This compound is commercially available and the bromo leaving group is situated at a benzylic position which is expected to be more activated towards nucleophilic attack. (Scheme 6.16).

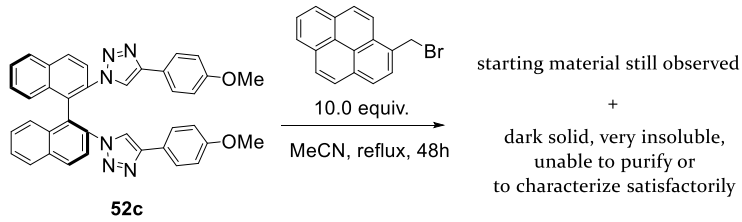

Scheme 6.16. Attempt to alkylate compound **62c** by using 1-bromomethylpyrene as the electrophile.

Performing the reaction in refluxing acetonitrile for 3 days led to incomplete conversion of the starting material as observed by TLC and NMR analysis of the crude mixture. A dark solid was formed which had very low solubility in most common solvents and no characterization of this compound can be provided. On the basis of these results it was hypothesized that a longer linker (more than 1C between N3 and the pyrene moiety) may result in a less rigid structure and should render more soluble diquaternary salts. Also, a complementary strategy was devised consisting on monoalkylating one of the two triazole rings in compounds **52** with a small alkyl group under controlled reaction conditions, and next, in a second step, to introduce the pyrene moiety by means of a second alkylation of the monoquaternary salt. This strategy brings the possibility of introducing only one pyrene moiety.

In order to introduce a longer linker between the triazole rings and the pyrene tags compounds **66a** and **66b** featuring a iodo and a tosyl leaving groups were synthesized and tested in the alkylation of **62c** (Table 6.2).

Table 6.2. Results obtained in the attempted alkylation of **52c** with iodo and tosyl derivatives **70a** and **70b**.

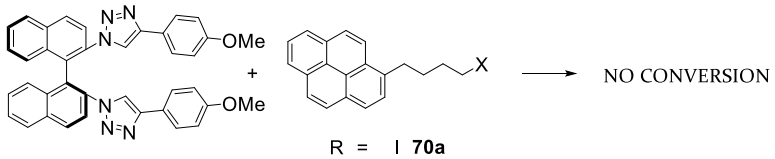

52c

R = I **70a**
R = OTs **70b**

Entry	X	(Equiv.)	Solvent	Additive	T(°C)	Time	Conversion(%)
1	OTs	8,0	MeCN	-	80	48	0
2	OTs	8,0	THF	-	80	48	0
3	I	2,0	MeCN	$AgPF_6$	80	30	0
4	I	8,0	MeCN	$AgBF_4$	80	48	0
5	I	8,0	MeCN	AgOTs	80	48	0
6	I	8,0	THF	-	60	48	0
7	I	8,0	DCE	-	60	48	0
8	I	8,0	DMF	-	60	48	partial

Conversion was evaluated by preparative TLC, and by ^{1}NMR analysis. DCE = 1,2-dichloroethane.

Alkylation with tosylate **70b** (entries 1,2) did not yield any alkylation product. Turning to the use of iodide **70a** no conversion of the starting material was observed for a range of conditions involving various reaction solvents in combination with silver salts, which as known to help in abstracting the halide anion in substitution reactions (entries 3-7). Only when DMF was used as the solvent some conversion of **52c** was observed by TLC and ^{1}NMR, but this product could not be appropriately purified and characterized. These results indicated that alkylation of bistriazoles **52** required the use of other reagents and/or reaction conditions.

6.2.1.1.2. *Synthetic strategy for the introduction of one or two pyrene moieties via alkylation*

Two particular tasks were addressed:

a) To synthesize a pyrene-containing molecule having a long alkyl linker chain (compared to 1-(bromomethyl) pyrene) and a greater

electrophilic character compared to iodo, bromo, or tosyl derivatives.

b) To explore the monoalkylation of bistriazoles **52** prior to the introduction of a pyrene function.

Monoalkylation of bistriazoles **52** was achieved through careful addition of methyl triflate (2 times 0,5 equiv.) to a precooled solution of the corresponding bistriazole at -15°C. After allowing the mixture to slowly reach room temperature reaction was continued for a total of 16h, and then another 0,5 equiv. of methyl triflate were added (scheme 6.17).

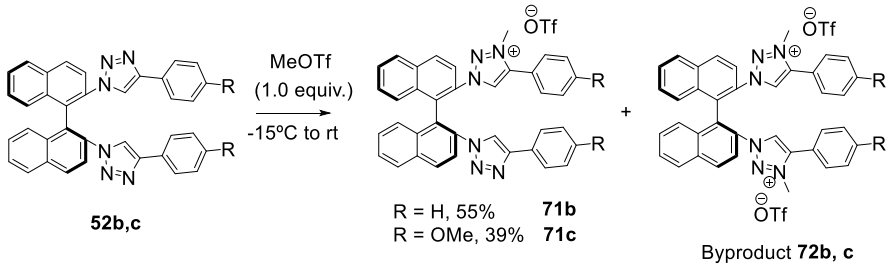

Scheme 6.17. Monalkylation of bistriazoles **52** with 1,0 equivalent of methyl triflate.

Formation of monoquaternary salts **71** was revealed by TLC and by ^{1}NMR of the crude reaction mixture, by the appearance of a new signal at *ca* 4,0 ppm corresponding to the methyl group attached to the N3 upon alkylation. Compounds **71** were obtained as off-white solids after purification by column chromatography. Slightly better yields were obtained for phenyl-substituted **71b** (55%), compared with 4-methoxyphenyl-substituted **71c** (39%). In both cases, in spite of the slow addition of MeOTf at low temperature, some dialkylated products **68** were formed, and they could also be recovered after chromatographic purification. Characterization is only provided for the case of dimethylated compound **72b**.[83]

Whereas alkylation of 1,2,3-triazole rings has been performed in quantitative yields by using methyl triflate,[56] the introduction of other groups at the N3 position through alkylation with their corresponding triflate derivatives has also been accomplished, albeit in lower yields.[85]

Therefore, a procedure was designed for the preparation of 4-(pyren-1-yl)butyl triflate **70c**, starting from commercially available 4-pyrenebutanol **70d**. By simply adding trifluoromethanesulfonic anhydride to a solution of 4-pyrenebutanol and NEt_3 at 0°C the desired alkyl triflate was obtained in up to 80% yield (scheme 6.18) Identity of this compound was confirmed by ^{1}NMR, where the signal corresponding to the methylene group next to the triflate shifted downfield from 4,01 ppm to 4,59 ppm upon formation of compound **66c**. In the next sections freshly prepared 4-(pyren-1-yl)butyl triflate was used, although this compound can be stored in the fridge for several days without degradation.

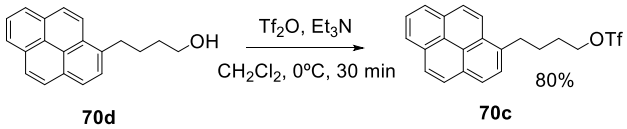

Scheme 6.18. Synthesis of triflate derivative **70c**.

Subsequently, 4-(pyren-1-yl)butyl triflate **70c** was used in the alkylation of compounds **52b** and **71b** (Scheme 6.19). Reaction of **71b** with an excess of the triflate reagent[85] resulted in complete conversion of the starting material after 24 hours as judged by TLC and ^{1}H NMR analysis (Scheme 6.19, route a). Some product loss always occurred upon purification by column chromatography on silica gel, which brought down the isolated yield of 69 to 67%. Attempts to purify **73** by means of precipitation using various solvent mixtures never yielded the pure compound. In the NMR spectra of this compound each signals corresponds to a single nucleus because of the symmetry loss due to the introduction of distinct alkyl groups on the two triazoles (Figure 6.8, a). Characterization by standard techniques was possible due to the good solubility of this diquaternary salt in typical deuterated solvents ($CDCl_3$ for instance). By using the same procedure, reacting **52b** with and excess of 4-(pyren-1-yl)butyl triflate **70c**, compound **74** bearing two pyrene tags was obtained in up to 54% yield (Scheme 6.19, route b). Purification was also achieved by means of column chromatography on silica gel. Full characterization of this new compound by standard techniques was possible due to its good solubility in common organic solvents.

Pyrene-tagged chiral [Rh(bis(NHC))] complexes. Synthesis, characterization and immobilization onto MWCNTs. Preliminary studies in asymmetric catalysis

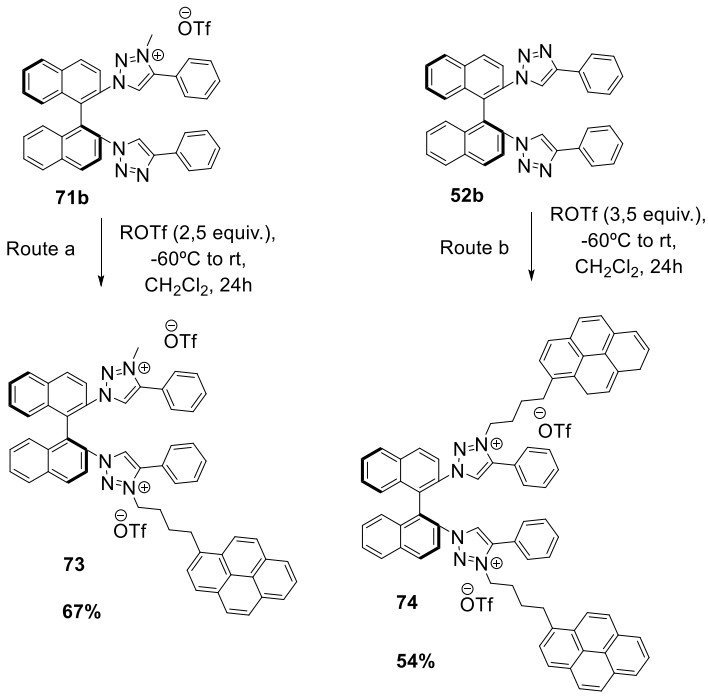

Scheme 6.19. Alkylation of compounds **52b** and **71b** to obtain compounds **73** and **74** containing one, or two pyrene tags.

Compared with **73**, NMR spectra of **74** are much simpler, and each signal corresponds to two equivalent nuclei due to the symmetry of the molecule (Figure 6.8, b).

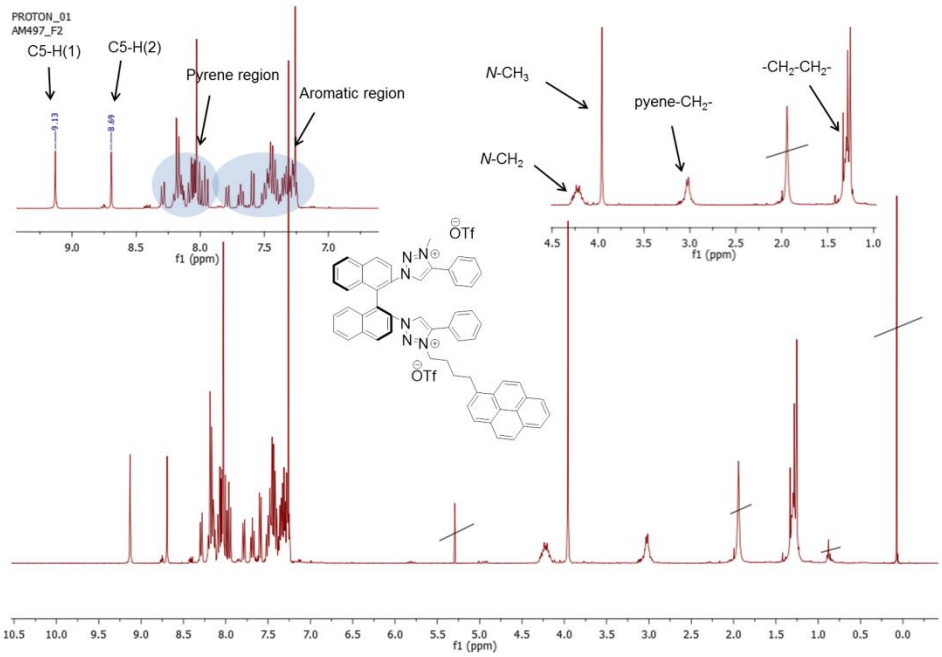

Figure 6.8. ^{1}H NMR spectrum of compound **73**.

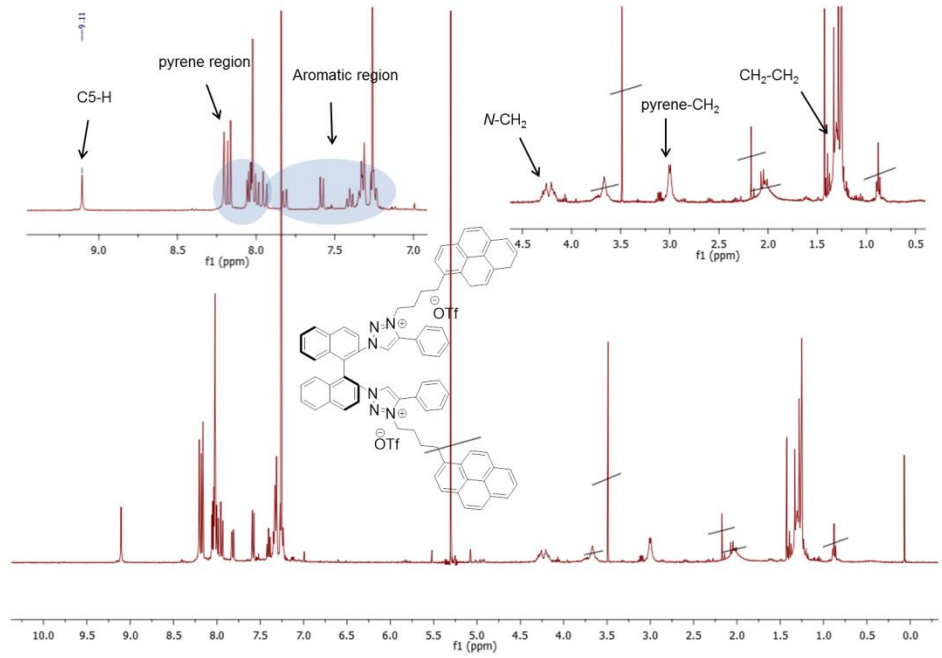

Figure 6.9. ^{1}H NMR spectrum of compound **74**.

Pyrene-tagged chiral [Rh(bis(NHC))] complexes. Synthesis, characterization and immobilization onto MWCNTs. Preliminary studies in asymmetric catalysis

6.2.1.2. Introduction of pyrene moieties via click CuAAC (Pathway B).

An alternative strategy for the introduction of pyrene moieties into the BINAM-bistriazole framework through "click" chemistry was envisioned. By switching the alkyne partner in the CuAAC[86] from phenylacetylene to propargyl pyrenebutyl ether **75**, compound **76** could be obtained (Scheme 6.20). When the same reaction conditions using $Cu(SO_4)\cdot 5H_2O$ were applied as in the synthesis of bistriazoles **52**, no conversion was observed. Instead, an in situ formed catalyst by stirring a solution of CuI and $P(OPh)_3$ was more effective for this transformation and compound **76** bearing two pyrene tags was obtained in 34% yield after chromatographic purification. Further optimization of the reaction conditions may possibly lead to higher isolated yields.

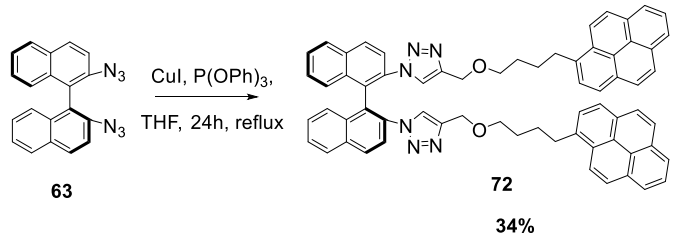

63 **72** **34%**

Scheme 6.20. Synthesis of compound **76** bearing two pyrene tags *via* CuCAAC.

Due to time constraints full exploration of this alternative route cannot be reported; nonetheless conversion of two-pyrene-tagged **72** into a bistriazolium salt precursor should be possible through alkylation with a suitable electrophile (MeOTf for instance).

6.2.2. Synthesis and characterization of [Rh(bis(NHC)(COD)](OTf) complexes

For the preparation of cationic Rh(I) complexes bearing chelating biscarbene ligands derived from ditriflate salts **72b**, **73** and **74**, the protocol reported by Elsevier for the preparation of closely related Rh(I) complex **59** was followed (Figure 6.9).[54]

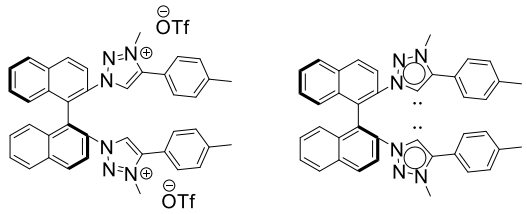

53 54

Figure 6.9. Preligand ditriflate salt **53**, and bis(NHC) ligand **54** reported by Elsevier et al.[54]

The most common strategies for the metalation of 1,3,4-substituted-1,2,3-triazolium salts consist on transmetallation from a silver complex, direct C-H activation, base-mediated proton abstraction/C-H activation, or in-situ generation of the free carbene.[56] Usually, silver-carbene complexes are effective carbene transfer agents. This ability to effectively transmetalate the carbene ligand to another transition metal center is due to the lability of the silver-carbene bond in solution. Evidence of this lability is the fact that most silver-carbene ^{13}C NMR signals appear as broad singlets, or are even not seen due to the fluxional behavior of the [Ag(NHC)] species. However, some cases have been reported where well-resolved Ag-C couplings were observed implying non-lability, and resulting in increased thermal stability.[12] Elsevier reported the synthesis of a dimeric silver complex $[Ag(\mathbf{54})]_2$ obtained by treatment of ditriflate salt **53** with Ag_2O . A characteristic carbene shift was observed by ^{13}C NMR (δ = 167,2 Hz) integrated by two doublets due to the strong coupling of the $C_{carbene}$ with the two silver isotopes ($^1J^{107}AgC$ = 171.2 Hz, $^1J^{109}AgC$ = 197.5 Hz). This observation suggesting a strong Ag-C bond was confirmed by unsuccessful attempts to transmetallate this bidentate ligand to a Pd precursor.

Alternatively, treating the ditriflate salt **53** with a dimeric metal precursor in the presence of tBuOK yielded the corresponding chelating Pd, Rh and Ir complexes (Scheme 6.21).

For the case of N3-alkylated triazolium salts, formation of the free carbene is not expected to occur by using tBuOK (pKa = 22) and stronger bases such as $KN(SiMe_3)_2$ (pKa = 26) are required.[77,87]

Pyrene-tagged chiral [Rh(bis(NHC))] complexes. Synthesis, characterization and immobilization onto MWCNTs. Preliminary studies in asymmetric catalysis

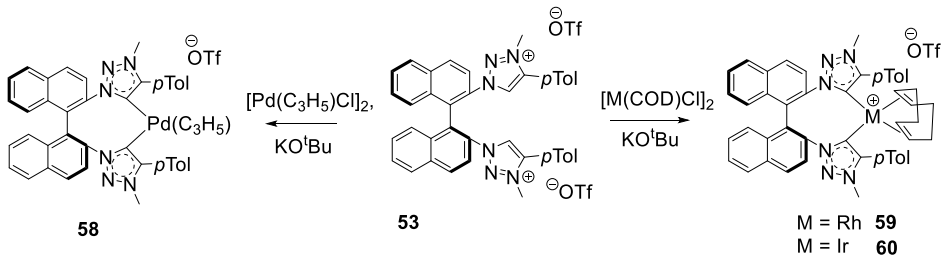

Scheme 6.21. Synthesis of chelating Pd, Rh, and Ir complexes **58**, **59** and **60** obtained by treatment of ditriflate salt precursor **51·2HOTf** with KO^{t}Bu in the presence of a suitable metal precursor.

Possibly, metalation proceeds not through the free carbene but through activation of the acidic C5-H bond by an in situ formed M-tBuO species. Analogously to the examples provided by Bertrand et al.,[82] under these conditions chelate bistriazolylidene complexes were obtained exclusively, without the formation of any dinuclear species.[39,88]By following the same procedure the expected Rh(I) chelate complexes bearing biscarbene ligands were obtained from **72b**, **73** and **74** as yellow-brown solids in good yields after purification by precipitation in THF/Et_2O (Scheme 6.22). Formation of any dinuclear species was not observed. These complexes exhibited very similar NMR features as the Rh complex reported by Elsevier et al.[54]

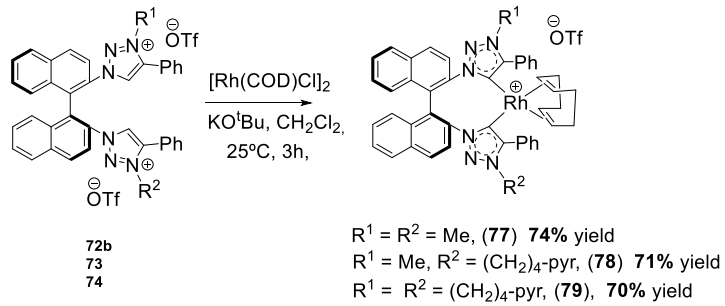

Scheme 6.22. Synthesis of Rh(I) complexes **77**, **78**, and **79**, by using the same protocol as reported by Elsevier for analogous Rh complexes.

The first evidence for the formation of the carbene species came from the disappearance of the low field singlet signal(s) corresponding to the C5-H protons, and from the presence of the signals corresponding to the Rh-

bound COD moiety as seen by ^{1}H NMR analysis (Figure 6.10 and Figure 6.11).

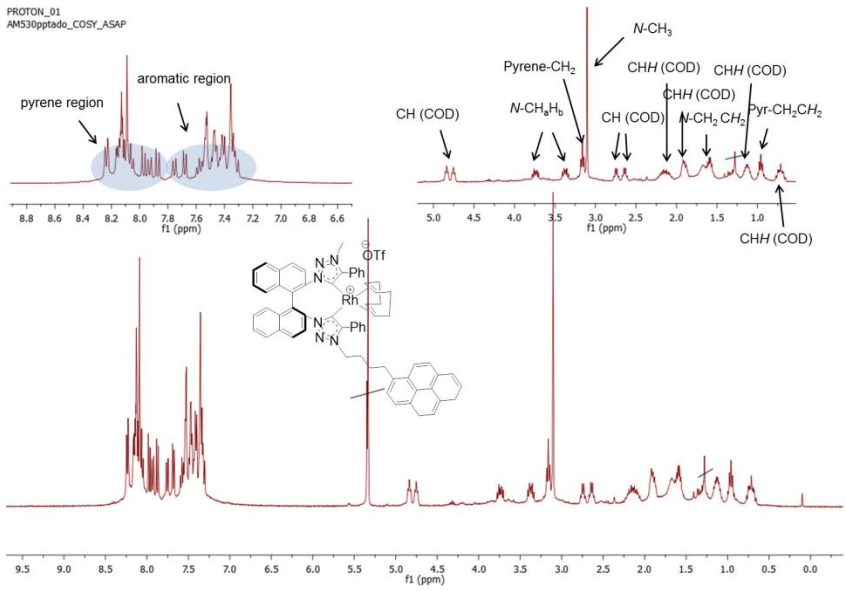

Figure 6.10. ^{1}H NMR spectrum of complex **78**.

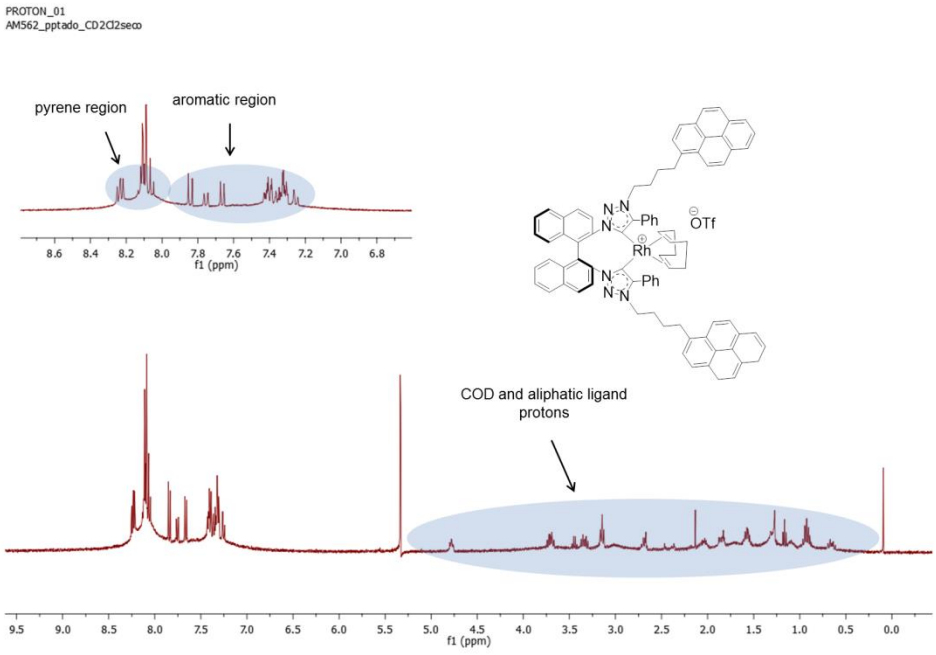

Figure 6.11. ^{1}H NMR spectrum of complex **79**.

Pyrene-tagged chiral [Rh(bis(NHC))] complexes. Synthesis, characterization and immobilization onto MWCNTs. Preliminary studies in asymmetric catalysis

Meaningfully, in the case of complex **78**, signals corresponding to sp^2 protons in the COD moiety appeared as two pairs of multiplets, each multiplet corresponding to a single proton, which is in agreement with the non-symmetric chemical environment of this complex. For complexes **78** and **79**, the diastereotopic methylene protons sitting on the carbon next to the triazole (NCH_AH_B) become more different in chemical shift ($\Delta\delta$ = 0,04 ppm in the salt precursors vs $\Delta\delta$ = 0,4 ppm in the corresponding Rh(I) chelate complexes) as a result of the more rigid environment upon coordination of the ligand to the Rh center. ^{13}C NMR analysis shows the downfield shift of the C5 on the triazole towards the 170-174 ppm range ($^1J_{Rh\text{-}C}$ = 50,6-56,9 Hz) upon formation of the Rh-carbene complexes which is in accordance with the shifts and coupling constants found in similar [Rh(NHC)] complexes.[26] The three new Rh(I) complexes were also characterized by HR-MS.

6.2.3. Non covalent immobilization of complexes 78 and 79 onto MWCNT's. Characterization of hybrid materials 80 and 81.

Immobilization of pyrene-tagged complexes **78** and **79** onto MWCNT's *via* π-π stacking interactions was achieved following the procedure depicted in Scheme 6.23 .

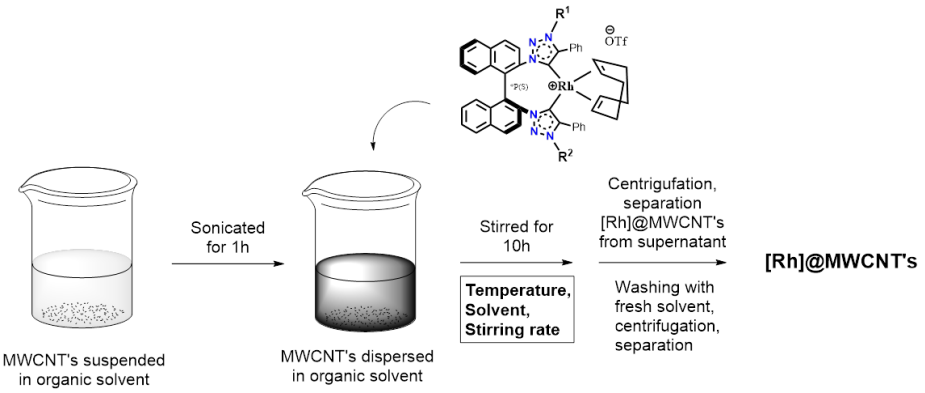

Scheme 6.23. Experimental procedure for the non-covalent immobilization of [Rh(bis(NHC))] complexes **78** and **79** onto MWCNT's.

The hybrid materials were obtained in a very straightforward manner by simply stirring a solution of the corresponding pyrene-functionalized Rh complex in the presence of a suspension of MWCNT's.[63,67] After 10 hours, the hybrid, functionalized MWCNTs are separated by centrifugation. Immobilization of **78** and **79** was carried out according to this simple procedure. The influence of both the solvent[64] and the presence of one, or two pyrene tags on the amount of catalyst effectively immobilized onto the surface of MWCNT's was evaluated (Table 6.3).[89] Using CH_2Cl_2 and stirring the heterogeneous mixture at room temperature for 10 hours resulted in a hybrid material containing 3,74% weight of **78** as measured by ICP-OES (entry 1).

Table 6.3. Amount of [Rh(bis(NHC))] complex immobilized onto MWCNT's for **78**, and **79** in two different solvents.

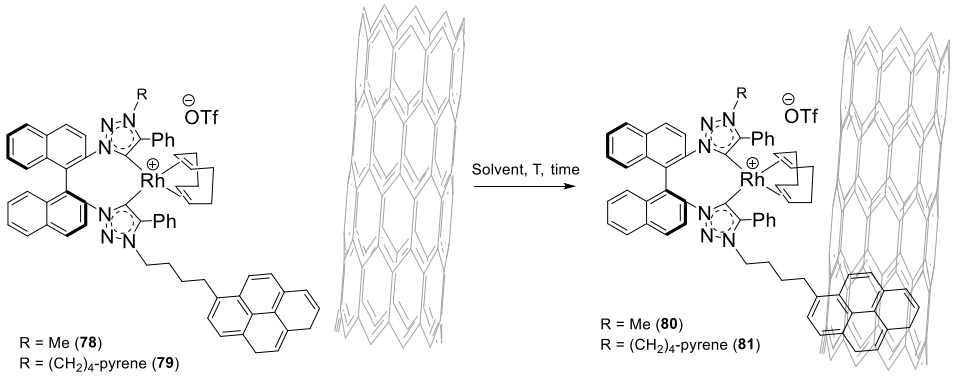

Entry	Complex	Solvent	[Rh](% w/w)[a]	% immobilization[b]
1	78	CH_2Cl_2	3,74	41
2	79	CH_2Cl_2	5,88	65
3	78	AcOEt	6,6	73
4	79	AcOEt	0,061	0,07

Conditions: 9 mg [Rh]/90 mg MWCNT's in the four experiments. [a] ICP-OES analysis of the Rh content in the hybrid materials and correlating to the molecular weight of each complex [Rh]. [b] Referred to the total 9 mg of [Rh] used

When complex **79** bearing two pyrene was stirred in the presence of MWCNT's under the same conditions a 5,88 weight % of the latter complex was encountered in the corresponding hybrid material indicating a direct correlation between the number of pyrene "anchors" and the catalyst loading under these conditions. However, in both experiments

complete immobilization of the total organometallic complex added did not take place.

Performing the immobilization on ethyl acetate provided different results. For the case of the single-pyrene-tagged **78**, the final hybrid material **80** contained a 6,6% weight of this complex (entry 3), representing an incorporation degree of 0,73 which compares favorably to the use of CH_2Cl_2 as the solvent (entry 1). However, performing the immobilization of double-pyrene-tagged **79** onto the MWCNT's very low catalyst loadings were obtained after ICP-OES analysis of the hybrid material **81** (entry 4).

An easy explanation for this result could be the poor solubility of complex **79** in AcOEt at room temperature. Other solvents such as acetone[100] or THF are worth being explored in order to facilitate stronger interactions between the pyrene moieties and the walls of the MWCNT's.

Characterization of the hybrid [Rh]@MWCNT's materials 80 and 81

The obtained hybrid materials were analyzed using various techniques. ICP-OES was used to quantitatively analyze the Rh content in the functionalized MWCNTs (Table 6.5, see experimental part for details). Analysis by XPS (X-ray photoelectron spectroscopy) showed a signal at 309,5 eV which corresponds to the presence of Rh(I) ions on the surface of the solid. Moreover, the other elements coming from the Rh complexes (N, O, F, S) were also detected, although the ratios between these elements did not always correspond to the theoretical values.

UV-Vis spectrometry has been used for the characterization of related hybrid materials in a quantitative manner by application of the Beer's Law,[98] and also in a qualitative manner to prove the incorporation of a "homogeneous" metal complex into a hybrid solid material.[87] In order to examine the nature of the immobilized Rh species in the hybrid materials, three samples were prepared: a) the corresponding soluble pyrene-decorated Rh complex; b) unfunctionalized MWCNT's; c) the corresponding hybrid material. Direct UV-Vis analysis of the hybrid materials did not provide any characteristic absorbance peaks arising from surface-immobilized Rh complexes could. Therefore, an indirect

analysis was performed in which the corresponding hybrid materials were sonicated in DMF prior to UV-Vis spectrometry. In this manner characteristic absorbance bands were detected exactly at the same wavelength as observed in the related homogeneous Rh complexes (Figures 6.12 and 6.13). These bands very likely arise from solubilized Rh species, and the fact that they are not shifted with respect to the original homogeneous Rh complexes, may be understood as an evidence of the unchanged nature of the pyrene-functionalized Rh complexes upon heterogenization, as expected.

Finally, distribution of the metallic atoms over the surface of the solid was investigated by means of, EDX (Energy-Dispersive photoelectron spectroscopy) and a homogeneous mapping of the metal was found (figure 6.14).

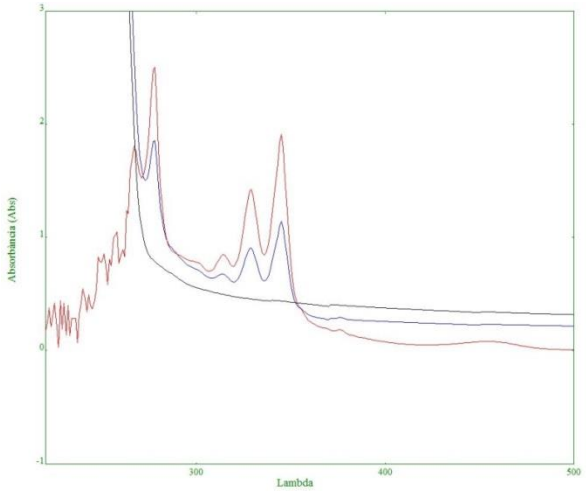

Figure 6.12. UV-Vis analysis of **80**. The plot corresponds to: unfunctionalized MWCNT's (black line) vs **78** (red line) vs **80** (blue line).

Pyrene-tagged chiral [Rh(bis(NHC))] complexes. Synthesis, characterization and immobilization onto MWCNTs. Preliminary studies in asymmetric catalysis

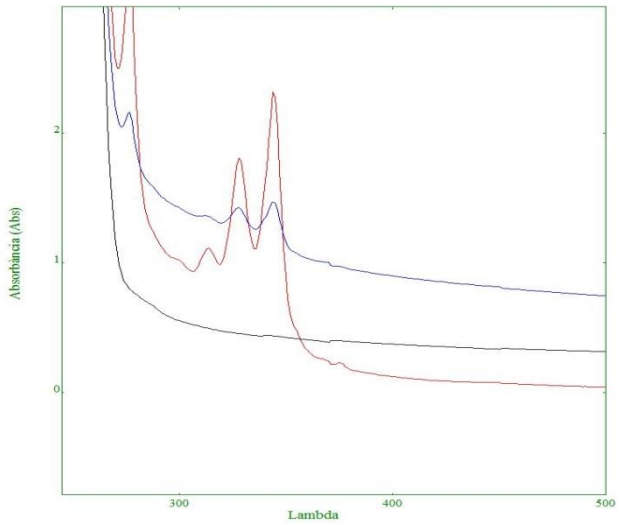

Figure 6.13. UV-Vis spectroscopic analysis of **81**. The plot corresponds to: unfunctionalized MWCNT's (black line) vs **79** (red line) vs **81** (blue line).

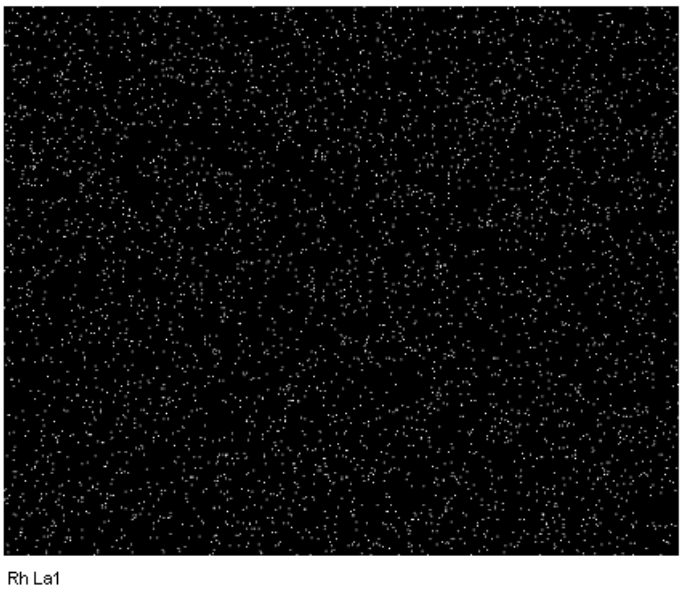

Figure 6.14. EDX analysis of hybrid material **80** showing a homogeneous distribution of Rh ions on the surface of the solid.

6.2.4. Evaluation of Rh(I) complex 77 as precatalyst in asymmetric reduction processes

In order to gain insight on the catalytic potential of the heterogenized complexes presented above, non-immobilizable **77** was used as a model in preliminary catalytic tests. The results obtained by using this precatalyst in various catalytic processes will be presented and discussed.

6.2.4.1. Asymmetric hydrosilylation of ketones

In view of the close similarity of **77** to complex **59**, asymmetric hydrosilylation of ketones appeared to be an appropriate transformation to test the efficiency of **77**. The best results reported by Elsevier et al. were achieved in the hydrosilylation of the bulky isobutyrophenone **82** (see Scheme 6.9). Therefore, isobutyrophenone was chosen in order to test the activity and selectivity of complex **77** and also for comparison with **59**.

Using a 50% excess of diphenylsilane at 25°C, resulted in only 25% conversion, and 7% enantioselectivity (Entry 1, table 6.4). A slight increase in the reaction temperature resulted in moderate conversion, but the enantioselectivity decreased to 2%. Assuming that 39 due to its steric demand should contribute to the selectivity of the reaction, bulkier tertiary silane partners were tested in the hydrosilylation of **82**. However, performing the reaction at 30°C using either triphenylsilane or triisopropylsilane, resulted in no conversion of the starting material (entries 3, 4). These results are not much surprising though; a recent study on the hydrosilylation of ketones using [Rh(I)bis(NHC)] complexes proposed that hydrosilylation using monohydrosilanes proceeds via a different reaction mechanism and the reaction rate is reduced by several orders of magnitude compared to the use of dihydrosilanes.[90,91,92,93]

Mechanistic evidences recently reported by Herrmann and Kuhn could explain the low ee obtained,[94] although the reduced activity of **77** compared to that of Elsevier's catalysts remains unclear.

Pyrene-tagged chiral [Rh(bis(NHC))] complexes. Synthesis, characterization and immobilization onto MWCNTs. Preliminary studies in asymmetric catalysis

Table 6.4. Evaluation of precatalyst **77** in the asymmetric hydrosilylation of **82**.

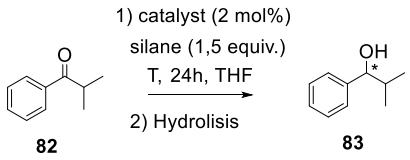

Entry	Silane	T(°C)	Conversion(%)[a]	Yield(%)[a]	ee(%)
1	H_2SiPh_2	25	25	25	7
2	H_2SiPh_2	30	60	60	2
3	$HSiPh_3$	30	0	-	-
4	HSi^iPr_3	30	0	-	-

[a]Conversions, yields and ee's were calculated by GC-FID using mesitylene as internal standard.

6.2.4.2. Asymmetric hydroboration of alkenes

Various chiral bidentate ligands, mostly diphosphines or mixed phosphine/heterodonor bidentate ligands have successfully promoted the asymmetric hydroboration of terminal alkenes, yielding the branched regioisomer selectively and in high ee.[95] Therefore, complex **77** displays both the structural and the chemical requirements for this catalytic process. Results obtained in the hydroboration of styrene (**84**) with pinacolborane using precatalyst **77** are presented in Scheme 6.24.

Reaction proceeded to complete conversion, but to our disappointment an equimolar mixture of *sec*-phenylethanol and 2-phenylethanol was obtained. This result only compares slightly worse to Rh(I)/BINAP system (70:30),[96] and is slightly better to the regioselectivity provided by Wilkinson's catalyst (35:65).[95] Unfortunately, Analysis of the reaction mixture by chiral GC-FID revealed that no enantioinduction was achieved under these conditions, since *sec*-phenylethanol was obtained as a racemic mixture. This results obviously compares unfavorably with those

obtained by Rh(I)/BINAP (40% ee)[96] and more unfavorably with Rh(I)/(R,S)-JosiPhos (84% ee).[96]

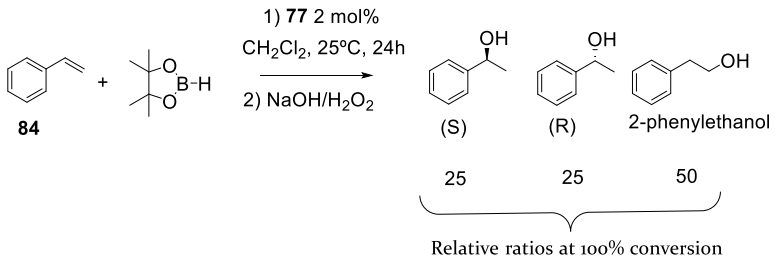

Scheme 6.24. Evaluation of precatalyst **77** in the asymmetric hydroboration of styrene (**84**) using pinacolborane.

In view of this result it was decided to apply complex **77** in a different catalytic process

6.2.4.3. Asymmetric hydrogenation of olefins

Asymmetric hydrogenation of prochiral olefins has arguably been the most widely studied transformation in enantioselective transition metal catalysis.[97] In this reaction, rhodium catalysts modulated by optically pure diphosphines have proven outstandingly efficient.[98] Hydrogenation of functionalized alkenes has also been reported by catalysts based on chiral bis(NHC) with promising results.[99] Thus, precatalyst **77** was tested in the hydrogenation of two benchmark substrates, dimethyl itaconate **80** and the more challenging α-methyl stilbene **85** (Table 6.6).

Running the reaction under very mild reaction conditions, room temperature and 3 bars of H_2 resulted in no conversion for any of the two substrates after 24 hours (entries 1, 2). Increasing the temperature to 40°C and the H_2 pressure to 45 bar proved effective in the case of substrate **80** since complete conversion was obtained under these conditions (entry 3). However, analysis of the product revealed a racemic mixture. This lack of enantioselectivity was accompanied by the observation of a dark grey precipitate on the walls of the reaction vessel, that suggested the degradation of the catalyst and formation of metallic Rh(0). The substrate **81** was not hydrogenated under the same conditions (entry 4).

Table 6.6. Catalytic hydrogenation of substrates **85** and **86** using precatalyst **77**.

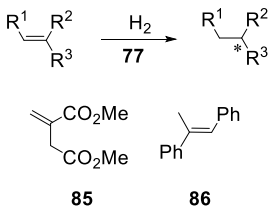

Entry	Substrate	T(°C)	P(bar)	Conv.(%)	Sel.(%)	Ee(%)
1	**85**	25	3	0	-	-
2	**86**	25	3	0	0	-
3	**85**	40	45	100	100	0
4	**86**	40	45	0	-	-

Conditions: 0,5 mnmol substrate, 1 mol % catalyst, 3 mL CH_2Cl_2, 24h. Conversion measused by ^{1}H NMR relative to mesitylene added as external standard. ee % analyzed by chiral GC-MS.

These results suggest that complex **77** may perform better as a catalyst in a process other than hydrogenation, and therefore further evaluation of the reactivity of this type of Rh(I) complexes under alternative reaction conditions is clearly needed.

6.3. Conclusions

Development of two different synthetic strategies was achieved for the functionalization of the chiral 1,1'-binaphtyl-2.2'-bis(4-aryl-1,2,3-triazol) backbone. A first strategy involved the introduction of the pyrene tag through alkylation of the bistriazole compounds **52**. From the various electrophiles tested to grant the pyrene-functionalized triazolium compounds, the best results were achieved by using 4-(pyren-1-yl)butyl triflate **70c**. Moreover, it was found that monomethylation of bistriazole **52b** followed by alkylation with 4-(pyren-1-yl)butyl triflate led to bistriazolium preligand ditriflate salt **73**, containing only one pyrene tag, whereas direct alkylation of **52b** with a small excess of 4-(pyren-1-yl)butyl triflate yielded **74** containing two pyrene tags. Additionally to the alkylation strategy, pyrene tags could also be introduced in the ligand

backbone through Cu-catalyzed [3+2] alkyne-azide cycloaddition. Compound **76** was obtained in this way.

Following a reported synthetic protocol for the preparation of related [Rh(I)(bis(NHC))], the functionalized ditriflate salts were treated with ^{t}BuOK, in the presence of $[Rh(\mu\text{-}Cl)(COD)]_2$ to obtain Rh(I) chelate complexes **77**,, **75**, and **79**. Purification of these complexes was accomplished by precipitation techniques, and not by chromatographic separation. Yields above 70% were obtained for the three Rh complexes.

Pyrene containing Rh complexes **78** and **79** were immobilized onto MWCNT's *via* π-π stacking interactions. Two factors were identified to influence the amount of complex that could be incorporated onto the surface of MWCNT's. First, the number of pyrene tags showed a positive effect, and higher loadings of complex **79** were obtained in the hybrid material compared to single-tagged complex **78**. The second factor influencing the π-π stacking interactions was the nature of the solvent, and ethyl acetate provided higher loadings compared to dichloromethane. The final hybrid materials were characterized by different techniques, namely ICP-OES, EDX, XPS, and UV-Vis spectroscopy. A homogeneous distribution of the complexes over the surface of the solid was observed. The Rh ions in the immobilized complexes still presented a +1 oxidation state. This finding, together with UV-Vis analysis show strong evidence indicative that the complexes remain intact upon immobilization.

Preliminary tests were performed in the application of precatalyst **77** in asymmetric reduction processes. Hydrosilylation of isobutyrophenone proceeded sluggishly, and the product was obtained in very poor enantiomeric excess. Higher activity was displayed by the same complex in the hydroboration of styrene. Moderate regioselectivity towards the branched isomer was achieved. However, a racemix mixture of the two enantiomers was detected. Lastly, **77** was active in the hydrogenation of dimethyl itaconate, but the product was obtained as a racemic mixture, apparently due to catalyst decomposition to metallic rhodium. Further exploration of these novel Rh complexes is currently ongoing.

6.4. Experimental part

General

Reactions were carried out using standard bench-top techniques unless the use of a Schlenk flask is specified, in which case Schlenk-line inert atmosphere techniques were used. Where stirring of the reaction mixture is indicated, magnetic stirring using a Teflon-coated stir bar was employed throughout. Commercially supplied compounds were used without further purification. Dry solvents were prepared by distillation from Na/benzophenone, CaH_2 or P_2O_5, or collected from a Braun SPS800 solvent purification system. Solution-state NMR spectra were obtained at the *Servei de Recursos Científics i Tècnics* (SRCiT), URV, with Varian (Agilent) Mercury VX400 or NMR System400 400 MHz spectrometers and calibrated to residual solvent peaks. Chemical shifts for ^{1}H and $^{13}C\{^{1}H\}$ NMR spectra are reported relative to TMS. ICP analyses were conducted at the *Serveis Tècnics de Recerca de la Universitat de Girona* using an ICP-OES, Agilent 5100 instrument. Samples were digested in concentrated HNO_3 under microwave irradiation before being diluted for analysis. HR-MS (ESI-TOF) analyses were performed at the SRCiT, on an Agilent Time-of-Flight 6210 spectrometer or at High resolution mass spectra (HRMS) were recorded/measured on a Bruker MicrOTOF-Q II™ instrument using ESI or Cryospray ionization sources at *Serveis Tècnics of the Universitat de Girona*. Samples were introduced into the mass spectrometer ion source by direct infusion using a syringe pump and were externally calibrated using sodium formate. The instrument was operated in the positive ion mode. Measurement of the samples by UV-Vis spectroscopy was carried out in a VWR W3100 PC spectrophotometer. Samples were appropriately diluted and placed in a quartz cuvette. Energy-dispersive X-Ray analysis of solid samples were conducted at the SRCiT using a SEM Jeol 6400 microscope. XPS experiments were performed at Unitat d'Anàlisi de Superfícies
CCiTUB in a PHI 5500 MultiTechnique System (From Physical Electronics) with a monochromatic X-ray source (Aluminium Kalfa line of 1486,6 eV energy and 350 W), placed perpendicular to the analyzer axis and calibrated using the 3d5/2 line of Ag with a full width at half

maximum (FWHM) of 0,8 eV. The analyzed area was a circle of 0,8 mm diameter, and the selected resolution for the spectra was 187,5 eV of Pass Energy and 0,8 eV/step for the general spectra and 23,5 eV of Pass Energy and 0,1 eV/step for the spectra of the different elements in the depth profile spectra. A low energy electron gun (less than 10 eV) was used in order to discharge the surface when necessary. All measurements were made in a ultra high vacuum (UHV) chamber pressure between $5 \cdot 10^{-9}$ and $2 \cdot 10^{-8}$ Torr.

Other than solvents, reagents obtained from commercial sources were used without further purification. The multi-walled carbon nanotubes (MWCNTs) were purchased from HeJi, Inc. (Zengcheng city, China) in bulk form with >99% purity, 150 μm average length and 10–20 nm diameter. $[Rh(\mu\text{-}Cl)(COD)]_2$ was prepared following a reported procedure.[100]

Experimental procedures

In all cases the synthetic procedures will refer to the (S)-enantiomers; The described procedures also allowed for the obtaining of the (R)-enantiomers with similar results.

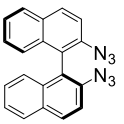

(*S*)-2,2'-diazido-1,1'-binaphthalene, 51. Tert-butyl nitrite (2,7 mL, 22.6 mmol, 12 eq.) was added to a suspension of (S)-(-)-1,1'-binaphythyl-2,2'-diamine **50** (535 mg, 1. 9 mmol, 1 eq.) in tert-butanol (5 mL). After stirring for 5 min at 25°C, water (1 mL) and sodium azide (773 mg, 11.3 mmol, 6 eq.) were added. The solution was stirred for 2 h. The product was extracted with dichloromethane (5 mL), dried over Na_2SO_4, concentrated under vacuum and washed with hexane. The azide was obtained as an orange solid and was used without further purification. Yield = 440 mg, (70 %) **^{1}H NMR** (400 MHz, $CDCl_3$): δ = 8.05 (d, *J* = 8.8 Hz, 1H, Ar-H), 7.92 (d, *J* = 8.0 Hz, 1H, Ar-H), 7.51 (d, *J* = 8.8 Hz, 1H, Ar-H), 7.44 (m, 1H, Ar-H), 7.30 (m, 1H, Ar-H), 7.06 (d, *J* = 8.3 Hz, 1H, Ar-H). Peaks match the literature values.[54]

(S)-2,2'-bis(4-phenyl-1H-1,2,3-triazol-1-yl)-1,1'-binaphthalene (S)-2,2'-diazido-1,1'-binaphthalene, 52b. 51 (168 mg, 0.5 mmol, 1 eq.), $CuSO_4 \cdot 5H_2O$ (50 mg, 0.2 mmol, 0.4 eq.), sodium ascorbate (79 mg, 0.4

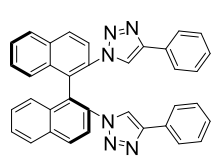

mmol, 0.8 eq.), potassium carbonate (69 mg, 0.5 mmol, 1 eq.) and phenylacetylene (110 µL, 1 mmol, 2.0. eq.) were added to a round bottom flask containing tetrahydrofurane:water (1:1) (7 mL). Then, the mixture was heated at 60°C for 48h. The reaction mixture was poured in dichloromethane (50 mL). The organic fraction was washed with ammonia (20% w/w aqueous solution, 3 x 20 mL), until no blue copper colour was observed), dried over anhydrous Na_2SO_4 and concentrated under vacuum. Hexane (50 mL) was added to the crude in order to furnish the triazole as an off white powder which was filtered off and used without further purification. Yield = 223 mg, 83%; **^{1}H NMR** (400 MHz, $CDCl_3$): δ = 8.11 (d, J = 8.7 Hz, 2H, Ar-H), 7,97 (d, J = 8.2 Hz, 2H, Ar-H), 7.82 (s, 2H, Tz-H), 7.74 (d, J = 8,7 Hz, 2H, Ar-H), 7.59 (m, 6H, Ar-H), 7.33 (m, 10H, Ar-H). **^{13}C{^{1}H} NMR** (100,6 MHz, CDCl3) δ 134.52, 133.30, 132.51, 131.92 (tz-CH), 130.05, 128.78, 128.56, 128.18, 127.86, 127.73, 126.33, 126.07, 125.64, 123.22. HR-MS: m/z = 541,2134, calcd. for C36H25N6 [M+H+]: 541,2141;

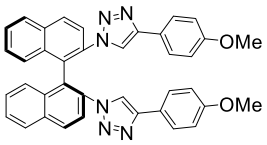

(*S*)-2,2'-bis(4-(methoxy)phenyl-1*H*-1,2,3-triazol-1-yl)-1,1'-binaphthalene, 52c (S)-2,2'-diazido-1,1'-binaphthalene **51** (168 mg, 0.5 mmol, 1 eq.), $CuSO_4{\cdot}5H_2O$ (50 mg, 0.2 mmol, 0.4 eq.), sodium ascorbate (79 mg, 0.4 mmol, 0.8 eq.), potassium carbonate (.69 mg, 0.5 mmol, 1.0 eq.) and 4-ethynylanisole 130 mg, 1.0 mmol, 2.0 eq.) were added to a round bottom flask containing tetrahydrofurane:water (1:1, 7 mL). This mixture was heated at 60°C with stirring for 48h. Then, the mixture was poured in dichloromethane (50 mL). The organic fraction was washed with ammonia (20% w/w aqueous solution, 3 x 20 mL, until no blue copper colour was observed), dried over anhydrous Na_2SO_4 and concentrated under vacuum. Hexane (50 mL) was added to the crude in order to furnish the triazole as an off white powder which was filtered off and used without further purification. Yield: 195 mg (65%). **^{1}H NMR** (400 MHz, $CDCl_3$) δ 8.09 (d, *J* = 8.7 Hz, 2H, Ar-H), 7.95 (d, *J* = 8.2 Hz, 2H, Ar-H), 7.73 (d, *J* = 8.8 Hz 2H, Ar-H), 7.69 (s, 2H, tz-H), 7.54 (m, 2H, Ar-H), 7.49 (d, *J* = 8,4 Hz, 4H, Ph-H), 7,31-7,42 (m, 4H, Ar-H), 6,85 (d, 4H, Ph-H), 3,78 (s, 6H, -OCH_3). **^{13}C{^{1}H} NMR** (100,6 MHz, $CDCl_3$): δ = 159.63, 133.26,

132.54, 131,62, 131,29, 130.78 (tz-H), 130,60, 130,21, 129,08, 128.53, 128,30, 128.14, 127.68, 127,26, 126.93, 126.34, 123.20, 114.21, 55.31 (-OCH_3).

(*S*)-2,2'-bis(4-(methyloxy-4'-pyren-yl-butyl))-1*H*-1,2,3-triazol-1-yl)-1,1'-binaphthalene, 76. 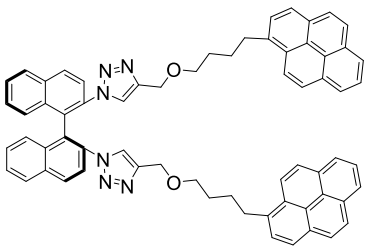 Triphenyl phosphite (7,52 µL; 0,0278 mmol; 0,30 equiv.) was dissolved in dry THF (3 mL); Then CuI (4,81 mg; 0,0253 mmol; 0,275 equiv.) was added, and this solution was stirred for 10 minutes at room temperature. Then propargyl pyrenebutyl ether[101] **75** (132 mg; 0,253 mmol; 2,75 equiv.) was added followed by (S)-2,2'-diazido-1,1'-binaphthalene **51** (31 mg, 0,092 mmol, 1 eq.) and this mixture was heated at 70°C for 24h. After this time, the volatiles were removed under vacuum and the pure product was obtained after purification by chromatography on silica using petroleum ether/ethyl acetate (1,5:1). Yield: 31 mg (34%). **^{1}H NMR** (400 MHz, $CDCl_3$) δ 8.24 (d, *J* = 9,3 Hz, 2H, Ar-H), 7.94-8,16 (m, 12H, Ar-H), 7.84 (d, *J* = 7.8 Hz 2H, Ar-H), 7.65 (d, *J* = 7.8 Hz, 2H, Ar-H), 7.58 (d, *J* = 8,2 Hz 2H, Ar-H), 7.42 (d, *J* = 8,9 Hz, 2H, Ar-H), 7,40 (s, 2H, Tz-H), 7,29 (m, 2H, Ar-H), 7,19 (m, 2H, Ar-H), 7,12 (d, *J* = 8,5 Hz 2H, Ar-H), 4,38 (s, 4H, Tz-*CH_2*O-), 3,28 (t, *J* = 7,7 Hz, 4H, O*CH_2*CH_2), 3,14 (t, *J* = 6,3 Hz, 4H, CH_2*CH_2*pyr), 1,77 (m, 4H, *int-CH_2*), 1,59 (m, 4H, *int-CH_2*). **^{13}C{^{1}H} NMR** (100,6 MHz, $CDCl_3$): δ = 144,47, 136,87, 134,52, 132,98, 131,98, 131,41, 130,89, 130,43, 129,77, 128,62, 128,24, 127,90, 127,51, 127,39, 127,35, 127,22, 126,59, 125,95, 125,81, 125,07, 124,85, 124,79, 124,69, 123,95, 123,49, 123,01, 69,66, 63,75, 33,32, 29,63, 28,43. HR-MS: exact mass = 960,4148, calcd. mass for $C_{66}H_{52}N_6O_2$: 960,4152.

4-(pyren-1-yl)butyl triflate, 70c. 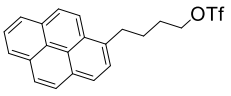 A solution of 1-pyrenebutanol **70d** (200 mg, 0.729 mmol, 1 eq.) and Et_3N (150 µL, 1.094 mmol, 1.5 eq.)in DCM (3 mL) was cooled down to 0°C. To this solution trifluoromethanesulphonic anhydride (0.18 mL, 1.094 mmol, 1.5 eq.)was slowly added. The mixture was stirred at 0 ºC for 30 minutes, and then quenched with $NaHCO_3$ (4 mL aq. saturated solution) and extracted with Et_2O (3x12 mL). The combined organic fractions were washed with brine, dried over $MgSO_4$, filtered and concentrated in vacuo. The residue was filtered through a

plug of silica eluting with CH_2Cl_2 and then dried under vacuum to yield a light brown dense oil which becomed a solid after staying at 4°C for 2 days. Yield = 236 mg, (80 %). **^{1}H NMR** (400 MHz, $CDCl_3$) δ 8,23 (d, *J* = 9.2 Hz, 1H, Ar-H), 8,12-8,20 (m, 4H, Ar-H), 7,98-8,05 (m, 3H, Ar-H), 7.85 (d, *J* = 7.8 Hz, 1H, Ar-H), 4.57 (t, *J* = 5.9 Hz, 2H, TfO-CH_2-), 3.41 (t, *J* = 7.2 Hz, 2H, pyrene-CH_2-), 1,99 (m, 4H, -CH_2 CH_2). Peaks match the literature values.[83]

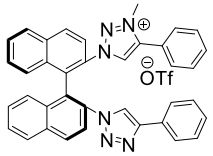

(*S*)-3-methyl-4-phenyl-1-(2'-(4-phenyl-1*H*-1,2,3-triazol-1-yl)-[1,1'-binaphthalen]-2-yl)-1*H*-1,2,3-triazol-3-ium trifluoromethanesulfonate, 71b. A solution of **52b** (272 mg, 0,5 mmol, 1 eq) in dichloromethane (14 mL) was cooled to -15°C. To this solution, methyl triflate (29 µL, 0.26 mmol, 0.5 eq) was added dropwise. This mixture was allowed to slowly warm to room temperature, as it was stirred for 16h. After this time, this procedure was repeated again (addition of another 0,5 equiv. of MeOTf at -15°C then allowed to slowly warm up to room temperature). After another 16h, the solvent was evaporated, and the crude product was purified by column chromatography on SiO_2 using CH_2Cl_2 first as the mobile phase, then (CH_2Cl_2:MeOH) (97:3) and finally (CH_2Cl_2:MeOH) (93:7) the mobile phase to yield the desired compound as a light brown solid. Yield = 194 mg (55%). **^{1}H NMR** (400 MHz, $CDCl_3$) δ 8.276 (d, J = 8,7 Hz, 1H, Ar-H), 8.21 (m, 1H, Ar-H), 8.07-8,13 (m, 3H), 7.82 (d, *J* = 8.8 Hz, 1H, Ar-H), 7.80 (d, *J* = 7,7 Hz, 1H, Ar-H), 7.7 (m, 2H, Ar-H), 7.38-7,57 (m, 11H), 7.27-7,37 (m, 4H), 4.09 (s, 3H, NCH_3). **^{13}C{^{1}H} NMR** (91 MHz, $CDCl_3$) δ 153,43, 134.31, 133.13 (triazole-CH), 131.88, 131.74, 129.79, 129.54, 129.32, 129.25, 129.12, 129.04, 128.89, 128.78, 128.66, 128.46, 126.67, 126.37, 125.74, 123.09, 121.45, 38.77 (triazole-CH_3). ESI-MS m/z, relative intensity: 555.2, 556.2, 557.2.

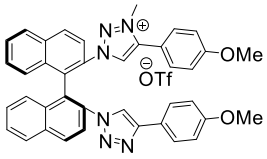

c[1,1'-binaphthalen]-2-yl)-1*H*-1,2,3-tria-zol-3-ium trifluoromethansulfonate, 71c. A solution of **52c** (143 mg, 0,238 mmol, 1 eq) in anhydrous dichloromethane (7 mL) was cooled down to -15°C. To this solution methyl triflate (40 µL, 0.36 mmol, 0.5 eq) was added dropwise to which it was previously cooled

down to 0 ºC in an ice bath during 20 min. Then, once the methyl triflate was added, the solution was warmed up to room temperature with vigorously stirring. After 16h, the procedure was repeated again (addition of another 0,5 equiv. of MeOTf at -15°C then allowed to slowly warm up to room temperature) and the reaction mixture was left stirring overnight. Once the solvent was evaporated, the crude product was purified by column chromatography on SiO_2 using CH_2Cl_2 first, then 100:4 (CH_2Cl_2:MeOH) as the mobile phase to yield the desired compound as an off white solid. Yield = 71 mg (39%). **^{1}H NMR** (400 MHz, $CDCl_3$): δ = 8.25 (d, J = 8,5 Hz, 1H, Ar-H), 8.24 (d, J = 8,4 Hz, 1H, Ar-H), 8.06 – 8.15 (m, 3H, Ar-H), 7.81 (d, *J* = 8.8 Hz, 1H, Ar-H), 7.75 – 7.65 (m, 2H, Ar-H), 7.62 (s, 1H,Tz-H), 7.57-7,47 (m, 3H, Ar-H), 7.45-7,33 (m, 5H, Ar-H), 7,14 (s, *1*H, Tz-H), 6.98 (d, *J* = 8,8 Hz, 2H, Ph-H), 6,85 (d, J = 8,9 Hz, 2H, Ph-H), 4,08 (s, 3H, NCH_3), 3,82 (s, 3H, OCH_3), 3,79 (s, 3H, OCH_3). **^{13}C{^{1}H} NMR** (91 MHz, $CDCl_3$) δ 162.25, 159.92, 143.11, 133.10 (triazole-CH), 132.63, 132.34, 132.16, 132.06, 131.73, 131.28, 129.22, 129.11, 129.08, 128.99, 128.78, 128.58, 128.35, 128.16, 127.80, 127.10, 126.56, 126.40, 123.14, 123.07, 115.04, 114.30, 113.18, 55.54 (-OCH_3), 55.33 (-OCH_3), 38.64 (triazol-CH_3). ESI-MS m/z, relative intensity: 615.3, 616.3, 617.3.

(*S*)-1,1'-([1,1'-binaphthalene]-2,2'-diyl)bis(3-methyl(phenyl)-1*H*-1,2,3-tria-zol-3-ium) trifluoromethanesulfonate, 72b.

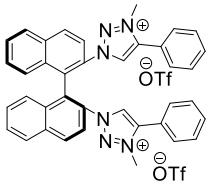

Although it can be obtained directly by reaction of **52b** with 2 equiv. MeOTf, we didn't pursue this compound and it was always obtained as a by-product in the synthesis of **71b** where it was collected after chromatographic purification of the crude reaction mixture and it was the last band to elute (CH_2Cl_2/MeOH)(93:7). The title compound was obtained as an off-white solid in *ca.* 30% yield. **^{1}H NMR** (400 MHz, $CDCl_3$): δ = 9,03 (s, 2H, Tz-H), 8.41 (d, *J* = 8,8 Hz, 2H, Ar-H), 8.22 (d, *J* = 8,9 Hz, 2H, Ar-H), 8.16 (d, *J* = 8.2 Hz, 2H, Ar-H), 7.74 (ddd, *J* = 8,1 Hz, 6,9Hz, 1,1 Hz, 2H, Ar-H), 7.58-7,45 (m, 12H, Ar-H), 7.32 (d, *J* = 8.1 Hz, 2H, Ar-H), 3.98 (s, 6H, NCH_3). **^{13}C{^{1}H} NMR** (91 MHz, $CDCl_3$) δ 143.84, 134.01, 132.60 (triazole-CH), 132.53, 132.07, 131.95, 130,88, 130,71, 129.52, 129.37, 129.18, 129.10, 129.06, 127,90, 126.75, 126.60, 122.82, 121.18, 38.97 (triazole-CH_3). HR-MS (ESI-TOF): m/z = 779,2344, calcd. for $C_{46}H_{40}N_6Rh$ ([M-CF_3SO_3]$^+$): 779,2364

Pyrene-tagged chiral [Rh(bis(NHC))] complexes. Synthesis, characterization and immobilization onto MWCNTs. Preliminary studies in asymmetric catalysis

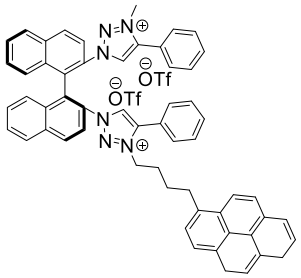

(S)-3-methyl-4-phenyl-1-(2'-(4-phenyl-3-(4-(pyren-1-yl)butyl)-1H-1,2,3-triazol-3-ium-1-yl)-[1,1'-binaphthalen]-2-yl)-1H-1,2,3-triazol-3-ium trifluoromethanesulfonate, 73. A solution of compound **71b** (155 mg, 0,220 mmol, 1 equiv.) was dissolved in anhydrous dichloromethane (9 mL), and this solution was cooled down to -60°C. With rapid stirring, a solution of freshly prepared 4-(pyren-1-yl)butyl triflate **70c** (0,550 mmol, 2,5 equiv.) in dichloromethane (3 mL) was slowly added. The brown mixture was allowed to slowly warm up to room temperature as it was stirred for 24 hours. After this time, a brown reaction residue was obtained after evaporation of the volatiles under vacuum, and this residue was purified by column chromatography on silica, by using a mobile phase gradient with increasing polarity: CH_2Cl_2 → CH_2Cl_2/MeCN (80:20) → CH_2Cl_2/MeCN (50:50) → CH_2Cl_2/MeCN/MeOH (50:45:5) → CH_2Cl_2/MeCN/MeOH (45:45:10). An off-white solid was obtained. Yield = 163 mg (67%).(However, in the most cases, isolated yield was not above 40%). **^{1}H NMR** (400 MHz, $CDCl_3$): δ = 9,15 (s, 1H, Tz-H), 8.71 (s, 1H, Tz-H), 8.31 (d, *J* = 8,8 Hz, 1H, Ar-H), 8.25-7,95 (m, 12H, Ar-H), 7.80 (d, *J* = 8,0 Hz, 1H, Ar-H), 7.70 (m, 1H, Ar-H), 7.61 (d, *J* = 7,8 Hz, 1H, Ar-H), 7,54-7,25 (m, 15H, Ar-H), 4,23 (m, 2H, NCH_2), 3,97 (s, 3H, NCH_3), 3,04 (m, 2H, CH_2-pyrene), 1,3 (m, 4H, -CH_2CH_2-). **^{13}C{^{1}H} NMR** (100,6 MHz, $CDCl_3$): δ = 143.96, 143.53, 134,88, 133.96, 132,72, 132,67, 132,60, 132,34, 131,96, 131,92, 131,84, 131,82, 131,35, 130,76, 129,97, 129,64, 129,49, 129,47, 129,38, 129,34, 129,24, 129,12, 129,08, 129,01, 128,90, 128,73, 128,46, 127,49, 127,46, 127,32, 127,10, 126,86, 126,46, 126,40, 126,01, 125,10, 124,99, 124,93, 124,88, 124,81, 123,31, 122,93, 122,70, 122,08, 121,07, 121,01, 118,89, 52,39 (NCH_2), 39,29 (NCH_3), 32,20, 29,69, 27,30. HR-MS (ESI-TOF): m/z = 406,1799, calcd. for $C_{57}H_{44}N_6$ ($[M-(CF_3SO_3)_2]^{2+}$): 406,1808.

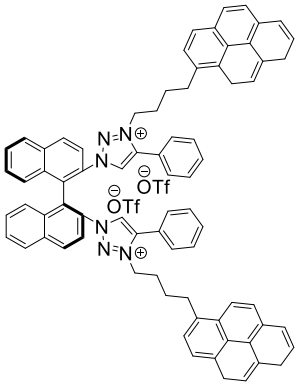

(S)-1,1'-([1,1'-binaphthalene]-2,2'-diyl)bis(4-phenyl-3-(4-(pyren-1-yl)butyl)-1H-1,2,3-triazol-3-ium), 74. A solution of bistriazole **52b** (168 mg, 0,31 mmol, 1.0 equiv.) in anhydrous dichloromethane (5 mL) was cooled down to -60°C. To this solution freshly prepared 4-(pyren-1-yl)butyl triflate (1,09 mmol, 3,5 equiv.) was added slowly dissolved in 3 mL dichloromethane, and it was left with stirring for 24 hours as it was allowed to slowly warm to room temperature. After completion of the reaction, the volatiles were evaporated under vacuum and the dark brown residue was dissolved in 2 mL dichloromethane and purified by chromatography on silica, using petroleum ether/ethyl acetate (2:1) first, and then CH_2Cl_2/MeOH (91:9). After concentration of the second fraction by stripping the mobile phase a light brown solid was obtained. Yield: 225 mg (54%). **^{1}H NMR** (400 MHz, $CDCl_3$): δ = 9,11 (s, 2H, Tz-H), 8.18 (m, 8H, Ar-H), 7,82 (d, *J* = 7,8 Hz, 2H, Ar-H), 7.58 (d, *J* = 7,8 Hz, 2H, Ar-H), 7,41 (m, 2H, Ar-H), 7.33 (m, 8H, Ar-H), 7,26 (m, 4H, Ar-H), 4,25 (m, 4H, NCH_2), 3,00 (m, 4H, CH_2-pyrene), 1,30 (m, 8H, CH_2CH_2). **^{13}C{^{1}H} NMR** (100,6 MHz, DMSO(d_6)): δ = 143,51, 134,98, 133,90, 132,57, 132,33, 131,79, 131,76, 131,33, 130,75, 129,90, 129,38, 129,32, 129,00, 128,89, 128,84, 128,76, 128,43, 127,44, 127,42, 127,05, 126,86, 126,81, 126,58, 125,97, 125,05, 124,95, 124,89, 124,86, 124,77, 122,94, 122,83, 122,16, 120,97, 118,98, 52,28 (NCH_2), 32,15 (CH_2-pyr), 29,71 (NCH_2CH_2), 27,24 (CH_2CH_2-pyr). HR-MS (ESI-TOF): m/z = 527,2371, calcd. for $C_{76}H_{58}N_6$ ($[M-(CF_3SO_3)_2]^{2+}$): 527,2362

General procedure for the metalation of bistriazolium ditriflate salts:

In a schlenk flask, the corresponding salt (0,20 mmol, 1,0 equiv.) and $[RhCl(COD)]_2$ (0,1 mmol, 0,5 equiv.) were dissolved in dry THF (8mL). Then KO^{t}Bu (0,80 mmol, 4,0 equiv.) was added to this orange solution at 25°C with stirring resulting in a rapid darkening of the solution. This mixture was stirred for 3 hours, and then it was filtered through celite under air, and quickly washed with more dry THF until the filtrates didn't show any yellow colour. THF was subsequently evaporated from the filtrates, and the residue was left under vacuum for two hours to remove

any remaining free COD. Then this residue was dissolved in 1 mL of THF and a current of Ar was passed through the septum until the minimum volume of solvent needed to dissolve the crude complex was left, to which cold Et_2O was added. A light brown solid precipitated out of the solution; the supernatants were decanted *via* cannula and the solid was washed with cold Et_2O (3 x 3 mL) and decanted until the washings had no colour. This solid was left for 2 hours under vacuum to remove any residual solvents.

{(*S*)-2,2_-Bis[3-methyl-4-(phenyl)-1,2,3-triazol-5-ylidene]-1,1-binaphthyl}(η4-cyclooctadiene)rhodium(I) triflate, 77.

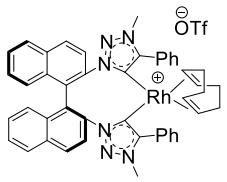

Yield: 74%. **^{1}H NMR** (400 MHz, $CDCl_3$): δ = 8,16 (d, J = 8,6 Hz, 2H, Ar-H), 7,96 (d, 8,6 Hz, 2H, Ar-H), 7,90 (d, 8,2 Hz, 2H, Ar-H), 7,59-7,35 (m, 16H, Ar-H), 4,77 (m, 2H, COD-CH), 3,10 (m, 6H, NCH_3), 2,65 (m, 2H, COD-CH), 2,19 (m, 2H, COD-CH*H*), 1,90 (m, 2H, COD-CH*H*), 1,12 (m, 2H, COD-CH*H*), 0,72 (m, 2H, COD-CH*H*). **^{13}C{^{1}H} NMR** (100,6 MHz, $CDCl_3$): δ = 173,62 (d, J = 50,7 Hz, Tz-C5), 145,79 (Ar-C_q), 137,89 (Ar-C_q), 134,02 (Ar-C_q), 132,46 (Ar-C_q), 132,11 (Ar-C_q), 131,40 (Ar-C_{Ar}), 130,59 (Ar-C_{Ar}), 130,57 (Ar-C_{Ar}), 129,30 (Ar-C_{Ar}), 129,25 (Ar-C_{Ar}), 128,77 (Ar-C_{Ar}), 128,55 (Ar-C_{Ar}), 128,09 (Ar-C_{Ar}), 127,93 (Ar-C_{Ar}), 122,67 (Ar-C_{Ar}), 92,93 (d, J = 9,2 Hz, COD-CH), 86,99 (d, J = 7,5 Hz, COD-CH), 36,82 (NCH_3), 36,18 (COD-CH_2), 26,75 (COD-CH_2). HR-MS (ESI-TOF, [M-CF_3SO_3]$^+$) *m/z* calc. for $C_{46}H_{40}N_6Rh$ 779.2364, found 779.2344.

{(S)-2-[(3-methyl-4-phenyl)-1,2,3-triazol-5-ylidene), 2'-[(3-(4-pyren-1-yl butyl)-4-phenyl-1,2,3-triazol-5-ylidene]-(1,1'-binaphtyl)}(η4-cyclooctadiene)rhodium(I) triflate, 78.

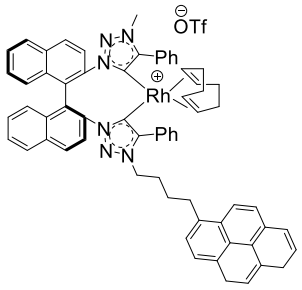

Yield: 71%. **^{1}H NMR** (400 MHz, $CDCl_3$): δ = 8,20 (d, J = 7,3 Hz, 2H), 8,15-7,99 (m, 8H, Ar-H), 7,93 (d, J = 8,6 Hz, 1H, Ar-H), 7,89 (d, J = 8,1 Hz, 1H, Ar-H), 7,84 (d, J = 8,6 Hz, 1H, Ar-H), 7,72 (d, J = 8,2 Hz, 1H, Ar-H), 7,64 (d, J = 7,9 Hz, 1H, Ar-H), 7,58-7,25 (m, 16H, Ar-H), 4,80 (m, 1H, COD-CH), 4,72 (m, 1H, COD-CH), 3,71 (m, 1H, NCH*H*), 3,33 (m, 1H, NCH*H*), 3,12 (t, J = 7,5 Hz, 2H, CH_2-

pyr), 3,07 (s, 3H, NCH_3), 2,71 (m, 1H, COD-CH*H*), 2,60 (m, 1H, COD-CH), 2,11 (m, 2H, COD-CH*H*), 1,87 (m, 2H, COD-CH*H*), 1,55 (m, 2H, NCH_2CH_2), 1,09 (m, 2H, COD-CH*H*), 0,92 (m, 2H, CH_2CH_2-pyr), 0,68 (m, 2H, COD-CH*H*). **$^{13}C\{^1H\}$ NMR** (100,6 MHz, $CDCl_3$): δ = 174,14 (d, J = 50,6 Hz, Tz-C5), 172,82 (d, J = 50,8 Hz, Tz-C5), 146,14 (Ar-C_q), 145,93 (Ar-C_q), 138,35 (Ar-C_q), 138,31 (Ar-C_q), 136,42 (Ar-C_q), 134,47 (Ar-C_q), 134,46 (Ar-C_q), 132,91 (Ar-C_q), 132,71 (Ar-C_q), 132,55 (Ar-C_q), 132,42 (Ar-C_q), 132,38 (Ar-C_q), 131,83 (Ar-C_q), 131,71 (Ar-CH), 131,63 (Ar-CH), 130,99 (Ar-C_q), 130,94 (Ar-CH), 130,88 (Ar-CH), 130,04 (Ar-CH), 129,72 (Ar-CH), 129,68 (Ar-CH), 129,50 (Ar-C_q), 129,31 (Ar-CH), 129,16 (Ar-CH), 128,92 (Ar-CH), 128,82 (Ar-CH), 128,68 (Ar-CH), 128,48 (Ar-CH), 128,45 (Ar-CH), 128,31 (Ar-CH), 128,23 (Ar-CH), 128,16 (Ar-CH), 127,80 (Ar-CH), 127,06 (Ar-CH), 126,10 (Ar-CH), 125,99 (Ar-CH), 125,86 (Ar-CH), 125,78 (Ar-CH), 124,06 (Ar-CH), 123,28 (Ar-CH), 123,05 (Ar-CH), 93,51 (d, J = 9,1 Hz, 1H, COD-CH), 93,00 (d, J = 9,0 Hz, COD-CH), 87,44 (d, J = 7,5 Hz, COD-CH), 87,08 (d, J = 7,4 Hz, COD-CH), 50,50 (NCH_2), 37,18 (NCH_3), 36,53 (COD-CH_2), 36,53 (COD-CH_2), 33,24 (CH_2-pyr), 28,89 (-CH_2CH_2-), 28,42 (-CH_2CH_2-), 27,10 (COD-CH_2), 27,02 (COD-CH_2). HRMS (ESI-TOF, $[M\text{-}CF_3SO_3]^+$) *m/z* calc. for $C_{46}H_{40}N_6Rh$ 1021,3460, found 1021,3435.

{(*S*)-2,2_-Bis[3-(1-pyren-yl butyl)-4-(phenyl)-1,2,3-triazol-5-ylidene]-1,1-binaphthyl}(η4-cyclooctadiene)rhodium(I) triflate, 79.

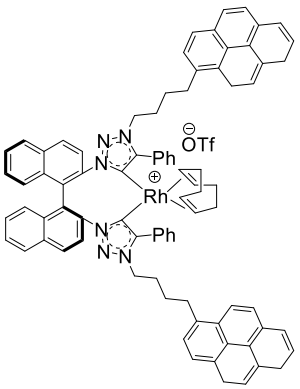

Yield: 74%. **^1H NMR** (400 MHz, $CDCl_3$): δ = 8,19 (m, 4H, Ar-H), 8,1-7,94 (m, 14H, Ar-H), 7,80 (d, 8,6 Hz, 2H, Ar-H), 7,71 (d, J = 8,3 Hz, 2H, Ar-H), 7,62 (d, J = 7,9 Hz, 2H, Ar-H), 7,41-7,18 (m, 16H, Ar-H), 4,73 (m, 2H, COD-CH), 3,65 (m, 2H, NCH*H*), 3,29 (m, 2H, NCH*H*), 3,10 (t, J = 7,1 Hz, 4H, CH_2-pyr), 2,63 (m, 2H, COD-CH), 1,99 (m, 2H, COD-CH*H*), 1,79 (m, 2H, COD-CH*H*), 1,55 (m, 4H, -CH_2CH_2-), 1,09 (m, 2H, COD-CH*H*), 0,88 (m, 4H, -CH_2CH_2-), 0,63 (m, 2H, COD-CH*H*). **$^{13}C\{^1H\}$ NMR** (100,6 MHz, CD_2Cl_2): δ = 172,25 (d, J = 50,6 Hz, Tz-C5), 145,63 (Ar-C_q), 137,85 (Ar-C_q), 135,84 (Ar-C_q), 134,94 (Ar-C_q), 132,22 (Ar-C_q), 131,96, 131,39, 131,03 (Ar-C_q), 130,56 (Ar-C_q), 130,40, 129,55 (C_q), 129,24, 129,10 (Ar-C_q), 128,96, 128,80 (C_q), 128,37 (C_q), 128,24 (C_q), 127,91, 127,75, 127,61, 127,36, 126,56, 125,68, 125,63, 125,48, 125,44, 125,37, 125, 36, 125,27, 123,52, 122,75, 92,74 (d, J = 9,2 Hz, COD-CH), 86,70 (d, J = 7,5 Hz,

COD-CH), 49,98 (NCH_2), 36,06 (COD-CH_2), 32,80 (CH_2-pyr), 30,19 (CH_2CH_2), 28,60 (COD-CH_2), 28,38 (CH_2CH_2). HRMS (ESI-TOF, [M-CF_3SO_3]$^+$) *m/z* calc. for $C_{84}H_{68}N_6Rh$ 1263,456, found 1263,4529.

General procedure for the immobilization of pyrene-tagged complexes onto MWCNT's.

MWCNT's (90 mg) were suspended on the specified solvent (25 mL). This suspension was sonicated for 1 hour at 25°C. Subsequently, the Rh complex was added (9 mg) to the dispersed MWCNT's, and this mixture was stirred at 25°C for 10 hours. After this time, the mixture was centrifugated, and the supernatant was decanted. The functionalized MWCNT's were washed twice (2 x 5 mL) with the solvent used for the immobilization procedure. The washings were centrifuged and decanted. The solid material was dried under vacuum until a black powdery solid was obtained.

General procedure for the catalytic hydrosilylation of isobutyrophenone (80).

In a schlenk flask **77** (2 mol%) was dissolved in dry THF (1 mL). To this solution isobutyrophenone (**81**) (39 µL, 0,25 mmol) was added followed by mesitylene (35,5 µL, 0,25 mmol), and by the silane reagent (0,375 mmol, 1,5 equiv.). This solution was left with stirring for 24h at room temperature. After this time 1 mL of H_2O was added and then 1,5 mL of HCl(aq.) 2M. After stirring for 5 minutes, Et_2O (5ml) was added and the organic phase was separated. The aqueous phase was extracted with additional Et_2O (5 mL). The combined organic layers were passed through a short plug of silica and eluted with 3 mL CH_2Cl_2 and they were analysed by chiral GC-FID using a CP-Chiralsil-Dex CB column (length: 25 m, internal diameter: 0.25 mm, film thickness: 0.25 µm. Method: carrier gas: 120 kPa He, temperature: 90 °C, rate 0,5 °C/min to 120 °C and hold for 3 min; rt = 35,73 min, 36,22 min for the two enantiomers of product **82**.

General procedure for the catalytic hydroboration of styrene (83).

In a flame-dried schlenk flask **77** (2 mol%) was dissolved in 1 mL $CHCl_2$. Styrene (**83**) (58 µL, 0,5 mmol) was added and this solution was stirred at

25°C for 10 minutes. Pinacol borane (88 µL, 0,585 mmol, 1,17 equiv.) was subsequently added and this solution was stirred for 24h at 25°C. After reaction time 0,3 mL of the mixture were pippeted out, concentrated and passed through a plug of silica, by elution with petroleum ether/ethyl acetate (20:1). After evaporation of the volatiles the residue was dissolved in $CDCl_3$ and analysed by ^{1}NMR. The remaining 0,7 mL of the reaction mixture where cooled down to 0°C, and NaOH aq. 3M (1,5 mL) and H_2O_2 (1 mL) were successively added. This biphasic mixture was stirred at 0°C for 30 minutes and then for 1 hour at room temperature. The organic phase was separated and the aqueous phase was extracted with CH_2Cl_2 (2 x 2 mL). The combined organic layers were washed with NaCl (aq.), dried with anhydrous $MgSO_4$ and concentrated to dryness. This residue was analysed by ^{1}H NMR and the enantiomeric excess was determined by chiral GC-FID using a CP-Chiralsil-Dex CB column (length: 25 m, internal diameter: 0.25 mm, film thickness: 0.25 µm. Method: carrier gas: 120 kPa He, temperature: 130 °C for 10 min, rate 10 °C/min to 180 °C and hold for 3 min.; rt = 3.18 min, 3,33 min for the two enantiomers of the branched regioisomer.

General procedure for the catalytic hydrogenation of 80 and 81.

Under an Ar atmosphere, catalyst **77** (1 mol%) was introduced in a vessel equipped with a magnetic stirrer and placed inside a stainless 5-positions 10 mL stainless steel autoclave. Catalyst **77** was dissolved in CH_2Cl_2 (3 mL) and then, the corresponding substrate (0,5 mmol) was added. The autoclave was pressurized with hydrogen to the indicated pressure and this mixture was stirred for 24 h at the indicated temperature. After carefully releasing the pressure, the reaction mixture was filtered through a short plug of silica and analyzed by NMR and chiral GC using a CP-Chiralsil-Dex CB column (length: 25 m, internal diameter: 0.25 mm, film thickness: 0.25 µm. Method: carrier gas: 120 kPa He, temperature: 60 °C for 35 min, rate 2 °C/min to 100 °C and hold for 1 min.; rt = 36,80 min, 37,10 min for the two enantiomers of hydrogenated **84** .

Pyrene-tagged chiral [Rh(bis(NHC))] complexes. Synthesis, characterization and immobilization onto MWCNTs. Preliminary studies in asymmetric catalysis

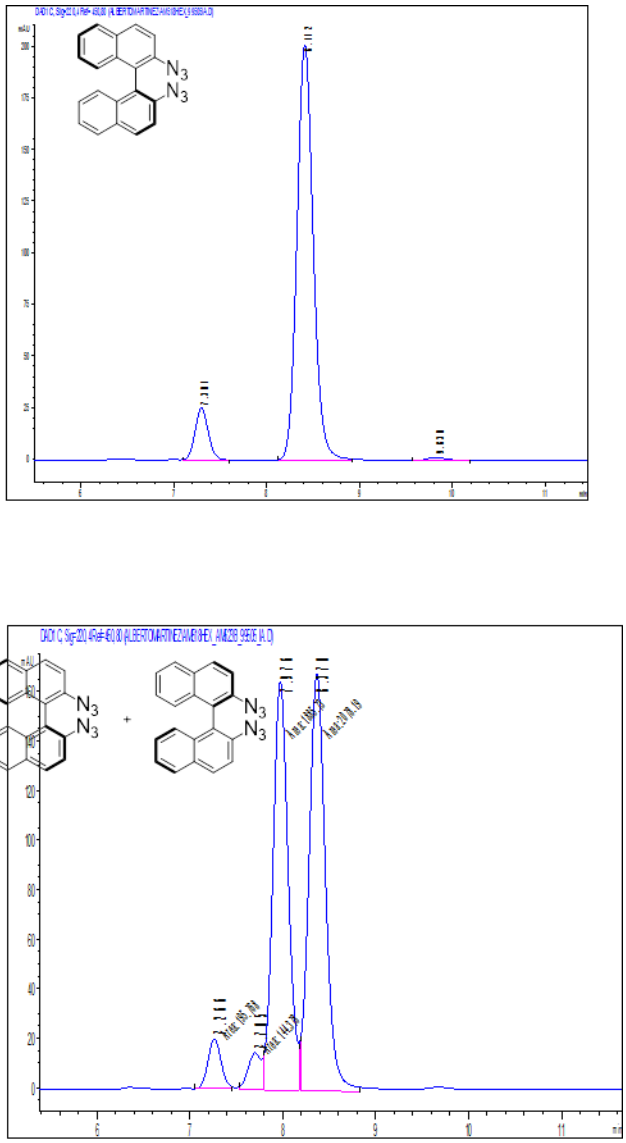

Figure S6.1. HPLC analysis of pure (*S*)-2,2'-diazido-1,1'-binaphthalene ((S)-**51**) (on top) and an equimolar mixture of (S)-**51** and (R)-**51**.

VI.5. References

[1] *N-heterocyclic carbenes in transition metal catalysis*; Topics in Organometallic Chemistry, 21; ed. F. Glorius, Wiley-VCH Verlag GmbH & Co: Weinheim, Germany, **2006**.
[2] R.H. Crabtree, *Coord. Chem. Rev.,* **2007**, *251, 595.*
[3] G. Bertrand, *J. Organomet. Chem.,* **2005**, *690*, 5397.
[4] M. Poyatos, J. A. Mata, E. Peris, *Chem. Rev.* **2009,** *109,* 3677.
[5] E. Peris, R. H. Crabtree, *Coord. Chem. Rev.*, **2004**, *248*, 2239.
[6] X.L. Hu, K. Meyer, *J. Organomet. Chem.* **2005**, *690*, 5474.
[7] R. McKie, J.A. Murphy, S.R. Park, M.D. Spicer, S.Z. Zhou, *Angew. Chem. Int. Ed.* **2007**, *46*, 6525.
[8] A.T. Normand, K.J. Cavell, *Eur. J. Inorg. Chem.* **2008**, 2781.
[9] E. Mas-Marzá, M. Poyatos, M. Sanaú, E, Peris, *Organometallics* **2004**, *23*, 323.
[10] D. Pugh, A.A. Danopoulos, *Coord. Chem. Rev.* **2007**, *251*, 610.
[11] C.H. Leung, C.D. Incarvito, R.H. Crabtree, *Organometallics* **2006**, *25*, 6099.
[12] Y.A. Wanniarachchi, M.A. Khan, L.M. Slaughter, *Organometallics,* **2004**, *23*, 5881.
[13] C. Buron, L. Stelzig, O. Guerret, H. Gornitzka, V. Romanenko, G. Bertrand, *J. Organomet. Chem.* **2002**, *664*, 70.
[14] O. Guerret, S. Sole, H. Gornitzka, M. Teichert, G. Trinquier, G. Bertrand, *J. Am. Chem. Soc.* **1997**, *119*, 6668.
[15] A.J. Boydston, K.A. Williams, C.W. Bielawski, *J. Am. Chem. Soc.* **2005**, *127*, 12496.
[16] J. Schwarz, V.P.W. Bohm, M.G. Gardiner, M. Grosche, W.A. Herrmann, W. Hieringer, G. Raudaschl-Sieber, *Chem. Eur. J.*, **2000**, *6*, 1773.
[17] M. Poyatos, E. Mas-Marza, J.A. Mata, M. Sanaú, E. Peris, *Eur. J. Inorg. Chem.* **2003**, 1215.
[18] M. Muehlhofer, T. Strassner, W.A. Herrmann, *Angew. Chem. Int. Ed.*, **2002**, *41*, 1745.
[19] W.A. Herrmann, C.P. Reisinger, M. Spiegler, *J. Organomet. Chem.*, **1998**, 557, 93.
[20] M. Albrecht, R.H. Crabtree, J. Mata, E. Peris, *Chem. Commun.*, **2002**, 32.
[21] M. Poyatos, M. Sanaú, E. Peris, *Inorg. Chem.*, **2003**, *42*, 2572.
[22] W.-L. Duan, M. Shi, G.–B. Rong, *Chem. Commun.*, **2003**, 2916.
[23] F.A. Westerhaus, B. Wendt, A. Dumrath, G. Wienhoefer, K. Junge, M. Beller, *ChemSusChem,* **2013**, *6*, 1001.
[24] S. Burling, L.D. Field, H.L. Li, B.A. Messerle, P. Turner, *Eur. J. Inorg. Chem*. **2003**, *2003*, 3179.
[25] J.A. Mata, M. Poyatos, E. Peris, *Coord. Chem. Rev.*, **2007**, *251*, 841.
[26] R.L. Lowry, M.K. Veige, O. Clément, K.A. Abboud, I. Ghiviriga, A.S. Veige, *Organometallics,* **2008,** *27,* 5184.
[27] R.H. Crabtree, *J. Organomet. Chem.* **2005**, *690*, 5451.
[28] H.B. Kagan, L. Langlois, T.P. Dang, *J. Organomet. Chem.* **1975**, *90*, 353.
[29] L.H. Gade, S. Bellemin-Lapponaz, *Coord. Chem. Rev.* **2007**, *251*, 718.
[30] D. S. Clyne, J. Jin, E. Genst, J. C. Gallucci and T. V. RajanBabu, *Org. Lett.*, **2000**, *2*, 1125.
[31] M. C. Perry, X. Cui and K. Burgess, *Tetrahedron: Asymmetry*, **2002**, *13*, 1969.

Pyrene-tagged chiral [Rh(bis(NHC))] complexes. Synthesis, characterization and immobilization onto MWCNTs. Preliminary studies in asymmetric catalysis

---

[32] M. S. Jeletic, I. Ghiviriga, K. A. Abboud and A. S. Veige, *Organometallics*, **2007**, *26*, 5267.
[33] C. Marshall, M. F. Ward and W. T. A. Harrison, *J. Organomet. Chem.*, **2005**, *690*, 3970.
[34] C. Marshall, M. F. Ward and W. T. A. Harrison, *Tetrahedron Lett.*, **2004**, *45*, 5703.
[35] L. J. Liu, F. Wang and M. Shi, *Eur. J. Inorg. Chem.*, **2009**, 1723.
[36] H. Song, L. N. Gu and G. Zi, *J. Organomet. Chem.*, **2009**, *694*, 1493.
[37] H. Clavier, J. C. Guillemin, M. Mauduit, *Chirality*, **2007**, *19*, 471.
[38] G. Bonnet, R. E. Douthwaite, R. Hodgson, *Organometallics*, **2003**, *22*, 4384.
[39] K. S. Schneider, J. Schwarz, G.D. Frey, E. Herdtweck, W.A. Herrmann, *J. Organomet. Chem.*, **2007**, *692*, 4560.
[40] R. Zhang, Q. Xu, X. Zhang, T. Zhang, M. Shi, *Tetrahedron: Asymmetry* **2010**, 1928.
[41] T. Zhang, M. Shi, M.X. Zhao, *Tetrahedron* **2008**, *64*, 2412.
[42] M.S. Jeletic, M.T. Jan, I. Ghiviriga, K.A. Abboud, A.S. Veige, *Dalton Trans.*, **2009**, 2764.
[43] M. Shi, H.X. Qian, *Appl. Organomet. Chem.* **2006**, *20*, 771.
[44] M.Y. Machado, R. Dorta, *Synthesis (Stuttgart)* **2005**, 2473.
[45] A.R. Chianese, R.H. Crabtree, *Organometallics* **2005**, *24*, 4432.
[46] T. Scherg, S.K. Schneider, G.D. Frey, J. Schwarz, E. Herdtweck, W.A. Herrmann, *Synlett* **2006**, 2894.
[47] A. Meyer, M.A. Taige, T. Strassner, *J. Organomet. Chem.* **2009**, *694*, 1861.
[48] M.S. Jeletic, R.J. Lowry, J.M. Swails, I. Ghiviriga, A.S. Veige, *J. Organomet. Chem.*, **2011**, *696*, 3127.
[49] M.S. Jeletic, I. Ghiviriga, K.A. Abboud, A.S. Veige, *Dalton Trans.*, **2010**, *39*, 6392.
[50] Q. Xu, X. Gu, S. Liu, Q. Dou, M. Shi, *J. Org. Chem.* **2007**, *72*, 2240.
[51] S.H. Cao, M. Shi, *Tetrahedron: Asymmetry* **2010**, *21*, 2675.
[52] T. Chen, J.J. Jiang, Q. Xu, M. Shi, *Org. Lett.* **2007**, *9*, 865.
[53] E.N. Jacobsen, T.P. Yoon, *Science* **2004**, *299*, 1691.
[54] S.N. Sluijter, L.J. Jongkind, C.J. Elsevier, *Eur. J. Inorg. Chem.*, **2015**, *18*, 2948.
[55] P. Mathew, A. Neels, M. Albrecht, *J. Am. Chem. Soc.*, **2008**, *130*, *13534*.
[56] K.F. Donnelly, A. Petronilho, M. Albrecht, *Chem. Commun.*, **2013**, *49*, 1145.
[57] M. Meldal, C.W. Tornøe, *Chem. Rev.* **2008**, *108*, 2952.
[58] J. J. Bürgi, R. Mariz, M. Gatti, E. Drinkel, X. Luan, S. Blumentritt, A. Linden, R. Dorta, *Angew. Chem. Int. Ed.* **2009**, *48*, 2768.
[59] M. S. Jeletic, C. E. Lower, I. Ghiviriga, A. S. Veige, *Organometallics,* **2011**, *30*, 6034.
[60] D.J. Cole-Hamilton, Science, **2003**, *299*, 1702.
[61] C. Copéret, M. Chabanas, R.P. Saint-Arroman, J.M. Basset, *Angew. Chem. Int. Ed.*, **2003**, *42*, 156.
[62] From *Catalysis by metal complexes* **2010**, *33* (*Heterogenized Homogeneous Catalysts for Fine Chemicals Production)*. Ed. P. Barbaro, F. Liguori. Springer.
[63] C. Vriamont, M. Devillers, O. Riant, S. Hermans, *Chem. Eur. J.*, **2013**, *19*, 12009.

[64] G. Liu, B. Wu, J. Zhang, X. Wang, M. Shao, J. Wang, *Inorg. Chem.*, **2009**, *48*, 2383.
[65] S. Wittman, A. Schaetz, R.N. Grass, W.J. Stark, O. Reiser, *Angew. Chem. Int. Ed.*, **2010**, *49*, 1867.
[66] D. Didier, E. Schulz, *Tetrahedron: Asymmetry*, **2013**, *24*, 769.
[67] S. Sabater, J.A. Mata, E. Peris, *ACS Catal.*, **2014**, *4*, 2038.
[68] *Nanostructured Carbon Materials for Catalysis*, **2015**; eds. P. Serp, B. Machado, RSC, Cambridge.
[69] Y. L. Zhao, J. F. Stoddart, *Acc. Chem. Res*. **2009**, *42*, 1161.
[70] H. Huang, Q. Yuang, J. S. Sha, R. D. K. Misra, *Adv. Drug Delivery Rev*. **2011**, *63*, 1332.
[71] C. Schulz-Drost, V. Sgobba, C. Gerhards, S. Leubner, R. M. Krieck Calderon, A. Ruland, D. M. Guldi, *Angew. Chem. Int. Ed*. **2010**, *49*, 6425.
[72] C. Vijayakumar, B. Balan, M.-J. Kim, M. Takeuchi, *J. Phys. Chem. C*, **2011**, *115*, 4533.
[73] S Iijima, *Nature*. **1991**, *354*, 56.
[74] D. Tasis, N. Tagmatarchis, A. Bianco, M. Prato, *Chem. Rev.* **2006**, *106*, 1105.
[75] J.M. Sieben, A. Ansón-Casaos, F. Montilla, M.T. Martínez, E. Morallón, *Electrochimica Acta*, **2014**, *135*, 404.
[76] Q. Li, M. Zaiser, R.J. Blackford, C. Jeffree, Y. He, V. Koutsos, *Mat. Lett.*, **2014**, *125*, 116.
[77] R. Ansari, S. Malakpour, M, Faghihnasiri, S. Ajori, *Superlatt. and Microstruct*. **2013**, *64*, 220.
[78] J. Chen, M.A. Hamon, H. Hu, Y. Chen, A.M. Rao, P.C. Eklund, R.C. Haddon, *Science* **1998**, *282*, 95.
[79] R.J. Chen, Y.Z. Zhang, D. Wang, H. Dai, *J. Am. Chem. Soc.* **2001**, *123*, 3838.
[80] C. Estarellas, *Theoretical and experimental study of cooperative effects in noncovalent interactions.* Ph. D. Tesis, Illes Balears University, Spain, 2012.
[81] S. Latil, M. Heggie, J. Charlier, F. Tournus, *Phys. Rev.* **2005**, *72*, 075431.
[82] L. Xing, J.-H. Xie, Y.-S. Chen, L.-X. Wang, Q.-L. Zhou, *Adv. Synth. Catal,.* **2008**, *350*, 1013.
[83] Master Thesis by A. Cabré, Universitat Autònoma de Barcelona, **2015**.
[84] T.J. Curphey, K.S. Prasad, *J. Org. Chem.* **1972**, *37*, 2259-2266
[85] G. Guisado-Barrios, J. Bouffard, B. Donnadieu, G. Bertrand, *Angew. Chem. Int. Ed.* **2010**, *49*, 4759.
[86] H.C. Kolb, M.G. Finn, K.B. Sharpless, *Angew. Chem. Int. Ed.*, **2001**, *40*, 2004.
[87] J. Bouffard, B. K. Keitz, R. Tonner, G. Guisado-Barrios, G. Frenking, R. H. Grubbs and G. Bertrand, Organometallics, **2011**, *30*, 2617.
[88] M. Poyatos, W. McNamara, C. Incarvito, E. Clot, E. Peris, R.H. Crabtree, *Organometallics*, **2008**, *27*, 2128-2136
[89] J.A. Mann, J. Rodríguez-López, H.D. Abruña, W.R. Dichtel, *J. Am. Chem. Soc.* **2011**, *133*, 17614.
[90] I. Ojima, M. Nihonyanagi, T. Kogure, M. Kumagai, S. Horiuchi, K. Nakatsugawa, Y. Nagai, *J. Organomet. Chem.* **1975**, *94*, 449.
[91] I. Ojima, T. Kogure, M. Kumagai, S. Horiuchi, T. Sato, *J. Organomet. Chem.,* **1976**, *122*, 83.

Pyrene-tagged chiral [Rh(bis(NHC))] complexes. Synthesis, characterization and immobilization onto MWCNTs. Preliminary studies in asymmetric catalysis

---

[92] G.Z. Zheng, T.H. Chan, *Organometallics*, **1995**, *14*, 70.
[93] N. Schneider, M. Finger, C. Haferkemper, S. Bellemin-Laponnaz, P. Hofmann, L.H. Gade, *Angew. Chem., Int. Ed*. **2009**, *48*, 1609.
[94] P. Gigler, B. Bechlars, W.A. Herrmann, F.E. Kühn**,** *J. Am. Chem. Soc.* **2011**, *133*, 1589.
[95] A.-M. Carroll, T.P. O'Sullivan, P.J. Guiry, *Adv. Synth. Catal*., **2005**, *347*, 609.
[96] C.M. Crudden, Y.B. Hleba, A.C. Chen, *J. Am. Chem. Soc.*, **2004**, *126*, 9200.
[97] W.S. Knowles, *Angew. Chem. Int. Ed.* **2002**, *41*, 1998.
[98] B.D.Vineyard, W.S. Knowles, M.J. Sabacky, G.L. Bachman, D.J. Weinkauff, *J. Am. Chem. Soc.* **1977**, *99*, 5946.
[99] A. Arnanz, C. González-Arellano, A. Juan, G. Villaverde, A. Corma, M. Iglesias, F. Sánchez, *Chem. Commun*., **2010**, *46*, 3001.
[100] R.H. Crabtree, G. Giordano, *Inorg. Synth.* **1979**, *19*, 218.
[101] J.M. Lobez, T.M. Swager, *Angew. Chem. Int. Ed.* **2010**, 49, 95.

UNIVERSITAT ROVIRA I VIRGILI
HETEROGENIZED N-HETEROCYCLIC CARBENE METAL COMPLEXES FOR SELECTIVE CATALYSIS
Alberto Martínez Lombardía

Chapter 7

"Conclusions"

UNIVERSITAT ROVIRA I VIRGILI
HETEROGENIZED N-HETEROCYCLIC CARBENE METAL COMPLEXES FOR SELECTIVE CATALYSIS
Alberto Martínez Lombardía

General conclusions

Two families of well-defined NHC-based organometallic complexes incorporating functional groups for their subsequent immobilization onto a solid support were synthesized and characterized.

The first family consisted in Pd complexes that were immobilized onto oxide supports. The resulting hybrid materials were active in C-C coupling processes and in the chemoselective semi-reduction of alkynes and alkynols. Moreover, the recovery and re-use of the supported catalysts was possible in cross-coupling reactions under batch conditions, and these heterogenized catalysts could be employed in a packed bed reactor to perform Suzuki-Miyaura and Sonogashira couplings under continuous flow conditions.

The second family consisted in chiral Rh complexes bearing pyrene moieties that were subsequently immobilized onto MWCNTs through π–π stacking interactions. The synthesis and characterization of the ligands, organometallic complexes and the resulting hybrid materials were performed. However, due to lack of time, only preliminary catalytic tests could be carried out and further work will be needed to assess the efficiency of this family of supported catalysts.

- **CHAPTER 3**:

  - A modular synthetic approach involving the functionalization of the aromatic *para* positions of NHC ligands was successfully applied. Although in this work, an alkene tether was introduced, the installation of a variety of other functionality may be envisioned through this methodology.

  - The immobilization of Pd-NHC complexes onto silica gel, mesoporous silica MCM-41, γ-Al_2O_3 and TiO_2 could be performed in a one-pot three sequential steps protocol starting from alkene-functionalized imidazolium chloride salts.

  - The differences in metal loadings for these supports were attributed to the surface areas and to the concentration of hydroxyl groups in these oxide supports.

- A ^{13}C-labelled sample in C2 (carbene carbon) of an alkene-functionalized imidazolium chloride salt was prepared and ^{13}C NMR was used to track the carbene through the last steps until the final solid-supported complexes. This study revealed that the integrity of the metal-carbene species is not affected by the immobilization procedure.

- All the hybrid materials synthesized in this work were characterized by ICP-AES, and elemental analysis.

- **CHAPTER 4**:

  - The supported [Pd(NHC)] complexes catalyzed the Suzuki-Miyaura coupling of aryl bromides and chlorides with phenylboronic acids in excellent yields and selectivities. Ligands with bulkier substituents such as 2,6-diisopropylphenyl resulted in improved catalytic activity, and capping the residual hydroxyl groups at the surface of the support also had a beneficial effect on activity. Under the reaction conditions, the supported species undergo degradation, resulting in diminished activity. The causes for this decomposition are not clear, but several experiments indicated that this decomposition was not due to interactions with the support nor to the intramolecular thioether linkages, but to an intrinsic instability of the molecular species. This deactivation mechanism is slowed down under non-aqueous reaction conditions, and using toluene as solvents, the catalysts displayed improved recyclability in successive catalytic runs.

  - The influence of the support was also evaluated, and catalysts supported onto γ-Al_2O_3 and TiO_2 were more robust that their silica-supported analogues. Application of the supported catalysts under continuous flow conditions led to an increase in the reaction rate (measured TOF) up to one order of magnitude with respect to the corresponding batch process.

  - The supported catalysts were also active in the Sonogashira and Heck reactions. In the Heck reaction between *p*-bromoacetophenone and ethyl acrylate, complete conversions were achieved in the first run. However, recycling of the catalyst lead to a constant decrease in the catalyst performance.

- In the case of the Sonogashira coupling, the supported catalysts efficiently coupled *p*-bromoacetophenone with various alkynes. As in the case of the Suzuki-Miyaura coupling, recycling studies showed that γ-Al_2O_3- and TiO_2-supported materials were more robust than those immobilized on silica. Therefore, these materials were applied in the Sonogashira coupling between *p*-bromoacetophenone and phenylacetyene under continuous flow conditions without apparent decomposition after two hours on stream. A comparison of catalysts activity under batch or continuous flow conditions again revealed a higher TOF under continuous flow conditions.

- **CHAPTER 5**:

- The supported [Pd(NHC)] complexes were also active in the hydrogenation of internal alkynes under mild reaction conditions. Experiments were carried out both under batch and under continuous flow conditions and demonstrated the difficulty in preventing the over-reduction in to the alkanes, especially at high conversions. When hydrogenations were performed under continuous flow conditions, the selectivity varied over time under a set of specified reaction conditions, which indicated a change in the nature of the catalyst species.

- Alternatively to the use of H_2(g), transfer hydrogenation conditions using a (1:1) mixture of formic acid/trimethylamine as the hydrogen donor allowed for an improved control of the selectivity. To suppress the formation of alkane products, a sub-stoichiometric amount of PPh_3 was used. Using this catalytic system, internal and terminal alkynes and alkynols were transformed into the corresponding alkene products in high chemo- and stereoselectivity. Internal alkynes and alkynols were converted to (*Z*)-alkenes in high to excellent yields.

- In the presence of formic acid/trimethylamine, the supported catalysts isomerize (*Z*)-stilbene into (*E*)-stilbene. This catalytic activity was utilized in the indirect (*E*)-selective transfer semi-hydrogenation of diphenylacetylene, and (*E*)-stilbene was obtained in 90% yield.

- Recycling studies were performed for the transfer semi-hydrogenation of diphenylacetylene mediated by γ-Al_2O_3 and TiO_2-supported

catalysts in combination with PPh_3. Complete loss of activity was observed after the first run. Metal leaching was detected by ICP-OES analysis of the reaction mixtures, but does not appear as the only cause for the observed deactivation. A possible explanation to this drop in catalyst activity could be the agglomeration of Pd into clusters, nanoparticles and inactive bulk metal, based on the greyish color of the catalyst after the reaction. However, due to the low content of Pd in the solids, TEM and XRD analysis did not provide any further evidence of this phenomenon.

- **CHAPTER 6**:

  - Introduction of pyrene groups in the backbone of 1,1'-binaphtyl-2,2'-bis(4-phenyl-1,2,3-triazol) was performed through two strategies: alkylation of the bistriazole fragment, or CuAAC "click" chemistry.

    - Alkylation at the N3's of the triazole rings required the use of triflate reagents. The use of one equivalent of methyl triflate allowed for the obtention of a monomethylated intermediate monotriazolium compound which was subsequently alkylated with an excess of 4-(pyren-1-yl)butyl triflate to obtaina a diquaternary ditriflate salt bearing a single pyrene tag.

    - The second strategy involved Cu-catalyzed alkyne azyde cycloaddition using a key BINAM-derived diazide compound and propargyl pyrenebutyl ether. This strategy afforded a bistriazole compound containing 2 pyrene tags in 34% yield.

  - Following a reported protocol, the three synthesized bistriazolium ditriflate salts were metallated to form the corresponding [Rh(I)bis(NHC)] chelate complexes in yields above 70% after purification.

  - The Rh complexes containing one and two pyrene moieties were immobilized onto the surface of MWCNTs. The presence of two pyrene tags in the structure of the complex had a positive effect on the anchoring of the molecular complex, and higher loadings were observed compared to the complex bearing a single pyrene tag. The

final hybrid materials were characterized using various techniques such as EDX, XPS, UV-Vis, etc... The complexes revealed a homogeneous distribution over the surface of the support and evidence that nature of the molecular complexes remained unchanged upon immobilization was obtained.

- The non-pyrene-tagged Rh complex was used for testing the potential of these type of complexes in asymmetric reduction processes such as the hydrosilylation of isobutyrophenone, the hydroboration of styrene with pinacolborane and the hydrogenation of alkenes. However, although some catalytic activity was achieved under the conditions tested, very low enantiomeric induction was observed in all cases.